

JOURNAL OF

**CHROMATOGRAPHY A**

INCLUDING ELECTROPHORESIS AND OTHER SEPARATION METHODS

## EDITORS

U.A.Th. Brinkman (Amsterdam)  
 R.W. Giese (Boston, MA)  
 J.K. Haken (Kensington, N.S.W.)  
 C.F. Poole (London)  
 L.R. Snyder (Orinda, CA)  
 S. Terabe (Hyogo)

EDITORS, SYMPOSIUM VOLUMES,  
 E. Heftmann (Orinda, CA), Z. Deyl (Prague)

## EDITORIAL BOARD

D.W. Armstrong (Rolla, MO)  
 W.A. Aue (Halifax)  
 P. Boček (Brno)  
 P.W. Carr (Minneapolis, MN)  
 J. Crommen (Liège)  
 V.A. Davankov (Moscow)  
 G.J. de Jong (Groningen)  
 Z. Deyl (Prague)  
 S. Dilli (Kensington, N.S.W.)  
 Z. El Rassi (Stillwater, OK)  
 H. Engelhardt (Saarbrücken)  
 M.B. Evans (Hattfield)  
 S. Fanali (Rome)  
 G.A. Guiochon (Knoxville, TN)  
 P.R. Haddad (Hobart, Tasmania)  
 I.M. Hais (Hradec Králové)  
 W.S. Hancock (Palo Alto, CA)  
 S. Hjertén (Uppsala)  
 S. Honda (Higashi-Osaka)  
 Cs. Horváth (New Haven, CT)  
 J.F.K. Huber (Vienna)  
 J. Janák (Brno)  
 P. Jandera (Pardubice)  
 B.L. Karger (Boston, MA)  
 J.J. Kirkland (Newport, DE)  
 E. sz. Kováts (Lausanne)  
 C.S. Lee (Ames, IA)  
 K. Macek (Prague)  
 A.J.P. Martin (Cambridge)  
 E.D. Morgan (Keele)  
 H. Poppe (Amsterdam)  
 P.G. Righetti (Milan)  
 P. Schoenmakers (Amsterdam)  
 R. Schwarzenbach (Dübendorf)  
 R.E. Shoup (West Lafayette, IN)  
 R.P. Singhai (Wichita, KS)  
 A.M. Sioufi (Marseille)  
 D.J. Strýdom (Boston, MA)  
 T. Takagi (Osaka)  
 N. Tanaka (Kyoto)  
 K.K. Unger (Mainz)  
 P. van Zoonen (Bilthoven)  
 R. Verpoorte (Leiden)  
 Gy. Vigh (College Station, TX)  
 J.T. Watson (East Lansing, MI)  
 B.D. Westerlund (Uppsala)

## EDITORS, BIBLIOGRAPHY SECTION

Z. Deyl (Prague), J. Janák (Brno), V. Schwarz (Prague)

ELSEVIER

# JOURNAL OF CHROMATOGRAPHY A

INCLUDING ELECTROPHORESIS AND OTHER SEPARATION METHODS

**Scope.** The *Journal of Chromatography* publishes papers on all aspects of **chromatography, electrophoresis** and other separation methods. Contributions consist mainly of research papers dealing with chromatographic theory, instrumental developments and their applications. Section *A* covers all areas except biomedical applications of separation science which are published in section *B: Biomedical Applications*.

**Submission of Papers.** The preferred medium of submission is on disk with accompanying manuscript. Manuscripts (in English; four copies are required) should be submitted to: Editorial Office of *Journal of Chromatography A*, P.O. Box 681, 1000 AR Amsterdam, Netherlands, Telefax (+31-20) 485 2304. Review articles are invited or proposed in writing to the Editors who welcome suggestions for subjects. An outline of the proposed review should first be forwarded to the Editors for preliminary discussion prior to preparation. Submission of an article is understood to imply that the article is original and unpublished and is not being considered for publication elsewhere. For copyright regulations, see below.

**Subscription information.** For 1996 Vols. 715–748 of *Journal of Chromatography A* (ISSN 0021-9673) are scheduled for publication. Subscription prices for *Journal of Chromatography A + B* (combined), or for section *A* or *B* are available upon request from the publisher. Subscriptions are accepted on a prepaid basis only and are entered on a calendar year basis. Issues are sent by surface mail except to the following countries where air delivery via SAL is ensured: Argentina, Australia, Brazil, Canada, China, Hong Kong, India, Israel, Japan, Malaysia, Mexico, New Zealand, Pakistan, Singapore, South Africa, South Korea, Taiwan, Thailand, USA. For all other countries airmail rates are available upon request. Claims for missing issues must be made within six months of our publication (mailing) date. Please address all your requests regarding orders and subscription queries to: Elsevier Science B.V., Journal Department, P.O. Box 211, 1000 AE Amsterdam, Netherlands. Tel.: (+31-20) 485 3642; Fax: (+31-20) 485 3598. Customers in the USA and Canada wishing information on this and other Elsevier journals, please contact Journal Information Center, Elsevier Science Inc., 655 Avenue of the Americas, New York, NY 10010, USA, Tel. (+1-212) 633 3750, Telefax (+1-212) 633 3764.

**Abstracts/Contents Lists** published in Analytical Abstracts, Biochemical Abstracts, Biological Abstracts, Chemical Abstracts, Chemical Titles, Chromatography Abstracts, Current Awareness in Biological Sciences (CABS), Current Contents/Life Sciences, Current Contents/Physical, Chemical & Earth Sciences, Deep-Sea Research/Part B: Oceanographic Literature Review, Excerpta Medica, Index Medicus, Mass Spectrometry Bulletin, PASCAL-CNRS, Referativnyi Zhurnal, Research Alert and Science Citation Index.

**US Mailing Notice.** *Journal of Chromatography A* (ISSN 0021-9673) is published weekly (total 52 issues) by Elsevier Science B.V., (Sara Burgerhartstraat 25, P.O. Box 211, 1000 AE Amsterdam, Netherlands). Annual subscription price in the USA US\$ 6863.00 (US\$ price valid in North, Central and South America only) including air speed delivery. Second class postage paid at Jamaica, NY 11431. **USA POSTMASTERS:** Send address changes to *Journal of Chromatography A*, Publications Expediting, Inc., 200 Meacham Avenue, Elmont, NY 11003. Airfreight and mailing in the USA by Publications Expediting.

**Advertisements.** The Editors of the journal accept no responsibility for the contents of the advertisements. Advertisement rates are available on request. Advertising orders and enquiries may be sent to *International:* Elsevier Science, Advertising Department, The Boulevard, Langford Lane, Kidlington, Oxford, OX5 1GB, UK; Tel: (+44) (0) 1865 843565; Fax: (+44) (0) 1865 843952. *USA and Canada:* Weston Media Associates, Dan Lipner, P.O. Box 1110, Greens Farms, CT 06436-1110, USA; Tel: (203) 261 2500; Fax: (203) 261 0101. *Japan:* Elsevier Science Japan, Ms Noriko Kodama, 20-12 Yushima, 3 chome, Bunkyo-Ku, Tokyo 113, Japan; Tel: (+81) 3 3836 0810; Fax: (+81) 3 3839 4344.

**See inside back cover** for Publication Schedule and Information for Authors.

© 1995 ELSEVIER SCIENCE B.V. All rights reserved.

0021-9673/95/\$09.50

No part of this publication may be reproduced, stored in a retrieval system or transmitted in any form or by any means, electronic, mechanical, photocopying, recording or otherwise, without the prior written permission of the publisher, Elsevier Science B.V., Copyright and Permissions Department, P.O. Box 521, 1000 AM Amsterdam, Netherlands.

Upon acceptance of an article by the journal, the author(s) will be asked to transfer copyright of the article to the publisher. The transfer will ensure the widest possible dissemination of information.

**Special regulations for readers in the USA** – This journal has been registered with the Copyright Clearance Center, Inc. Consent is given for copying of articles for personal or internal use, or for the personal use of specific clients. This consent is given on the condition that the copier pays through the Center the per-copy fee stated in the code on the first page of each article for copying beyond that permitted by Sections 107 or 108 of the US Copyright Law. The appropriate fee should be forwarded with a copy of the first page of the article to the Copyright Clearance Center, Inc., 222 Rosewood Drive, Danvers, MA 01923, USA. If no code appears in an article, the author has not given broad consent to copy and permission to copy must be obtained directly from the author. The fee indicated on the first page of an article in this issue will apply retroactively to all articles published in the journal, regardless of the year of publication. This consent does not extend to other kinds of copying, such as for general distribution, resale, advertising and promotion purposes, or for creating new collective works. Special written permission must be obtained from the publisher for such copying.

No responsibility is assumed by the Publisher for any injury and/or damage to persons or property as a matter of products liability, negligence or otherwise, or from any use or operation of any methods, products, instructions or ideas contained in the materials herein. Because of rapid advances in the medical sciences, the Publisher recommends that independent verification of diagnoses and drug dosages should be made.

Although all advertising material is expected to conform to ethical (medical) standards, inclusion in this publication does not constitute a guarantee or endorsement of the quality or value of such product or of the claims made of it by its manufacturer.

☉ The paper used in this publication meets the requirements of ANSI/NISO Z39.48-1992 (Permanence of Paper).

Printed in the Netherlands



## CONTENTS

(Abstracts/Contents Lists published in *Analytical Abstracts*, *Biochemical Abstracts*, *Biological Abstracts*, *Chemical Abstracts*, *Chemical Titles*, *Chromatography Abstracts*, *Current Awareness in Biological Sciences (CABS)*, *Current Contents/Life Sciences*, *Current Contents/Physical, Chemical & Earth Sciences*, *Deep-Sea Research/Part B: Oceanographic Literature Review*, *Excerpta Medica*, *Index Medicus*, *Mass Spectrometry Bulletin*, *PASCAL-CNRS*, *Referativnyi Zhurnal*, *Research Alert* and *Science Citation Index*)

## REGULAR PAPERS

*Column Liquid Chromatography*

- Acenaphthene fluorescence derivatisation reagents for use in high-performance liquid chromatography  
by L.A. Gifford, F.T.K. Owusu-Daaku and A.J. Stevens (Manchester, UK) (Received 29 May 1995) . . . . . 201
- Separation of priority pollutant phenols on chemically modified poly(styrene-divinylbenzene) resins by high-performance liquid chromatography  
by C.W. Klampfl and E. Spanos (Linz, Austria) (Received 1 June 1995) . . . . . 213
- High-performance liquid chromatographic method for the separation of isomers of *cis*- and *trans*-2-amino-cyclopentane-1-carboxylic acid  
by A. Péter and F. Fülöp (Szeged, Hungary) (Received 23 May 1995) . . . . . 219
- Investigation of crudes of synthesis of neuropeptide Y by high-performance liquid chromatography–electrospray mass spectrometry  
by A. Casazza, O. Curcuruto and M. Hamdan (Verona, Italy) and A. Bisello and E. Peggion (Padova, Italy) (Received 19 May 1995) . . . . . 227
- Quantitation of monoclonal antibodies by perfusion chromatography–immunodetection  
by L. Gadowski and A. Abdul-Wajid (Edmonton, Canada) (Received 23 May 1995) . . . . . 241
- Unusual chromatographic behaviour and one-step purification of a novel membrane proteinase from *Bacillus cereus*  
by B. Fricke, T. Buchmann and S. Friebe (Halle, Germany) (Received 29 May 1995) . . . . . 247

*Field-Flow Fractionation*

- Experimental study on the separation of silica gel supports by gravitational field-flow fractionation. II. Sample preparation, stop-flow procedure and overloading effect  
by J. Pazourek and J. Chmelík (Brno, Czech Republic) (Received 19 May 1995) . . . . . 259

*Gas Chromatography*

- Derivation of solubility parameters of chlorinated dibenzofurans and dibenzo[*p*]dioxins from gas chromatographic retention parameters via SOFA  
by H.A.J. Govers, F.W.M. van der Wielen and K. Olie (Amsterdam, Netherlands) (Received 24 May 1995) . . . . . 267
- Repetitive liquid injection system for inverse gas chromatography  
by S. Panda, Q. Bu, K.S. Yun and J.F. Parcher (University, MS, USA) (Received 1 June 1995) . . . . . 279
- Assessment of some possibilities for improving the performance of gas chromatographic thermal conductivity detectors with hot-wire sensitive elements  
by I.P. Mitov and L.A. Petrov (Sofia, Bulgaria) (Received 18 April 1995) . . . . . 287
- Thermodynamic consideration of the retention mechanism in a poly(perfluoroalkyl ether) gas chromatographic stationary phase used in packed columns  
by R.C. Castells, L.M. Romero and A.M. Nardillo (La Plata, Argentina) (Received 19 May 1995) . . . . . 299
- Glycerol as a new dissolution medium for  $\alpha$ -,  $\beta$ - and  $\gamma$ -cyclodextrins for preparing stereoselective stationary phases for gas–liquid chromatography  
by D. Sybilska, M. Asztemborska, D.R. Zook and J. Goronowicz (Warsaw, Poland) (Received 19 May 1995) . . . . . 309
- Gas chromatographic–mass spectrometric characterization of some fatty acids from white and interior spruce  
by D.-J. Carrier, J.E. Cunningham, L.R. Hogge, D.C. Taylor and D.I. Dunstan (Saskatoon, Canada) (Received 19 May 1995) . . . . . 317

Headspace sampling and gas chromatographic–mass spectrometric determination of amphetamine and methamphetamine in betel by S.-M. Wang and Y.-C. Ling (Hsinchu, Taiwan) and L.-C. Tsai and Y.-S. Giang (Taoyuan, Taiwan) (Received 23 May 1995)	325
---	-----

*Supercritical Fluid Chromatography*

Determination of cholesterol in milk fat by supercritical fluid chromatography by W. Huber, A. Molero, C. Pereyra and E. Martínez de la Ossa (Cádiz, Spain) (Received 18 May 1995)	333
---	-----

*Electrophoresis*

Enantiomeric resolution using the macrocyclic antibiotics rifamycin B and rifamycin SV as chiral selectors for capillary electrophoresis by T.J. Ward, C. Dann III and A. Blaylock (Jackson, MS, USA) (Received 10 May 1995)	337
Optimization of the separation of $\beta$ -agonists by capillary electrophoresis on untreated and C <sub>18</sub> bonded silica capillaries by S. Chevolleau and J. Tulliez (Toulouse, France) (Received 23 May 1995)	345
Determination of aminopyrine and its metabolite by capillary electrophoresis–electrochemical detection by W. Zhou, J. Liu and E. Wang (Changchun, China) (Received 18 May 1995)	355

SHORT COMMUNICATIONS

*Column Liquid Chromatography*

GABA-B agonists: enantiomeric resolution of 4-amino-3- (5-chlorothien-2-yl)butyric acid and analogues on chiral crown ether stationary phase by C. Vaccher, P. Berthelot and M. Debaert (Lille, France) (Received 23 May 1995)	361
---	-----

*Gas Chromatography*

Nickel(II) chelates of some tetradentate Schiff bases as stationary phases for gas chromatography by M.Y. Khuhawar, A.A. Memon and M.I. Bhanger (Sindh, Pakistan) (Received 12 May 1995)	366
---	-----

*Planar Chromatography*

Modified and convenient preparation of silica impregnated with silver nitrate and its application to the separation of steroids and triterpenes by T.-S. Li, J.-T. Li and H.-Z. Li (Baoding, China) (Received 23 May 1995)	372
---	-----

*Electrophoresis*

Determination of the petroleum tracers nitrate and thiocyanate in subterranean waters by capillary ion electrophoresis by L. Song, Q. Ou and W. Yu (Lanzhou, China) and L. Fang and Y. Jin (Shanshan, China) (Received 9 May 1995)	376
---	-----

BOOK REVIEWS

Techniques and Practice of Chromatography (edited by R.P.W. Scott), reviewed by J. Janák (Brno, Czech Republic)	385
Ion Chromatography (edited by J. Weiss), reviewed by P.R. Haddad (Hobart, Australia)	387

AUTHOR INDEX	389
--------------	-----

NEWS SECTION	393
--------------	-----



















# Acenaphthene fluorescence derivatisation reagents for use in high-performance liquid chromatography

L.A. Gifford\*, F.T.K. Owusu-Daaku, A.J. Stevens

*Department of Pharmacy, University of Manchester, Oxford Road, Manchester M13 9PL, UK*

First received 3 March 1995; revised manuscript received 29 May 1995; accepted 29 May 1995

## Abstract

Acenaphthene-5-sulphonyl chloride (AcNSCl), acenaphthene-5-sulphonyl hydrazine (AcNH) and 5-bromoacetyl acenaphthene (AcBr) were synthesised and applied to the analysis of primary and secondary amines, carbonyl compounds and carboxylic acids, respectively. AcNSCl was used in the HPLC assay of 20 amino acids and 5 peptides. The AcNSCl derivatives were found to be 10–25 times more fluorescent than their corresponding dansyl derivatives; between-run analyses gave coefficients of variation of 2.8–7.3%. AcNSCl has a pseudo-first-order rate constant 1.5 times greater than dansyl chloride for the reaction with amino acids. AcNH derivatives of the ketosteroids were 10 times more fluorescent than the corresponding dansyl derivatives. Fluocinolone cream was analysed with this reagent. AcBr derivatives of carboxylic acids gave a 15–24-fold increase in sensitivity in comparison with the corresponding naphthacyl bromide derivatives. This reagent was used in pharmacokinetic studies of ibuprofen.

## 1. Introduction

Dansyl chloride (DNSCl) was introduced by Weber [1] as a highly fluorescent label for the analysis of proteins and has subsequently become one of the most sensitive agents for pre-column derivatisation of amino acids prior to analysis by high-performance liquid chromatography (HPLC) [2]. It is reactive towards a variety of bases including primary and secondary amino groups. Chayen et al. [3] employed dansyl hydrazine for the determination of trace levels of carbonyl compounds and Distler [4] used naphthacyl bromide for the determination of carboxylic acids. The fluorescent characteristics

of each of these reagents is attributable to the substituted naphthalene nucleus. The structurally similar acenaphthene moiety is reported as having a fluorescence yield 2.6 times greater than that of naphthalene [5]. This observation prompted this investigation into the synthesis and application of acenaphthene-based derivatisation agents in the HPLC analysis of trace amounts of biologically important molecules.

The structural identification of naphthalene sulphonates was subject to confusion in the scientific literature and in some reports the 3-substituted product was thought to have been produced whilst in others the 5-substituted one was reported as being the product [6]. Consequently, a spectroscopic study was performed on the acenaphthene derivatives synthesised here in order to provide the correct structural assign-

\* Corresponding author.

ments. The aim of the present work is to compare the properties and sensitivity of the acenaphthene derivatising agents with the corresponding dansyl and naphthacyl reagents. Analytical applications of the derivatives are also discussed.

## 2. Experimental

### 2.1. Chemicals

Acenaphthene, aluminium chloride, 1,2-dichloroethane, bromoacetylchloride, triethylamine, sodium carbonate and 2-naphthacyl bromide were obtained from Sigma Chemicals. Ibuprofen and flurbiprofen were gift samples obtained from Boots Chemical. Hydrochloric acid and acetonitrile (Hypersolv) were obtained from BDH Chemicals. Polygram precoated silica gel plastic sheets containing a fluorescent indicator were obtained from Camlab. Silica gel 0.125–0.250 mm, 60–120 mesh size was obtained from Fisons Chemicals, 1.5-ml amber-coloured polypropylene vials were obtained from Eppendorf.

### 2.2. Instrumentation

For isocratic separations a Kontron Analytical LC 414 pump was used in conjunction with a Rheodyne 7125 syringe loading sample injector.

Gradient elution chromatography was performed using a Hewlett-Packard 1090 M liquid chromatograph. A Perkin-Elmer LS 5 luminescence spectrometer with flow cell was used in detecting the fluorescent derivatives. For data analysis peak integration was performed using a Trilab 2000 from Trivector Scientific.

Mass spectroscopy was carried out on a DH88 Mass Spectroscopy Data System, NMR analysis was carried out on a Joel JNM EX 270 spectrophotometer and IR data was obtained on a Pye Unicam SP 100 spectrophotometer.

Class A glassware from Gallenkamp and Beatson Clark was used.

### 2.3. Synthesis of reagents

The synthetic route for the preparation of the derivatives is shown in Fig. 1. Acenaphthene (1) was bromoacetylated via a Friedel–Crafts reaction to yield 5-bromoacetyl acenaphthene (5) (AcBr). Acenaphthene-5-sulphonic acid (2) sodium salt was synthesised and then reacted with phosphorus pentachloride to yield acenaphthene-5-sulphonyl chloride (3) (AcNSCl). Further reaction of this product with hydrazine hydrate yielded the acenaphthene-5-hydrazide (4).

### 2.4. Acenaphthene-5-sulphonic acid sodium salt

An amount of 20 g acenaphthene was dissolved in 100 g of nitrobenzene and the solution

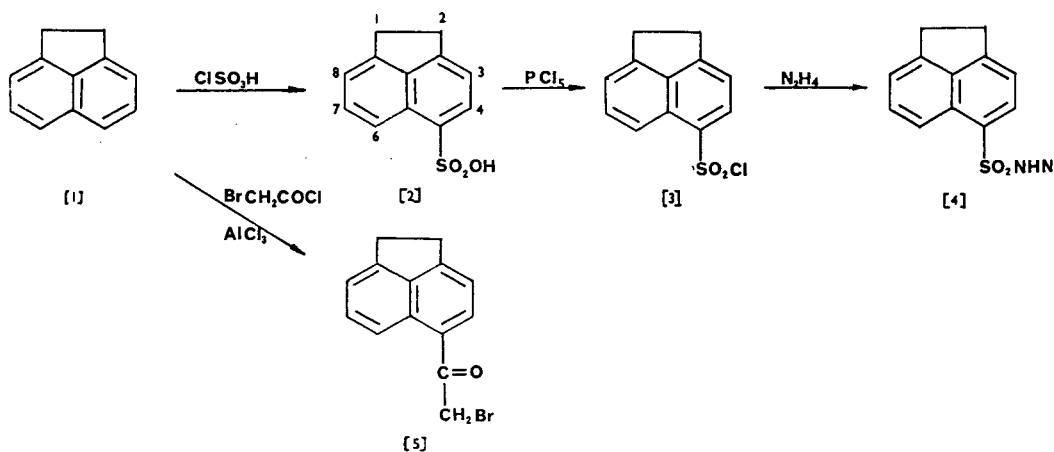


Fig. 1. Synthetic route for the preparation of AcNSO<sub>3</sub>H [2], AcNSCl [3], AcNH [4] and AcBr [5].

cooled to 0°C. Then 9 ml of chlorosulphonic acid was added dropwise with constant stirring and with the temperature maintained below 5°C during the addition. The temperature of the mixture was then allowed to rise to 20°C over half an hour. After diluting with 500 ml of water, the aqueous layer was separated from the nitrobenzene layer. Solid sodium carbonate was added to neutralise the aqueous solution. The neutralised solution was treated hot with sodium chloride until precipitation was observed. The mixture was then cooled in an ice bath for 1 h and then filtered. Traces of nitrobenzene and water were removed by heating at 140°C for 36–48 h. Obtained was 25 g, yield 76%, of a pale yellow solid, m.p. >300°C, m.p. anilide derivative 178°C.

NMR:  $\delta$ /ppm 2.95 (d, 4H,  $2 \times \text{CH}_2$ , H-1, H-2), 7.15 (d, 1H, Ar, H-3), 7.83 (d, 1H, Ar, H-4), 8.00 (d, 1H, Ar-6), 7.48 (t, 1H, Ar-7), 7.02 (d, 1H, Ar-8).

#### 2.5. Acenaphthene-5-sulphonyl chloride

An amount of 10 g of  $\text{AcNSO}_3\text{H}$  sodium salt was ground in a mortar with 3.5 g of phosphorus pentachloride for 3 min. Following the evolution of hydrogen chloride, cracked ice and water were added and the mixture vigorously stirred to wash out phosphoric acid, the presence of which would lead to decomposition of the product. The product was then extracted into 100 ml of ethyl acetate, washed with 5% sodium bicarbonate solution and then with distilled water until neutral. After drying over anhydrous sodium sulphate and evaporation of the solvent by a gentle stream of nitrogen, crude  $\text{AcNSCl}$  crystals were obtained. An amount of 200 mg of the crude product, dissolved in 2–3 ml of toluene, was applied to a  $2 \times 30$  cm column of silica gel H, prepared by filling a suitable glass column with a slurry of silica gel in toluene (25 g in 100 ml). Elution with toluene separated  $\text{AcNSCl}$  well ahead of its impurities as the first yellow band to be eluted. On crystallisation 150 mg of yellow crystals were obtained, yield 11.5%, m.p. 98–101°C. Elemental analysis: Calculated for  $\text{C}_{12}\text{H}_9\text{O}_2\text{ClS}$ : C 57.14%, H 3.57%, S 12.69%, Cl 13.88%; found: C 57.30%, H 3.80%, S 12.65%,

Cl 13.83%. NMR:  $\delta$ /ppm 3.46 (s, 4H,  $2 \times \text{CH}_2$ , H-1, H-2), 7.35 (d, 1H, Ar, H-3), 7.48 (d, 1H, Ar, H-8), 7.73 (t, 1H, Ar, H-7), 8.25 (d, 1H, AR, H-4), 8.35 (d, 1H, AR, H-6). Mass spectrum:  $m/z$  252 [ $\text{M}^+$ ], 153 (base peak).

#### 2.6. Acenaphthene-5-sulphonyl hydrazine (AcNH)

An amount of 1 g of  $\text{AcNSCl}$  was dissolved in 3 ml of tetrahydrofuran (THF) in a three-necked pear-shaped flask fitted with a Pasteur pipette, thermometer and dropping funnel. The mixture was cooled in an ice bath to 10°C while stirring and bubbling a gentle stream of nitrogen through it. Then 0.4 ml of an aqueous solution of 85% hydrazine hydrate was added dropwise through the dropping funnel while maintaining the temperature between 10–15°C. Stirring was continued for a further 15 min. The lower aqueous layer was drawn off and the upper THF layer was filtered through a bed of celite filter aid. The celite was washed with 1 ml THF to remove any adsorbed hydrazide. Two 10-ml portions of water were added to the THF layer while stirring vigorously. A buff flocculent precipitate resulted and the reaction mixture was cooled in a refrigerator for 1 h to complete the precipitation. The product was filtered through a Buchner funnel and washed several times with water and dried. It was then recrystallised from ethanol. Obtained was 0.95 g, 95% yield, m.p. 132–134°C. Elemental analysis: Calculated for  $\text{C}_{12}\text{H}_{12}\text{N}_2\text{O}_2\text{S}$ : C 58.06%, H 4.83%, N 11.29%, S 12.90%; found: C 58.6%, H 5.00%, N 11.31%, S 12.80%. NMR:  $\delta$ /ppm 3.23 (s, 2H,  $\text{NH}_2$ ), 3.45 (s, 4H,  $2 \times \text{CH}_2$ , H-1, H-2), 5.72 (s, 1H, NH), 7.35 (d, 1H, Ar, H-3), 7.43 (d, 1H, Ar, H-8), 7.62 (t, 1H, Ar, H-7), 8.18 (s, 1H, Ar, H-4), 8.22 (d, 1H, Ar, H-6). Mass spectrum:  $m/z$  248 [ $\text{M}^+$ ], 153 (base peak). IR: 1140, 1323, 1610, 3330  $\text{cm}^{-1}$ .

#### 2.7. 5-Bromoacetyl acenaphthene

A 1-l three-necked flask was fitted with a mechanical stirrer and a dropping funnel. An



amount of 43 g acenaphthene was dissolved in 200 ml dichloroethane and 43 g bromoacetyl chloride was added to the homogenous solution. The mixture was cooled to  $-5^{\circ}\text{C}$  in a freezing mixture of ice and salt. Then 38 g of aluminium chloride was added in small portions during 90 min with vigorous stirring, the temperature not being allowed to rise above  $3^{\circ}\text{C}$ . The stirrer was removed and the central neck stoppered. The side necks of the flask were respectively fitted with a capillary bleed tube and a vacuum line. The pressure was reduced for 30 min and an excess of crushed ice was added to separate the dichloroethane layer. The latter was washed successively with two 100-ml portions of dilute hydrochloric acid and 100 ml of 5% sodium carbonate solution. The dichloroethane layer was dried over magnesium sulphate, filtered and then distilled off under reduced pressure. The oily liquid obtained was transferred to a porcelain basin. After it had solidified, the top liquid layer was decanted and the remaining liquid blotted off with filter paper. The brownish coloured residue (yield 75%) contained about 50% unreacted acenaphthene as determined from the NMR spectrum. The residue was then purified by passing it through a  $2 \times 30$  cm column of silica gel, 60–120 mesh, and eluting with toluene. Fractions of the eluate were examined by performing TLC on silica gel sheets impregnated with fluorescent indicator using toluene as the partitioning solvent. Unreacted acenaphthene was thus found to elute from the column first, followed by the yellow AcBr fraction. On crystallisation the AcBr gave a yield of 40%, m.p.  $87\text{--}90^{\circ}\text{C}$ . Elemental analysis: Calculated for  $\text{C}_{14}\text{H}_{11}\text{OBr}$ : C 61.09%, H 4.00%, Br 29.09%; found: C 61.50%, H 4.05%, Br 29.3%. NMR  $^1\text{H}$ :  $\text{CDCl}_3/\text{TMS}$ ,  $\delta/\text{ppm}$ : 3.42 (s, 4H,  $2 \times \text{CH}_2$ , H-1, H-2), 4.57 (s, 2H,  $\text{CH}_2$ , H-2), 7.32 (d, 1H, Ar, H-3), 7.39 (d, 1H, Ar, H-8), 7.63 (t, 1H, Ar, H-7), 8.08 (d, 1H, Ar, H-4), 8.68 (d, 1H, Ar, H-6);  $^{13}\text{C}$ :  $\text{CDCl}_3/\text{TMS}$ ,  $\delta/\text{ppm}$ : 30.30, 30.64 (C-1 and C-2), 32.83 (C-2), 118.02 (C-3), 120.74 (C-8), 122.30 (C-6), 126.67, 129.76 (C-5 and C-5a), 130.93 (C-7), 133.01 (C-4), 139.78, 146.29, 154.47 (C-2a, C-2b and C-8a), 192.69 (C-1). Mass spectrum:  $m/z$  277

$[\text{M}^+]$ , 197 (base peak). IR (KBr) C=O:  $1685\text{ cm}^{-1}$ .

### 2.8. Derivatisation of amino acids with AcNSCl and DNSCl

Solutions of 1 ml containing 20  $\mu\text{mol}$  of a single individual amino acid were dispensed into separate 10-ml volumetric flasks, and a similar amount of alanine was added to each, to act as an internal standard. The flasks were made up to volume with 0.2 M sodium bicarbonate solution, pH 8.5. The resulting solution (A) was diluted 1:10 times to give solution (B). The (A) solutions were derivatised with DNSCl and the (B) solutions were derivatised with AcNSCl in the following manner. A 1-ml portion of the amino acid-alanine solution under study was pipetted into a 3-ml amber Eppendorf vial together with 1 ml of a 0.015% solution of the derivatising agent in dry acetone. After mixing the vial was capped tightly and maintained at  $47^{\circ}\text{C}$  for 30 min. The reaction was quenched by the addition of 200  $\mu\text{l}$  of 2% ethylamine and then allowed to reach room temperature. Separation of 20  $\mu\text{l}$  of the amino acid derivative solution was achieved using a Hypersil 5  $\mu\text{m}$ ,  $\text{C}_{18}$ ,  $250 \times 4.6$  mm I.D. column. A mobile-phase gradient was employed with 5% THF in 10 mM pH 4.2 acetate buffer (solvent A) and 10% THF in acetonitrile (solvent B). The gradient profile employed was 10% solvent B increasing to 40% solvent B over a 30 min period. This was maintained for a further 15 min and increased to 100% solvent B for 3 min. A flow-rate of 1 ml/min was maintained throughout. Reproducibility of these reaction conditions was determined by analysing a solution of valine containing 20  $\mu\text{mol}/\text{ml}$  to which had been added 20  $\mu\text{mol}$  alanine as internal standard. Within-run precision was determined by performing six analyses of a single sample in parallel with each other. Between-run precision was determined by performing the analysis of the same sample on six separate occasions. The fluorescent enhancement achieved with the AcNSCl reagent compared to the DNSCl reagent was determined from the ratio of the

chromatographic peak areas of the derivative peaks measured at their optimum fluorescence wavelengths and calculated for equivalent concentrations.

### 2.9. Peptide analysis with AcNSCl and DNSCl

Three peptides were investigated, Asp-Glu-Gly, Met-Leu-Phe and Val-Ala-Ala-Phe, at concentrations of 60  $\mu\text{g}/\text{ml}$  in water. The solutions were diluted by a factor of ten prior to analysis with AcNSCl.

#### *N-terminal analysis*

An amount of 100  $\mu\text{l}$  of the peptide solution under study was lyophilised by freeze drying and 50  $\mu\text{l}$  0.2 M sodium bicarbonate solution added. Then 50  $\mu\text{l}$  of a 0.5% solution of the derivatising agent in dry acetone was added and the mixture incubated at 47°C for 30 min. The reaction was quenched with 100  $\mu\text{l}$  of 2% ethylamine. The mixture was then lyophilised and hydrolysed with 100  $\mu\text{l}$  6 M HCl at 105°C for 16 h in a sealed glass vial. After further lyophilisation the residue was dissolved in 100  $\mu\text{l}$  of mobile phase prior to HPLC analysis as described for the analysis of amino acids.

#### *Amino acid composition*

An amount of 100  $\mu\text{l}$  of the peptide solution was lyophilised, 100  $\mu\text{l}$  6 M HCl was then added and the solution hydrolysed at 105°C for 16 h in a sealed glass vial. A 50- $\mu\text{l}$  portion of the hydrolysate was then lyophilised and dissolved in 15  $\mu\text{l}$  0.2 M sodium bicarbonate solution. Then 15  $\mu\text{l}$  of labelling agent was added and the solution incubated at 47°C for 30 min. The reaction was quenched with 100  $\mu\text{l}$  2% ethylamine and 20  $\mu\text{l}$  was subjected to HPLC analysis of constituent amino acids.

### 2.10. Derivatisation of 17-ketosteroids with AcNH and DNH

Solutions of progesterone (0.2 mg/ml) and TFA (2.5%) were prepared in toluene. AcNH or DNH (1 mg/ml) were prepared as solutions in ethanol–toluene (1:9, v/v). Of each of the ster-

oids 100  $\mu\text{l}$ , TFA and the labelling agent were placed in an amber-coloured vial and the solvent removed under vacuum at 60°C. The residue was reconstituted in 100  $\mu\text{l}$  acetonitrile and 20  $\mu\text{l}$  of the resulting solution analysed by gradient elution chromatography using a Hypersil C<sub>18</sub>, 5  $\mu\text{m}$ , 250  $\times$  4.6 mm I.D. column. The flow-rate was maintained at 2 ml/min using a binary solvent mixture. Solvent A was 0.5 g/l Tris buffer, pH 7, and solvent B was 90% acetonitrile in water. A linear gradient of 50% solvent A to 70% solvent B over 20 min was used for DNH derivatives whilst the same gradient over a 10-min period was used for AcNH derivatives. To determine the effect of AcNH concentration on derivative formation, solutions of progesterone were derivatised under identical conditions except that the volume of AcNH reagent utilised was varied from 10 to 100  $\mu\text{l}$ .

Fluocinolone acetonide cream was analysed by normal-phase HPLC following extraction and derivatisation. An amount of 11.25 g of Synalar Cream was transferred to a separating funnel with the aid of 100 ml of cyclohexane. Then 50 ml of methanol was added and the mixture shaken vigorously for 3 min. After standing for 15 min the lower layer was transferred to a second separating funnel containing 140 ml of distilled water and 100 ml of chloroform. The separating funnel was shaken for 3 min, the phases allowed to separate and a 3-ml portion of the chloroform placed in a screw-capped test tube containing 0.3 ml of hydrocortisone internal standard solution, 0.028% w/v in ethanol. Standard solutions of fluocinolone acetonide were prepared to cover the concentration range 0.02–1.00 mg/ml and 1 ml of each was dispensed into a screw-capped test tube containing 0.3 ml of internal standard solution. The solutions were then reacted with 1 ml of AcNH, 3 mg/ml, and derivatised following the procedure described by Chayen et al. [3] for the derivatisation of carbonyl compounds with DNH. The dried extracts were reconstituted in 200  $\mu\text{l}$  of mobile phase (dioxane–toluene 10:90) prior to separation on a 500  $\times$  1 mm I.D., 10  $\mu\text{m}$  silica microbore column. Excitation and emission wavelengths were as given in Table 1.

Table 1  
Fluorescence characteristics of acenaphthene derivatives

	(DNS) Dansyl derivative		AcNSCl derivative		Fluorescence enhancement (AcN/DNS)
	$\lambda_{ex}$ (nm)	$\lambda_r$ (nm)	$\lambda_{ex}$ (nm)	$\lambda_r$ (nm)	
Alanine					27
Arginine					25
Asparagine					24
Aspartic acid					35
Cysteine					25
Glutamic acid					30
Glutamine					30
Glycine					30
Histidine					25
Isoleucine	250	470	230 (300)	420	24
Leucine					26
Lysine					20
Methionine					25
Phenylalanine					22
Proline					20
Serine					27
Threonine					37
Tryptophan					25
Tyrosine					25
Valine					27
	DNH derivative		AcNH derivative		
Progesterone	340	520	230 (300)	350	10
Fluocinolone acetonide					10
	Naphthacyl derivative		AcBr derivative		
Propionic acid					25
Hexanoic acid	22				
Ibuprofen	250 (290)	410	250 (290)	450	16
Flurbiprofen					15

### 2.11. Derivatisation of carboxylic acids with AcBr

A modification of the method for the analysis of short-chain fatty acids using naphthacyl bromide (NBr) was followed [4]. All solutions were prepared in acetonitrile. An amount of 100  $\mu$ l of 0.04 M AcBr (or NBr) was added to 100  $\mu$ l 0.01 M carboxylic acid sample in a 1.5-ml amber-coloured vial. Then 100  $\mu$ l 3% triethylamine and 200  $\mu$ l acetonitrile were added and the contents of the vial thoroughly mixed and heated in a water bath at 75°C for 5 min. On cooling, 500  $\mu$ l

acetonitrile was added to give a total volume of 1 ml. When using AcBr as derivatising agent it was necessary to carry out a further dilution of 1 in 15 of the AcBr derivatives in order to be able to evaluate off-range peaks. Of the resulting solution 20  $\mu$ l was subjected to HPLC analysis using a Hypersil 5  $\mu$ m, C<sub>18</sub>, 250  $\times$  4.6 mm I.D. column and a mobile phase of 90% acetonitrile in water at a flow-rate of 1 ml/min. The effect of the molar concentration of the labelling agent on fluorescence intensity was determined over a four-fold concentration range. Excitation and emission wavelengths of the carboxylic acid



derivatives are shown in Table 1. Reproducibility of the derivatisation reaction was determined by analysing 100  $\mu\text{l}$  of 0.01 M ibuprofen containing an equivalent amount of flurbiprofen as internal standard. Within-run precision was determined by performing six analyses of a single sample in parallel with each other. Between-run precision was determined by performing the analysis of the same sample on six separate occasions.

### 2.12. Analysis of ibuprofen in rat plasma

Serial samples of plasma were obtained from rats previously administered with 50 mg/kg ibuprofen at a localised site of inflammation. An amount of 50  $\mu\text{l}$  of flurbiprofen internal standard (2  $\mu\text{g}/\text{ml}$ ) was added to 100  $\mu\text{l}$  of plasma sample. Then 25  $\mu\text{l}$  of 2 M HCl was added and the mixture vortexed for 15 s. Then 2 ml of iso-octane–2-propanol (85:15) was added and the ibuprofen extracted by rotary mixing for 5 min. The mixture was centrifuged at 3000 rpm for 10 min, after which time the upper organic layer was removed by pipette and evaporated under a stream of nitrogen at 45°C. Amounts of 25  $\mu\text{l}$  of AcBr reagent (5 mg/ml in acetonitrile) and 10  $\mu\text{l}$  3% triethylamine catalyst were added to the residue and then vortex mixed for 30 s. The mixture was transferred to an amber-coloured vial and incubated at 75°C for 5 min. The solvent was evaporated under vacuum and the residue reconstituted in 25  $\mu\text{l}$  acetonitrile prior to HPLC analysis using the method for carboxylic acid analysis previously described. Plasma samples from three different rats were collected over a 7 h period and the ibuprofen concentration determined by comparison with a calibration curve covering the concentration range 0–80  $\mu\text{g}/\text{ml}$ .

## 3. Results and discussion

### 3.1. Synthesis of 5-substituted acenaphthenes

Aromatic sulphonation of acenaphthene proceeds via an electrophilic substitution mechanism with the production of a mixture of 3-, 5-

and 3,5-substituted sulphonic acids [6]. Under the reaction conditions employed the 5-substituted sulphonic acid was found to be the major product formed. This was confirmed by  $^1\text{H}$  NMR spectroscopy and by confirmatory evidence of the anilide melting point [7]. AcNSCl and AcNH were prepared using the AcNSO<sub>3</sub>H and the syntheses were confirmed by  $^1\text{H}$  NMR and MS. Friedel–Crafts acetylations of acenaphthene have been reported to give both 5-acetyladenaphthene and 3-acetyladenaphthene [8], the proportion of the 5-isomer being predominant (98%) when the reaction is carried out in dichloroethane. The identity of the product formed in this study was confirmed as being 5-bromoacetyl acenaphthene by  $^1\text{H}$  and  $^{13}\text{C}$  NMR.

### 3.2. Fluorescence characteristics of acenaphthene and dansyl derivatives

The fluorescence excitation and emission wavelengths for the AcNSCl and DNSCl derivatives, observed in the solvent systems employed for chromatographic analysis, together with the ratio of the fluorescence intensities (AcNS/DNS) are shown in Table 1. As predicted from the relative quantum yields of acenaphthene and naphthalene, the fluorescence intensities of the acenaphthene derivatives are greater than those of the corresponding dansyl derivatives. The fluorescence enhancement observed in the amino acids when derivatised with AcNSCl is 20–37 times greater than that observed when derivatised with DNSCl. The maximum excitation and emission wavelengths are shifted to shorter wavelengths in the acenaphthene derivatives. The fluorescence intensity is a function of both the quantum yield of the parent fluorophore and the solvent composition. The fluorescence characteristics of solutions of DNSCl derivatives are dependent on the solvent being used [9]. With increasing dielectric constant of the solvent the emission wavelength is shifted to longer wavelengths and generally the quantum yield decreases. A similar effect is observed for the AcNSCl derivatives. Since the separation of amino acids is best performed using a gradient

elution system in which the dielectric constant of the mobile phase decreases with increased elution time, the fluorescence intensity of the derivatives is expected to increase at longer retention times. This effect offsets the slight loss in sensitivity expected due to the band spreading of late eluting components.

Fluorescence intensity as a function of pH was found to be constant over the pH range 1–14 for  $5 \cdot 10^{-5}$  M AcNSO<sub>3</sub>H in aqueous buffer solutions. Fig. 2 demonstrates the stability of the fluorophore to changes in pH. Protonation of the dimethylamino function at low pH reduces the fluorescent intensity of the DNSCI derivatives to that comparable with naphthalene. Due to the absence of the dimethylamino group in acenaphthene this effect is not encountered in the

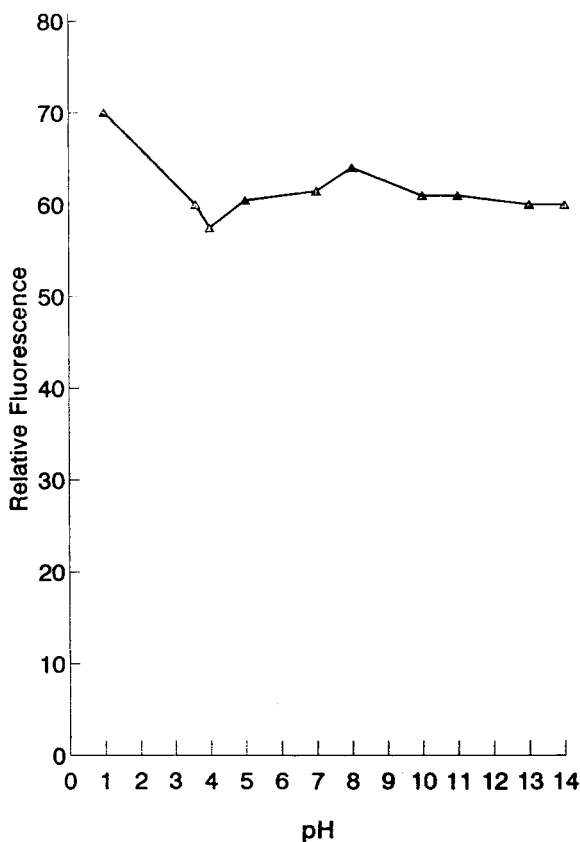


Fig. 2. Fluorescence emission of acenaphthene sulphonic acid versus pH.

AcNSCI derivatives. In strongly alkaline solution the amido group of primary-amine DNSCI derivatives ionises and causes a hypsochromic shift in the absorption maxima and of the emission maxima by about 10 nm [10]. This is also likely to occur for the AcNSCI derivatives; however, since high pHs are not normally employed for chromatographic separations, the AcNSCI derivatives are acceptable as being insensitive to pH change for practical purposes.

### 3.3. Rate of derivatisation reaction

The reaction between DNSCI or AcNSCI and an amino acid is bimolecular and the reaction appears second-order overall. However, if the concentration of the derivatising agent is in large excess, the reaction will become pseudo-first-order and the rate will depend upon the concentration of the amino acid A as described by the equation:

$$\ln[A] = -kt + \ln[A_0]$$

where  $[A]$  is the concentration of amino acid at time  $t$  and  $[A_0]$  the initial concentration of amino acid at time  $t_0$ . Fig. 3 shows the rate of formation of AcNS-valine and DNS-valine. The first-order rate constants being  $0.298$  and  $0.18 \text{ min}^{-1}$ , respectively. Under these reaction conditions AcNSCI reacts 1.5 times faster than DNSCI.

### 3.4. Reproducibility and recovery

In a study of the dansylation reaction Tapuhi et al. [11] showed that the addition of a primary amine to the dansylation reaction mixture after 35 min quenches the reaction and eliminates the possibility of side reactions occurring and thus enhancing reproducibility. The results from reproducibility studies using acenaphthene and dansyl reagents with the amino acid valine and the arylpropionic acid ibuprofen are shown in Table 2. In both cases the acenaphthene derivatives demonstrated a slight improvement in the precision of the determinations compared with the dansyl derivatisation. For the analysis of

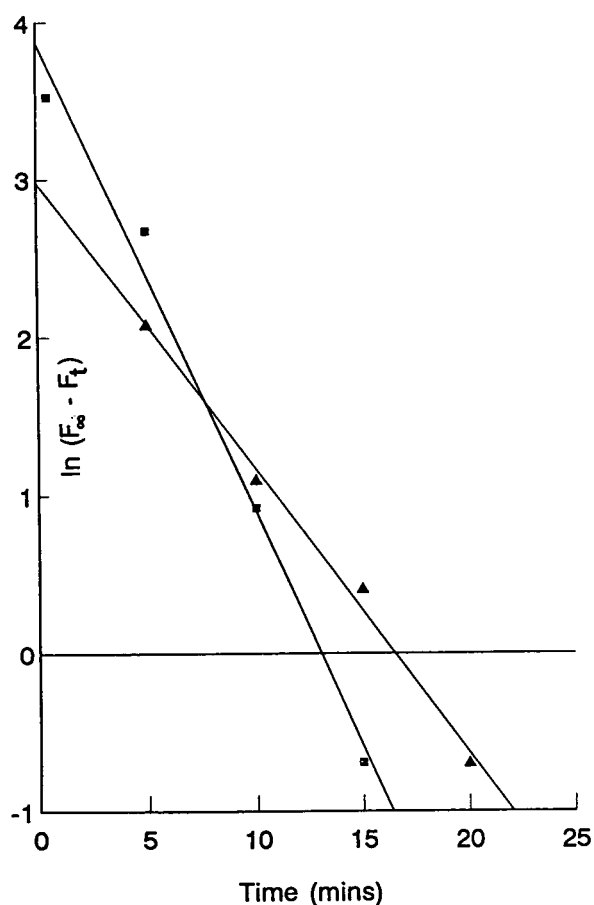


Fig. 3. Rates of formation of AcNS-valine (■) and DNS-valine (▲).

valine with AcNSCl linearity was observed over the concentration range 0–200 ng/ml.

Table 3 shows recoveries for assays performed in triplicate using each of the newly synthesised

acenaphthene derivatives. In each case the amount of analyte recovered was within 2% of the amount of analyte added. These results demonstrate an acceptable level of precision and accuracy for the derivatisation procedures using these derivatisation reagents.

### 3.5. Amino acid and peptide analysis

Fig. 4 shows the chromatographic separation of a mixture of nine amino acids together with the chromatogram for the blank. After the reagent hydrolysis product has eluted from the column at 5 min the baseline is clear of interference and is ideally suited to the analysis of amino acid mixtures. Relative to the corresponding DNSCl derivatives the AcNSCl derivatives have retention times which are approximately 1.2 times longer due to the greater hydrophobicity of the acenaphthene nucleus.

Five peptides were hydrolysed according to the method described in the Experimental section and the resulting solutions derivatised with AcNSCl and DNSCl. The peptides studied were Asp-Glu-Gly, Met-Leu-Phe, Val-Ala-Ala-Phe, Val-Gly-Asp-Glu and Val-Gly-Ser-Glu. In all cases the constituent amino acids were identified from the chromatograms obtained using both derivatising reagents. N-terminal analysis was performed by derivatising the peptides prior to hydrolysis, again the terminal amino acids were identified in each case from the chromatograph. Fig. 5 demonstrates the analysis of Val-Gly-Ser-Glu by this method. Val-AcNS was found to give a 100% recovery when subjected to the acid hydrolysis procedure, indicating that the AcNSCl

Table 2  
Reproducibility studies of acenaphthene derivatives

	Amount injected on-column (pg)	Within-run precision (C.V.%)	Between-run precision (C.V.%)
AcNS-valine	10.6	1.48	4.37
DNS-valine	106	2.33	5.13
AcBr-ibuprofen	9.7	0.62	2.90
NBr-ibuprofen	97	3.25	2.00

Using peak-height ratios,  $n = 6$ .

Table 3  
Recoveries of analytes following derivatisation

Sample	Derivatising agent	Amount added	Amount found	Recovery <sup>a</sup> (%)
Valine in buffer (ng/ml)	AcNSCl	100	104	104.0 <i>n</i> = 6
Fluocinolone in cream (mg/100 g)	AcNH	25	25.3	101.5 <i>n</i> = 3
Ibuprofen in plasma (ng/ml)	AcBr	100	102	102.0 <i>n</i> = 6

<sup>a</sup> *n* = number of samples analysed.

amino acid derivatives are stable to hydrolysis and could be used in qualitative amino acid analysis of protein hydrolysates. It should be noted that Gray [12] found that DNS-serine and

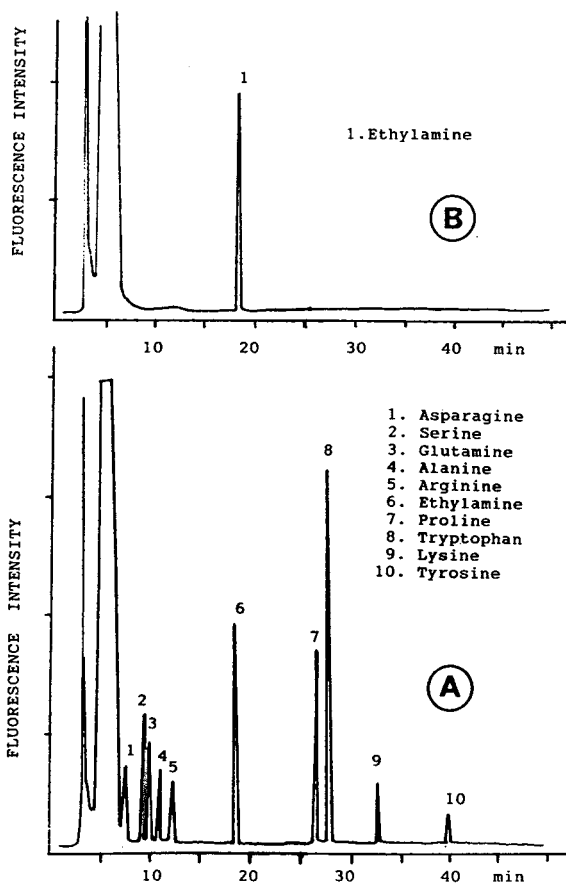


Fig. 4. (A) Chromatogram of a mixture of 1.25 nM of each of nine AcNS-amino acids. (B) Reagent blank.

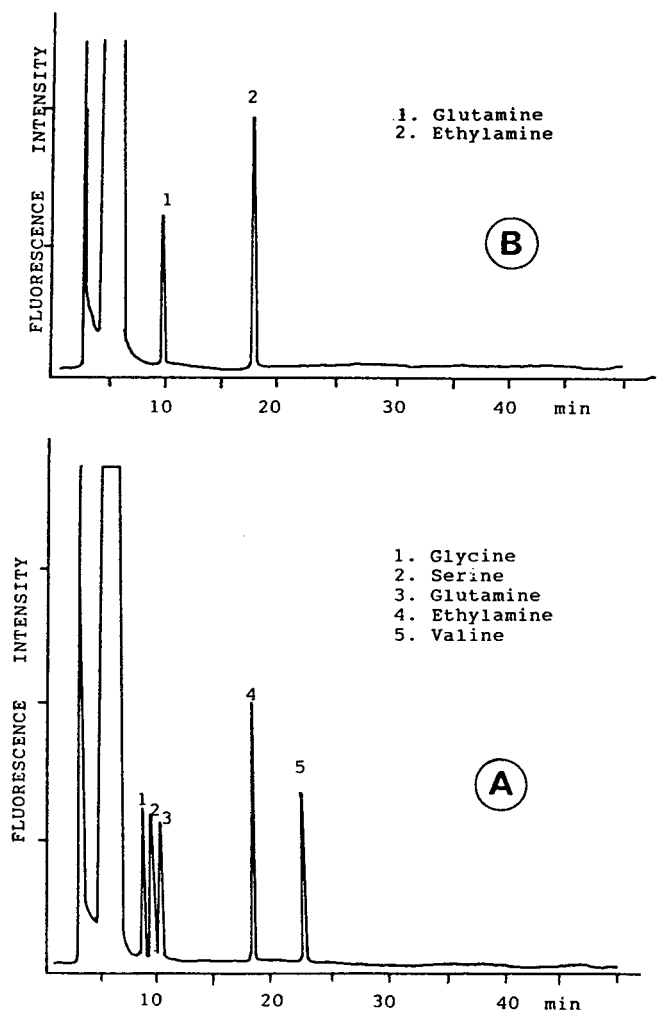


Fig. 5. (A) Chromatogram of constituent amino acids of 0.3 nM of the peptide Val-Gly-Ser-Glu following acid hydrolysis. (B) Chromatogram of terminal amino acid only.

DNS-proline did not give complete recovery when subjected to acid hydrolysis, and care should therefore be taken in quantitative determinations.

### 3.6. Steroid analysis

Steroids incorporating two carbonyl groups in the structure, such as progesterone, have been shown to form a mixture of mono- and bis-derivatives on reaction with DNH which can be individually identified by HPLC [13]. The relative amounts of each of the mono- and bis-derivatives is dependent on the concentration of DNH used. Fig. 6 shows the ratio of bis/mono formed over the concentration range 0.1–1.0 mg of AcNH used. This represents approximately 0.5–5.0 times molar excess of reagent. Under the reaction conditions used complete conversion to

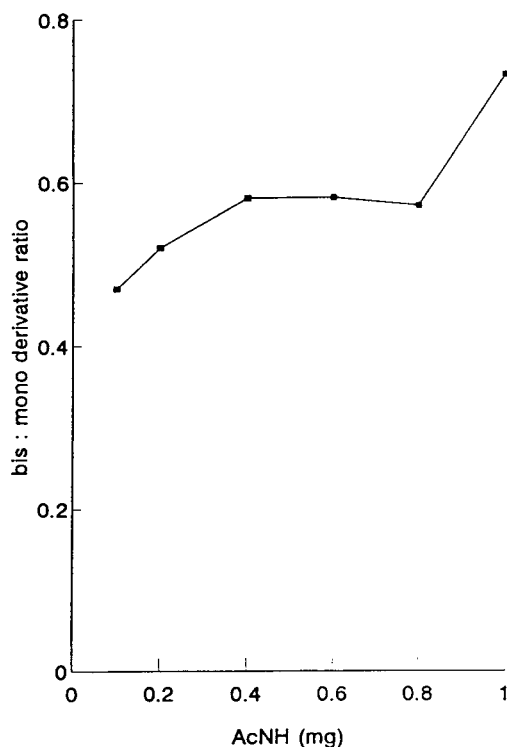


Fig. 6. Variation in the amounts of bis- and mono-derivatives of progesterone with increasing amounts of AcNH derivatising agent in the reaction mixture.

the bis-derivative was not achieved even in the presence of excess reagent.

Trace amounts of ketosteroids have been determined by reaction of the keto group with DNH to form highly fluorescent hydrazones [3]. The conjugate ketone  $\Delta^4$ -3-one reacts in the cold whereas the 17-ketosteroid requires an elevated temperature. The derivatisation of fluocinolone acetone with AcNH was performed in a boiling water bath for a period of 10 min. Chromatography of the resulting reaction mixture using a 15-fold molar excess of AcNH produced only a single peak for the bis component in contrast to the mixed mono and bis product at lower reagent concentrations. Linearity was observed over the concentration range 0–500 ng on column. The sample was analysed in triplicate and found to contain 0.0253% active ingredient, representing 101.5% of the label claim and validating this method.

### 3.7. Carboxylic acid analysis

2-Naphthacyl bromide is a fluorescent label used in the analysis of carboxylic acids [4]. The analogous compound 5-acenaphthacyl bromide was found to produce some 15–20 times more fluorescence when used to derivatise carboxylic acids than the naphthacyl derivative, see Table 1. On-column limits of detection for the short-chain carboxylic acids propanoic and hexanoic acid and the arylpropanoic acids ibuprofen and flurbiprofen were found to be 0.5 and 2.5 pmol, respectively. For the analysis of ibuprofen linearity was observed over the concentration range 0–200 ng/ml and the within- and between-run coefficients of variation were 0.62% and 2.9%, respectively.

The AcN-Br reagent was used to determine the concentrations of ibuprofen in rat plasma following regional administration of the drug to an inflamed site [14]. The levels of drug circulating in the plasma, following this method of delivery, were expected to be low and thus provide a suitable test for the sensitivity of the method. The precision of the method was found to be acceptable and was used to study the pharmacokinetic profile of ibuprofen. A typical

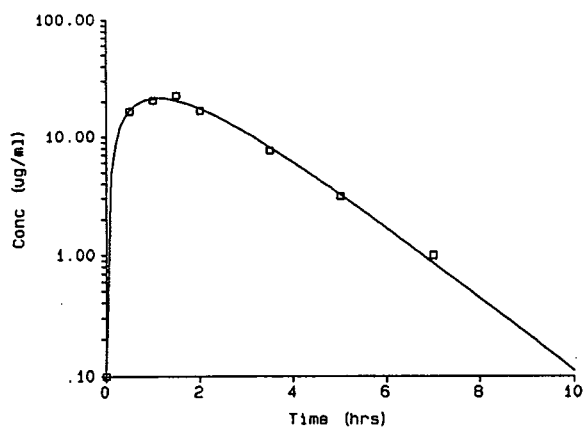


Fig. 7. Concentration–time profile of ibuprofen in rat plasma following administration of the drug at a regional site of delivery.

concentration–time profile is shown in Fig. 7. The mean half life from three subjects was determined as 1.57 h, compared with a value of 1.65 h determined at higher levels by HPLC–UV analysis [14].

## References

- [1] G. Weber, *Biochem. J.*, 51 (1952) 155.
- [2] M. Simmaco, D. De Biase, D. Barra and F. Bossa, *J. Chromatogr.*, 504 (1990) 129.
- [3] R. Chayen, R. Dvir, S. Gould and A. Harell, *Anal. Biochem.*, 42 (1971) 283.
- [4] W. Distler, *J. Chromatogr.*, 192 (1980) 240.
- [5] I.B. Berlman, *Handbook of Fluorescence Spectra of Aromatic Molecules*, 2nd ed., Academic Press, New York, NY, 1971.
- [6] H. Cerfontain and Z.R.H. Schaasberg-Nienhuis, *J. Chem. Soc. Perkin Trans.*, 2 (1974) 989.
- [7] Z. Rappoport (Editor), *Handbook of Tables for Organic Compound Identification*, 3rd ed., CRC Press, Boca Raton, FL, 1977.
- [8] P.H. Gore and M. Jehangir, *J. Chem. Soc. Perkin Trans.*, 1 (1974) 3007.
- [9] R.F. Chen, *Arch. Biochem. Biophys.*, 120 (1967) 609.
- [10] N. Seiler and M. Wiechmann, *Z. Anal. Chem.*, 220 (1966) 109.
- [11] Y. Tapuhi, D.E. Schmidt, W. Lidner and B.L. Karger, *Anal. Biochem.*, 115 (1981) 123.
- [12] W.R. Gray, *Methods Enzymol.*, 25 (1972) 121.
- [13] R. Weinberger, T. Koziol and G. Millington, *Chromatographia*, 19 (1984) 452.
- [14] A.J. Stevens, S.W. Martin, B.S. Brennan, M. Rowland and J.B. Houston, *J. Drug Targeting*, 2 (1994) 333.

# Separation of priority pollutant phenols on chemically modified poly(styrene–divinylbenzene) resins by high-performance liquid chromatography

Christian W. Klampff\*, Emmanouil Spanos

*Department of Analytical Chemistry, Johannes-Kepler University, A-4040 Linz, Austria*

First received 28 February 1995; revised manuscript received 1 June 1995; accepted 1 June 1995

---

## Abstract

A highly cross-linked porous poly(styrene–divinylbenzene) (PS-DVB) resin was prepared using the two-step microsuspension method. The retention behaviour of eleven phenols, listed as priority pollutants by the United States Environmental Protection Agency (EPA), was investigated using this resin with and without surface modification. The corresponding capacity factors ( $k'$ ) of these phenols were compared. Most of the tested compounds showed distinctly different elution behaviour on derivatized resins. A very fast separation of all eleven priority pollutant phenols (PPPs) could be achieved on a column packed with PS-DVB beads modified with *tert.*-butyl groups using gradient elution.

## 1. Introduction

The use of polymeric resins in reversed-phase high-performance liquid chromatography (RP-HPLC) has grown dramatically, since an increasing number of polymeric columns are commercially available [1]. The application of silica-based supports is limited by the low stability of silica at alkaline pH values and by the unwanted interactions between polar solutes and remaining free silanol groups not covered by the hydrophobic ligand. In particular PS-DVB-based resins show a high stability over the pH range 1–14 and provide excellent separations [2–5]. Additionally, PS-DVB particles permit the intro-

duction of numerous functional groups that change their surface chemistry and hence the chromatographic selectivity [6–11].

Sun and Fritz [6] showed that the modification of a XAD-4 and a spherical PS-DVB resin by incorporating different functional groups into the polymer has a major effect on the retention behaviour of various analytes. More hydrophobic resins have been prepared by the Friedel–Crafts reaction of different alkylchlorides with the benzene ring of the polymer. In a way identical to that for silica-based supports, the hydrophobicity of the resin can be controlled by the type of functional group incorporated in the resin.

In contrast to the resin described in the present work, most of the commercially available polymeric supports for HPLC are generally prepared by suspension polymerization followed by

---

\* Corresponding author.

a size classification procedure [12]. The PS-DVB support proposed here was polymerized using the two-step microsuspension method, which directly leads to monosized particles [13–17]. Therefore these polymer beads may be used for chromatography without any size classification procedure. Porosity and the degree of cross-linking are adjusted by the amount of an inert diluent, e.g. toluene, and the amount of a cross-linking agent, e.g. divinylbenzene, respectively, added during the polymerization step [18]. The high cross-linking degree of the PS-DVB resin studied in this paper leads to an increased ruggedness of the particles.

Numerous papers have been published dealing with the separation of substituted phenols by HPLC [5,19–29]. Some of the works investigate the retention behaviour of these solutes using different chromatographic columns, e.g. silica-based reversed-phase columns [19,28], a graphitized carbon column [20] or different polymer-based columns [5,6,21]. But to the best of our knowledge there are no reports addressed to the separation of all eleven priority pollutant phenols (PPPs) using a polymer-based column.

Therefore the aim of the present work was to synthesize and derivatize a highly cross-linked PS-DVB resin, using two different alkylating agents. The chromatographic behaviour of all eleven PPPs listed in the Environmental Protection Agency (EPA) Method 625 [30] was investigated on these polymer supports. The resin derivatized with *tert.*-butyl groups was found to be suitable for the separation of all eleven phenols.

## 2. Experimental

### 2.1. Equipment

A Waters 625 LC-system equipped with a Waters 600E system controller (Waters, Milford, MA, USA), a 9125 Rheodyne injector (Rheodyne, Cotati, CA, USA) equipped with a 50- $\mu$ l loop, an ABI 785A programmable absorbance

detector (Applied Biosystems, San Jose, CA, USA) and a HP 3359A chromatographic work-system (Hewlett-Packard, Palo Alto, CA, USA) were used for HPLC. For column packing a Knauer pneumatic HPLC pump (Knauer, Berlin, Germany) was used.

### 2.2. Reagents and chemicals

All chemicals used for the synthesis and derivatization of the polymeric resin were purchased from Merck (Darmstadt, Germany). HPLC gradient grade acetonitrile, methanol and analytical grade acetic acid were purchased from J.T. Baker (Deventer, Netherlands). Doubly distilled water was used.

Priority pollutant phenols (Merck) were dissolved in analytical grade methanol from J.T. Baker and the solutions stored at 4°C in the dark.

### 2.3. Columns

PS-DVB beads were prepared by a two-step microsuspension method similar to the procedure described elsewhere [13]. The resulting particles had a mean diameter of 4  $\mu$ m ( $\pm 0.3$   $\mu$ m), a specific surface area between 92 and 94  $m^2/g$  and a cross-linking degree of 50%. Part of the material was alkylated under Friedel–Crafts conditions. To a suspension of 5 g of the resin in octadecylchloride 0.5 g anhydrous aluminium chloride was added. The mixture was kept at 80°C for 20 h and then was diluted with 4 M hydrochloric acid, filtered and washed subsequently with water, methanol and acetone. The resulting PS-DVB particles with octadecylchains bound to the benzene ring of the resin were dried. In the same way *tert.*-butylchloride was reacted with the PS-DVB beads. All polymer resins were suspended in tetrahydrofuran, sonicated and packed into 30  $\times$  4 mm I.D. stainless-steel columns for 15 min at 35 MPa. Thio-urea was chosen to determine the hold-up time ( $t_0$ ) of the columns in this study.



### 3. Results and discussion

#### 3.1. Chromatographic behaviour

The chromatographic behaviour of eleven differently substituted PPPs has been investigated using different acetonitrile–water mixtures for isocratic elution. To both solvents 1% acetic acid was added to prevent peak tailing [29]. Fig. 1 shows the capacity factors of these phenols on a PS-DVB column as a function of the acetonitrile content of the eluent. Because of the scale of the diagram, pentachlorophenol is not shown in this plot. A flow-rate of 1 ml/min was used throughout these experiments unless specified other.

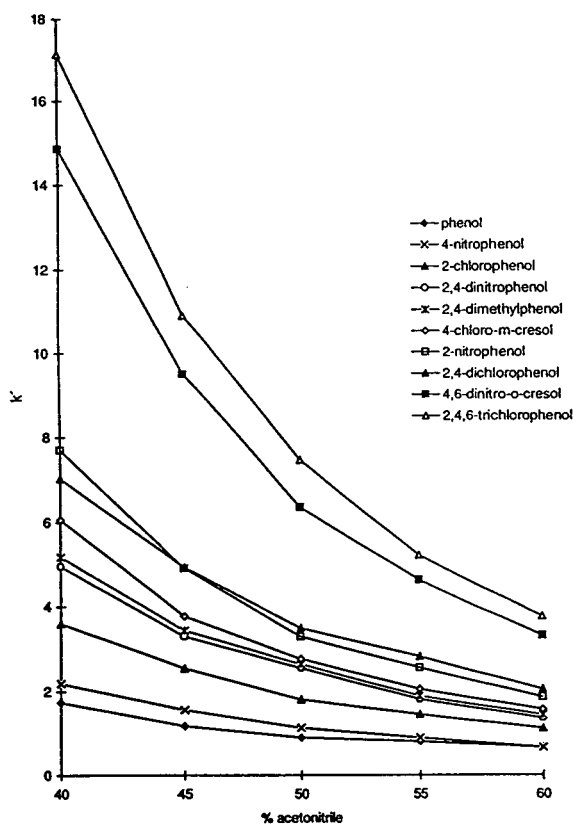


Fig. 1. The  $k'$ -values of ten PPPs as a function of the acetonitrile content of the eluent. Chromatographic conditions: column, PS-DVB, 4  $\mu$ m, 30  $\times$  4 mm I.D.; eluent, water (1% acetic acid)–acetonitrile (1% acetic acid); flow-rate, 1 ml/min.

Using the same eluent, the PPPs elute in identical order from underivatized PS-DVB as from the alkylated species. Published separations of these phenols using similar conditions but silica-based reversed-phase columns [28,29] show quite different results. The weakly retained phenols, e.g. phenol or 4-nitrophenol, as well as the strongly retained substances, e.g. 2,4-dinitro-*o*-cresol, 2,4,6-trichlorophenol or pentachlorophenol, show the same elution behaviour on PS-DVB-based resins as compared to silica-based materials. However, the elution order of the moderately retained compounds, starting from 2-chlorophenol and ending with 2-nitrophenol, considerably differs as compared with silica-based columns. This is clearly demonstrated in Table 1. This behaviour is believed to be caused by additional interactions between the  $\pi$ -electrons of the PS-DVB resin and orbitals of the solute species.

The acetonitrile content of the eluent changes the elution order of these PPPs on a PS-DVB column only in one case. As can be seen in Fig. 1, 2-nitrophenol is less retained than 2,4-dichlo-

Table 1  
Comparison of  $k'$ -values of 11 PPPs on a PS-DVB and a silica  $C_{18}$  reversed-phase liquid chromatography column

Compound	Capacity factors ( $k'$ )	
	PS-DVB	Silica $C_{18}$
Phenol	0.90	1.07
4-Nitrophenol	1.13	1.29
2-Chlorophenol	1.81	1.86
2,4-Dinitrophenol	2.55	1.77
2,4-Dimethylphenol	2.64	2.68
4-Chloro- <i>m</i> -cresol	2.77	3.11
2,4-Dichlorophenol	3.29	5.98
2-Nitrophenol	3.49	2.71
4,6-Dinitro- <i>o</i> -cresol	6.34	4.22
2,4,6-Trichlorophenol	7.45	6.85
Pentachlorophenol	17.36	18.75

PS-DVB: 30  $\times$  4 mm I.D., 4  $\mu$ m; eluent, water–acetonitrile–acetic acid (49.5:49.5:1); flow-rate, 1 ml/min.

Silica  $C_{18}$ : Radial Pak  $C_{18}$  cartridge (Waters, Milford, MA, USA), 100  $\times$  8 mm I.D., 5  $\mu$ m; eluent, water–acetonitrile–acetic acid (50:50:0.1); flow-rate 2 ml/min; data taken from Ref. [28].

rophenol on PS-DVB-based columns if the acetonitrile content of the eluent is less than 45%. Increasing the acetonitrile content of the eluent, 2,4-dichlorophenol elutes earlier than 2-nitrophenol. This observation does not only apply to underivatized PS-DVB but also to the alkylated resins used in this study.

### 3.2. Comparison of unmodified and modified PS-DVB resins

Alkylated and underivatized PS-DVB based columns were investigated. Comparing the  $k'$ -values of all eleven PPPs, it can be mentioned that generally  $k'$ -values increase by introducing alkyl groups to the benzene ring of the polymer due to the increase in sorbent hydrophobicity. As can be seen in Table 2, the resin derivatized with  $C_{18}$  chains shows a larger increase in  $k'$ -values than the resin substituted with *tert.*-butyl groups. This may be attributed to the higher hydrophobicity of the  $C_{18}$  chains compared with the *tert.*-butyl groups. The behaviour of 2,4,6-trichlorophenol, shown in Fig. 2, is a typical example of this fact. However, phenols containing a free nitro-group, e.g. 2,4-dinitrophenol, 4-nitrophenol or 4,6-dinitro-*o*-cresol, show different behaviour, which is illustrated in Fig. 3. The  $k'$ -values observed with the *tert.*-butyl-de-

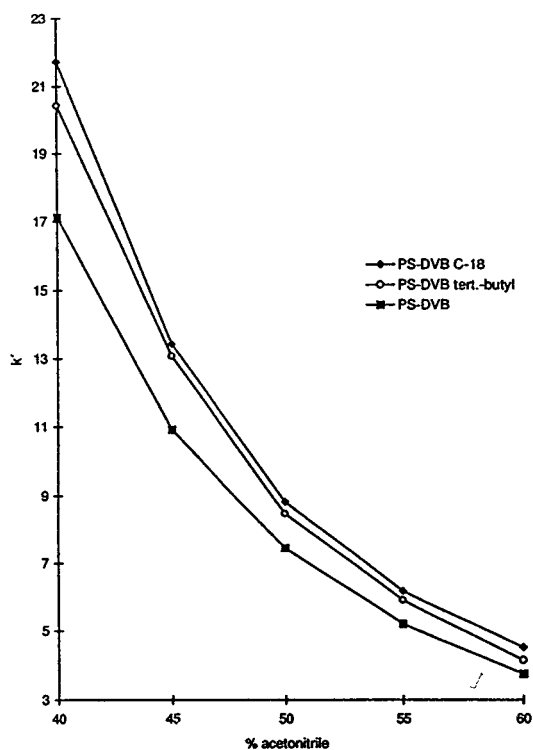


Fig. 2. The  $k'$ -values of 2,4,6-trichlorophenol as a function of the acetonitrile content of the eluent using alkylated and non-alkylated PS-DVB columns. Chromatographic conditions: column, 30 × 4 mm I.D.; eluent, water (1% acetic acid)–acetonitrile (1% acetic acid); flow-rate, 1 ml/min.

Table 2

Comparison of  $k'$ -values of 11 PPPs on alkylated and non-alkylated PS-DVB resins

Compound	Capacity factors ( $k'$ )		
	PS-DVB	PS-DVB $C_{18}$	PS-DVB <i>tert.</i> -butyl
Phenol	0.90	1.03	1.00
4-Nitrophenol	1.13	1.23	1.10
2-Chlorophenol	1.81	2.07	1.94
2,4-Dinitrophenol	2.55	2.74	2.20
2,4-Dimethylphenol	2.64	2.80	2.66
4-Chloro- <i>m</i> -cresol	2.77	3.19	3.09
2,4-Dichlorophenol	3.29	4.06	3.89
2-Nitrophenol	3.49	4.12	4.15
4,6-Dinitro- <i>o</i> -cresol 6.34	7.24	6.07	
2,4,6-Trichlorophenol	7.45	8.83	8.47
Pentachlorophenol	17.36	24.09	21.96

Chromatographic conditions: columns 30 × 4 mm I.D.; eluent, water–acetonitrile–acetic acid (49.5:49.5:1); flow-rate, 1 ml/min.

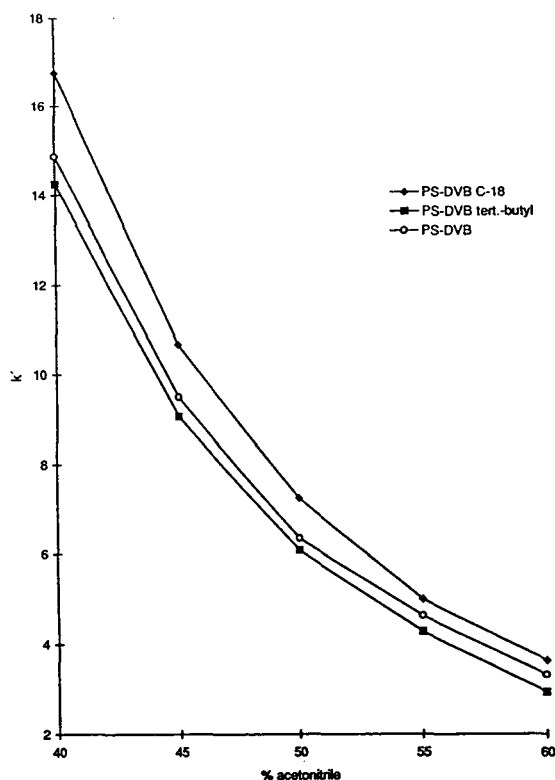


Fig. 3. The  $k'$ -values of 4,6-dinitro-*o*-cresol as a function of the acetonitrile content of the eluent using alkylated and non-alkylated PS-DVB columns. Chromatographic conditions: column, 30 × 4 mm I.D.; eluent, water (1% acetic acid)–acetonitrile (1% acetic acid); flow-rate, 1 ml/min.

derivatized resin are even lower than those with the underivatized resin. But it should be stressed that these more polar phenols do not reverse the retention order, as might be expected. The resin derivatized with the C<sub>18</sub> chains still leads to the highest  $k'$ -values even for these PPPs containing free nitro-groups. 2-Nitrophenol behaves like the phenols without nitro-groups due to the intramolecular hydrogen bonding.

The number of theoretical plates for these columns was determined for 4-chloro-*m*-cresol using a mixture of 50% acetonitrile and 50% water, both containing 1% of acetic acid for isocratic elution. It was found to be 450 for the columns filled with alkylated resin and 525 for the column filled with underivatized PS-DVB.

This corresponds to a value of 15 000 respectively 17 500 plates/m.

### 3.3. Separation of priority pollutant phenols

To achieve complete separation of all eleven PPPs on a PS-DVB-based column isocratic conditions with a low acetonitrile content were used to separate the first eight phenols (phenol–2,4-dichlorophenol), while the strongly retained phenols, e.g. 4,6-dinitro-*o*-cresol, 2,4,6-trichlorophenol and pentachlorophenol, were eluted by a steep gradient up to 95% acetonitrile. When using an eluent mixture containing 40% of acetonitrile, the resolution of e.g. 2,4-dinitrophenol and 2,4-dimethylphenol is very poor for both the PS-DVB and the PS-DVB C<sub>18</sub> column. The use of underivatized PS-DVB results in a resolution ( $R_s$ ) of just 0.08 while the C<sub>18</sub> derivatized resin gives an even worse  $R_s$  of 0.03. Whereas using the *tert.*-butyl-group containing resin increases the resolution of these two peaks to a value of 0.61. This fact is caused by the different behaviour of phenols containing free nitro-groups on the *tert.*-butyl-derivatized resin compared to that on underivatized and C<sub>18</sub>-derivatized polymer. Fig. 4 shows a high-speed separation of a standard mixture of all eleven PPPs on a *tert.*-butyl-derivatized PS-DVB column. Good separation of all investigated phenols could be achieved in less than 6.5 min using the chromatographic conditions specified in Fig. 4.

## 4. Conclusion

The results obtained in this work indicate that PS-DVB-based resins prepared by the two-step microsuspension method are an attractive alternative to silica-based columns in reversed-phase liquid chromatography. It is apparent that the introduction of alkyl groups into these PS-DVB resins has an appreciable effect on the retention times and  $k'$ -values. In some cases derivatized columns even offer an additional selectivity parameter, which could be shown in the case of the separation of eleven PPPs on a PS-DVB-based column containing *tert.*-butyl groups. This sepa-

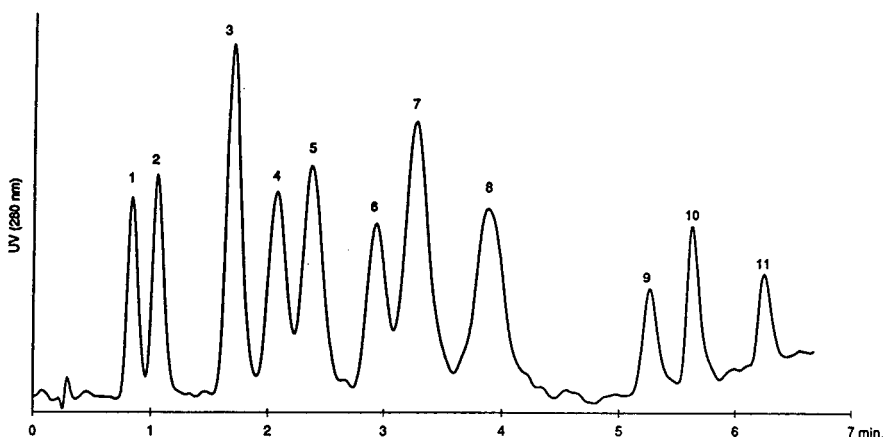


Fig. 4. Separation of a standard mixture of 11 PPPs. Chromatographic conditions: column, PS-DVB *tert.*-butyl, 4  $\mu$ m, 30  $\times$  4 mm I.D.; eluents, (A) water–acetic acid (99:1), (B) acetonitrile–acetic acid (99:1), 65% A and 35% B 4 min isocratic followed by a linear gradient to 95% B in 2 min; flow-rate, 1.5 ml/min; detection, UV 280 nm; peaks: 1 = phenol, 2 = 4-nitrophenol, 3 = 2-chlorophenol, 4 = 2,4-dinitrophenol, 5 = 2,4-dimethylphenol, 6 = 4-chloro-*m*-cresol, 7 = 2-nitrophenol, 8 = 2,4-dichlorophenol, 9 = 4,6-dinitro-*o*-cresol, 10 = 2,4,6-trichlorophenol, 11 = pentachlorophenol.

ration is less time-consuming than published separations using other chromatographic supports.

## References

- [1] J.R. Benson and D.J. Woo, *J. Chromatogr. Sci.*, 22 (1984) 386.
- [2] D.P. Lee, *J. Chromatogr. Sci.*, 20 (1982) 203.
- [3] R.L. Smith and D.J. Pietrzyk, *J. Chromatogr. Sci.*, 21 (1983) 282.
- [4] J.V. Dawkins, L.L. Lloyd and F.P. Warner, *J. Chromatogr.*, 352 (1986) 157.
- [5] H.A. MacLeod and G. Laver, *J. Chromatogr.*, 244 (1982) 385.
- [6] J.J. Sun and J.S. Fritz, *J. Chromatogr.*, 522 (1990) 95.
- [7] S.M. Ahmed, *Dispersion Sci. Technol.*, 5 (1984) 421.
- [8] R. Taylor, *Electrophilic Aromatic Substitution*, Wiley, Chichester, 1990.
- [9] M.J. Farrall and J.M.J. Frechet, *J. Org. Chem.*, 41 (1976) 3877.
- [10] R.L.L. Letsinger, M.J. Kornet and V. Mahadevan, *J. Am. Chem. Soc.*, 86 (1964) 5163.
- [11] N.P. Bullen, P. Hodge and F.G. Thorpe, *J. Chem. Soc. Perkin Trans.*, 1 (1981) 1863.
- [12] T. Ellingsen, O. Aune, J. Ugelstad and S. Hagen, *J. Chromatogr.*, 535 (1990) 147.
- [13] C.G. Huber, P.J. Oefner and G.K. Bonn, *Anal. Biochem.*, 212 (1993) 351.
- [14] C.G. Huber, P.J. Oefner and G.K. Bonn, *J. Chromatogr.*, 599 (1992) 113.
- [15] S. Wongyai, J.M. Varga and G.K. Bonn, *J. Chromatogr.*, 536 (1991) 155.
- [16] G. Bonn, C. Huber and P. Oefner, Austrian Patent Application, No. 2285/92, 1992.
- [17] J.W. Goodwin, J. Hearn, C.C. Ho and R.H. Ottewill, *Colloid Polym. Sci.*, 252 (1974) 464.
- [18] F. Nevejans and M. Verzele, *J. Chromatogr.*, 406 (1987) 325.
- [19] S. Yamauchi, *J. Chromatogr.*, 635 (1993) 61.
- [20] E. Forgács, T. Cserhádi and K. Valkó, *J. Chromatogr.*, 592 (1992) 75.
- [21] G. Marko-Varga and D. Barceló, *Chromatographia*, 34 (1992) 146.
- [22] W. Markowski, T.H. Dzido and E. Soczewinski, *J. Chromatogr.*, 523 (1990) 81.
- [23] M.D. Andrés, B. Cañas, R.C. Izquierdo, L.M. Polo and P. Alarcón, *J. Chromatogr.*, 507 (1990) 399.
- [24] C.P. Ong, H.K. Lee and S.F.Y. Li, *J. Chromatogr.*, 464 (1989) 405.
- [25] H.K. Lee, S.F.Y. Li and Y.H. Tay, *J. Chromatogr.*, 438 (1988) 429.
- [26] P. Alarcón, A. Bustos, B. Cañas, M.D. Andrés and L.M. Polo, *Chromatographia*, 24 (1987) 613.
- [27] F.P. Bigley and R.L. Grob, *J. Chromatogr.*, 350 (1985) 407.
- [28] N.G. Buckman, J.O. Hill, R.J. Magee and M.J. McCormick, *J. Chromatogr.*, 284 (1984) 441.
- [29] P.A. Realini, *J. Chromatogr. Sci.*, 19 (1981) 124.
- [30] EPA method 625, Base/Neutrals and Acids, U.S. Environmental Protection Agency, 1984.

# High-performance liquid chromatographic method for the separation of isomers of *cis*- and *trans*-2-amino-cyclopentane-1-carboxylic acid

Antal Péter<sup>a,\*</sup>, Ferenc Fülöp<sup>b</sup>

<sup>a</sup>Department of Inorganic and Analytical Chemistry, Attila József University, P.O. Box 440, H-6701 Szeged, Hungary

<sup>b</sup>Institute of Pharmaceutical Chemistry, Albert Szent-Györgyi Medical University, P.O. Box 121, H-6701 Szeged, Hungary

First received 28 February 1995; revised manuscript received 23 May 1995; accepted 23 May 1995

## Abstract

A method was developed for the separation of *cis*-(1*S*,2*R*)-, *cis*-(1*R*,2*S*)-, *trans*-(1*S*,2*S*)- and *trans*-(1*R*,2*R*)-2-amino-cyclopentane-1-carboxylic acids by using pre-column derivatization with the chiral derivatizing reagents 1-fluoro-2,4-dinitrophenyl-5-L-alanine amide and 2,3,4,6-tetra-O-acetyl-β-D-glucopyranosyl isothiocyanate. The method is suitable for the separation of both diastereomeric and enantiomeric pairs. The high-performance liquid chromatographic conditions (pH, eluent composition and different buffers) were varied to obtain optimal separation.

## 1. Introduction

In recent years, a number of investigations have been performed [1–5] to introduce alicyclic β-amino acids such as *cis*- and *trans*-2-amino-cyclopentane-1-carboxylic acids (*cis*- and *trans*-ACPC, Fig. 1) into peptides in order to increase their stability and to modify their biological activity. Also, *cis*- and *trans*-ACPC have been used in the syntheses of biologically active heterocycles [6–9].

Although the syntheses [10–12] and transformations of racemic *cis*- and *trans*-ACPC have long been known, interest in this field was

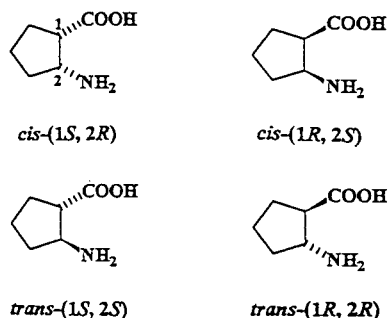


Fig. 1. Structures of four stereoisomers of *cis*-(1*S*,2*R*, 1*R*,2*S*)- and *trans*-(1*S*,2*S*, 1*R*,2*R*)-2-amino-cyclopentane-1-carboxylic acid.

\* Corresponding author. Address for correspondence until December 1995: Vrije Universiteit Brussel, ORGC-VUB, c/o Dr. D. Tourwe, Pleinlaan 2, B-1050 Brussels, Belgium.

enhanced when *cis*-(1*R*,2*S*)-ACPC (cispentacin) was found in nature [13–16].

Cispentacin [(–)-*cis*-(1*R*,2*S*)-ACPC] was isolated [13–16] by two independent laboratories from *Bacillus cereus* L450-B2 and *Streptomyces setonii* 7562. (–)-*cis*-ACPC exerts a marked protective effect against *Candida albicans* and *Cryptococcus neoformans* in mice [13–18]. Because of their biological importance, a number of methods have been developed [19–22] and patented [23–30] for the preparation of cispentacin. These methods mainly involve enzymatic separation techniques [31].

The difficulty to obtain many uncommon amino acids in a homochiral form underline the importance of having at hand effective chromatographic methods for the characterization and identification of enantiomers.

Several papers and reviews have been published on the development of enantioselective separations by means of liquid chromatographic techniques. Enantioselective separations involving high-performance liquid chromatographic (HPLC) methods can be divided into three main groups: direct separation on chiral stationary phases [32–34], separation on achiral columns with chiral eluents [34–36], and separation of the diastereoisomers formed by pre-column derivatization with chiral reagents [34,37–48].

The present paper deals with the separation of enantiomers of *cis*- and *trans*-ACPC by using pre-column derivatization with 1-fluoro-2,4-dinitrophenyl-5-L-alanine amide (FDAA, Marfey's reagent) or 2,3,4,6-tetra-O-acetyl-β-D-glucopyranosyl isothiocyanate (GITC). The separations were carried out in different buffer systems, acetonitrile or methanol being used as organic modifier. The effects of pH, mobile phase composition and organic modifier content on the separation were also investigated.

## 2. Experimental

### 2.1. Chemicals and reagents

(±)-*cis*-ACPC was prepared from cyclopentene via chlorosulphonyl isocyanate addition,

followed by aqueous hydrochloric acid treatment and ion-exchange chromatography [12]. (±)-*trans*-ACPC was synthesized by Michael addition of ammonia to 1-cyclopentenecarboxylic acid in a steel autoclave at 170°C for 80 h, followed by ion-exchange chromatography [10]. (–)-*cis*-(1*R*,2*S*)-ACPC and (+)-*trans*-(1*S*,2*S*)-ACPC were prepared from the corresponding esters by lipase acylation, followed by hydrolysis [49].

GITC was purchased from Aldrich (Steinheim, Germany), FDAA from Pierce Chemical (Rockford, IL, USA), and potassium dihydrogenphosphate, trifluoroacetic acid, sodium acetate, phosphoric acid, acetic acid of analytical reagent grade, acetonitrile and methanol of HPLC grade from Merck (Darmstadt, Germany). Buffers were prepared with doubly distilled water and further purified by filtration on a 0.45-μm filter, type HV, Millipore (Molsheim, France). The pH was adjusted with phosphoric acid, acetic acid and sodium hydroxide.

### 2.2. Apparatus

HPLC analyses were performed on an M-600 low-pressure-gradient pump equipped with an M-996 photodiode-array detector and a Millennium 2010 Chromatography Manager data system (Waters Chromatography, Division of Millipore, Milford, MA, USA) and on an L-6000 liquid chromatographic pump (Merck Hitachi, Tokyo, Japan) equipped with a UV 308 detector (Labor MIM, Budapest, Hungary) and an HP 3395 integrator (Hewlett-Packard, Waldbronn, Germany).

The columns used were Lichrospher 100 RP18 (125 × 4 mm I.D.), 5 μm particle size (Merck, Darmstadt, Germany).

### 2.3. Derivatization of amino acids for chromatographic analysis

An amount of 0.5–1 mg of *cis*- or *trans*-ACPC was derivatized with FDAA by the method of Marfey [43] and with GITC by the method of Nimura et al. [40].

### 3. Results and discussion

Control of the carboxylate group ionization requires the control of pH, i.e. buffering of the mixed aqueous–organic modifier phase system, in order to maintain equilibrium constancy within the column. The  $pK$  values of ACPC are not known; for 1-amino-cyclopentane-1-carboxylic acid,  $pK_1 = 10.31$  and  $pK_2 = 2.40$  [50]. The effect of pH on the separation was investigated in the 0.01 M potassium dihydrogenphosphate (pH 2–6)–acetonitrile system; the results can be found in Fig. 2. It is clear from Fig. 2 that the  $k'$  values are higher at lower pH, while at  $pH < 3$  and at  $pH > 5$   $k'$  varies slightly with a change in pH. These results led to the choice of three systems to keep the ionization at a constant level: a 0.1% aqueous solution of trifluoroacetic acid, which is often used in the separation of derivatized amino acids and peptides, 0.01 M potassium dihydrogenphosphate at pH 3, and 0.01 M sodium acetate at pH 3.

#### 3.1. Separation of ACPC–GITC derivatives

Separations were carried out in the three systems, with methanol or acetonitrile as organic modifier; the results are given in Tables 1 and 2. Table 1 demonstrates that decrease of the

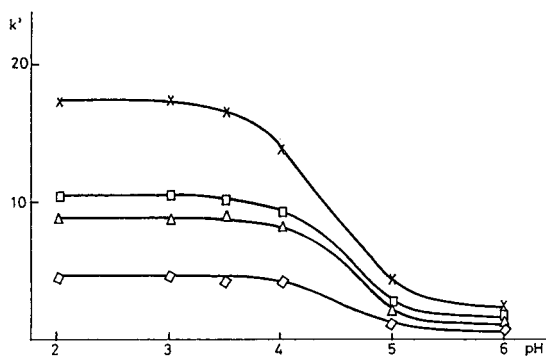


Fig. 2. Dependence of retention factor ( $k'$ ) of four diastereoisomers of ACPC–FDAA derivatives on pH of buffer. Column, Lichrospher 100 RP18; flow-rate, 0.8 ml/min; detection, 340 nm; mobile phase, 0.01 M potassium dihydrogenphosphate (pH 2–6)–acetonitrile (70:30). ( $\diamond$ ) *cis*-(1*R*,2*S*) derivative; ( $\triangle$ ) *cis*-(1*S*,2*R*) derivative; ( $\square$ ) *trans*-(1*S*,2*S*) derivative; ( $\times$ ) *trans*-(1*R*,2*R*) derivative.

methanol content results in an increase in  $k'$  for all four enantiomers, while the  $\alpha$  and  $R_s$  values also improve.

The optimal mobile-phase composition contains 42.5% or less methanol. In this case, the four enantiomers can be separated with  $R_s$  higher than 1.5. Comparison of the three buffer systems reveals only slight differences. Better resolutions were generally obtained in phosphate buffer, but at the same time the  $k'$  value of the last peak, i.e. the total time of analysis, was the largest in this system. The elution order of the peaks was identified by comparing the individual  $k'$  values with standards prepared by enzymatic resolution. These experiments showed that the first peak corresponds to the *trans*-(1*S*,2*S*), the second to the *trans*-(1*R*,2*R*), the third to the *cis*-(1*R*,2*S*) and the fourth to the *cis*-(1*S*,2*R*) isomer (Fig. 3).

When acetonitrile was applied as organic modifier, decrease of the acetonitrile content of the mobile phase resulted in behaviour similar to that observed in the methanol-containing system. Resolutions similar to those observed in the methanol-containing mobile phase could be achieved with much larger  $k'$  values (Table 2). This corresponds with our earlier findings [51,52]: in acetonitrile-containing systems, a similar resolution of diastereoisomers of some unusual aromatic amino acids with GITC can be attained at higher  $k'$  values as compared with the methanol-containing systems. With regard to the buffer systems, phosphate seems favourable with respect to resolution and peak shape. The elution order of the four enantiomers is the same as that observed in methanol.

The described method is suitable for the determination of less than 0.1% minor isomer content in excess of the major isomer.

#### 3.2. Separation of ACPC–FDAA derivatives

The results of separations with methanol as organic modifier are given in Table 3. The elution order, determined by comparison with standards, was *cis*-(1*R*,2*S*), *cis*-(1*S*,2*R*), *trans*-(1*S*,2*S*) and *trans*-(1*R*,2*R*) isomer (Fig. 3). This

Table 1  
Dependence of retention factor ( $k'$ ), separation factor ( $\alpha$ ) and resolution ( $R_s$ ) of ACPC–GITC derivatives on eluent composition

Eluent composition	$k'$				$\alpha_{t,t}$	$\alpha_{t,c}$	$\alpha_{c,c}$	$R_{s,t,t}$	$R_{s,t,c}$	$R_{s,c,c}$
	<i>trans</i>		<i>cis</i>							
	(1S,2S)	(1R,2R)	(1R,2S)	(1S,2R)						
TFA–CH <sub>3</sub> OH										
55:45	5.38	5.93	6.53	7.25	1.10	1.10	1.11	0.75	0.80	0.65
57.5:42.5	6.55	8.34	11.41	13.36	1.27	1.36	1.17	2.04	2.50	1.53
60:40	8.69	11.50	15.88	18.97	1.32	1.38	1.19	2.67	3.50	1.91
KH <sub>2</sub> PO <sub>4</sub> –CH <sub>3</sub> OH										
55:45	4.17	5.55	8.14	9.70	1.33	1.47	1.19	1.26	2.14	0.90
57.5:42.5	5.83	8.00	11.80	14.40	1.37	1.48	1.22	1.96	3.35	2.03
60:40	8.50	12.11	17.90	22.17	1.42	1.48	1.24	3.63	4.40	2.40
NaOAc–CH <sub>3</sub> OH										
55:45	4.67	5.69	7.60	9.72	1.22	1.34	1.27	1.45	2.04	1.16
57.5:42.5	5.86	7.37	10.02	11.71	1.26	1.36	1.17	2.04	2.84	2.01
60:40	8.29	10.56	14.70	17.13	1.28	1.39	1.17	2.13	3.38	2.30

Column, Lichrospher 100 RP18; flow-rate, 0.8 ml/min; detection, 250 nm; TFA, 0.1% aqueous solution of trifluoroacetic acid; KH<sub>2</sub>PO<sub>4</sub>, 0.01 M aqueous solution of potassium dihydrogenphosphate (pH 3); NaOAc, 0.01 M aqueous solution of sodium acetate (pH 3);  $\alpha_{t,t}$  and  $R_{s,t,t}$  represent separation of *trans*-(1S,2S) and *trans*-(1R,2R) derivatives;  $\alpha_{t,c}$  and  $R_{s,t,c}$  represent separation of *trans*-(1R,2R) and *cis*-(1R,2S) derivatives;  $\alpha_{c,c}$  and  $R_{s,c,c}$  represent separation of *cis*-(1R,2S) and *cis*-(1S,2R) derivatives.

Table 2  
Dependence of retention factor ( $k'$ ), separation factor ( $\alpha$ ) and resolution ( $R_s$ ) of ACPC–GITC derivatives on eluent composition

Eluent composition	$k'$				$\alpha_{t,t}$	$\alpha_{t,c}$	$\alpha_{c,c}$	$R_{s,t,t}$	$R_{s,t,c}$	$R_{s,c,c}$
	<i>trans</i>		<i>cis</i>							
	(1S,2S)	(1R,2R)	(1R,2S)	(1S,2R)						
TFA–CH <sub>3</sub> CN										
77.5:22.5	20.98	24.80	32.48	36.46	1.18	1.31	1.12	1.75	2.96	1.35
KH <sub>2</sub> PO <sub>4</sub> –CH <sub>3</sub> CN										
77.5:22.5	17.58	21.36	30.14	34.41	1.22	1.41	1.14	2.31	4.26	1.71
NaOAc–CH <sub>3</sub> CN										
77.5:22.5	16.06	20.09	28.70	33.54	1.25	1.43	1.17	1.84	3.10	1.42

Column, Lichrospher 100 RP18; flow-rate, 0.8 ml/min; detection, 250 nm; TFA, 0.1% aqueous solution of trifluoroacetic acid; KH<sub>2</sub>PO<sub>4</sub>, 0.01 M aqueous solution of potassium dihydrogenphosphate (pH 3); NaOAc, 0.01 M aqueous solution of sodium acetate (pH 3);  $\alpha_{t,t}$  and  $R_{s,t,t}$  represent separation of *trans*-(1S,2S) and *trans*-(1R,2R) derivatives;  $\alpha_{t,c}$  and  $R_{s,t,c}$  represent separation of *trans*-(1R,2R) and *cis*-(1R,2S) derivatives;  $\alpha_{c,c}$  and  $R_{s,c,c}$  represent separation of *cis*-(1R,2S) and *cis*-(1S,2R) derivatives.



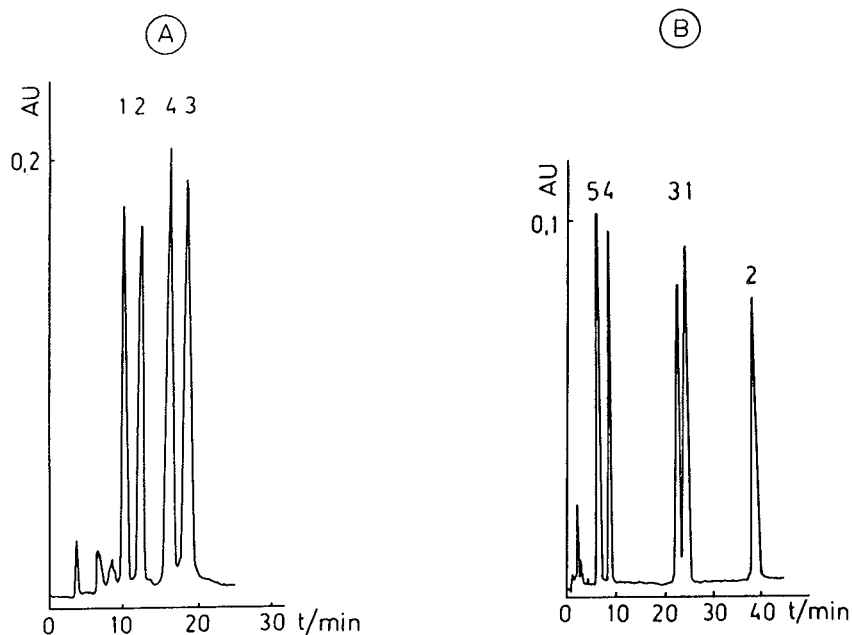


Fig. 3. Representative chromatograms of separation of four diastereoisomers of ACPC derivatives. (A) GITC derivatives, (B) FDAA derivatives. Column, Lichrospher 100 RP18; flow-rate, 0.8 ml/min; detection, (A) 250 nm, (B) 340 nm; mobile phase, (A) 0.01 M sodium acetate (pH 3)–methanol (57.5:42.5), (B) 0.01 M sodium acetate–methanol (77.5:22.5). Peaks: 1 = *trans*-(1*S*,2*S*) derivative; 2 = *trans*-(1*R*,2*R*) derivative; 3 = *cis*-(1*S*,2*R*) derivative; 4 = *cis*-(1*R*,2*S*) derivative; 5 = unreacted FDAA.

*cis/trans* sequence is the reverse of that observed for the GITC derivatives.

At a given eluent composition, the  $k'$  values of the diastereoisomers in the trifluoroacetic acid system are the highest, and the resolutions are also the best here. As can be seen in Fig. 3, the *cis*-(1*R*,2*S*) and *cis*-(1*S*,2*R*) isomers and the *trans*-(1*S*,2*S*) and *trans*-(1*R*,2*R*) isomers separate very well. The peaks of the *cis*-(1*S*,2*R*) and *trans*-(1*S*,2*S*) isomers are close, and good separation requires optimization of the conditions. Peak number 5, which elutes first, corresponds to unreacted reagent.

The results of separations in the acetonitrile-containing system are shown in Table 4. The elution order of the four enantiomers is the same as that observed in methanol. In the eluent system with a buffer–acetonitrile ratio of 70:30, the unreacted FDAA elutes after, and very close to, the *cis*-(1*R*,2*S*) isomer. Complete separation of these two peaks can be achieved at 25% acetonitrile content. Comparison of the three buffer systems at a given eluent composition

reveals that the  $k'$  values are the lowest in sodium acetate, while the resolutions are better in the trifluoroacetic acid and phosphate buffer systems. There is no significant difference in separation capability between the two organic modifiers, methanol and acetonitrile.

The chiral purity of ACPC isomers can also be determined by derivatization with FDAA. The detection limit is less than 0.1% for the minor isomer in the presence of the major isomer.

#### 4. Conclusions

The described procedure can be applied for the separation and identification of four enantiomers: *cis*-(1*S*,2*R*)-, *cis*-(1*R*,2*S*)-, *trans*-(1*S*,2*S*)- and *trans*-(1*R*,2*R*)-2-aminocyclopentane-1-carboxylic acid. The method permits a check on the configuration of the amino acid after synthesis, and hence optimization of the conditions of synthesis. In general, the GITC derivatives give better resolution than the FDAA derivatives for

Table 3

Dependence of retention factor ( $k'$ ), separation factor ( $\alpha$ ) and resolution ( $R_s$ ) of ACPC–FDAA derivatives on eluent composition

Eluent composition	$k'$				$\alpha_{c,c}$	$\alpha_{c,t}$	$\alpha_{t,t}$	$R_{s;c,c}$	$R_{s;c,t}$	$R_{s;t,t}$
	<i>cis</i>		<i>trans</i>							
	(1 <i>R</i> ,2 <i>S</i> )	(1 <i>S</i> ,2 <i>R</i> )	(1 <i>S</i> ,2 <i>S</i> )	(1 <i>R</i> ,2 <i>R</i> )						
TFA–CH <sub>3</sub> OH										
50:50	3.75	10.92	13.26	21.36	2.91	1.21	1.61	8.90	2.36	5.41
52.5:47.5	4.95	14.89	16.67	27.51	3.01	1.12	1.65	10.25	2.37	6.41
55:45	6.80	21.26	23.14	38.97	3.12	1.09	1.68	14.72	2.40	8.67
KH <sub>2</sub> PO <sub>4</sub> –CH <sub>3</sub> OH										
50:50	3.50	10.81	11.43	18.58	3.08	1.05	1.62	8.70	1.05	6.20
52.5:47.5	4.51	14.14	15.25	25.13	3.13	1.08	1.65	9.34	1.08	6.62
55:45	6.36	20.59	22.41	37.52	3.23	1.09	1.67	15.01	1.52	8.61
NaOAc–CH <sub>3</sub> OH										
50:50	2.77	7.95	8.70	13.79	2.87	1.09	1.59	6.36	0.91	4.10
52.5:47.5	3.56	10.04	11.32	18.97	2.82	1.12	1.67	6.97	1.25	4.77
55:45	4.96	15.00	16.12	20.64	3.02	1.08	1.28	11.40	1.36	8.14

Column, Lichrospher 100 RP18; flow-rate, 0.8 ml/min; detection, 340 nm; TFA, 0.1% aqueous solution of trifluoroacetic acid; KH<sub>2</sub>PO<sub>4</sub>, 0.01 M aqueous solution of potassium dihydrogenphosphate (pH 3); NaOAc, 0.01 M aqueous solution of sodium acetate (pH 3);  $\alpha_{c,c}$  and  $R_{s;c,c}$  represent separation of *cis*-(1*R*,2*S*) and *cis*-(1*S*,2*R*) derivatives;  $\alpha_{c,t}$  and  $R_{s;c,t}$  represent separation of *cis*-(1*S*,2*R*) and *trans*-(1*S*,2*S*) derivatives;  $\alpha_{t,t}$  and  $R_{s;t,t}$  represent separation of *trans*-(1*S*,2*S*) and *trans*-(1*R*,2*R*) derivatives.

Table 4

Dependence of retention factor ( $k'$ ), separation factor ( $\alpha$ ) and resolution ( $R_s$ ) of ACPC–FDAA derivatives on eluent composition

Eluent composition	$k'$				$\alpha_{c,c}$	$\alpha_{c,t}$	$\alpha_{t,t}$	$R_{s;c,c}$	$R_{s;c,t}$	$R_{s;t,t}$
	<i>cis</i>		<i>trans</i>							
	(1 <i>R</i> ,2 <i>S</i> )	(1 <i>S</i> ,2 <i>R</i> )	(1 <i>S</i> ,2 <i>S</i> )	(1 <i>R</i> ,2 <i>R</i> )						
TFA–CH <sub>3</sub> CN										
70:30	5.32	10.49	11.90	19.20	1.97	1.14	1.61	6.89	1.58	5.85
72.5:27.5	6.89 <sup>a</sup>	16.26	18.68	32.70	–	1.14	1.75	–	2.19	8.77
KH <sub>2</sub> PO <sub>4</sub> –CH <sub>3</sub> CN										
70:30	5.01	8.97	10.24	16.70	1.79	1.14	1.63	5.78	1.27	4.67
72.5:27.5	6.46 <sup>a</sup>	14.03	16.24	27.86	–	1.16	1.72	–	2.60	9.18
NaOAc–CH <sub>3</sub> CN										
70:30	3.78	7.85	8.70	14.23	2.07	1.11	1.64	5.60	1.16	4.53
72.5:27.5	5.34	12.09	13.29	22.98	2.26	1.10	1.73	10.03	1.38	6.83

Column, Lichrospher 100 RP18; flow-rate, 0.8 ml/min; detection, 340 nm; TFA, 0.1% aqueous solution of trifluoroacetic acid; KH<sub>2</sub>PO<sub>4</sub>, 0.01 M aqueous solution of potassium dihydrogenphosphate (pH 3); NaOAc, 0.01 M aqueous solution of sodium acetate (pH 3);  $\alpha_{c,c}$  and  $R_{s;c,c}$  represent separation of *cis*-(1*R*,2*S*) and *cis*-(1*S*,2*R*) derivatives;  $\alpha_{c,t}$  and  $R_{s;c,t}$  represent separation of *cis*-(1*S*,2*R*) and *trans*-(1*S*,2*S*) derivatives;  $\alpha_{t,t}$  and  $R_{s;t,t}$  represent separation of *trans*-(1*S*,2*S*) and *trans*-(1*R*,2*R*) derivatives.

<sup>a</sup> The peak of the *cis*-(1*R*,2*S*) derivative coincides with that of unreacted FDAA.

all four enantiomers. Of the three buffer systems applied in the case of the GITC derivatives, the phosphate buffer seems best; in the case of the FDAA derivatives, trifluoroacetic acid seems most efficient. With respect to the two organic modifiers, the methanol-containing mobile phase system seems to be more efficient than the acetonitrile-containing one. The elution order of the diastereomers of the *cis* and *trans* isomer derivatives with GITC was opposite to that of the FDAA derivatives.

The detection limit for the minor isomer is less than 0.1% in excess of the major isomer.

### Acknowledgements

This work was supported in part by a grant from the Hungarian Research Foundation (OTKA T 14898). The authors express their thanks to Prof. Liisa Kanerva and Péter Csomós (Department of Chemistry, University of Turku, Finland) for the enzymatic resolutions of *cis*- and *trans*-ACPC.

### References

- [1] D.F. Mierke, G. Nössner, P.W. Schiller and M. Goodman, *Int. J. Peptide Protein Res.*, 35 (1990) 35.
- [2] T. Yamazaki, A. Pröbstl, P.W. Schiller and M. Goodman, *Int. J. Peptide Protein Res.*, 37 (1991) 364.
- [3] T. Yamazaki, Y.F. Zhu, A. Pröbstl, R.K. Chadha and M. Goodman, *J. Org. Chem.*, 56 (1991) 6644.
- [4] T. Yamazaki and M. Goodman, *Chirality*, 3 (1991) 268.
- [5] Z. Huang, A. Pröbstl, J.R. Spencer, T. Yamazaki and M. Goodman, *Int. J. Peptide Protein Res.*, 42 (1993) 352.
- [6] G. Bernáth, *Acta Chim. Hung. Mod. Chem.*, 129 (1992) 107.
- [7] G. Bernáth, L. Gera, G. Göndös, Z. Ecsery, M. Hermann, M. Szentiványi and E. Janváry, *Hung. Patent 172460* (*Chem. Abstr.*, 94 (1981) 175144).
- [8] F. Fülöp, G. Csirinyi and G. Bernáth, *Acta Chim. Hung.*, 125 (1988) 193.
- [9] F. Fülöp, K. Pihlaja, J. Mattinen and G. Bernáth, *Tetrahedron*, 43 (1987) 1863.
- [10] H. Pleiniger and K. Schneider, *Chem. Ber.*, 92 (1959) 1594.
- [11] G. Bernáth, K.L. Láng, G. Göndös, P. Márai and K. Kovács, *Acta Chim. Acad. Sci. Hung.*, 74 (1972) 479.
- [12] E. Nativ and P. Rona, *Isr. J. Chem.*, 10 (1972) 55.
- [13] M. Konishi, M. Nishio, K. Saitoh, T. Miyaki, T. Oki and H. Kawaguchi, *J. Antibiot.*, 42 (1989) 1749.
- [14] T. Oki, M. Hirano, K. Tomatsu, K. Numata and H. Kamei, *J. Antibiot.*, 42 (1989) 1756.
- [15] T. Iwamoto, E. Tsujii, M. Ezaki, A. Fujie, S. Hashimoto, M. Okuhara, M. Koshaka, H. Imanaka, K. Kawabata, Y. Inamoto and K. Sakane, *J. Antibiot.*, 43 (1990) 1.
- [16] K. Kawabata, Y. Inamoto, K. Sakane, T. Iwamoto and S. Hashimoto, *J. Antibiot.*, 43 (1990) 513.
- [17] J.O. Capobianco, D. Zakula, M.L. Coen and R.C. Goldman, *Biochem. Biophys. Res. Commun.*, 190 (1993) 1037.
- [18] N. Naruse, S. Yamamoto, H. Yamamoto, S. Kondo, S. Masuyoshi, K. Numata, Y. Fukagawa and T. Oki, *J. Antibiot.*, 46 (1993) 685.
- [19] C. Evans, R. McCague, S.M. Roberts, A.G. Sutherland and R. Wisdom, *J. Chem. Soc. Perkin Trans. 1*, (1991) 2276.
- [20] T. Konosu and S. Oida, *Chem. Pharm. Bull.*, 41 (1993) 1012.
- [21] S.G. Davies, O. Ichihara and I.A.S. Walters, *Synlett*, (1993) 461.
- [22] H. Nakano, Y. Okuyama, K. Iwasa and H. Hongo, *Tetrahedron Asymmetry*, 5 (1994) 1155.
- [23] N. Oishi, S. Maeno, M. Kobayashi, H. Sugiyama and K. Toyaka, *Jpn. Kokai Tokkyo Koho JP 63 83,040* (*Chem. Abstr.*, 109 (1988) 165710).
- [24] K. Sakane, K. Kawabata and Y. Inamoto, *Jpn. Kokai Tokkyo Koho JP 02 49,758* (*Chem. Abstr.*, 113 (1990) 40012).
- [25] K. Sakane, K. Kawabata and Y. Inamoto, *Jpn. Kokai Tokkyo Koho JP 02 174,753* (*Chem. Abstr.*, 114 (1991) 24607).
- [26] M. Miyauchi, E. Tsujii, M. Ezaki, H. Hashimoto and M. Okuhara, *Eur. Pat. Appl. EP 298,640* (*Chem. Abstr.*, 114 (1991) 24607).
- [27] S. Oida and T. Konosu, *Jpn. Kokai Tokkyo Koho JP 04 243,870* (*Chem. Abstr.*, 118 (1993) 80923).
- [28] C.T. Evans, S.M. Roberts and A.G. Sutherland, *PCT Int. Appl. WO 92 18,477* (*Chem. Abstr.*, 118 (1993) 168892).
- [29] Y. Mikami, G.M. Scaronone, N. Kurita, Y.K. Nobuyuki, K. Yazawa and M. Miyaji, *Nippon Ishinkin Gakkai Zasshi*, 33 (1992) 355 (*Chem. Abstr.*, 118 (1993) 76906).
- [30] P.J. Crowley, D. Youle and S.P. Heaney, *PCT Int. Appl. WO 94 03,061* (*Chem. Abstr.*, 120 (1994) 263835).
- [31] S.M. Roberts, *Pure Appl. Chem.*, 64 (1992) 1933.
- [32] W.H. Pirkle and J. Finn, in J. Morrison (Editor), *Asymmetric Synthesis, Vol. I, Analytical Methods*, Academic Press, New York, 1983, Ch. 6.
- [33] W.F. Lindner and C. Petterson, in I. Wainer (Editor), *Liquid Chromatography in Pharmaceutical Development: an Introduction*, Aster, Springfield, VA, 1985, Part 1.

- [34] D.W. Armstrong and S.M. Han, *CRC Crit. Rev. Anal. Chem.*, 19 (1988) 175.
- [35] V.A. Davankow, A.A. Kurganov and A.S. Bochkov, *Adv. Chromatogr.*, 22 (1983) 71.
- [36] C. Petterson, *Trends Anal. Chem.*, 7 (1988) 209.
- [37] W.F. Lindner, in L. Crane and B. Zief (Editors), *Chromatographic Chiral Separations*, Marcel Dekker, New York, 1987, p. 91.
- [38] W.F. Lindner, in J.F. Lawrence and R.W. Frei (Editors), *Chemical Derivatization in Analytical Chemistry*, Vol. 2, Plenum Press, New York, 1982, p. 145.
- [39] T. Nambara, in W.S. Hancock (Editor), *CRC Handbook of HPLC for the Separation of Amino Acids, Peptides and Proteins*, Vol. I, CRC Press, Boca Raton, FL, 1984, p. 383.
- [40] N. Nimura, H. Ogura and T. Kinoshita, *J. Chromatogr.*, 202 (1980) 375.
- [41] T. Kinoshita, Y. Kasahara and N. Nimura, *J. Chromatogr.*, 210 (1981) 77.
- [42] N. Nimura, A. Toyama and T. Kinoshita, *J. Chromatogr.*, 316 (1984) 547.
- [43] P. Marfey, *Carlsberg Res. Commun.*, 49 (1984) 591.
- [44] S. Einarsson, B. Josefsson, P. Möller and D. Sanchez, *Anal. Chem.*, 59 (1987) 1191.
- [45] H. Brückner and C. Gah, *J. Chromatogr.*, 555 (1991) 81.
- [46] H. Brückner, R. Wittner and H. Godel, *Chromatographia*, 32 (1991) 383.
- [47] H. Brückner and B. Strecker, *Chromatographia*, 33 (1992) 586.
- [48] S. Einarsson and G. Hansson, in C.T. Mant and R.S. Hodges (Editors), *High Performance Liquid Chromatography of Peptides and Proteins*, CRC Press, Boca Raton, FL, 1991, p. 369.
- [49] L. Kanerva, P. Csomós, F. Fülöp and G. Bernáth, *Tetrahedron*, submitted for publication.
- [50] A.E. Martell and R.M. Smith (Editors), *Critical Stability Constants*, Vol. 1, Plenum, Press, 1974.
- [51] A. Péter, G. Tóth and D. Tourwé, *J. Chromatogr. A*, 668 (1994) 331.
- [52] A. Péter, G. Tóth, E. Olajos, F. Fülöp and D. Tourwé, *J. Chromatogr. A*, 705 (1995) 257.



ELSEVIER

Journal of Chromatography A, 715 (1995) 227–240

JOURNAL OF  
CHROMATOGRAPHY A

## Investigation of crudes of synthesis of neuropeptide Y by high-performance liquid chromatography–electrospray mass spectrometry

Andrea Casazza<sup>a</sup>, Ornella Curcuruto<sup>a</sup>, Mahmoud Hamdan<sup>a,\*</sup>, Alessandro Bisello<sup>b</sup>, Evaristo Peggion<sup>b</sup>

<sup>a</sup>Mass Spectrometry Laboratory, Analytical Sciences Department, Centro Ricerche Glaxo, Via A. Fleming 4, 37134 Verona, Italy

<sup>b</sup>Centro Studio Biopolimeri, Dipartimento Chimica Organica, Università di Padova, Via Marzolo 4, 35131 Padova, Italy

First received 6 March 1995; revised manuscript received 19 May 1995; accepted 22 May 1995

### Abstract

Neuropeptide Y (NPY) and its modified form, [Leu<sup>31</sup>,Pro<sup>34</sup>]NPY, are both thirty six amino acids long and they have relative molecular masses of 4250 and 4220. Solid-phase synthesis of both peptides resulted in complex crudes of reaction, which were investigated by means of combined high-performance liquid chromatography–electrospray mass spectrometry (HPLC–ES-MS). The combination of these two powerful analytical techniques allowed rapid and reliable identification of the target peptides and furnished comprehensive information on other reaction products, which were mainly peptidic chains containing a smaller number of amino acids compared to those present in the intact peptides. The possible origin of such side-products and the eventual purification and unambiguous identification of both peptides are discussed.

### 1. Introduction

Electrospray ionization (ESI) mass spectrometry (MS) has been extensively used for the characterization of small proteins [1–4] and peptides [5,6].

Neuropeptide Y (NPY) was first sequenced by Tatemoto [7] and is considered a major regulatory peptide both in the central and the peripheral nervous system [8]. In the central system, NPY is believed to be involved in the regulation of food intake, memory processing and circadian rhythm. In the peripheral nervous system, the

same peptide functions as transmitter in sympathetic nerves, where it acts together with norepinephrine in the regulation of vascular tone. NPY has also been identified as a therapeutic agent against shocks restoring blood pressure to its normal level [9,10]. In general, substantial and pure quantities are needed for three-dimensional structural characterization of this peptide. Most of present day synthesis of peptides and small proteins is mainly based on the solid-phase method, first introduced by Merrifield [11]. In this procedure of synthesis, a progressively growing peptidic chain is bounded to an insoluble resin by the carboxylic function of the C-terminal amino acid. The synthesis

\* Corresponding author.

proceeds through successive couplings between the activated amino acids and the free amine function of the peptidic chain already linked to the insoluble resin. This synthetic procedure commonly results in unwanted products associated with the absence of one or more amino acids. To reduce the number of such products and to simplify inevitable high-performance liquid chromatography (HPLC) separation, the capping procedure is often adopted [11]. Such a procedure involves the acetylation of the unreacted amine functions following each coupling process. The complexity of the resulting crude of synthesis renders combined HPLC–mass spectrometry an indispensable analytical tool for fast and reliable identification of the target peptide and associated side-products.

## 2. Experimental

All presented mass spectrometric measurements were obtained using a single-quadrupole instrument (VG Platform, Fisons Instruments, Manchester, UK), which has an upper mass range of 3000. Direct-injection (no HPLC separation) measurements were performed using a Phoenix 20 CU pump (Fisons Instruments); a mobile phase composed of acetonitrile–water (50:50; v/v), 10  $\mu$ l/min flow-rate, a 10- $\mu$ l loop and sample concentrations of 20 pmol/ $\mu$ l (artificial mixture) and 85 mg/l (crude of synthesis) were used.

### 2.1. Analytical HPLC

Initial analytical HPLC of the two crudes of synthesis was performed using the following conditions: Perkin-Elmer 3B HPLC pump (Perkin-Elmer and Applied Biosystem, Foster City, CA, USA) equipped with a Perkin-Elmer LC75 UV spectrophotometer, a Perkin-Elmer 56 recorder and a Perkin-Elmer Sigma 15 data station; Vydac narrow-bore C<sub>18</sub> RP, 300 Å (150 × 2.1 mm I.D., 5  $\mu$ m particle size) column (Vydac, Hesperia, CA, USA); 200  $\mu$ l/min flow-rate, 220

nm wavelength and 1 mg/ml sample concentration. The solvents used in the gradient method were: solvent A, acetonitrile–water (3:1, v/v) containing 0.1% trifluoroacetic acid (TFA); solvent B, water containing 0.1% TFA and sample concentration of 1 mg/ml. The gradient sequence was: time (*t*) 0–3 min 24% A, which over 64 min reached 66.6% A, remaining constant for 5 min, and going to 100% A in 10 min. The same HPLC conditions were used for the analysis of [Leu<sup>31</sup>,Pro<sup>34</sup>]NPY crude of synthesis with two variations: 216 nm instead of 220 nm wavelength and gradient sequence from (*t*) 0–3 min: 40% A, which over 29 min reached 49.5% A, remaining constant for 5 min and going to 100% A in 3 min.

### 2.2. HPLC–MS

The analytical conditions were: Phoenix 20CU HPLC pump (Fisons Instruments); VG Platform mass spectrometer (Fisons Instruments) equipped with an electrospray ion source, Ultramex 5 C<sub>18</sub> (250 × 1 mm I.D.) column (Phenomenex, Torrance, CA, USA); 30  $\mu$ l/min flow-rate, 2- $\mu$ l loop and sample concentration of 0.25 mg/ml. The gradient solvents used were the same as described above. The gradient sequences were: (a) artificial mixture: from 30% A to 70% A in 30 min, (b) NPY crude of synthesis: from 45% A to 89% A in 50 min, and (c) [Leu<sup>31</sup>,Pro<sup>34</sup>]NPY crude of synthesis: from 65% A to 75% A in 40 min.

### 2.3. Preparative HPLC

The analysis conditions were: Shimadzu LC-8A pump, Shimadzu-6A UV detector, Shimadzu C-R6A chromatopack data station (Shimadzu Europe, Duisburg, Germany), Deltapack C<sub>18</sub> RP (300 × 1.9 mm I.D., 15  $\mu$ m particle size) column, 20 ml/min flow-rate and 220 nm wavelength. The gradient sequence was: *t* = 0 100% B, reaching 73.4% B in 10 min, 33.4% B in 150 min, remaining constant for 10 min and reaching 100% A in 2 min.

## 2.4. Synthesis

The synthesis of NPY and [Leu<sup>31</sup>,Pro<sup>34</sup>]NPY was based on solid-phase methods using an automated peptide synthesizer (Applied Biosystem 431A). The resin (Bachem Feinchemikalien, Bubendorf, Switzerland) contained Fmoc-4-methoxy-4'-(carboxypropyl)-benzylamine linked to alanyl-aminomethyl-polystyrene-1% divinylbenzene (substitution 0.6 mmol/g). For NPY the activation of the Fmoc-amino acid was performed in situ with HBTU–HOBT–DIPEA. A four-fold excess of the activated amino acid was used and acetylation of the unreacted amino functions was performed at the end of each coupling step using 10% acetic anhydride in NMP. For [Leu<sup>31</sup>,Pro<sup>34</sup>]NPY the activation was performed with HOBT–DCC in NMP for 30 min. A four-fold excess of the active ester was used but no capping was done. In both syntheses every Arg(Mtr) was recoupled. After completion of the sequence the peptide was cleaved from the solid support with simultaneous deprotection of the side chains using a mixture of TFA–thioanisole–phenol–ethanedithiol–water (84:4:6:4:3) at 25°C for 4 h. After filtration and removal of the volatiles, the residual Mtr groups were cleaved with TFA–thioanisole–trimethylsilylbromide (6:1:1) at 0°C for 1 h. The mixture was then concentrated under reduced pressure, water was added and the solution was extracted with diethyl ether. The crude peptides were recovered by lyophilization.

## 2.5. Materials

Fmoc-L-Pro-OH, Fmoc-L-Ala-OH, Fmoc-L-Glu-(OtBu)-OH, Fmoc-L-Asp(OtBu), Fmoc-L-Leu-OH, Fmoc-L-Arg(Mtr)-OH, Fmoc-L-Tyr(tBu)-OH, Fmoc-L-Ser(tBu)-OH, Fmoc-L-His(Trt)-OH, Fmoc-L-Ile-OH, Fmoc-L-Asn(Trt)-OH, Fmoc-L-Thr(tBu)-OH, Fmoc-L-Gln-(Trt)-OH were purchased from Applied BioSystems; Fmoc-L-Ala-NCA, Fmoc-L-Arg(Mtr)-NCA, Fmoc-L-Ser(tBu)-NCA, Fmoc-L-Leu-NCA, Fmoc-Ile-NCA, Fmoc-L-Asn(Trt)-NCA, Fmoc-Thr(tBu)-NCA, Fmoc-Gln(Trt)-

NCA were purchased from Propeptide (Vert-le-Petit, France).

N-Methylpyrrolidone (NMP), dichloromethane, piperidine, 1-hydroxybenzo-triazole, N,N'-dicyclohexylcarbodiimide, acetic anhydride and trifluoroacetic acid were purchased from Applied BioSystems; diisopropylethylamine, ethanedithiol and thioanisole from Fluka Chemie (Buchs, Switzerland); acetonitrile and phenol from Carlo Erba Reagenti (Milan, Italy).

## 3. Results and discussion

It is commonly argued that under certain ion source conditions, electrospray ionization can yield simple ES mass spectra with negligible fragmentation allowing reasonable identification of the molecular identities within a mixture without the need for chromatographic separation prior to the mass spectrometric analysis. However, the usefulness of this characteristic of ES ionization is highly dependent on the complexity of the investigated medium and the chemical nature of its components. To underline this observation, three mixtures are considered, where the first is artificially made by mixing equal concentrations of [Leu<sup>31</sup>,Pro<sup>34</sup>]NPY ( $M_r$  4220), [D-Phe<sup>12</sup>]bombesin ( $M_r$  1628) and alytesin ( $M_r$  1534), while the second and third mixtures are the crudes of synthesis of NPY and [Leu<sup>31</sup>,Pro<sup>34</sup>]NPY obtained in two different procedures of synthesis. These analysis were performed using 30°C source temperature, 35 V extraction (cone) voltage and 3 kV capillary voltage.

### 3.1. Artificial mixture of [Leu<sup>31</sup>,Pro<sup>34</sup>]NPY, [D-Phe<sup>12</sup>]bombesin and alytesin

Equal concentrations (20 pmol/ $\mu$ l) of the three peptides in acetonitrile–water (50:50, v/v) were directly injected into the ion source. The resulting ES mass spectrum in Fig. 1a contains the multiply charged ions 1056 [M + 4H]<sup>4+</sup> and 604 [M + 7H]<sup>7+</sup> of [Leu<sup>31</sup>,Pro<sup>34</sup>]NPY. The singly and doubly protonated alytesin are observed at A ( $m/z$  1535) and A2 ( $m/z$  768), while the

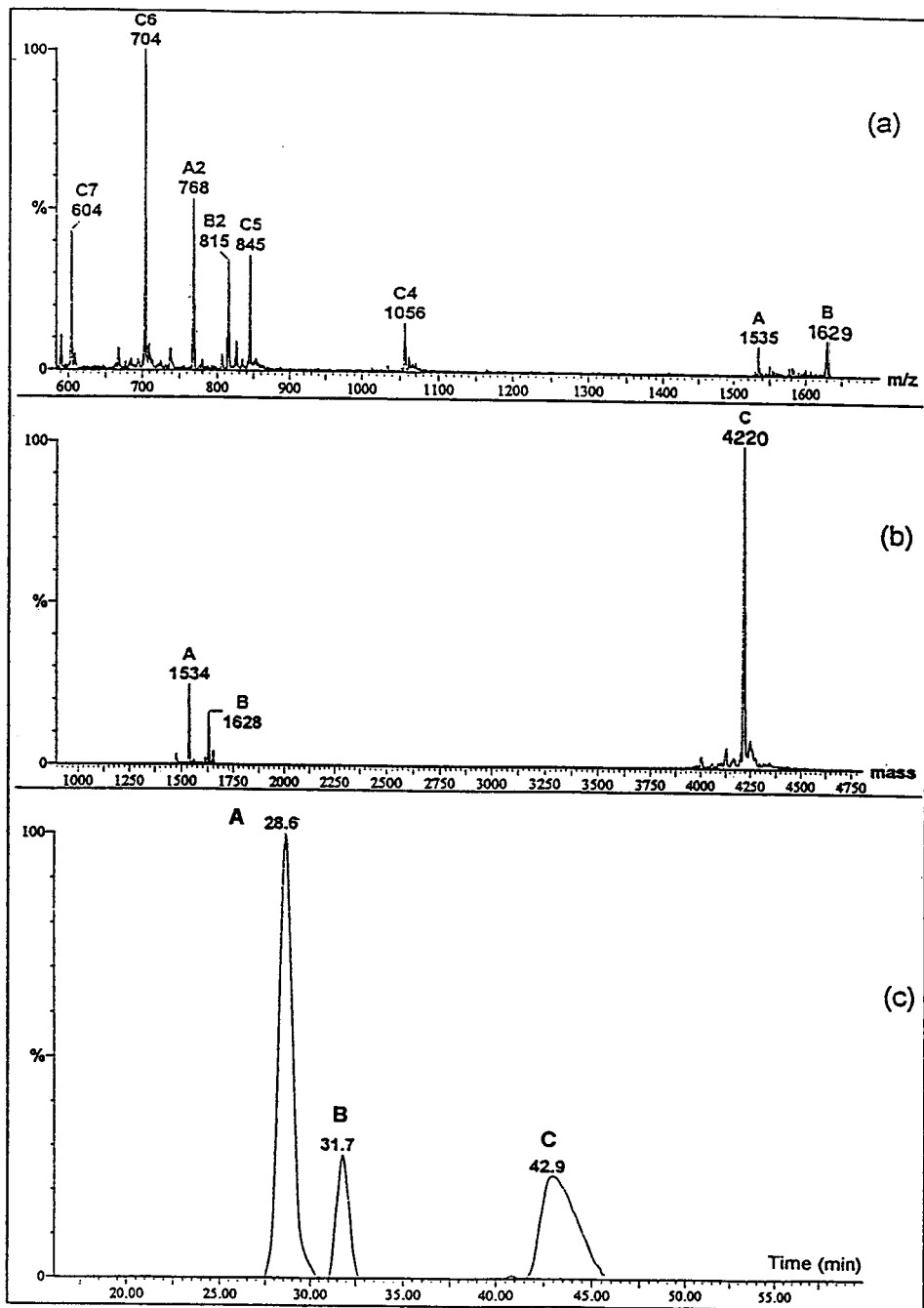


Fig. 1. (a) Charge-state distribution in the ES mass spectrum of an artificial mixture containing alytesin, [Phe<sup>12</sup>]bombesin and [Leu<sup>31</sup>,Pro<sup>34</sup>]NPY injected into the ion source without chromatographic separation; (b) measured relative molecular masses of the three peptides obtained by algorithmic transformation of the above charge-state distributions and (c) total-ion current (TIC) chromatogram of HPLC-ES-MS of the same mixture, with peak A (alytesin), peak B ([Phe<sup>12</sup>]bombesin) and peak C ([Leu<sup>31</sup>,Pro<sup>34</sup>]NPY).



corresponding ions of [D-Phe<sup>12</sup>]bombesin are observed at B ( $m/z$  1629) and B2 ( $m/z$  815). Algorithmic transformation of the three charge-state distributions yielded the relative intensities of the three ion species in the mixture as a function of their relative molecular masses (Fig. 1b).

The investigation of the same mixture by HPLC–ES–MS resulted in the total-ion current (TIC) chromatogram in Fig. 1c. The three peaks with the retention times ( $t_R$ ) 28.6, 31.7 and 42.9 min are attributed to altytesin, [D-Phe<sup>12</sup>]bombesin and [Leu<sup>31</sup>,Pro<sup>34</sup>]NPY, respectively.

The ES mass spectra under these peaks (Figs. 2a,b,c) contain charge-state distributions which are not substantially different from those reported in Fig. 1a. This agreement between the two sets of ES data obtained with and without HPLC separation was not evident in the data of the crudes of synthesis, which are discussed below. Apart from this deduction, the data pertaining to the artificial mixture served two purposes. First, optimization of the ion source conditions prior to the investigation of completely unknown crudes of synthesis and second, the same data furnished valuable information on the charge-states distribution of [Leu<sup>31</sup>,Pro<sup>34</sup>]NPY in the presence of other components in the electro-sprayed solution.

### 3.2. HPLC–ES–MS of the NPY crude of synthesis

Solid-phase synthesis [10] of the peptide NPY yielded a crude mixture which upon investigation by gradient HPLC resulted in the UV chromatogram in Fig. 3a. As well as the target NPY ( $t_R = 40.4$  min), the chromatogram contains other, unidentified peaks with the indicated retention times. The complexity of the crude was further confirmed by its ES mass spectrum (Fig. 3b) obtained by direct injection into the ion source of a solution containing  $8.5 \cdot 10^{-2}$  mg/ml dissolved in acetonitrile–water (50:50, v/v) and using a 10  $\mu$ l/min flow-rate. The multiply charged ions marked A4–A7 are attributed to  $[M + 4H]^{4+}$  and  $[M + 7H]^{7+}$  of the NPY, while

other significant charge-state distributions marked B3–B6 and C3–C4 are assigned to two fragments with relative molecular masses 3492 and 2271, respectively.

The identification of other significant peaks in the same spectrum required further HPLC–ES–MS measurements. To gain further information on the various components observed in the UV chromatogram, HPLC–ES–MS analysis was performed. However, before performing such analysis, the analytical HPLC parameters were modified to allow micro-bore column analysis. Such modification had two advantages: improved concentration detection limits and a lower flow-rate (30  $\mu$ l/min) more adequate for electrospray ionization.

The HPLC–ES–MS of the crude of synthesis resulted in the total-ion current chromatogram in Fig. 3c, in which the target NPY is observed at the retention time of 36.8 min. The ES mass spectrum under this peak (Fig. 4a) exhibits the multiply charged ions (A3–A6) of the NPY.

The ES mass spectra under the TIC peaks with the retention times 38.5 and 45.0 min are given in Fig. 4b,c. The first spectrum contains a single charge-state distribution (A2–A4) yielding a relative molecular mass of 2270, while the spectrum in Fig. 4c exhibits two charge-state distributions, A and B, which yielded the relative molecular masses 3490 and 2852. Based on the mass spectra in Fig. 4 and other mass spectra which are not presented here, the relative molecular masses and most likely amino acid composition of the various peptidic chains within the crude of synthesis are summarized in Table 1. Close inspection of this table reveals that most of the acetylated peptidic chains contain 8–16 amino acids [Ac(28–36), Ac(20–36)]. These and similar incomplete (difficult) sequences are commonly observed in solid-phase peptide synthesis.

The chemistry related to repeated sequential coupling of amino acid residues to a growing terminal section of a peptide attached to a lightly cross-linked solid resin has been extensively investigated [12]. Couplings considered difficult and/or of low yield tend to occur with particular sequences. These difficulties have been variously attributed to association complexes, swelling

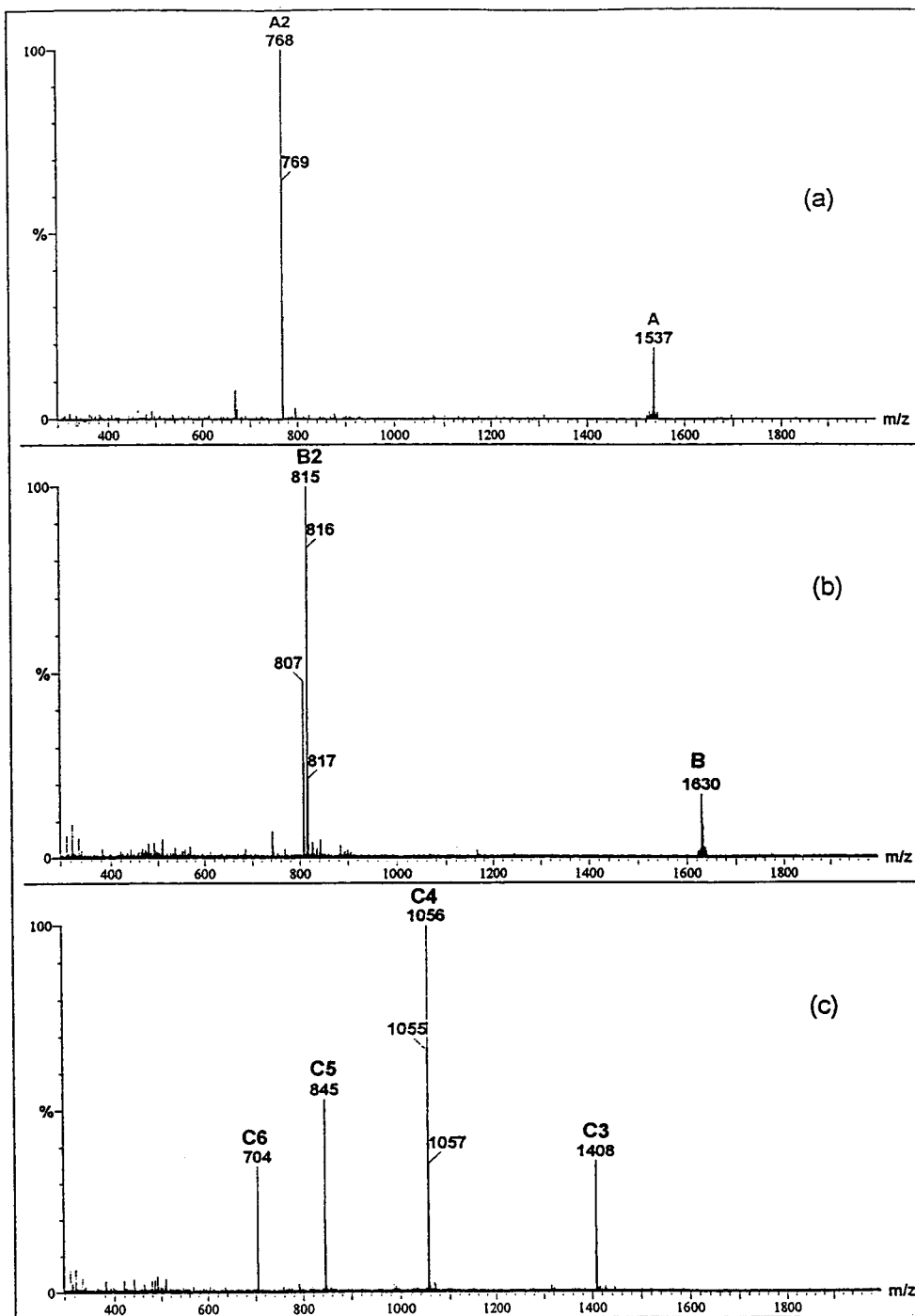


Fig. 2. Charge-state distributions under the TIC peaks in Fig. 1c; (a)  $t_R = 28.6$  min, (b) 31.7 min, and (c) 42.9 min.

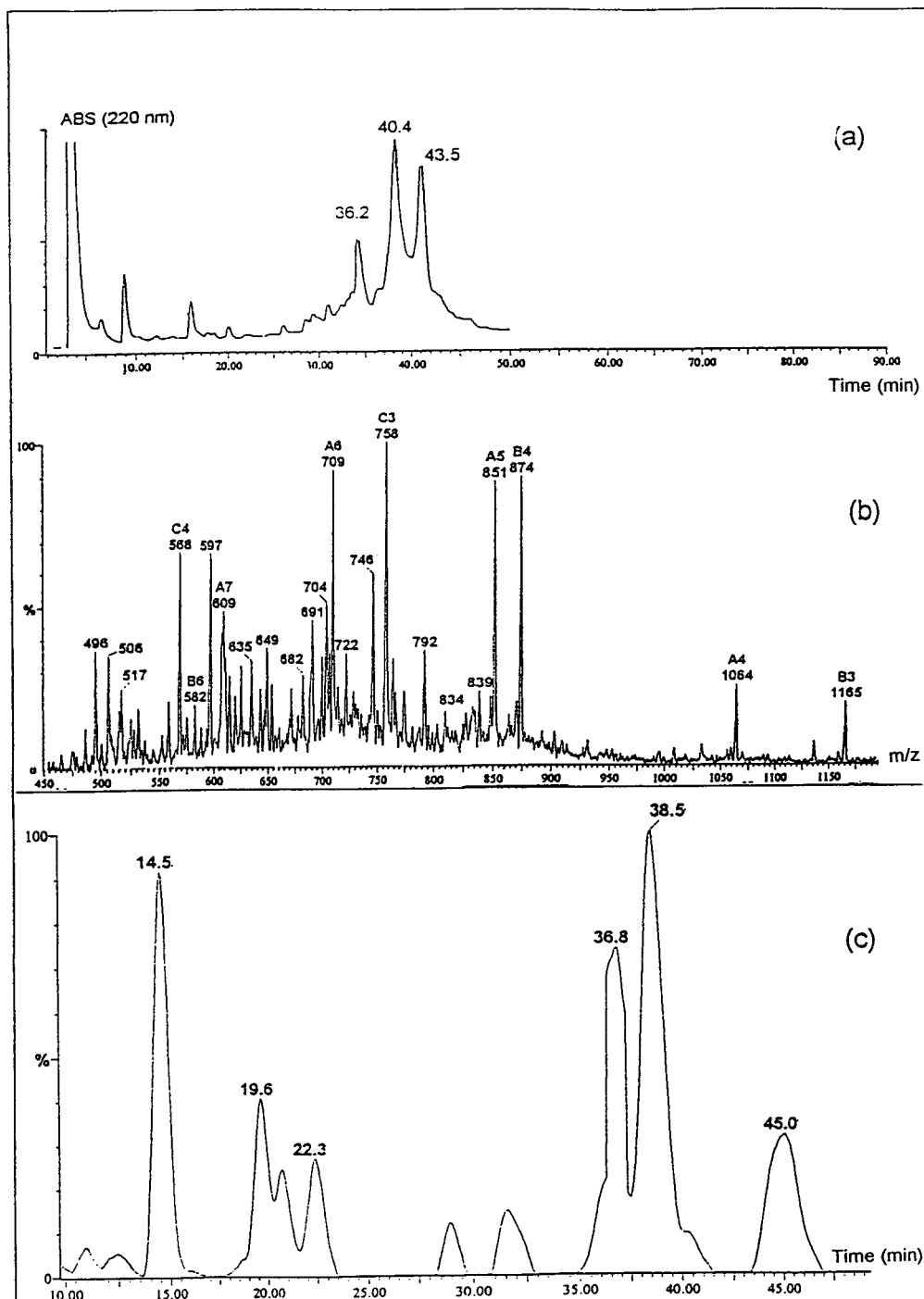


Fig. 3. (a) UV (220 nm) chromatogram of the NPY crude of synthesis, (b) charge-state distributions in the ES mass spectrum of the mixture injected into the ion source without chromatographic separation and (c) TIC chromatogram obtained by HPLC-ES-MS of the same mixture.

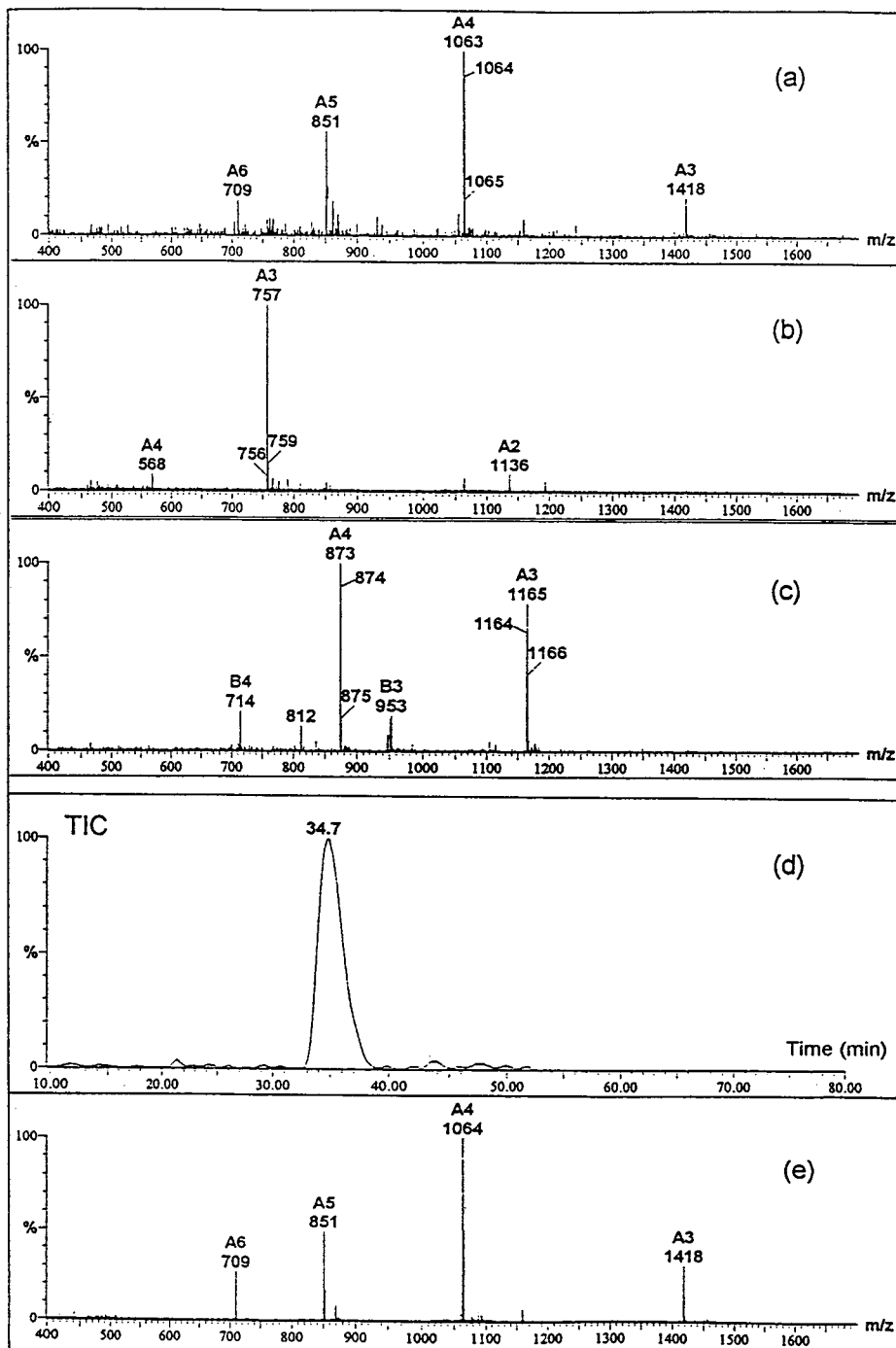


Fig. 4. Charge-state distributions in the ES mass spectra under the TIC peaks in Fig. 3c at the retention times ( $t_R$ ) of: (a) 36.8 min, (b) 38.5 min and (c) 45.0 min; (d) TIC chromatogram of the purified NPY, and (e) charge-state distribution in the ES mass spectrum under the NPY peak (d).

Table 1  
Relative molecular masses ( $M_r$ ) of acetylated chains and the numeric position ( $x$ ) of the final amino acid attached

$x$	$M_r = \text{Ac}(x - 36)$	$x$	$M_r = \text{Ac}(x - 36)$	
36	222	18	2496	
35	378	17	2609	
34	506	16	2724	
33	662	15	2853	
32	763	14	2924	
31	876	13	3021	
30	989	*	3092	
29	1103	11	3207	
28	1216	*	10	3336
27	1379	*	9	3393
26	1516	*	8	3490
25	1672	*	7	3604
24	1785	*	6	3719
23	1856	*	5	3816
22	1943	*	4	3944
21	2106	*	3	4031
20	2269	*	2	4128
19	2425		–	

The symbol \* refers to the peptidic chains which have been identified in the present work.

problems and hydrogen-bond aggregation of the growing peptide chains [13,14]. Although it has been always assumed that the solid support could isolate the growing peptide chains, creating chemically dilute environments [15], it has now been shown that site–site reactions between different chains do occur, resulting in incomplete sequences.

Based on the data presented, it is evident that the use of HPLC–ES–MS allowed reliable identification of the target NPY and it underlined the need for further purification. This was done using preparative HPLC followed by HPLC–ES–MS analysis, which resulted in a single TIC peak centered at  $t_R = 34.7$  min (Fig. 4d), under which the ES mass spectrum in Fig. 4e was obtained. The observation of a single charge-state distribution (A3–A6) centered at  $m/z$  1063 infers the presence of a single identity with a relative molecular mass of 4250 corresponding to the NPY peptide.

### 3.3. HPLC–ES–MS of [Leu<sup>31</sup>,Pro<sup>34</sup>]NPY crude of synthesis

The method of synthesis of this peptide did not involve capping. In other words, acetylation was not applied to the sites where coupling was not successful. In theory, such procedure is expected to result in a more complicated crude of synthesis compared to that obtained in the synthesis of NPY. Such expected complexity and in particular the lack of resolution is clearly evident in the UV chromatogram in Fig. 5a. The total-ion current (TIC) chromatogram of the same crude of synthesis obtained using 30  $\mu\text{l}/\text{min}$  flow-rate, Ultramex column and positive ES ionization is given in Fig. 5b.

The qualitative differences between the two chromatograms in Fig. 5 can be attributed to two reasons. First, the two chromatograms were generated under different experimental conditions including different columns, different sample concentrations and different flow-rates. Second, the top chromatogram refers to UV absorption by various components present in solution, while the bottom chromatogram reflects the protonation efficiency of gas-phase molecules.

The ES mass spectrum (Fig. 6a) under the twin peak with retention times 21.7 and 22.9 min contains three charge-state distributions, marked A, B and C.

The first distribution (A3–A6) is attributed to the target compound [Leu<sup>31</sup>,Pro<sup>34</sup>]NPY, while the distributions (B3–B5) and (C3–C5) are due to incomplete peptidic chains with relative molecular masses of 4110 and 3816, respectively.

The dominant TIC peak centered at 13.0 min is due to a relatively pure component with relative molecular mass of 1486, while the peak at  $t_R = 27.9$  min contains two molecular identities with relative molecular masses of 3978 (A), and 747 (B), respectively.

The data in Figs. 5 and 6 underlined the need for further purification of the target compound. Such purification was performed in two stages, involving preparative HPLC followed by a relatively slow gradient HPLC, which resulted in the UV chromatogram in Fig. 7a. The observation of

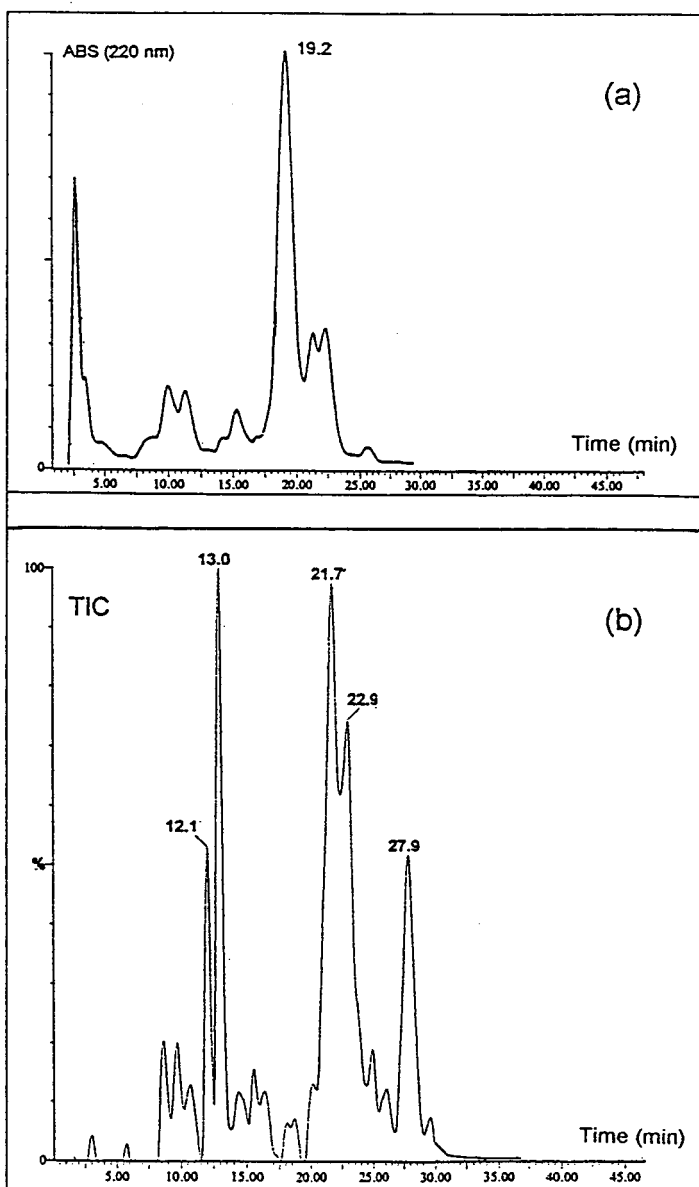


Fig. 5. UV (220 nm) chromatogram of  $[\text{Leu}^{31},\text{Pro}^{34}]\text{NPY}$  crude of synthesis and (b) TIC chromatogram of the same mixture obtained by HPLC-ES-MS.

a single Gaussian peak and the absence of substantial baseline noise gives the impression of a pure product. This apparent purity is not confirmed by the ES mass spectrum under this peak (Fig. 7b), which contains two charge-state distributions, (A3–A5) and (B3–B5), which

upon transformation (Fig. 7c) gave two molecular masses, 4220  $[\text{Leu}^{31},\text{Pro}^{34}]\text{NPY}$ , and 4106.

The observation of the latter molecular identity can be simply attributed to collision-induced dissociation of the intact peptide in the intermediate region of the ion source, which is held at

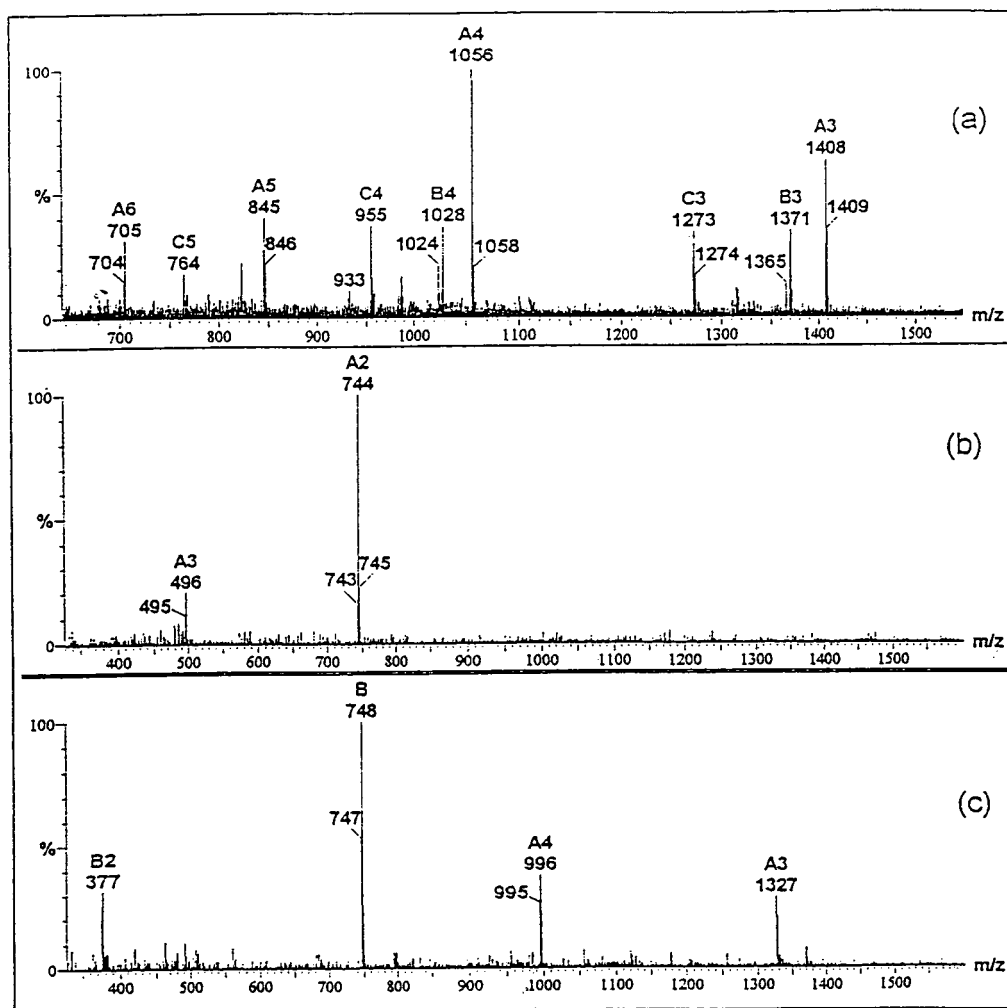


Fig. 6. Charge-state distributions in the ES mass spectra under the TIC peaks in Fig. 5b at the retention times: (a) 21.7–22.9 min, (b) 13.0 min, and (c) 27.9 min.

a pressure of ca. 0.1 mbar. This interpretation, however, cannot be fully sustained for a number of reasons. First, both C- and N-terminals contain tyrosine ( $M_r$  181), which excludes the loss of 114 as the first step of dissociation; second, peak slicing by means of preparative HPLC resulted in three fractions pertaining to the leading part of the peak, the center and the trailing part, which were isolated and examined by ES mass spectrometry.

The transformed mass spectra in Fig. 8a,b,c indicate that the leading part of the purified

HPLC peak contains exclusively  $[\text{Leu}^{31}, \text{Pro}^{34}] \text{NPY}$ , while the central and trailing portions of the same peak contain the same peptide as well as a second component with a molecular mass of 4106. The absence of the latter molecular identity from the leading portion of the HPLC peak is a clear indication that this component is not the result of fragmentation within the ion source.

Considering the HPLC–ES–MS data and the procedure of synthesis, the molecular mass 4106 is attributed to the absence of one of the as-

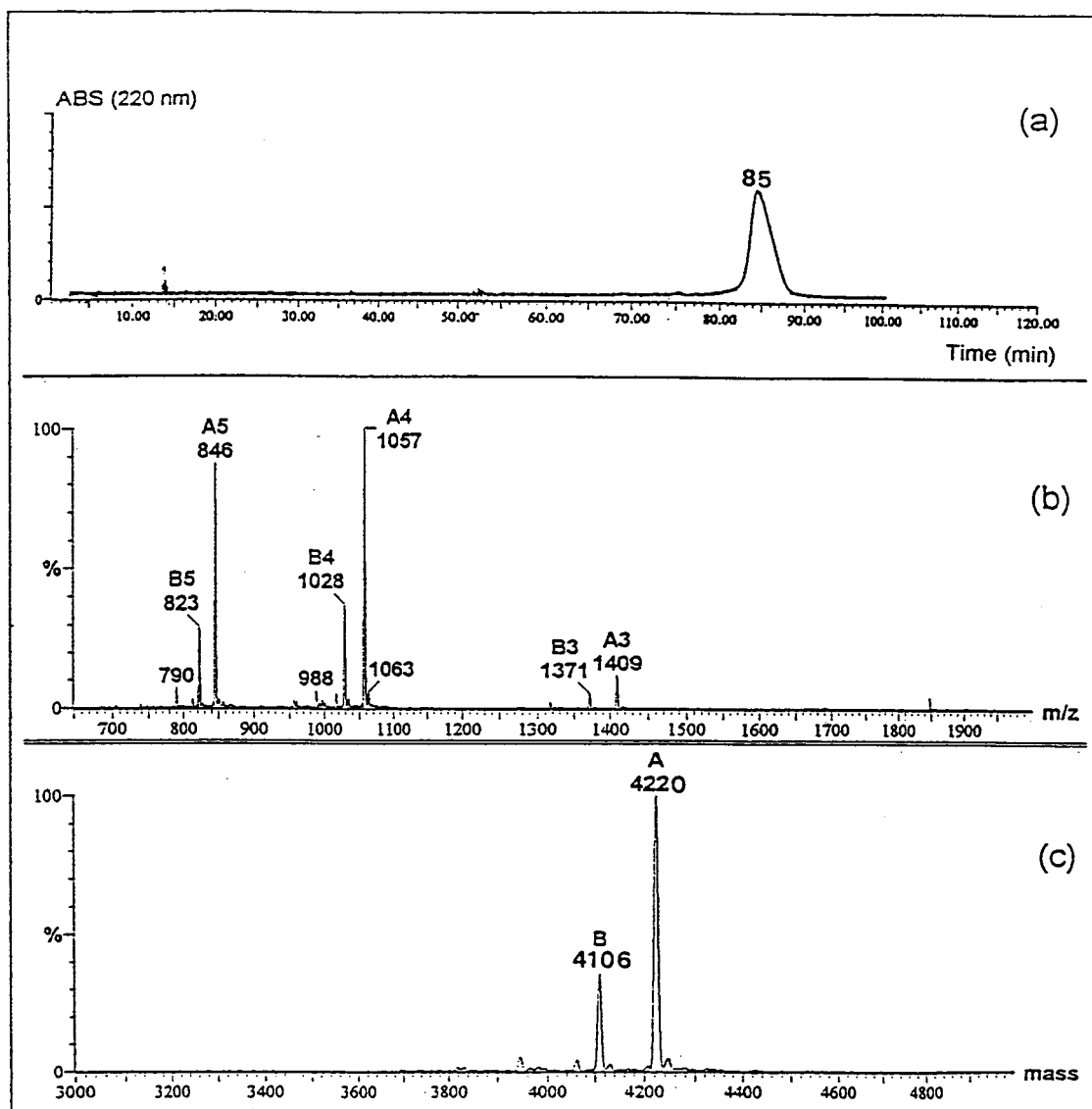


Fig. 7. (a) UV (220 nm) chromatogram obtained by preparative HPLC of  $[\text{Leu}^{31}, \text{Pro}^{34}]$ NPY crude of synthesis, (b) charge-state distributions in the ES mass spectrum under the above peak and (c) measured relative molecular masses obtained by algorithmic transformation of the charge-state distributions.

paragine residues ( $M_r$  114) from the amino acids sequence of  $[\text{Leu}^{31}, \text{Pro}^{34}]$ NPY.

#### 4. Conclusions

The combination of HPLC and electrospray ionization mass spectrometry provides an effi-

cient analytical tool for fast separation and reliable identification of the major components present in a fairly complex medium, which are commonly encountered in the crudes of synthesis of large peptides and small proteins. The mildness and mass specific capabilities of ES mass spectrometry permitted the following deductions. First, unambiguous identification of the



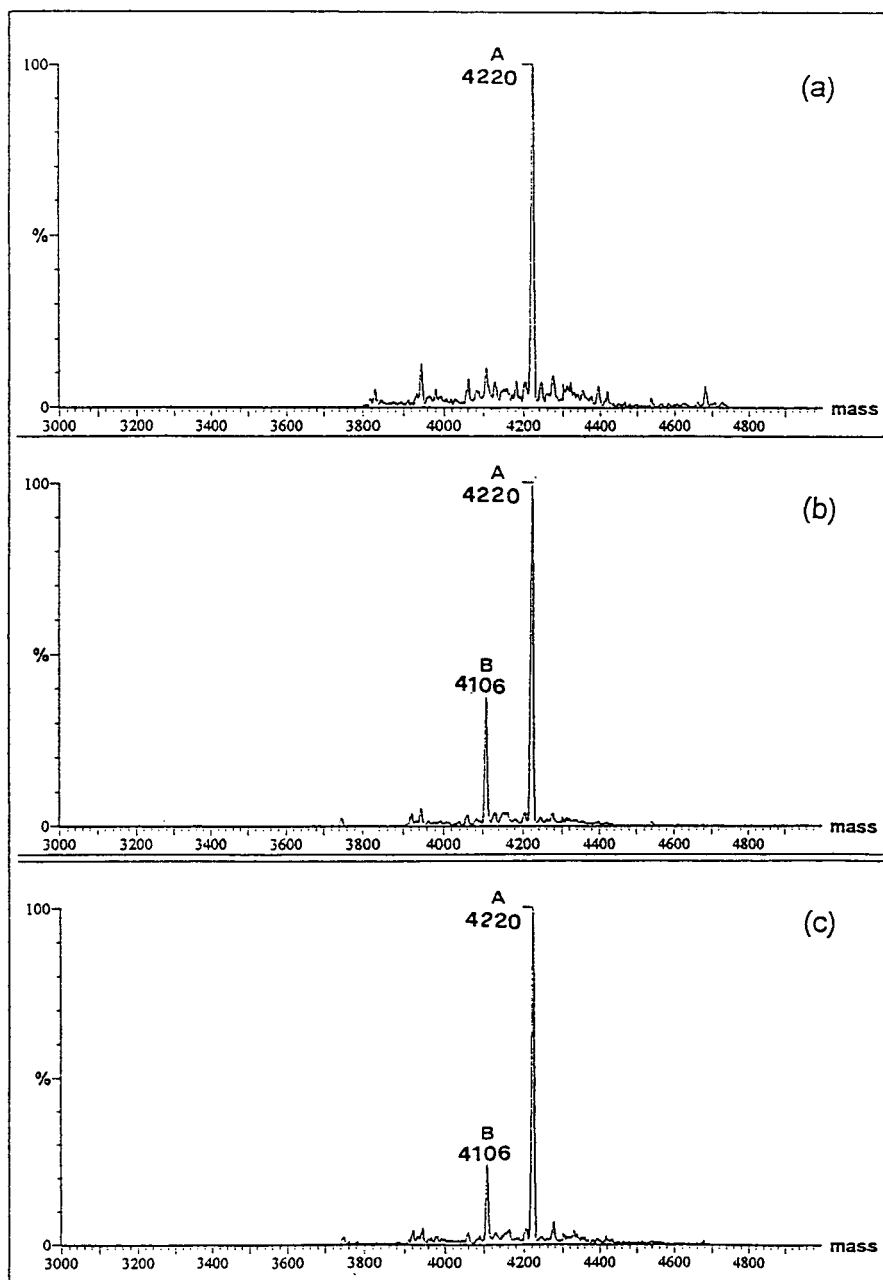


Fig. 8. Measured relative molecular masses obtained by algorithmic transformation of the charge-state distributions of the three fractions obtained by preparative HPLC slicing of the peak in Fig. 7a: (a) leading fraction, (b) central fraction, and (c) trailing fraction.

target peptides in the various stages of chromatographic separation and purification. Second, reliable molecular mass identification of various incomplete peptidic chains within the resulting crudes of synthesis and third, differentiation between two peptidic components within a single chromatographic peak which, because of their closely related amino acid sequence, could not be distinguished by HPLC alone.

## References

- [1] A.P. Bruins, T.R. Covey and J.D. Henion, *Anal. Chem.*, 59 (1987) 2642.
- [2] J.A. Loo, H.R. Udseth and R.D. Smith, *Anal. Biochem.*, 179 (1989) 404.
- [3] R. Feng and Y. Konishi, *Anal. Chem.*, 64 (1992) 2090.
- [4] J.B. Fenn, M. Mann, C.K. Meng, S.F. Wong and C.M. Whitehouse, *Science*, 246 (1989) 64.
- [5] B.T. Chait and S.B.H. Kent, *Science*, 257 (1992) 1884.
- [6] P.A. Scindler, A. Van Dorosselaer and A.M. Falik, *Anal. Biochem.*, 213 (1993) 256.
- [7] K. Tatemoto, *Proc. Natl. Acad. Sci. USA*, 79 (1982) 5485.
- [8] H.V. Mutt and K. Fuxe (Editors), *Neuropeptides*, 14th Nobel Symposium, Raven Press, New York, 1989.
- [9] D. Evequoz, B. Waeber, J.F. Aubert, J.P. Fluckinger, J. Nussberger and H.R. Brunner, *Circ. Res.*, 62 (1988) 23.
- [10] D. Evequoz, B. Waeber, R. Corder, T. Nussberger, R. Gaillard and H.R. Brunner, *Life Sci.*, 41 (1987) 2573.
- [11] R.B. Merrifield, *J. Am. Chem. Soc.*, 85 (1963) 2149.
- [12] G. Barany and R.B. Merrifield, in E. Gross and J. Meienhofer (Editors), *The Peptides*, Vol. 2, Academic Press, New York, 1974, pp. 1–284.
- [13] S. Kent and I. Clark-Lewis, in K. Alitalo, P. Partanen and A. Vaheri (Editors), *Synthetic Peptides in Biology and Medicine*, Elsevier, Amsterdam, 1986.
- [14] R.B. Merrifield, *Br. Polym. J.*, 16 (1984) 173.
- [15] K.K. Bhargava, V.K. Sarin, N.L. Trang, A. Cerami and R.B. Merrifield, *J. Am. Chem. Soc.*, 105 (1983) 3247.

## Quantitation of monoclonal antibodies by perfusion chromatography–immunodetection

L. Gadowski, A. Abdul-Wajid\*

*Analytical Development, Biomira, 2011-94 Street, Edmonton, Alb. T6N 1H1, Canada*

First received 9 February 1995; revised manuscript received 23 May 1995; accepted 23 May 1995

### Abstract

The ImmunoDetection PG (protein G) cartridge which is based on perfusion chromatography has been evaluated for the quantitation of murine monoclonal antibody (IgG1) in biological fluids. The results indicate a low intra-day coefficient of variation (C.V.)  $\leq 5\%$  and a sample analysis time of 5.5 min. A standard curve generated using injection of known amounts of monomeric antibody against the eluted peak area shows linearity ( $r^2 = 0.99$ ) over the 0.1–100  $\mu\text{g}$  range. The minimum detectable concentration (MDC) at 280 nm is about 2  $\mu\text{g}/\text{ml}$  which can be decreased to 200 ng/ml if the antibody elution is monitored at 214 nm. Under these conditions the C.V. is  $\leq 5\%$ . Accuracy of the quantitation is independent of operator, solution composition, sample pH and the ionic strength, all of which are factors to consider in performing immunoassays. Antibody samples containing aggregated and fragmented  $F_c$  regions of the antibody will interfere with this method of quantitation. An optimized validated method for the quantitation of antibody is described. This mode of perfusion chromatography could be applied in the biopharmaceutical field due to its speed, efficiency and sensitivity.

### 1. Introduction

The rapid quantitation of monoclonal antibodies in complex biological fluids is a requirement in quality control laboratories dealing with biologics in the presence of excipients, salts, stabilizers and buffers. It is also a requisite in other biopharmaceutical settings such as hybridoma laboratory, fermentation, purification and determination of process recovery. Typically these needs are met by the use of enzyme-linked immunosorbent assay (ELISA) and radioimmunoassay (RIA) techniques. These techniques are sensitive in the pg/ng range but they are complex, time-consuming and operator and tech-

nique dependent and give high coefficients of variation (C.V.s). In addition, they require either radiolabeling of or conjugation of fluorescent labels/tags or enzymes to the primary or secondary antibody.

High-performance liquid affinity chromatography (HPLAC) utilizing protein G offers a rapid, precise and specific technique for the quantitation of antibodies [1–3]. An antibody to human growth hormone (hGH) has been quantitated using HPLAC in conjunction with fluorescence detection with a minimum detection limit of 250 ng/ml [4]. Combination of a protein G column and reversed-phase column chromatography has been successfully used for the quantitation of an antibody and contaminants and to checking the purity of the antigen [5]. The use of

\* Corresponding author.

ImmunoDetection (ID) protein G (PG) cartridges for immunoassays is a novel technique which combines the resolving power of perfusion chromatography with the precision and speed of HPLC. This immunoassay setup offers many advantages for the quantitation of antibodies in terms of its adaptability to conventional HPLC systems, its efficiency, and its operator independence [6]. Tru-Scint AD is a monoclonal antibody used for the *in vivo* radio-imaging of adenocarcinomas. It is a murine antibody (IgG1) raised against synthetic asialo-Tn antigen [7]. The exact nature of the epitope recognized by this monoclonal antibody is still under investigation. The antibody is formulated as a lyophilized powder containing sucrose as an excipient and stabilizer. It is reconstituted at the clinic using USP grade sodium pertechnetate Tc-99m injection solution. We have investigated the utility of perfusion chromatography for the quantitation of this monoclonal antibody. We studied various parameters which affect the reproducibility of this method. A method is described for the quantitation of the Tru-Scint AD antibody at various stages of the processing, product development and manufacturing.

## 2. Experimental

The ID sensor PG cartridge (55 × 12 mm I.D.) (Perceptive Biosystem, Cambridge, MA, USA) was connected to a Beckman HPLC equipped with a Model 166 detector module, a Model 126 programmable solvent delivery module and System Gold software (Beckman, CA, USA). Analytical grade sodium mono- and diphosphate and hydrochloric acid were from Fisher Scientific (Ottawa, Ont., Canada) and Curtin Matheson Scientific (Houston, TX, USA), respectively. All samples and buffers were filtered through a 0.2- $\mu$ m filter before loading on the cartridge. The standard curve of monoclonal antibody over the ranges 100 ng–5  $\mu$ g and 5–100  $\mu$ g per 50  $\mu$ l, was developed using the following gradient system. The standards and samples were injected on a pre-equilibrated cartridge at a flow-rate of 0.5 ml/min followed by washing with equilibration

buffer (10 mM phosphate buffer pH 7.2 containing 150 mM NaCl) at 2 ml/min for 1.5 min. The monoclonal antibody was eluted with elution buffer (2.5 mM HCl pH 2.6 containing 150 mM NaCl) at a flow-rate of 2 ml/min and monitored at 280 nm or 214 nm as appropriate. The integrated peak areas of antibody standards were plotted against the injected amounts using the Curve fit option of the System Gold software and the unknown samples were extrapolated from this standard curve.

The antibody concentration was determined using an extinction coefficient of  $\epsilon_{280}^{1\%} = 1.59$  with the aid of a Beckman DU 640 spectrophotometer (Beckman, Fullerton, CA, USA).

The aggregated dimeric antibody was generated by irradiating the monomeric antibody with UV light, followed by purification of the aggregated antibodies on a size-exclusion column TSK G3000 (600 × 7.7 mm I.D.) (Beckman). The protein concentration of the aggregated antibody was determined by the Bradford method [8] using a Bio-Rad kit.

## 3. Results and discussion

A typical standard chromatogram of 10  $\mu$ g of eluted monoclonal antibody on this PG cartridge is shown in Fig 1. The elution time of the antibody was quite reproducible at  $2.7 \pm 0.1$  min ( $n = 20$ ). The turn-around time for sample analysis is only 5.5 min. The standard curve is generated by loading monomeric monoclonal antibody on the PG cartridge and integrating the peak areas of the eluted antibody detected at 280 nm (curve not shown). The maximum and minimum capacities of the cartridge as recommended by the manufacturer are 100  $\mu$ g and 100 ng, respectively. We found the standard curve to be linear ( $r^2 = 0.99$ ) over this range.

Using this standard curve we quantitated monomeric monoclonal antibodies from several complex mixtures such as cell supernatants, lyophilized antibodies with excipients, salts, buffers etc. While validating this technique for the quality control of antibodies, we investigated various parameters which could affect this quan-

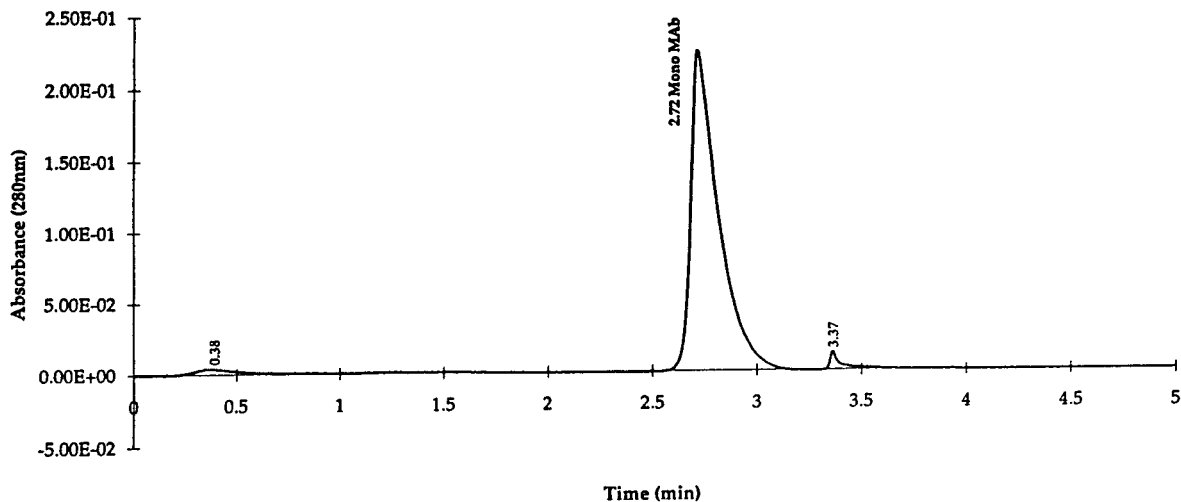


Fig. 1. Elution profile of Tru-Scint AD antibody on protein G cartridge: 10  $\mu$ g of antibody were injected as described in Experimental.

titative method and the concentration of the antibodies.

The inter-day and intra-day coefficients of variation are  $\leq 9\%$  and  $\leq 5\%$ , respectively, while monitoring the eluted peak at 280 nm. As expected the C.V. increases with a decrease of the amount of antibody injected (data not shown). By switching the monitoring wavelength to 214 nm the inter-day C.V. can be lowered to  $< 4\%$  and the sensitivity and limit of detection to 200 ng/ml (data not shown). This is comparable to the 250 ng/ml found for fluorescence-based quantitation of human growth hormone antibody [4]. The advantage of protein G based HPLC is that no labeling of the antibodies with the fluorescent dye Texas red is required.

The non-retained peak (0.38 min), i.e. the flow-through, was checked for the presence of the antibody by collecting and re-injecting the solution. No antibody could be found (data not shown). This suggests that, in this concentration range and with the injection flow-rate used, the total amount of antibody loaded is bound to the cartridge matrix. We did not observe the 50% unbound fraction seen by other investigators [10], who used an ImmunoDetection CO cartridge where the antigen was immobilized on the cartridge. This inconsistency may be due to

differences in the immobilization mechanism between the PG and CO cartridges.

The accuracy of the present technique was established by comparing the determined antibody content of a purified antibody sample with the results obtained using another method such as absorbance at 280 nm using the specific extinction coefficient and ELISA. When compared with the absorbance method the present method showed an antibody recovery of  $\sim 96\%$ . The method was also compared with an ELISA using few antibody samples obtained from a cell culture and at various steps of purification. It appears that both methods are comparable for each set of samples. With ELISA all samples showed amounts ca. 20–25% higher. The differences could be explained by the specificity of the ID PG method, which quantitates only native antibody—either in monomeric or aggregated form—whereas the ELISA may also score interfering substances and degraded epitopes.

The effect of excipients such as sucrose, buffers and the presence of salts on the quantitation of Tru-Scint AD MAb-L4 antibody was evaluated. The lyophilized antibody containing 3% excipient sucrose was reconstituted in saline and about 27  $\mu$ g of the antibody was injected on the ID PG cartridge. On elution it showed a re-

covery of  $\sim 96\%$ . There is no significant difference in the determination of the antibody in the presence of excipients, salts and stabilizers.

The effect of dimer aggregates was investigated in terms of their ability to bind to the protein G and their effect on the determination of monomeric IgG concentration, as they present a potential intrinsic contaminant in our product on prolonged storage. To evaluate the effect we purified the dimers using HPLC size-exclusion chromatography (data not shown). The dimers were injected and quantitated using the ImmunoDetection PG cartridge. The purified dimer bound to the protein G and showed a broad elution profile (Fig 2). On extrapolation of its concentration from a standard curve generated using monomeric antibody, we recovered a higher ( $\sim 157\%$ ) amount of antibody than was loaded onto the cartridge as determined by the Bio-Rad kit. This was not surprising, as this method is based on the absolute mass which is proportional to the peak area. This confirms that dimer-containing samples will interfere with the

determination of monomeric antibody concentration.

Results from samples containing aggregates should be interpreted with caution. One can establish the effect of various percentages of dimer on the determination of monomeric antibody concentration by spiking the samples with appropriate amounts of dimer.

We investigated the effect of the pH and the ionic strength of the antibody sample. Sample pHs of 4.0 and 11.0 did not have any effect on the ability of the antibody to bind to the PG cartridge. Similarly, increasing the salt concentration in the sample up to  $0.3\text{ M}$  NaCl did not show any effect on binding and retention of antibody (data not shown). This versatility is important in downstream processing involving various antibody samples of high and low pH and ionic strengths. We have used this method to directly analyze such samples without any processing.

The ImmunoDetection method using the perfusion chromatography PG matrix described

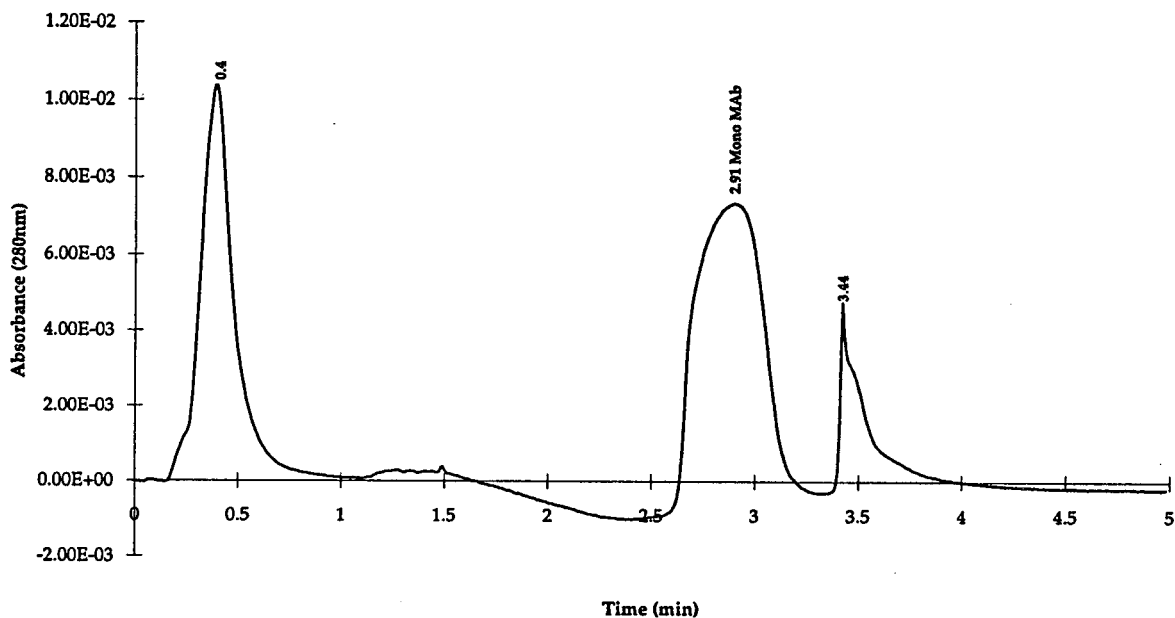


Fig. 2. Elution profile of aggregated antibody on protein G cartridge: ca.  $3.1\ \mu\text{g}$  of aggregated antibody at  $62.2\ \mu\text{g}/\text{ml}$  (as determined by the Bio-Rad protein assay) was injected, eluted and quantitated using the standard protocol detailed in Experimental.

here has multiple applications in quantifying various subtypes of antibody, such as IgG1, IgG2, IgG3 and IgG4, due to its broad specificity [9], from complex biological fluids in a more consistent and rapid way. This type of immunoassay shows a low C.V., broad dynamic range and high reproducibility due to operator independence. As the method is based on the integration of total peak area—which is proportional to the mass—one needs to be aware of the presence of aggregates and other F<sub>C</sub>-binding fragments of antibody in the sample which might interfere with the determination of monomeric antibody concentration. One should be aware of differences in the glycosylation pattern of the antibodies when comparing one monomeric antibody standard curve against differently glycosylated monomeric antibodies, as differences result in a change of the peak area per unit of mass. To quantitate any unknown antibody sample, one needs to establish that the differences in the glycosylation patterns are minimal between the unknown sample and the standard antibody which is used to generate the curve. Compared to ELISA and RIA this method offers higher analytical precision, faster sample throughput and lower C.V.s. In addition, this type of chromatography can be performed using conventional HPLC equipment, which makes it an attractive technique in biopharmaceutical settings such as quality control, bioprocess development and downstream purification where it can be used to determine the recovery and mass balance.

### Acknowledgements

The authors thank Paola Chabot and Sandra Overgaard, Bioprocess Development, Biomira, for providing the bioprocess samples along with the ELISA data for comparison.

### References

- [1] G.S. Blank and D. Vetalin, *Anal. Biochem.*, 190 (1990) 317.
- [2] S.K. Roy, D.V. Weber and W.C. McGregor, *J. Chromatogr.*, 303 (1984) 225.
- [3] R.R. Walters, *Anal. Chem.*, 57 (1985) 1099A.
- [4] A. Riggan and E.F. Regnier, *Anal. Chem.*, 63 (1991) 468.
- [5] J.L. Janis and E.F. Regnier, *Anal. Chem.*, 61 (1989) 1901.
- [6] N.B. Afeyan, N.F. Gordon and F.E. Regnier, *Nature*, 358 (1992) 603.
- [7] A.A. Noujaim, T.R. Sykes, A.J. McEwan, G.D. McClean, S.A. McQuarrie, G. Stanczyk and B.M. Longenecker, in R.P. Baum et al. (Editors), *Clinical Use of Antibodies*, Kluwer Academic Publishers, Dordrecht, Netherlands, 1991, p. 151.
- [8] M. Bradford, *Anal. Biochem.*, 72 (1976) 248.
- [9] S. Ohlson, R. Nilsson, U. Niss, B. Kjellberg and C. Freiburghans, *J. Immunol. Methods*, 114 (1988) 175.
- [10] M.M. Scherberman and J.T. Collins, *Anal. Biochem.*, 217 (1994) 241.





## Unusual chromatographic behaviour and one-step purification of a novel membrane proteinase from *Bacillus cereus*

Beate Fricke<sup>a,\*</sup>, Thomas Buchmann<sup>a</sup>, Sieglinde Friebe<sup>b</sup>

<sup>a</sup>*Institute of Physiological Chemistry, Medical Faculty, Martin Luther University Halle–Wittenberg, Holly Straße 1, Halle (Saale), Germany*

<sup>b</sup>*Institute of Biochemistry, Faculty of Life Sciences, Martin Luther University, Halle (Saale), Germany*

First received 14 February 1995; revised manuscript received 29 May 1995; accepted 29 May 1995

---

### Abstract

Cell envelopes of *Bacillus cereus* contain a casein-cleaving membrane proteinase (CCMP) and an insulin-cleaving membrane proteinase (ICMP), which differ in their substrate and inhibitor specificity from all *Bacillus* proteinases described previously. They remained localized in the cytoplasmic membrane after treatment with lysozyme and mutanolysin and they are strongly attached to the membrane compared with other known membrane proteinases. Only high a concentration of the zwitterionic detergent sulfobetain SB-12 enabled an effective solubilization of both membrane proteinases. The usual conventional purification methods, such as chromatofocusing, ion-exchange chromatography and hydrophobic interaction chromatography in the presence of detergent concentrations beyond their critical micelle concentration, could not be applied to the purification, because the solubilized membrane proteinases bound strongly and irreversibly to the chromatographic matrix. In the search for other purification methods, we used a tentacle ion-exchanger (EMD trimethylaminoethyl-Fractogel) to reduce the hydrophobic interactions between the proteinases and the matrix. All contaminating proteins could be removed by a first gradient of sodium chloride without elution of CCMP; a second gradient with isopropanol and a decreasing salt concentration resulted in an efficiently purified CCMP. The ICMP was irreversibly denaturated.

Purified CCMP is a member of the metalloproteinase family with a pH optimum in the neutral range and a temperature optimum of 40°C, whose properties differ from the serine-type membrane proteinase of *Bacillus subtilis* described by Shimizu et al. [Agric. Biol. Chem., 47 (1983) 1775]. It consists of two subunits in sodiumdodecyl sulfate–polyacrylamide gel electrophoresis (SDS–PAGE) under reducing conditions ( $M_r$  53 000 and 65 000); however, the molecular mass of the purified enzyme could not be determined by size exclusion or SDS–PAGE, because the purified enzyme aggregated at the top of the gel matrix. CCMP solubilized before the purification process, could be eluted in the presence of 0.1% octylphenol-poly(ethyleneglycol ether)<sub>9–10</sub> (Triton X-100) in two peaks of  $M_r$  56 000 and 128 000, respectively.

We discuss this special chromatographic behaviour of the CCMP from *Bacillus cereus*, with regard to the strong hydrophobic interactions of the enzyme with the chromatographic matrix and additional self-aggregation, which could only be dissolved by solvents such as isopropanol.

---

\* Corresponding author.

## 1. Introduction

Membrane proteins can be released from membranes by treatment with detergents, which surround the hydrophobic regions of the membrane proteins and mediate their solubility in aqueous media [2–4]. At high detergent/membrane protein concentration ratios, the detergent molecules replace the phospholipid molecules from the protein surface and protein–detergent micelles are formed [5–7]. In this solubilized state, the membrane proteins can be subjected to various purification methods in the presence of detergent above its critical micellar concentration (CMC). For example, solubilized leader peptidase from *E. coli* was purified by hydrophobic interaction chromatography on phenyl-sepharose in the presence of the non-ionic detergent Triton X-100 [8–11]. The neutral endopeptidase from kidney microvilli could be purified by ion-exchange chromatography in its detergent form [12–14]. Generally, the purification of membrane proteins is more difficult than that of soluble proteins, because mixed micelles between phospholipids and different membrane proteins and detergent molecules can be generated during the solubilization process and the interactions between the membrane proteins and the chromatographic matrix are customarily decreased in the presence of detergent. Therefore many membrane proteins were first purified in their protease form without their hydrophobic anchor [15,16]. Additionally, integral membrane proteins, such as receptor or transport proteins are often markedly dependent on membrane phospholipids, which form the typical environment for these proteins in the membrane. Removal or dilution of the phospholipids during and after the solubilization, may result in a significant reduction in protein stability and subsequently in the loss of biological activity [17–20].

We were especially interested in the purification of the membrane proteinases from *Bacillus cereus* in their detergent form. The behaviour of the solubilized proteinases from *B. cereus* during various purification procedures was very unusual and different from that of other membrane

proteins in their amphipathic forms, as described in the previous literature. In the present article we examine the interactions of the membrane proteinases from *B. cereus* with different gel matrices and describe a new way to dissolve this unusually strong binding of membrane proteins with the chromatographic matrix.

## 2. Experimental

### 2.1. Chemicals

Sulfobetain SB-12, Triton X-100, SDS, trypsin, lysozyme from chicken egg white, marker proteins for size exclusion chromatography (catalase, aldolase, bovine albumin, ovalbumin, dinitrophenyl alanine) and the synthetic peptide substrates Ala-pNA, Glu-pNA, Bz-D,L-Arg-pNA, Suc-Ala-Ala-Val-pNA, Suc-Ala<sub>3</sub>-pNA, Glp-Phe-Leu-pNA and Fa-Gly-Leu-NH<sub>2</sub> (FAGLA) were obtained from Serva (Heidelberg, Germany). The detergents sodium cholate, sodium deoxycholate, Brij 35 and Triton X-100 were purchased from Ferak (Berlin, Germany). CHAPSO, octylthioglucoside, EMD TMAE-Fractogel-650(S) and marker proteins for SDS–polyacrylamide gel electrophoresis (SDS–PAGE) (myoglobin, soya-bean trypsin inhibitor, carboanhydrase, ovalbumin, bovine serum albumin, glutamate dehydrogenase, ovotransferrin, phosphorylase b,  $\beta$ -galactosidase, myosin) were obtained from Merck (Darmstadt, Germany). DEAE-Sephacel and Sephacryl S-200 were purchased from Pharmacia (Freiburg, Germany).

Mutanolysin (4200 units/mg) and Fa-Leu-Gly-Pro-Ala-NH<sub>2</sub> (FALGPA) were from Sigma (Deisenhofen, Germany). RNase, DNase I from bovine pancreas and the protease inhibitors Pefabloc, PMSF, pCMB, phosphoramidon, leupeptin, antipain and elastatinal were manufactured by Boehringer (Mannheim, Germany). All other chemicals were of analytical grade.

### 2.2. Organism and culture conditions

*B. cereus* is included in our strain collection and was characterized by Dr. Verburg (German

Collection for Microorganisms, Braunschweig). The bacteria were grown in a medium consisting of 20 g/l yeast extract (Difco) in a phosphate buffer medium [21]. The cultivation was carried out in a fermenter Biostat S (Fa. Braun, Melsungen, Germany) with a 7-l working volume at 37°C, a pH regulated at 7.0 and an aeration rate of 7 l/min until the end of the logarithmic phase (6–8 h cultivation time).

### 2.3. Cell disintegration

Freshly harvested cells were washed three times with an excess of sodium chloride solution (5 g/l) and diluted in Tris–HCl buffer (pH 7.5, 0.05 M, buffer A) to a dry weight of about 100 mg/ml. After adding the same volume of glass beads (diameter 0.10–0.11 mm), the cells were disintegrated by stirring in an ice bath. The cell homogenate was separated from the glass beads and the few intact cells by centrifugation (4000 g, 15 min), and the glass beads were washed three times. The combined supernatants were submitted to ultracentrifugation (90 000 g, 60 min) and separated into the particulate (crude cell envelope) and the soluble fraction (cytosol). The crude cell envelope fraction was resuspended in buffer A, washed again under the same conditions and stored at –20°C.

### 2.4. Protease-releasing experiments with lysozyme, mutanolysin, nuclease and trypsin

Washed cell envelopes (10 ml) were homogenized and diluted in 25 ml Tris–HCl buffer (0.05 M, pH 7.5, buffer A). First a 5-ml sample was taken as blank value. Then 10 000 units mutanolysin were added to the remaining cell envelope suspension. The suspension was shaken on a rotatory shaker at 37°C and samples (5 ml) were taken every 15 min over a 75-min period. All samples were collected in an ice bath and centrifuged (60 000 g, 1 h). Sediments were suspended in 5 ml buffer A. The lysozyme (20 mg) and nuclease treatment (10 mg RNase, 10 mg DNase) were carried out in the same way in buffer A.

For trypsin treatment, cell envelopes (8 ml)

were diluted twice in buffer A and trypsin solution (1.2 mg in 6 ml buffer A) was added. The suspension was shaken and samples (3 ml) were taken at timed intervals of 10 min (0–60 min). After the different incubation times, 1 ml Pefabloc (2 mg/ml) was added to inhibit the trypsin action. All samples were centrifuged under the conditions described above, to separate the protease-solubilized enzyme and the activities of CCMP and ICMP in sediments and supernatants were determined.

### 2.5. Solubilization

Washed crude cell envelopes were suspended in Tris–HCl buffer (0.05 M, pH 7.5), mixed with an equal volume of detergent in different concentrations and shaken (150 rpm) for 1 h at room temperature. Solubilized protein in the supernatant was separated from the insoluble sediment by ultracentrifugation (90 000 g, 60 min). The sediments were dissolved and homogenized in buffer with the same detergent concentration as in the corresponding supernatants.

For the solubilization procedure prior to purification of the enzymes, detergent–buffer (8% w/v sulfobetain SB-12 in buffer A) and the same volume of washed cell-envelopes were mixed and treated as described above.

In the supernatant and in the sediment, the proteolytic activities (azocasein assay, [<sup>125</sup>I]insulin assay) and the protein concentration (BCA method) were determined. The solubilize was then stored at –20°C.

### 2.6. Determination of proteolytic activities

Proteolytic activities were determined with azocasein and insulin, by measuring the generation of TCA-soluble coloured or radioactive peptides in the TCA supernatants. For the determination of the insulin-cleaving proteinase, <sup>125</sup>I-labeled insulin (100 000 dpm/assay) was incubated with the enzyme-containing fractions and the radioactive, TCA-soluble peptides generated by the proteolytic action were measured in a  $\gamma$ -counter (LB-2104, Berthold) as described before [22]. Cleavage of azocasein was tested by

the method of Langner et al. [23] and expressed in proteolytic units (PU, 1 PU = 1 nmol azocasein cleaved per second at 37°C). Hydrolysis of synthetic *p*-nitranilide (pNA) substrates (0.5 mM) was photometrically determined at 405 nm in an end-point assay. After incubation at 37°C for various periods of time, protein was precipitated by the addition of TCA (5% final concentration) and sedimented by centrifugation. The clear supernatants were readjusted by sodium hydroxide to neutral pH. Cleavage of the thermolysin substrate Fa-Gly-Leu-NH<sub>2</sub> and of the collagenase substrate Fa-Leu-Gly-Pro-Ala-NH<sub>2</sub> was determined at 345 nm in a continuous spectrophotometric assay [24].

For inhibition assays, the protease-containing fractions were preincubated for 30 min at room temperature; then the usual assay with azocasein or [<sup>125</sup>I]insulin was carried out.

### 2.7. Protein determination

In the presence of detergents interfering with the Lowry method, the BCA method [25] was used for the determination of the protein content, according to the manufacturer's instructions (BioRad, Munich, Germany).

### 2.8. Lipid extraction

A general lipid extraction procedure with chloroform–methanol with some modifications was applied for the isolation of lipids from *B. cereus* [26]. Methanol–chloroform (2:1, v/v) was added to a suspension of crude cell envelopes containing 40–50 mg bacterial dry weight/ml, in a ratio of 3.75 ml per ml cell suspension. The mixture was shaken (120 rpm) in an Erlenmeyer flask for several hours at room temperature. After filtration, the supernatant was decanted and the residue was resuspended in 4.75 ml of methanol–chloroform–water (2:1:0.8, v/v). The mixture was then shaken and filtered. Amounts of 2.5 ml each of chloroform and water were added to the combined supernatants, and the mixture was separated in a separatory funnel. The lower chloroform phase was dried in a rotary evaporator (30–35°C). The lipid residue

was dissolved in a small amount of diethyl ether, subdivided into small portions, evaporated to dryness and stored under nitrogen at –20°C.

### 2.9. Determination of the molecular masses

The purity and the molecular mass of CCMP were assessed by SDS–PAGE in a Tris–glycine buffer system [27] using various gel concentrations. The enzyme samples were mixed with 1% SDS, 2% mercaptoethanol and sodium-EDTA to prevent autolysis of the protease during heat denaturation (3 min, 100°C). The gels were stained according to a silver-staining method [28].

The molecular mass of CCMP was also determined by size exclusion with Sephacryl S-200, adding different detergents and also the phospholipids of *B. cereus* to the elution buffer to examine the aggregation behaviour of CCMP [buffer A with 0.2 M NaCl and with or without detergents and phospholipids–0.1% (w/v) Triton X-100, 0.2% (w/v) sulfobetain SB-12, and 0.1 mg/ml *B. cereus* phospholipid].

## 3. Results

The membrane proteinases of *B. cereus* were difficult to solubilize. High concentrations of Triton X-100, Brij 35, octylthioglucoside and related non-ionic detergents were ineffective in releasing the enzymes from the cell envelopes. Treatment with mutanolysin and lysozyme had no significant effect—a clear sign that the proteases are not cell wall constituents (Table 1). Only the zwitterionic detergent sulfobetain SB-12 was able to release both an insulin-cleaving (ICMP, data not shown) and a casein-cleaving proteinase (CCMP) from the cell envelopes (Fig. 1).

These enzymes retained their full activity in the solubilized state for days without the addition of phospholipids during the solubilization process. Dilution of the solubilizate caused enzyme activation with decreasing detergent concentration, especially for ICMP (Fig. 2). Only at a sulfobetain SB-12 concentration in the

Table 1  
Solubilization of the membrane-bound proteinases by various reagents and detergents

Treatment	CCMP (%)	ICMP (%)
Nuclease	8.5	7.2
Lysozyme (75 min)	9.0	7.5
Mutanolysin (75 min)	8.8	7.9
Trypsin (60 min)	11.0	8.0
Triton X-100 (1% w/v)	16.0	7.3
1 M NaCl after Triton X-100 (2% w/v)	15.8	10.5
Brij 35 (1% w/v)	10.9	12.6
Octylthioglucoside (0.5% w/v)	6.5	10.5
CHAPSO (1% w/v)	7.8	3.7
SDS (0.2%)	10.8	32.6
Sodium deoxycholate (1% w/v)	35.0	27.6
Sulfobetain SB-12 (4% w/v)	79.2	88.4

Cell envelopes were prepared by stirring with glass beads. The solubilization extent is expressed in percentage of the sum of proteolytic activities in the supernatants and sediments after the treatment.

[<sup>125</sup>I]insulin assay below its CMC of 0.12 g/100 ml [29] could this proteinase be measured.

### 3.1. Enzyme purification

All attempts to purify the enzymes by usual chromatographic methods were unsuccessful. At neutral pH in the presence of various detergents the proteinases were bound well on DEAE-Sephacel, but neither 2 M sodium chloride nor increased detergent concentrations (up to 4% w/v sulfobetain SB-12) nor decreasing the pH (acetate buffer pH 3.6) were able to elute the enzymes. Both proteinases (ICMP and CCMP) remained bound to the top of the column and were finally inactivated by the acidic pH. The solubilized proteinases were bound to a chromatofocusing column of polybuffer exchanger PBE-94 and again could not be eluted. Hydrophobic interaction chromatography on phenyl-sepharose and also on the less hydrophobic butyl-sepharose resulted in irreversible binding of the proteinases. Only the use of HA-Ultrogel and subsequent size-exclusion chromatography on Sephadex G-150 in the presence of 0.2% (w/v) sulfobetain led to a partially purified casein-cleaving membrane proteinase (unpublished results). The tentacle ion-exchanger EMD TMAE-Fractogel was selected for the purifica-

tion procedure, to reduce the interactions between the membrane proteinases and the gel matrix and to prevent possible deformation of the enzymes during ionic binding to the matrix.

The solubilizate containing 4% (w/v) sulfobetain SB-12 was dialyzed overnight against excess buffer A containing 2 mM CaCl<sub>2</sub> and 0.2% SB-12 (buffer B). Sulfobetain SB-12 is easy to remove by dialysis because of its high CMC [29]. A column of Fractogel EMD TMAE-650(S) (150 × 10 mm) connected to a fast protein liquid chromatographic (FPLC) apparatus (Pharmacia, Uppsala, Sweden) was preequilibrated with buffer B. After loading the dialyzed solubilizate, the column was washed with buffer B (2 ml/min) until the optical density at 280 nm was reduced to its initial value. The gradients consisted of different concentrations of NaCl and isopropanol.

The best purification (Table 2) was obtained when the first gradient was ranged from 100% buffer B and 0% buffer C (buffer B with 1 M NaCl) to 0% buffer B and 100% buffer C in 60 min (2 ml/min) with subsequent washing for 15 min with buffer C. The second gradient consisted of 100% buffer C and 0% buffer D (buffer B with 0.5 M NaCl and 50% (v/v) isopropanol) to 0% buffer C and 100% buffer D in 90 min (2 ml/min) (Fig. 3).

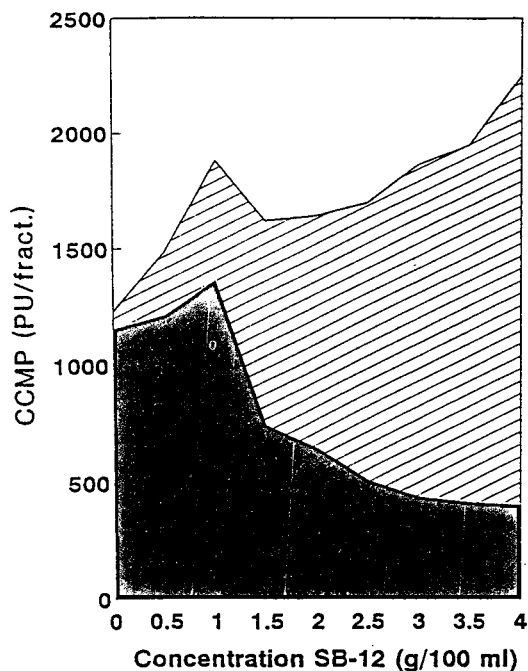


Fig. 1. Solubilization of the CCMP from *B. cereus* with sulfobetain SB-12. Washed cell envelopes were suspended in Tris-HCl buffer (pH 7.5, 0.05 M, buffer A) and mixed with an equal volume of the detergent sulfobetain SB-12 in the same buffer. The suspension was shaken for 60 min at room temperature and separated by centrifugation at 90 000 g for 60 min. Proteolytic activities in supernatants and sediments were determined after dialysis of the fractions against buffer A with 0.2% sulfobetain SB-12.

A higher sodium chloride concentration in the first gradient (up to 2 M NaCl) caused formation of small salt crystals in the buffer containing isopropanol during the second gradient and the chromatographic matrix was damaged by the pressure occurring in the column. Only a salt concentration of 1.0 M is soluble in a buffer with 50% (v/v) isopropanol. An increased salt concentration (above 0.5 M) in buffer D led to a stronger attachment of the proteinase to the chromatographic matrix, and the enzyme was eluted at a higher isopropanol concentration in a less purified state.

The sensitivity of CCMP for isopropanol was tested and the enzyme was found to be as sensitive as chymotrypsin. ICMP was inactivated at low isopropanol concentrations (Fig. 4).

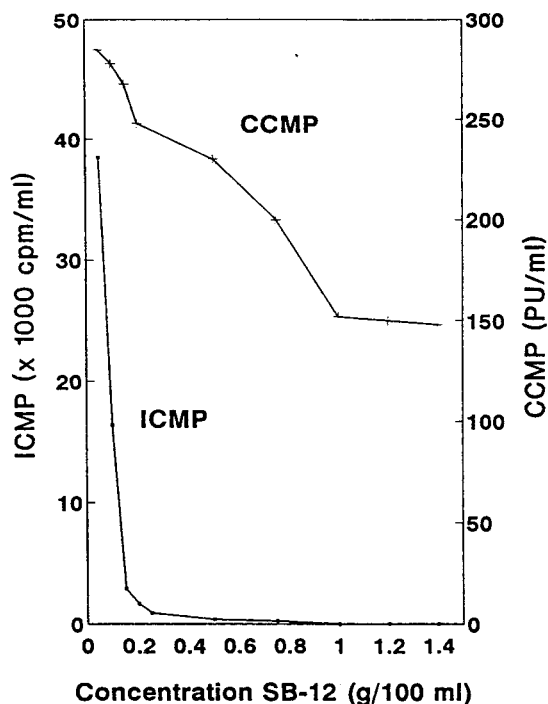


Fig. 2. Dependence of the proteolytic activity on the detergent concentration in the proteinase assay. Supernatant from sulfobetain SB-12 solubilization with high proteolytic activity was diluted with buffer A to a defined detergent concentration in the proteolytic assay and the proteolytic activity was determined in the usual way with azocasein and [ $^{125}$ I]insulin.

### 3.2. Detergent and phospholipid dependence of CCMP

The membrane proteinases retain their activity during solubilization without the addition of phospholipids even at high detergent concentrations and remain active for days at 4°C in this solubilized state. A 50-fold dilution of the solubilized membrane proteases in detergent-free buffer activated the proteolytic activity; this activation is due to the dilution of the reversible inactivating detergent sulfobetain SB-12. This indicates that the resulting lack of phospholipids had no inactivating effect (Fig. 2). Addition of *B. cereus* phospholipids to the solubilizate did not increase the activity of the enzymes during the subsequent dilution. The strong interaction of the enzymes with the chromatographic matrix

Table 2  
Solubilization and purification of CCMP from *B. cereus*

Purification step	Protein (mg/fraction)	Proteolytic activity (PU/fraction)	Recovery (%)	Purification factor
Washed cell envelopes	19	352.0	100	1
Solubilize with 4% sulfobetain SB-12	12	522.1	148	2.4
Dialyze against 0.2% sulfobetain SB-12	10	246.0	70	1.1
Eluate from TMAE-Fractogel	0.07	102.5	29	63

during FPLC on EMD TMAE-Fractogel can not be decreased by the addition of phospholipids to the elution buffer together with high salt concentrations. In the presence of Triton X-100 (0.1%), strong dilution of the phospholipid content of the solubilize during size exclusion was possible without precipitation or inactivation of the solubilized enzyme.

By contrast, purified CCMP after FPLC on TMAE-Fractogel could not be eluted from the same column under identical conditions, because

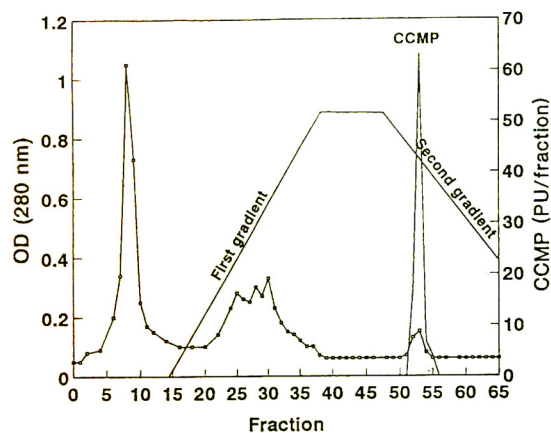


Fig. 3. Purification of CCMP by ion-exchange chromatography on a column of EMD TMAE-Fractogel 650(S) (150 × 10 mm). The column was equilibrated and prewashed with Tris-HCl buffer (pH 7.5, 0.05 M, buffer B) containing 2 mM CaCl<sub>2</sub> and 0.2% sulfobetain SB-12. Elution was performed by two gradients, a first gradient from 100% buffer B and 0% buffer C (buffer B with 1 M NaCl) to 0% buffer B and 100% buffer C and a second gradient from 100% buffer C and 0% buffer D (buffer B with 0.5 M NaCl and 50% (v/v) isopropanol) to 0% buffer C and 100% buffer D with a flow-rate of 2 ml/min.

of strong self-aggregation of the purified hydrophobic enzyme.

### 3.3. Inhibition behaviour and substrate specificity of the purified enzyme

The purified CCMP shows the typical inhibition pattern of a metalloprotease when reacted with sulfhydryl reagents like pCMB (Table 3), but the enzyme is different from the thermolysin-like enzymes in its behaviour with phosphoramidon. Neither the *p*-nitranilide substrates of aminopeptidases, subtilisins, trypsin-like and chymotrypsin-like proteases tested, nor the typical thermolysin substrate FAGLA and the collagenase substrate FALGPA, were cleaved. In its inhibition behaviour and activity with synthetic peptide substrates the purified CCMP

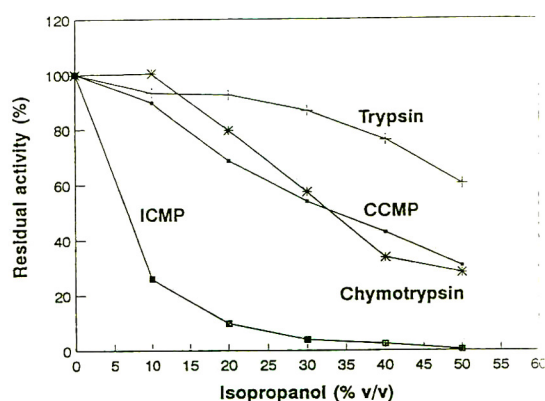


Fig. 4. Influence of isopropanol on the activity of CCMP and ICMP of *B. cereus*, trypsin and chymotrypsin.



Table 3  
Influence of different inhibitors and metal ions on purified CCMP from *B. cereus*

Concentration (final concentration in the assay)	Inhibition (%)
<i>o</i> -Phenanthroline (1 mM)	100
EDTA (1 mM)	100
pCMB (1 mM)	75
Benzamidine hydrochloride (5 mM)	0
PMSF (1 mM)	24
Pefabloc (1 mM)	24
Phosphoramidon (10 $\mu$ M)	0
Elastatinal (10 $\mu$ M)	0
Chymostatin (10 $\mu$ M)	0
Leupeptin (10 $\mu$ M)	0
Antipain (10 $\mu$ M)	0
Ca <sup>2+</sup> (1 mM)	0
Mg <sup>2+</sup> (1 mM)	0
Mn <sup>2+</sup> (1 mM)	24
Co <sup>2+</sup> (1 mM)	71
Zn <sup>2+</sup> (1 mM)	74

The proteinase was preincubated with different inhibitors and metal ions for 30 min at room temperature.

differs from all extracellular and endocellular *Bacillus* proteases described so far.

### 3.4. Determination of the molecular mass

The crude solubilizate (after solubilization with sulfobetain SB-12) was subjected to the size-exclusion procedure under various conditions (addition of *B. cereus* lipid, addition of 2 mmol Ca<sup>2+</sup>, content of 0.2% sulfobetain SB-12, or 0.1% Triton X-100 in the elution buffer). Two peaks with azocaseinolytic activity (corresponding to molecular masses of 56 000 and 128 000, respectively, Fig. 7) were eluted in similar positions, but with a different percentage partition between them and with different amounts of activity, depending on the buffer used (Fig. 6a–c). In the presence of phospholipids in the elution buffer, the two peaks with azocaseinolytic activity were unified by the formation of mixed phospholipid–detergent–protein micelles (Fig. 6d). The elution behaviour of the purified enzyme was markedly changed; aggregation of the enzyme led to a complex which could not be eluted with detergent buffer.

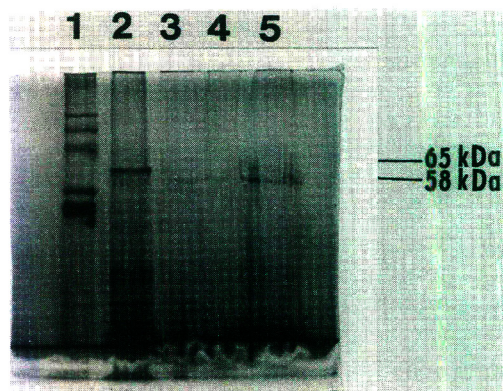


Fig. 5. SDS–PAGE with silver-staining. Different electrophoretic mobility of the purified CCMP depending on the treatment before the SDS–PAGE. Lane 1: calibration proteins, lane 2: solubilizate after dialysis (with 5% ME and 1% SDS boiled for 5 min at 100°C), lane 3: purified CCMP (without ME and SDS, without boiling), lane 4: purified CCMP (without ME, boiled with 1% SDS for 5 min at 100°C, lane 5: purified CCMP (boiled for 5 min with 5% ME and 1% SDS).

The purified CCMP did not enter 7% SDS–PAGE gels, not even after boiling for 5 min with 1% SDS (data not shown). By the addition of mercaptoethanol, two diffuse protein bands of  $M_r$  53 000 and 65 000 could be detected for the purified enzyme after silver-staining (Fig. 5, lane 5), corresponding well in their molecular masses to the results of the size-exclusion chromatography (Fig. 7).

## 4. Discussion

*Bacillus* species are known to secrete several proteases during their transition to the stationary phase. Besides three relatively major proteases (alkaline serine proteases–subtilisins, neutral metalloproteases–thermolysin-like proteases and bacillopeptidase F—a serine protease with high esterolytic activity) there are also several minor extracellular proteases, which could be demonstrated only after constructing deletion mutants for the major extracellular proteases (for a review see Ref. [30]). Intracellular serine proteases (ISP) with high structural similarities



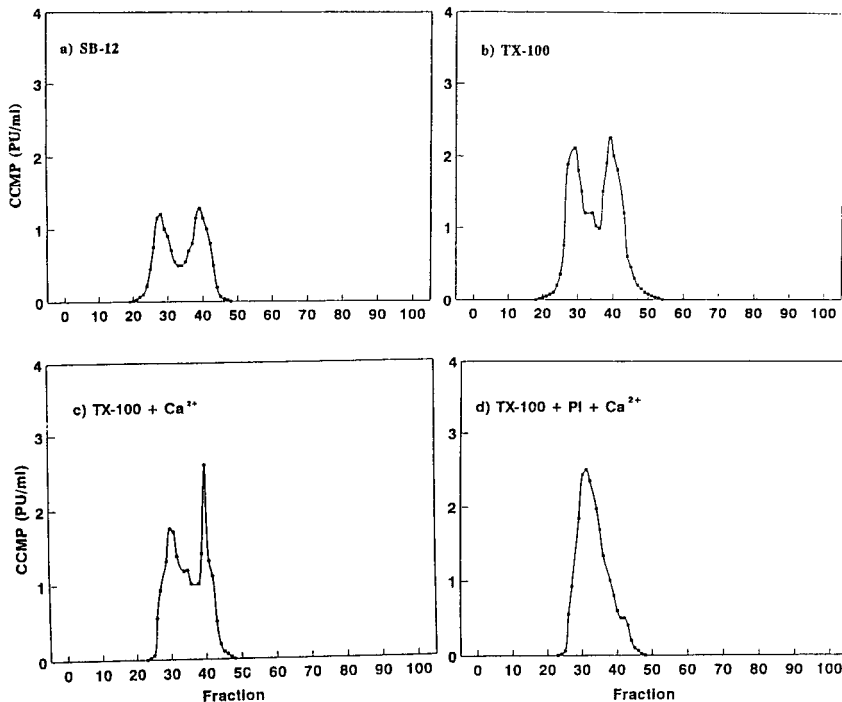


Fig. 6. Elution behaviour of the CCMP from a column of Sephacryl S-200 under the influence of different detergents, phospholipids and metal ions. The same amount of solubilizate was loaded onto the column ( $800 \times 10$  mm I.D.) in all instances, the elution was performed at a rate of 1 ml/20 min with a Tris-HCl buffer (pH 7.5, 0.05 M, 0.2 M NaCl) with the following additions: (a) elution with 0.2% SB-12, (b) elution with 0.1% Triton X-100, (c) elution with 0.1% Triton X-100 and 2 mM  $\text{CaCl}_2$ , (d) elution with 0.1% Triton X-100, 2 mM  $\text{CaCl}_2$ , and additionally 1 mg *B. cereus* lipids/ml buffer.

to subtilisins seem to play an important role in the sporulation process [31,32].

We could isolate a novel membrane proteinase called CCMP from *B. cereus* with unusually strong hydrophobic properties and a high tendency to self-aggregation. Strongin et al. [33] reported that the membrane proteinase isolated from *B. subtilis* is very similar to the cytoplasmic serine protease. Mäntsälä and Zalkin [34] extracted the cell membrane of *B. subtilis* YY88 with a very low detergent concentration (0.1% Triton X-100) and found that the greater part of the membrane proteinase activities corresponded to the extracellular serine and metalloproteases in their immunological reactivity and substrate specificity [34]. The only membrane proteinase which is distinct from all other reported *Bacillus* proteases in its special behaviour as an amphipathic protein, was purified from *B. subtilis*

IFO 3027 [1]. This membrane-bound proteinase could only be solubilized by butanol extraction or a high Triton X-100 concentration in the presence of 1 M salt. In buffers of low ionic strength, the enzyme precipitated and could only be purified in the presence of detergent and 0.5 M sodium chloride. This solubilization behaviour is different from that of the CCMP from *B. cereus*; Triton X-100, even together with high salt concentrations, was not able to release the membrane proteinases from the cell envelopes (Tables 1, 4). Other differences are the different behaviour with class-specific inhibitors and the substrate specificity (Table 4).

There are several reasons why a protein may bind to the top of a column:

1. The protein is in a particulate state and therefore not able to pass the column matrix.

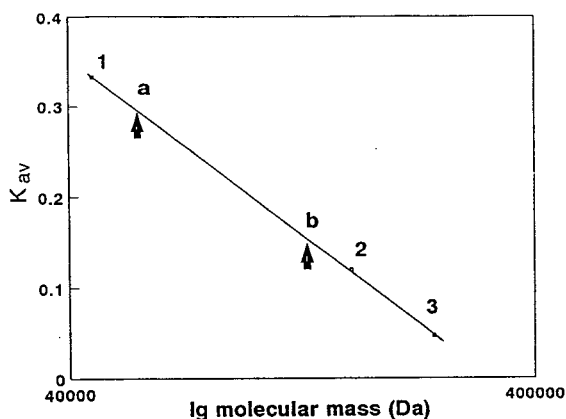


Fig. 7. Size-exclusion chromatography on Sephacryl S-200 (800 × 10 mm). Determination of the molecular mass of the CCMP in the solubilize in comparison with calibration proteins (1: bovine serum albumin, 2: aldolase, 3: catalase) resulting in two molecular masses (a: 56 000, b: 128 000). Elution of the proteolytic activity was performed at a rate of 1 ml/20 min with a Tris-HCl buffer (pH 7.5, 0.05 M) containing 0.1% Triton X-100 and 0.2 M NaCl; calibration proteins were eluted with the same buffer, but without detergent addition.

2. A lack of phospholipids due to protein dilution during the chromatographic step causes the precipitation of the protein.
3. As a result of the interaction between protein and chromatographic matrix the conformation of the protein is changed and it binds to the chromatographic matrix.

Since repeated preparative ultracentrifugation of the solubilized enzyme did not result in enzyme sedimentation and a separation of the crude enzyme after solubilization by size-exclusion chromatography was also possible, the first possibility can be excluded. In contrast to the membrane proteinases from *B. cereus*, phospholipid-dependent membrane proteins react with rapid and often irreversible inactivation to a dilution of the solubilize; for example the tetrodotoxin binding component from the electroplax of *Electrophorus electricus* is completely inactivated after a solubilize dilution in as short

Table 4

Comparison between the CCMP from *B. cereus* and the membrane proteinase from *B. subtilis* IFO 3027 [1]

	CCMP from <i>B. cereus</i>	Membrane proteinase from <i>B. subtilis</i>
Molecular mass		
SDS-PAGE		62 000
Size exclusion		540 000
pH optimum	6.5–7.5	11
Inhibition by	Residual activity	Residual activity
PMSF (1 mM)	100%	0%
EDTA (5 mM)	0%	100%
Leupeptin (100 µg/ml)	100%	100%
Antipain (100 µg/ml)	100%	56%
Chymostatin (50 µg/ml)	100%	18%
Cleavage of Suc-(L-Ala) <sub>3</sub> -pNA per 1 PU	no hydrolysis	0.17 · 10 <sup>-3</sup> µmol/min
Cleavage of Z-(L-Ala) <sub>2</sub> -L-Leu-pNA per 1 PU	no hydrolysis	54 · 10 <sup>-3</sup> µmol/min
Solubilization by 1 M LiCl after Triton X-100 (2% w/v)	solubilized activity 8%	solubilized activity 63.4%

a time as just one hour at room temperature [17]. The transport activity of the branched-chain amino acid transport system of *Lactococcus lactis* was recovered only when solubilization was performed in the presence of acidic phospholipids [35]. Such phospholipid-dependent membrane proteins always need the presence of a minimal phospholipid content (a phospholipid mixture or one defined phospholipid) during each purification step [36–39] independent of their function as an enzyme or a membrane receptor or as a transport protein; often such phospholipid-dependent proteins are integral membrane proteins.

We discuss the strong aggregation of the membrane proteinases from *B. cereus* in ion-exchange chromatography as the binding of protein by ionic interactions and subsequent conformational changes with resulting strong hydrophobic interactions of the enzyme. TMAE-Fractogel is a tentacle gel with long hydrophilic polymer chains with repeating ion-exchange groups, and was chosen to reduce the interactions mentioned above. However, the enzyme showed the same behaviour as on ion-exchange gels without tentacles (DEAE-Sephacel, chromatofocusing ion-exchanger PBE 74). Addition of phospholipids could not reduce the aggregation of the proteinases on the TMAE-Fractogel. Isopropanol used for the elution of the bound CCMP from the anion-exchange column (Fig. 4), also serves in affinity chromatography to solve hydrophobic interactions between the affinity ligands and the bound enzyme. It is used, for example, in the affinity chromatography on bacitracin-sepharose to elute thermolysin [40,41] and in the affinity chromatography with peptidyl methyl ketones as ligands for the elution of papain and thermitase [42]. We postulate that isopropanol solves the hydrophobic interactions of the CCMP with the chromatographic matrix. Both proteinases are strong hydrophobic proteins, as was demonstrated by phase-separation experiments. After salt addition to solubilizates in non-ionic detergents, the membrane proteinases of *B. cereus* are concentrated in the detergent phase [21].

The purified CCMP tends to self-aggregation

(Figs. 5, 6). Only after treatment with mercaptoethanol were two discrete protein bands detected in SDS-PAGE after silver-staining. In samples with untreated enzyme or enzyme boiled with SDS, no protein could be detected (Fig. 5).

ICMP was only detectable in column eluents after FPLC on TMAE-Fractogel in very low amounts. Cleavage of intact insulin is a property of only few proteinases—for example, IDE (insulin-destroying enzyme [43–45]); most proteinases are only able to cleave the single insulin chains. It is possible that the insulin cleavage in the membranes and in the solubilizate is the result of a common action of different enzymes or that ICMP is very labile in the purification process. Since pooling of the fractions after chromatography did not result in restoration of the insulin-destroying activity, and ICMP is very sensitive to detergents (Fig. 2) and organic solvents (Fig. 4), we will test various stabilizing agents for the purification of this enzyme and search for other purification possibilities, such as solvent-solvent extraction.

### Abbreviations

BCA	bichinchinonic acid,
Bz	benzoyl,
Brij 35	dodecylpoly(ox- yethyleneglycol ether) <sub>23</sub> ,
CCMP	casein-cleaving membrane proteinase,
CHAPSO	3-(3-cholamidopropyldimeth- ylammonio)-2-hydroxy-prop- ane sulfonate,
CMC	critical micelle concentration,
DEAE	diethylaminoethyl,
Fa	furylacroleyl,
Glp	pyroglutamyl,
ICMP	insulin cleaving membrane proteinase,
Mutanolysin	endo-N-acetyl muramidase from <i>Staphylococcus globis- porus</i> ,
Pefabloc	4-(2-aminoethyl)benzylsulfo- nyl fluoride,

pCMB	<i>para</i> -chloromercuri benzoate,
PMSEF	phenylmethanesulfonyl fluoride,
pNA	<i>para</i> -nitranilide,
SDS	sodiumdodecyl sulfate,
Suc	succinyl,
Sulfobetain SB-12	N-dodecyl-N,N-trimethyl-3-ammonio-1-prop-anesulfonate,
TCA	trichloroacetic acid,
TMAE	trimethylaminoethyl,
Triton X-100	octylphenol-poly-(ethyleneglycol ether) <sub>9–10</sub> ,
Z	benzyloxycarbonyl.

## References

- [1] Y. Shimizu, T. Nishino and S. Murao, *Agric. Biol. Chem.*, 47 (1983) 1775–1782.
- [2] A. Helenius and H. Soderlung, *Biochim. Biophys. Acta*, 307 (1973) 287–300.
- [3] A. Helenius and K. Simons, *Biochim. Biophys. Acta*, 415 (1975) 29–79.
- [4] L.M. Hjelmeland, *Methods Enzymol.*, 124 (1986) 135–164.
- [5] A. Helenius, D.R. McCaslin, E. Fries and S. Tanford, *Methods Enzymol.*, 56 (1979) 734–749.
- [6] A. Helenius, E. Fries and J. Kartenbeck, *J. Cell Biol.*, 75 (1977) 866–880.
- [7] D. Lichtenberg, R.J. Robson and E.A. Dennis, *Biochim. Biophys. Acta*, 737 (1983) 285–304.
- [8] I.K. Dev and P.H. Ray, *J. Biol. Chem.*, 259 (1984) 11114–11120.
- [9] A.J.M. Driessen and W. Wickner, *Proc. Natl. Acad. Sci. USA*, 87 (1990) 3107–3111.
- [10] P.B. Wolfe, P. Silver and W. Wickner, *J. Biol. Chem.*, 257 (1982) 7898–7902.
- [11] C. Zwizinski, T. Date and W. Wicker, *J. Biol. Chem.*, 255 (1980) 7973–7977.
- [12] J.A. Cromlish, N.G. Serdal and M. Chretien, *J. Biol. Chem.*, 261 (1986) 10850–10859.
- [13] I.S. Fulcher and A.J. Kenny, *Biochem. J.*, 211 (1983) 743–753.
- [14] S.G. George and A.J. Kenny, *Biochem. J.*, 134 (1973) 43–57.
- [15] M.A. Kerr and A.J. Kenny, *Biochem. J.*, 137 (1974) 477–488.
- [16] P.E. Butler, M.J. McKay and J.S. Bond, *Biochem. J.*, 241 (1987) 229–235.
- [17] W.S. Agnew and M.A. Raftery, *Biochemistry*, 18 (1979) 1912–1919.
- [18] W.A. Catterall, L.C. Morrow and R.P. Harthorne, *J. Biol. Chem.*, 254 (1979) 11379–11387.
- [19] P. Mende, H.V.J. Kolbe, B. Kadenbach, I. Stipani and F. Palmieri, *Eur. J. Biochem.*, 128 (1982) 91–95.
- [20] H. Tokuda, K. Shiozuka and S. Mizushima, *Eur. J. Biochem.*, 192 (1990) 583–589.
- [21] B. Fricke, *Anal. Biochem.*, 212 (1993) 154–159.
- [22] B. Fricke and H. Aurich, *Arch. Microbiol.*, 157 (1992) 451–456.
- [23] J. Langner, A. Wakil, M. Zimmermann, S. Ansorge, P. Bohley, H. Kirschke and B. Wiederanders, *Acta Biol. Med. Ger.*, 31 (1973) 1–18.
- [24] J. Feder and J.M. Schuck, *Biochemistry*, 9 (1970) 2784–2791.
- [25] P.K. Smith, R.I. Krohn, G.T. Hermanson, S.K. Mallia, F.H. Gartner, M.D. Provenzano, E.K. Fujimoto, N.M. Goetze, B.J. Olson and D.C. Klenk, *Anal. Biochem.*, 150 (1985) 76–85.
- [26] M. Kates, in T.S. Work and E. Work (Editors), *Laboratory Techniques in Biochemistry and Molecular Biology*, Vol. 3, *Technics of Lipidology: Isolation, Analysis and Identification of Lipids*, Elsevier, New York, 1975.
- [27] U.K. Laemmli, *Nature*, 227 (1970) 680–686.
- [28] J. Heukeshoven and R. Dernick, *Electrophoresis*, 6 (1985) 103–112.
- [29] A. Gonenne and R. Ernst, *Anal. Biochem.*, 87 (1978) 28–38.
- [30] X.-S. He, R. Brückner and R.H. Doi, *Res. Microbiol.*, 142 (1991) 797–803.
- [31] Y.-S.E. Cheng and A.I. Aronson, *Arch. Microbiol.*, 115 (1977) 61–66.
- [32] Y.-S.E. Cheng and A.I. Aronson, *Proc. Natl. Acad. Sci. USA*, 74 (1977) 1254–1258.
- [33] A.Y. Strongin, L.S. Izotova, Z.T. Abramov, L.M. Ermakova, D.I. Gorodetsky and V.M. Stepanov, *Arch. Microbiol.*, 119 (1978) 287–293.
- [34] P. Mäntsälä and H. Zalkin, *J. Bacteriol.*, 141 (1980) 493–501.
- [35] G. in 't Veld, T. de Vrije, A.J.M. Driessen and W.N. Konings, *Biochim. Biophys. Acta*, 1104 (1992) 250–256.
- [36] E.A. Evans, R. Gilmore and G. Blobel, *Proc. Natl. Acad. Sci. USA*, 83 (1986) 581–585.
- [37] A. Mancini, R. Roberti, L. Binaglia, A. El Missiri and L. Freysz, *Membrane Biochem.*, 10 (1993) 43–52.
- [38] M.J. Newman and T.H. Wilson, *J. Biol. Chem.*, 255 (1980) 10583–10586.
- [39] J.T. YaDeau and G. Blobel, *J. Biol. Chem.*, 264 (1989) 2928–2934.
- [40] V.M. Stepanov and G.N. Rudenskaya, *J. Appl. Biochem.*, 5 (1983) 420–428.
- [41] J.M. Irvine, G.H. Coombs and M.J. North, *FEMS Microbiol. Lett.*, 110 (1993) 113–120.
- [42] K. Peters, S. Fittkau, A. Steinert and D. Ströhl, *J. Chromatogr.*, 648 (1993) 91–99.
- [43] J.S. Bond and P.E. Butler, *Annu. Rev. Biochem.*, 56 (1987) 333–364.
- [44] J.A. Affholter, V.A. Fried and R.A. Roth, *Science*, 242 (1988) 1415–1418.
- [45] W.C. Duckworth, *Endocrinol. Rev.*, 9 (1988) 319–345.



ELSEVIER

Journal of Chromatography A, 715 (1995) 259–265

JOURNAL OF  
CHROMATOGRAPHY A

# Experimental study on the separation of silica gel supports by gravitational field-flow fractionation

## II. Sample preparation, stop-flow procedure and overloading effect

Jiří Pazourek\*, Josef Chmelík

*Institute of Analytical Chemistry, Academy of Sciences of the Czech Republic, Veveří 97, CZ-611 42 Brno, Czech Republic*

First received 20 February 1995; revised manuscript received 19 May 1995; accepted 19 May 1995

### Abstract

Two kinds of silica were studied: a commercial porous chromatographic support with a broad size distribution and a special non-porous silica with a very narrow size distribution. The preparation of sample suspensions in aqueous solution of the non-ionic detergent Tween 60 was optimized and the influence of the amount of particles injected and of the stop-flow time on separation was investigated. A study of the overloading effect showed a dramatic increase in the mean retention ratio with increasing amount of particles. Considering previous observations, an explanation of the overloading effect in gravitational field-flow fractionation is suggested.

### 1. Introduction

Gravitational field-flow fractionation (GFFF) belongs to the family of field-flow fractionation (FFF) techniques where an external force field acts perpendicularly to a carrier liquid flow with a non-uniform velocity profile. Concentration profiles of sample components result from the applied field and the component properties and directly determine the elution times. GFFF utilizes the Earth's gravity as the external force field which drives analyte particles (usually micrometre-sized particles because of the relatively weak field) towards the channel bottom that is placed horizontally (accumulation wall). However, there are other forces acting on particles in the

flow, viz., hydrodynamic lift forces. In contrast to gravity, they can drive the particles away from the channel accumulation wall. The retention ratios observed are usually higher than those calculated on the basis of the simple steric model that presumes the particles to roll on the accumulation wall. This means that lift forces cause the focusing (hyperlayer) elution mode [1,2]. The vertical position of the zones in the flow velocity profile is determined by the particle size and density because the gravitational force (the mass) depends on the size and density, and hydrodynamic lift forces depend on the size. GFFF has been applied to the separation and characterization of various particulate materials, e.g. glass, silica gel and latex beads [3–8] and blood cells [9,10].

Particulate samples in FFF cannot be consid-

\* Corresponding author.

ered as point-like, having no interactions among themselves or with the accumulation wall. The influence of particle–particle and particle–wall interactions on retention behaviour has been studied [8,11,12]. However, even without such interactions, the retention behaviour differs from ideal behaviour because of the finite sample concentration. Increasing samples concentration causes deviations of the sample concentration profile and flow velocity profile from their ideal infinite dilution limits: Hoyos and Martin [13] made a detailed analysis of the influence of finite concentration on retention in sedimentation FFF (SdFFF). They explained theoretically previous observations [14] on tailing and increases in retention ratio with increasing amount of sample (polystyrene latex beads of diameter of 460 nm). However, as they noted, the model cannot be applied in the focusing separation mode.

This paper is the second part of a study examining the separation and characterization of silica gel particles by GFFF; the first part [8] dealt with the selection of an optimum carrier liquid and characterization of the lift forces activity in GFFF. The aim of this part was to find an optimum means of sample preparation (preparation of suspensions of particulate materials) and to explain the effect of overloading, both of which are prerequisites to interpreting GFFF experiments.

## 2. Experimental

### 2.1. Equipment

The experimental arrangement was described elsewhere [6–8]. The separation channel was cut in an 80- $\mu\text{m}$  spacer, which was placed between two mirror-quality float glass plates and clamped between two Plexiglas blocks. The channel had dimensions 20  $\times$  360 mm (dead volume 0.53 ml). The inlet and outlet triangles of the channel had heights of 3 cm. The pump was an HPP 4001 (Laboratory Instruments, Prague, Czechoslovakia). A UVM 4 spectrophotometric detector (Development Workshops, Prague, Czechoslovakia)

was used at 265 nm (optical path 5.7 mm).

### 2.2. Materials

The samples were non-porous silica gel spheres of diameter  $1.43 \pm 0.01 \mu\text{m}$  (a kind gift from Professor E. Kováts, SFIT Lausanne, Switzerland, denoted here as 1.4- $\mu\text{m}$  particles) and a sample of commercial porous silica of diameter  $4.78 \pm 1.12 \mu\text{m}$  (Tessek, Prague, Czech Republic, denoted here as 5- $\mu\text{m}$  particles). Their sizes were determined by electron microscopy. The sample suspensions were of concentration 0.025–200 mg/ml. The carrier liquid was a 0.1% solution of Tween 60 (Fluka, Buchs, Switzerland) in distilled water with final density 1.00 g/ml.

## 3. Results and discussion

### 3.1. Sample preparation

The most common procedure for the preparation of suspensions is homogenization of the particulate material in a detergent solution. The detergent prevents concentration of the solid particles on interfaces during manipulation (sampling, injection, transport through the channel). However, porous materials suspended in liquids (such as common silica gel supports) can contain gas cavities on the particle surface. Problems with such samples can arise not only because of worse wetting but also because the cavities influence the apparent density, which directly affects the retention ratio observed. Giddings and Moon [15] concluded that suspensions of porous silica particles contained air activities even after sonication for 6 h. Therefore, we verified three methods of preparation of porous silica samples.

Fractogram A in Fig. 1 was obtained from a sample prepared by simply putting porous 5- $\mu\text{m}$  silica particles in a 0.1% aqueous solution of Tween 60 and shaking. Fractogram B was recorded after 5 min of sonication of the suspension of the same composition and fractogram C

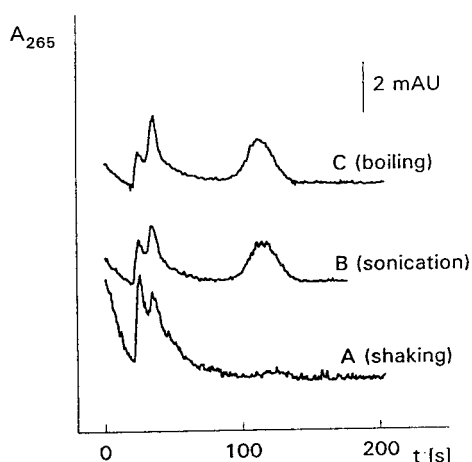


Fig. 1. Optimization of sample preparation procedure. Samples were porous 5- $\mu\text{m}$  silica gel particles of concentration 1 mg/ml in a 0.1% solution of Tween 60. Fractogram A, recorded after shaking the silica powder in the suspension medium only; B, sample after 10 min of sonication; C, sample after 15 min of boiling, tempering and following 1 min of sonication. Flow-rate, 0.99 ml/min; volume injected, 1  $\mu\text{l}$ .

after 15 min of boiling, following tempering and 1-min sonication of a silica particle suspension in 0.1% Tween 60. It is obvious that the retained peak in fractogram A is almost hidden in an anomalous 'noisy' baseline. This is probably a result of chaotic elution of badly wetted particles having a broad particle density distribution while after sonication of the suspension this density distribution was reduced and the retained peak was well pronounced (fractogram B). No significant changes in peak dispersion or retention ratio in fractogram C were observed after boiling, which should release contingent cavities, so we concluded that sonication in the detergent solution was an adequate as the sample preparation procedure for the samples used, and in all subsequent experiments we used suspensions of silica particles in 0.1% Tween 60 prepared only by 1-min sonication.

### 3.2. Stop-flow procedure and relaxation

The relaxation in FFF usually reduces and non-equilibrium contribution to the total peak dispersion because during the relaxation time (in

the absence of the carrier liquid flow) the analyte is expected to form an equilibrium concentration profile suitable for subsequent elution. However, in experiments with particulate samples, the process of sedimentation has to be taken into account. After the sample injection into a channel, the particles are randomly distributed across the whole channel thickness. If the carrier liquid flow is not interrupted, then the particles in the upper and central planes migrate at higher velocities than those located closer to their equilibrium positions near the accumulation wall. This is a consequence of the parabolic flow profile. The particles injected into the upper channel region must pass through the central region because they also sediment. Therefore, the initial sample distribution causes a distinction of elution velocities and thereby contributes to peak broadening. In order to avoid these effects, one has to use either a special split or frit inlet system [16,17] or a stop-flow procedure. In the stop-flow procedure, the sample is injected at a reduced flow-rate and in this way is introduced into the rectangular region of the channel spacer (just behind the spacer inlet triangle). Then the flow is stopped and the sample is affected only by the external field. Finally, the flow is resumed at the elution flow-rate.

In our system, we stop the flow to let the particles settle (to reach a sedimentation equilibrium) in order to reduce their vertical distribution before the elution. This strategy follows from the analysis of the lift forces function [7,18]: in the absence of any external field acting perpendicularly to the flow direction, there are three equilibrium positions across the channel thickness where particles can be focused during the elution owing to hydrodynamic lift forces activity: expressed in dimensionless distance  $\delta$  denoting the relative distance of a particle center from the channel bottom, the three positions are 0.19, 0.50 and 0.81, respectively. This would mean that particles of the same size and density could be focused in three different positions (and consequently they could exhibit different retention ratios, namely 1 and 1.5) if they have been distributed randomly across the whole channel thickness at the beginning of elution. A similar

conclusion holds (there are three distinguished retention ratios as a maximum) if an external field (e.g., gravitational) acts [8]. This means that in GFFF not only peak dispersion but also the retention time is influenced by the initial sample distribution and thus experimental data are not always easy to interpret. In order to simplify the interpretation, it is advantageous to stop the flow after the injection and to let the sample particles settle to the accumulation wall. The time period without flow can be termed the stop-flow time rather than the relaxation time as it was described above that the procedure does not form a concentration profile of particles kept during subsequent elution; the settled particles have only the same starting position. When the flow is reapplied, the hydrodynamic forces drive the particles off the accumulation wall to an equilibrium position where the lift forces are exactly balanced by the gravitational forces. This equilibrium position cannot be reached without the carrier liquid flow (before the elution). The same starting point of all particles is advantageous because identical particles reach their equilibrium positions at the same rate and have the same mean velocity along the channel. A time period necessary for the vertical movement of the particles from their starting position to their equilibrium position (induced by the lift forces) can be called the relaxation time. It has been found previously that this time is relatively short (a few seconds) [7,8,19].

The theoretical time for the settlement of 1.4- $\mu\text{m}$  particles (calculated as the sedimentation time of the particle across the channel height) is 50 s. In order to observe any influence of the stop-flow time, we performed experiments at high flow-rates when the retention time was comparable to this stop-flow time (Fig. 2). Without any flow interruption, the particles eluted from the channel in an asymmetric peak with a left edge retention ratio of 1.5 and a tail overlapping the position of  $R = 1$  ( $t_0 = 6.4$  s); no retained peak was observed (see Fig. 2, fractogram A). In fractogram B in Fig. 2, one can see a retained peak. This means that particles reached a suitable position within 10 s of the stop-flow time. After longer stop-flow times we obtained

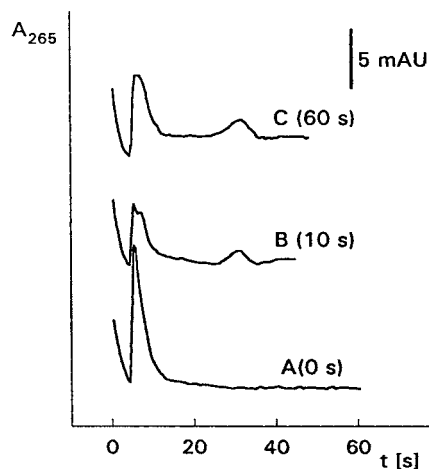


Fig. 2. The stop-flow procedure. The time at each fractogram shows the proper stop-flow time. Experimental conditions: sample, 1.4- $\mu\text{m}$  silica gel particles of concentration 0.25 mg/ml; volume injected, 1  $\mu\text{l}$ ; flow-rate, 5.00 ml/min.

retained peaks with the same retention ratio and dispersion as shown in fractogram C for 60 s. This means that it is not necessary to wait for the complete sedimentation time. It seems that it is sufficient if the particles reach the lower half of the channel where they will be focused during subsequent elution under the influence of the lift and gravitational forces.

### 3.3. Overloading

We also studied the influence of the sample volume and concentration on the retention. In Fig. 3 are shown overlapped fractograms obtained with 1.4- $\mu\text{m}$  particles at two constant concentrations with variable injection volumes. It is evident that an increase in injection volume causes a decrease in the mean retention time and an increase in the peak dispersion by tailing. A similar evolution of series of peaks was observed with 5- $\mu\text{m}$  particles (data not shown). In Fig. 4 are displayed fractograms of 5- $\mu\text{m}$  particles recorded at two constant injection volumes and variable concentrations. One can see that an increase in concentration results in a decrease in the mean retention time which is similar to the observations shown in Fig. 3. Analogous fractog-



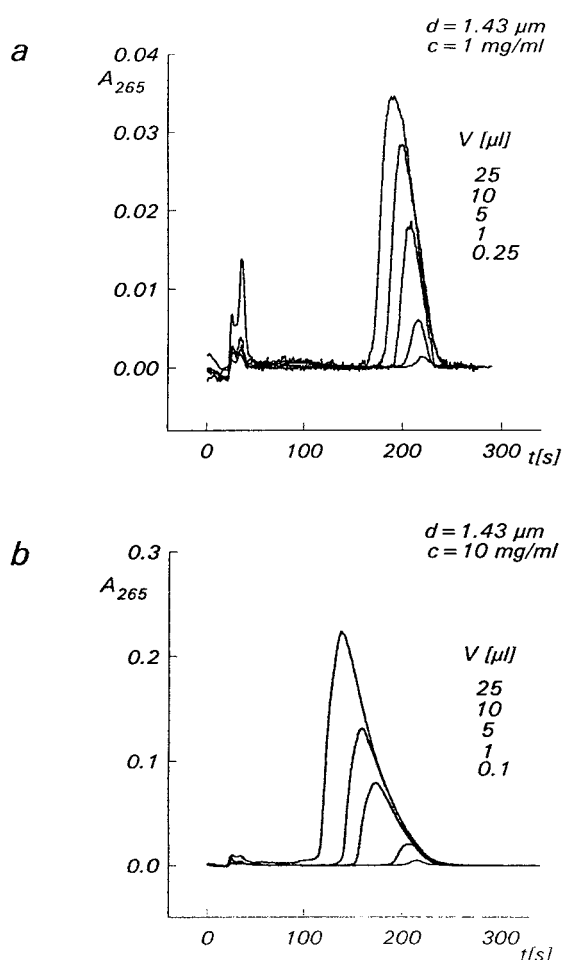


Fig. 3. Overloading effects in GFFF at constant sample concentration. The  $V$  values are the volumes injected; the smaller the volume, the smaller is the peak maximum. Concentrations of 1.4- $\mu\text{m}$  silica gel suspension, (a) 1 and (b) 10 mg/ml; flow-rate, 0.99 ml/min.

rams were obtained at 1.4- $\mu\text{m}$  particles (data not shown).

Previous observation on overloading effects in FFF showed various results: fronting of peaks and a decrease in retention ratio (the sample was polystyrene of molecular mass 200 000–670 000), or tailing and a decrease in retention ratio (the sample was polystyrene of molecular mass 860 000) in flow FFF [20]. In experiments with SdFFF, Kirkland et al. [21] reported an increase

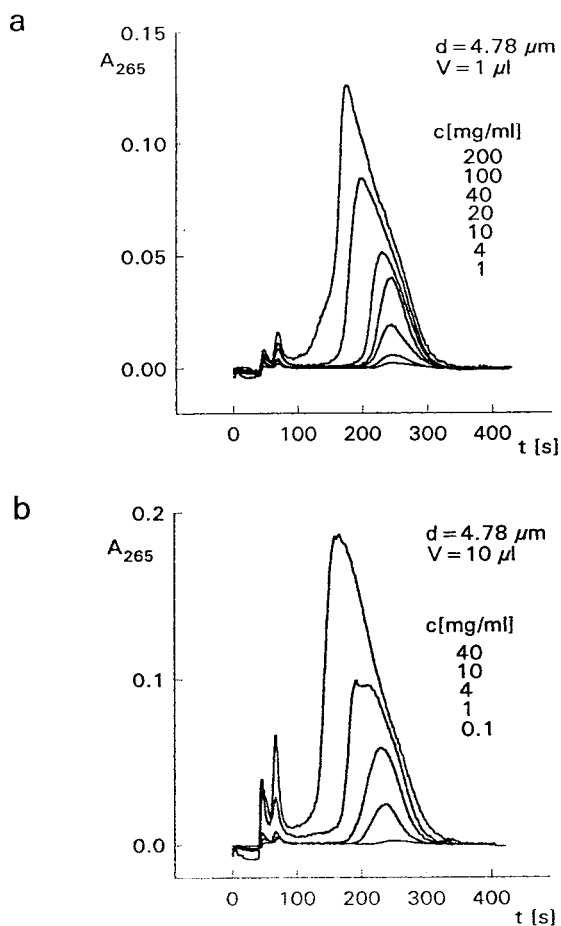


Fig. 4. Overloading effects in GFFF at constant sample volume. The  $c$  values are the concentrations of sample injected; the lower the concentration, the smaller is the peak maximum. Volumes of 5- $\mu\text{m}$  silica gel suspension, (a) 1 and (b) 10  $\mu\text{l}$ ; flow-rate, 0.49 ml/min.

in retention ratio with constant peak width (polystyrene latex beads of diameter 176 nm).

As is obvious from our GFFF experiments, we observed tailing peaks and an increase in retention ratio, which is in contrast to the above-mentioned observations of other workers. A key to understanding this is a difference in separation modes: whereas under normal conditions (with an exponential concentration distribution [20,21]) samples of nanometre size are pressed towards the accumulation wall and the hydrodynamic lift forces are not pronounced, in our

experiments particles  $>1 \mu\text{m}$  are focused in zones above the channel bottom much higher than presumed from simple steric exclusion.

Moreover, we observed a similar evolution of peak characteristics (i.e., an increase in the retention ratio and tailing) for both variable concentration at a constant sample volume and vice versa. This behaviour implies that the retention is determined mainly by the product of concentration and volume ( $cV$ ), i.e., the number of particles, rather than by the concentration or volume of the sample. We tried to confirm this idea by comparing experiments performed with constant product  $cV$ . Fig. 5 shows fractograms of  $5\text{-}\mu\text{m}$  silica and Fig. 6 similar fractograms for  $1.4\text{-}\mu\text{m}$  silica, all obtained at  $cV=1 \mu\text{g}$ . It is clear that the peaks in each triad are virtually identical, although the concentrations or volumes differ even 40-fold for both kinds of particles.

An explanation of the observed increase in retention ratio with increasing number of particles can be based on the course of the lift forces function (see Fig. 7). The magnitude of the lift forces is highest at the channel bottom and then rapidly decreases. Because we examined only retained peaks ( $R < 1$ ), the zones were always focused between the channel bottom and the position  $\delta = 0.19$ . During the elution process,

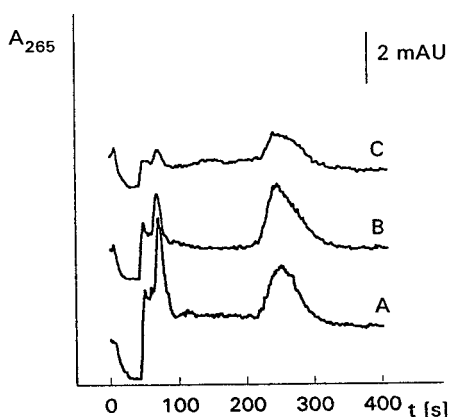


Fig. 5. Fractograms of  $5\text{-}\mu\text{m}$  particles obtained at constant product  $cV=1 \mu\text{g}$ . Fractogram A,  $c=0.1 \text{ mg/ml}$  and  $V=10 \mu\text{l}$ ; B,  $c=1 \text{ mg/ml}$  and  $V=1 \mu\text{l}$ ; C,  $c=4 \text{ mg/ml}$  and  $V=0.25 \mu\text{l}$ . Flow-rate,  $0.49 \text{ ml/min}$ .

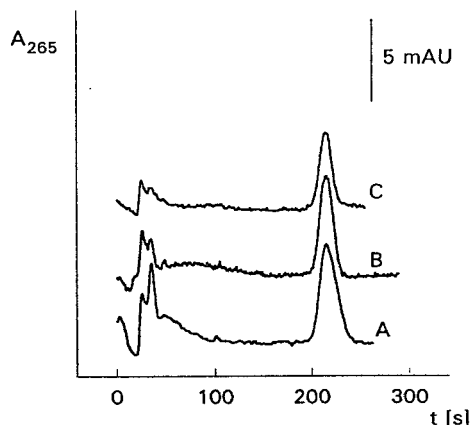


Fig. 6. Fractograms of  $1.4\text{-}\mu\text{m}$  particles obtained at constant flow product  $cV=1 \mu\text{g}$ . Fractogram A,  $c=0.1 \text{ mg/ml}$  and  $V=10 \mu\text{l}$ ; B,  $c=1 \text{ mg/ml}$  and  $V=1 \mu\text{l}$ ; C,  $c=10 \text{ mg/ml}$  and  $V=0.1 \mu\text{l}$ . Flow-rate,  $0.99 \text{ ml/min}$ .

particles oscillate around their equilibrium position  $\delta_0$  where the magnitude of the lift forces  $F$  equals the Archimedes mass of particles  $G = \pi d^3 g \Delta\rho/6$  ( $d$  is the particle diameter,  $g$  is gravitational acceleration and  $\Delta\rho$  is the density difference between particles and carrier liquid). Particles in a lower position  $\delta_1 < \delta_0$  are pushed back upward to the equilibrium position faster ( $F_1 \gg G$ ) than those from the upper positions  $\delta_2 > \delta_0$  ( $F_2 < G$ ). Hence the particles occupy the upper positions in higher numbers, so the zone centre of gravity exhibits a higher mean velocity (a higher retention ratio) because of the parabolic flow profile. This mechanism can also explain our observations in Figs. 5 and 6, where the same numbers of particles exhibited the same retention ratio and peak dispersion independently of the injected volume/concentration.

A conclusion following from our explanation is that overloading effects in GFFF are minimized if the experiments are carried out with the minimum number of particles.

#### Acknowledgement

This work was supported by Grant 203/93/0351 from the Grant Agency of the Czech Republic.

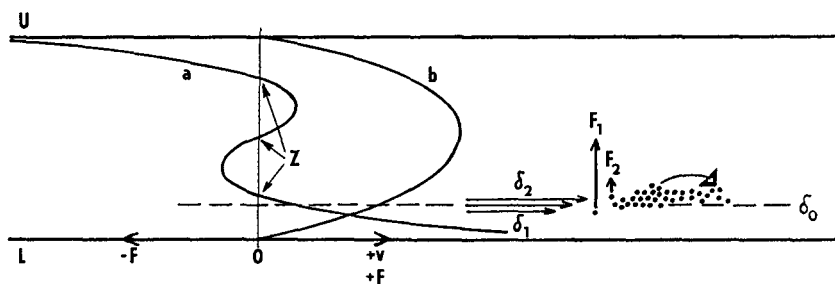


Fig. 7. Schematic representation of overloading effects in GFFF channel. U and L represent the upper and lower channel walls, curves a and b represent the courses of the lift forces and flow velocity profile, respectively,  $-F$  and  $+F$  show the orientation of the lift forces and  $+v$  shows the direction of the carrier liquid flow. The dashed line  $\delta_0$  represents the location of the particle equilibrium position where  $F = G$ , and  $Z$  denotes three positions inside the channel where  $F = 0$  ( $\delta$  is the dimensionless distance of a particle centre from the channel bottom and equals 0.19, 0.50 and 0.81, respectively). Three arrows represent the streamlines near the particle equilibrium position: the middle arrow is at the position  $\delta_0$  where  $F = G$  and corresponds to the retention ratio of very diluted samples, the bottom arrow is at the position  $\delta_1 < \delta_0$  where  $F_1 \gg G$  and particles are rapidly transported to the equilibrium position and the top arrow is at the position  $\delta_2 > \delta_0$  where  $F_2 < G$  and the velocity of the carrier liquid flow is higher. Hence these particles move faster along the channel than the particles at  $\delta_0$  and it is the cause of the observed increase in the mean retention ratio.

## References

- [1] J.C. Giddings, *Sep. Sci. Technol.*, 18 (1983) 765.
- [2] J. Janča and J. Chmelík, *Anal. Chem.*, 56 (1984) 2481.
- [3] J.C. Giddings and M.N. Myers, *Sep. Sci. Technol.*, 13 (1978) 637.
- [4] J.C. Giddings, M.N. Myers, K.D. Caldwell and J.W. Pav, *J. Chromatogr.*, 185 (1979) 261.
- [5] K.D. Caldwell, T.T. Nguyen, M.N. Myers and J.C. Giddings, *Sep. Sci. Technol.*, 14 (1979) 935.
- [6] J. Pazourek, P. Filip, F. Matulík and J. Chmelík, *Sep. Sci. Technol.*, 28 (1993) 1859.
- [7] J. Pazourek and J. Chmelík, *Chromatographia*, 35 (1993) 591.
- [8] J. Pazourek, E. Urbánková and J. Chmelík, *J. Chromatogr.*, 660 (1994) 113.
- [9] P.J. Cardot, J. Gerota and M. Martin, *J. Chromatogr.*, 93 (1991) 568.
- [10] E. Urbánková, A. Vacek, N. Nováková, F. Matulík and J. Chmelík, *J. Chromatogr.*, 583 (1992) 27.
- [11] M.E. Hansen and J.C. Giddings, *Anal. Chem.*, 61 (1989) 811.
- [12] Y. Mori, K. Kimura and M. Tanigaki, *Anal. Chem.*, 62 (1990) 2668.
- [13] M. Hoyos and M. Martin, *Anal. Chem.*, 66 (1994) 1718.
- [14] M.E. Hansen, J.C. Giddings and R. Beckett, *J. Colloid Interface Sci.*, 132 (1989) 300.
- [15] J.C. Giddings and H.M. Moon, *Anal. Chem.*, 63 (1991) 2869.
- [16] S. Lee, M.N. Myers and J.C. Giddings, *Anal. Chem.*, 61 (1989) 2439.
- [17] M.K. Liu, P.S. Williams, M.N. Myers and J.C. Giddings, *Anal. Chem.*, 63 (1991) 2115.
- [18] V.L. Kononenko and J.K. Shimkus, *J. Chromatogr.*, 520 (1990) 271.
- [19] P.S. Williams, *Sep. Sci. Technol.*, 29 (1994) 11.
- [20] K.D. Caldwell, S.L. Brimhall, Y. Gao and J.C. Giddings, *J. Appl. Polym. Sci.*, 36 (1988) 703.
- [21] J.J. Kirkland, W.W. Yau and W.A. Doerner, *Anal. Chem.*, 52 (1980) 1944.



# Derivation of solubility parameters of chlorinated dibenzofurans and dibenzo[*p*]dioxins from gas chromatographic retention parameters via SOFA

Harrie A.J. Govers\*, Frans W.M. van der Wielen, Kees Olie

*Department of Environmental and Toxicological Chemistry, Amsterdam Research Institute for Substances in Ecosystems, University of Amsterdam, Nieuwe Achtergracht 166, 1018 WV Amsterdam, Netherlands*

First received 24 March 1995; revised manuscript received 24 May 1995; accepted 24 May 1995

---

## Abstract

Molar heat of vaporization, molar liquid volume and Scatchard–Hildebrand solubility parameters of chlorinated dibenzofurans (PCDFs) and dibenzo[*p*]dioxins (PCDDs) were derived from (semi-)empirical values of heat of vaporization, (subcooled) liquid density and gas chromatographic Kovats retention indices. To this end a thermodynamic prediction model (SOFA), recently developed, was extended by an exchange entropy contribution representing molecular orientational disorder. The parameters derived were validated using experimental values of relative retention times on stationary phases of different polarities.

Accurate to extremely accurate results were obtained with standard errors of regression close to experimental inaccuracy and high correlation coefficients comparing favourably to existing methods of prediction. The parameters derived performed quite well for apolar to moderately polar stationary phases. For polar phases inaccuracy increased significantly. The method has several advantages compared to other methods used for the prediction of chromatographic retention.

---

## 1. Introduction

Due to their high accuracy, rapid obtainability, versatility and to the low amounts of substances required, chromatographic retention parameters are being used for the determination and estimation of partition constants and other physico-chemical properties of organic compounds. The pertinent methods may be suited to individual compounds and, as often occurs in environmental chemistry, to series of structurally related or congeneric compounds. A basic re-

quirement is a theoretical model connecting the chromatographic retention parameter to the partition constant. In its most simple form this model may be a monolinear Collander-type regression relationship as used for the determination of the partition coefficient between *n*-octanol and water ( $K_{ow}$ ) and the HPLC reversed-phase capacity factor ( $k'$ ) for series of compounds [1].

In order to obtain a more accurate and general relationship we have recently proposed the SOFA (solubility parameters for fate analysis) thermodynamic model [2]. This model has proved capable to accurately predict  $K_{ow}$ , Kovats

\* Corresponding author.

GC retention indices ( $I$ ) on different columns, (subcooled) liquid vapour pressure ( $P$ ), aqueous solubility ( $S_w$ ), Henry's law constant ( $H$ ) and  $k'$  of methylchlorobenzenes. Predictions were isomer specific. Chromatographic retention parameters were predicted at a level of accuracy that compared favourably to experimental accuracy. In the SOFA model, which will be summarized in the Method section, the first step is the derivation of the compound's key descriptors, i.e. its heat of vaporization ( $\Delta H/\text{cal mol}^{-1}$ ), molar liquid volume ( $V/\text{cm}^3 \text{mol}^{-1}$ ) and calculated from these: its Scatchard–Hildebrand solubility parameter [ $\delta/(\text{cal cm}^{-3})^{1/2}$ ] [3]. The latter is an energy density of the liquid defined by  $\Delta H$ ,  $V$ , gas constant ( $R/\text{cal mol}^{-1} \text{K}^{-1}$ ) and absolute temperature ( $T/\text{K}$ ):

$$\delta = [(\Delta H - RT)/V]^{1/2} \quad (1)$$

For the derivation of key descriptors accurate experimental data of descriptors, chromatographic retention parameters or other partition constants have to be used. Once the key descriptors have been derived they can be applied to the prediction of in principle all other partition properties.

Here we derive the key descriptors of the environmentally relevant compound series of the polychlorinated dibenzofurans (PCDFs) and dibenzo[ $p$ ]dioxins (PCDDs) in order to use them elsewhere for the prediction of partition constants such as bioconcentration factors and sediment sorption constants [4]. Simultaneously we would like to find out the model's potential to accurately predict GC retention of these compounds on stationary phases of varying polarity. To this end it turns out to be necessary to extend the SOFA model by the inclusion of a novel molecular orientational disorder entropy contribution. For the derivation of key descriptors we use Kovats retention indices ( $I$ ) determined by Hale et al. [5] and Donnelly et al. [6] on apolar DB5 columns. The model is validated using relative retention times (RRT) determined by Ryan et al. [7] on columns of different polarity. The predictions are compared with the results obtained by other methods [6,8–12].

## 2. Method

### 2.1. The SOFA model equations of $I$ and RRT

SOFA enables a consistent prediction of all types of partition constants, including chromatographic retention parameters [2]. The mixing process of a solute,  $i$ , in a solvent (stationary phase),  $s$ , is modelled as an exchange of molecules in similar lattices filled with just solute or solvent molecules. If solute and solvent molecules have approximately identical shapes and dimensions, only one lattice can describe liquid solute, solvent and solution. An exchange enthalpy contribution can be understood as the result of the energy gain from the formation of solute–solvent interactions and the energy loss from breaking solute–solute and solvent–solvent interactions. An exchange entropy contribution, deviating from the random-mixing ideal-solution expression, may result especially when strong solute–solvent interactions are present, which limit the number of accessible lattice configurations. If solute and solvent molecules are markedly dissimilar, a combinatorial entropy contribution may arise from the extra lattice space in solution available for the smaller molecule compared with the space in a lattice filled with just small molecules. Based on this model an expression can be derived for the logarithm of the activity coefficient of the solute in the solvent at infinite dilution:  $\ln \gamma_{i,s} = H_{i,s}^{\text{ex}} + S_{i,s}^{\text{ex}} + S_{i,s}^{\text{co}}$  (see Ref. [2] for details). In this expression  $i$  stands for the solute and  $s$  for the stationary phase or solvent. The exchange enthalpy contribution is  $H_{i,s}^{\text{ex}} = V_i[\delta_i^2 + \delta_s^2 - 2\delta_i\delta_s c_{1,i,s}(c_{2,i,s}\delta_s + \delta_i)]/RT$ . Constants  $c_{1,i,s}$  and  $c_{2,i,s}$  occur in this contribution, which are characteristic for the class of compound, here denoted by  $I$ , and the solvent. The exchange entropy contribution reads  $S_{i,s}^{\text{ex}} = X_{I,s} + c_{3,I,s} \ln A_i$ , where  $X_{I,s}$  represents the class-solvent specific effect of molecular substitutional disorder and  $c_{3,I,s}$  that of orientational disorder. The latter implies an extension of an expression presented before [2]. The descriptor,  $A_i$ , stands for the maximum number of orientations a solute molecule can take at a lattice point [13]. In solution the maximum

number will be reduced by molecular interaction, represented by  $c_{3,1,s}$ . The combinatorial entropy contribution,  $S_{i,s}^{co} = \ln(V_i/V_s) - V_i/V_s + 1$ .

In addition the SOFA model relates the vapour pressure,  $P_i$ , of the solute with its heat of vaporization:  $\ln P_i = a_1 - b_1 \Delta H_i / RT$  (see Ref. [2] for details), where  $a_1$  is a class-specific constant for the entropy of vaporization and  $b_1$  for the contribution of  $\Delta H_i$ . Finally, we remark that numerical values of  $a$ ,  $b$ ,  $c$  and  $X$  constants have to be derived by fitting to experimental data as described in sections below.

In this way a model equation for  $\ln RRT$  is obtained from the specific retention volume,  $V_g$ , of congener  $i$  and the reference compound ( $r$ ), where  $V_{g,i}$  is a function of the congener's vapour pressure, its activity coefficient and the molecular mass of the stationary phase ( $M_s$ ) [14]. After substitution of our model expression for the vapor pressure and activity coefficient one obtains:

$$\begin{aligned} \ln RRT_{i,s} &= \ln V_{g,i,s} - \ln V_{g,r,s} \\ &= -\ln P_i - \ln \gamma_{i,s} + \ln (298.12R/M_s) \\ &\quad - \ln V_{g,r,s} = b_1 \Delta H_i \\ &\quad - V_i [\delta_i^2 + \delta_s^2 - 2\delta_i \delta_s c_{1,1,s} (c_{2,1,s} \delta_s + \delta_i) \\ &\quad \quad / (\delta_s + c_{2,1,s} \delta_i)] / RT \\ &\quad - a_{0,1} - a_{1,1} (T - 298.15) \\ &\quad - a_{2,1} (T - 298.15)^2 - X_{1,s} - c_{3,1,s} \ln A_i \\ &\quad - \ln (V_i/V_s) + V_i/V_s \\ &\quad + \ln (298.15R/M_s) - \ln V_{g,r,s} \end{aligned} \quad (2)$$

In Eq. 2 the entropy contribution to the vapour pressure ( $a_1$ ) is approximated by a second order polynomial function of temperature, as we would like to obtain an accurate expression for the temperature dependence of RRT. This temperature dependence further requires the knowledge of the temperature at which a certain congener,  $i$ , is eluted during a linearly programmed gas chromatographic run. This temperature,  $T$ , is calculated from the boiling point temperatures,  $T_{bp}$ , of the pertinent ( $i$ ), the first ( $b$ ) and last ( $e$ ) eluting congeners, and the elution temperatures of  $b$  and  $e$  according to Eq. 3:

$$T = T_b + (T_e - T_b)(T_{bp,i} - T_{bp,b}) / (T_{bp,e} - T_{bp,b}) \quad (3)$$

The elution temperatures  $T_b$  and  $T_e$  can be inferred from experimental data and the boiling points are estimated from the heat of vaporization (at 298.15 K) by the inverse of the semi-empirical Hildebrand rule [15]:

$$\Delta H = -2950 + 23.7T_{bp} + 0.02T_{bp}^2 \quad (4)$$

In a similar way a model equation, Eq. 5, is obtained for Kovats retention index  $I_{i,s}$  from the activity coefficients  $\gamma_{i,s}$ ,  $\gamma_{z,s}$ ,  $\gamma_{z+1,s}$  and vapour pressures  $P_i$ ,  $P_z$ ,  $P_{z+1}$  of the solute,  $i$ , and the  $n$ -alkanes with  $z$  or  $z + 1$  carbon atoms eluting just before and after  $i$ , respectively (see Ref. [2], Eq. 13). In this equation the entropy of vaporization constants  $a_1$  and  $a_z$ , with  $Z$  denoting the class of  $n$ -alkanes, were considered to be independent of temperature.  $\Delta X_{1,Z,s}$  represents a difference of substitutional exchange entropy effects between the classes  $I$  and  $Z$ . Eq. 5 holds for an isothermal chromatographic run. In case of a linearly programmed run the mean temperature can be taken as an approximation.

$$\begin{aligned} I_{i,s} - 100z &= \{b_1 \Delta H_i / RT - b_z \Delta H_z / RT \\ &\quad - V_i [\delta_i^2 + \delta_s^2 - 2\delta_i \delta_s c_{1,1,s} (c_{2,1,s} \delta_s \\ &\quad \quad + \delta_i) / (\delta_s + c_{2,1,s} \delta_i)] / RT + V_z [\delta_z^2 + \delta_s^2 \\ &\quad \quad - 2\delta_z \delta_s c_{1,z,s} (c_{2,z,s} \delta_s + \delta_z) / (\delta_s \\ &\quad \quad + c_{2,z,s} \delta_z)] / RT - a_1 + a_z - \Delta X_{1,Z,s} \\ &\quad - c_{3,1,s} \ln A_i + c_{3,z,s} \ln A_z \\ &\quad - \ln (V_i/V_z) + (V_i - V_z) / V_s\} \\ &\quad \cdot 100 / \{b_z (\Delta H_{z+1} - \Delta H_z) / RT \\ &\quad - V_{z+1} [\delta_{z+1}^2 + \delta_s^2 \\ &\quad \quad - 2\delta_{z+1} \delta_s c_{1,z,s} (c_{2,z,s} \delta_s + \delta_{z+1}) / (\delta_s \\ &\quad \quad + c_{2,z,s} \delta_{z+1})] / RT + V_z [\delta_z^2 + \delta_s^2 \\ &\quad \quad - 2\delta_z \delta_s c_{1,z,s} (c_{2,z,s} \delta_s + \delta_z) / (\delta_s \\ &\quad \quad + c_{2,z,s} \delta_z)] / RT - c_{3,z,s} (\ln A_{z+1} \\ &\quad \quad - \ln A_z) - \ln (V_{z+1}/V_z) + (V_{z+1} \\ &\quad \quad - V_z) / V_s\} \end{aligned} \quad (5)$$

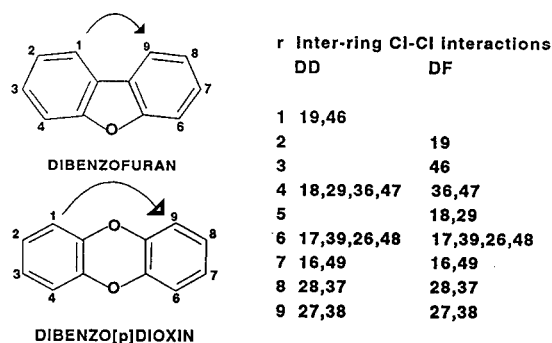


Fig. 1. Skeleton structures of dibenzofuran (DF) and dibenzo[*p*]dioxin (DD). Skeleton numbers denote the positions of chlorine atoms. The inter-ring ( $r=1-9$ ) chlorine-chlorine interactions are denoted by the corresponding skeleton number pairs. If several pairs occur in an entry, e.g. entry 6 under heading DD and DF, it is meant that these pairs obtain equal  $x$  values in Eq. 6. As shown for interactions  $r=1$  (DD) and  $r=2$  (DF) between atoms 1 and 9, the pair interactions may differ for DD and DF.

## 2.2. Fragment parameters for $\Delta H$ , $V$ and $A$

$\Delta H$ ,  $V$  and  $A$  are descriptors for pure solutes or solvents. For solutes,  $\Delta H_i$  and  $V_i$  ( $=x$ ) are calculated in an extended fragment model. It includes the contribution of the parent compound ( $x_{0,DF,DD}$ ), dibenzofuran or dibenzo[*p*]dioxin, the contribution of Cl atoms ( $x_{Cl}$ ), of interactions between Cl atoms positioned *ortho* (*o*), *meta* (*m*) and *para* (*p*) to each other in the same ring ( $x_{ClCl_{o,m,p}}$ ), between Cl atoms *ortho*, *meta* or *para* to the central CC bond in di-

benzofuran ( $x_{ClCl_{o,m,p}}$ ), between Cl atoms *ortho*, *meta* or *para* to a central O atom ( $x_{ClO_{o,m,p}}$ ) and between Cl atoms on different rings ( $x_{ClCl_r}$ ). The latter (nine) interactions are defined in Fig. 1. By counting the number of times ( $n_{Cl}$ ,  $n_{ClCl_{o,m,p}}$ , ...) a certain interaction occurs within a congener molecule all 136 PCDFs and 76 PCDDs can be identified uniquely. In Table 2 the values for the identifiers of octachloro-DF/DD are included as an example.

The total value of  $\Delta H_i$  or  $V_i$  is obtained by summation of the foregoing contributions multiplied by the number of times they occur in the molecule:

$$x = x_0 + n_{Cl} \cdot x_{Cl} + \dots + n_{ClCl_9} \cdot x_{ClCl_9} \quad (6)$$

As shown in Eq. 1,  $\delta_i$  can be calculated directly from  $V_i$ ,  $\Delta H_i$  and  $RT$ . As shown in Table 1, for the stationary chromatographic phases estimated values of  $V_s$  and  $\delta_s$  can be obtained from experimental values. The  $\Delta H_z$  and  $V_z$  values of *n*-alkanes and the temperature dependencies of  $\Delta H$  and  $V$  are approximated by simple empirical relationships as applied before [2].

$A_i$ , the maximum number of molecular (congener) orientations at a lattice point, is approximated by the number of ways the C, H, O or Cl atoms in the molecule can be permuted in the molecular skeleton ( $n$  denotes the number of atoms):

$$A_i = [nC + nH + nO + nCl]! / [nC!nH!nO!nCl!] \quad (7)$$

Table 1  
Molar liquid volume ( $V$ ) and solubility parameter ( $\delta$ ) of gas chromatographic stationary phases at 298.15 K

Liquid phase (-silicone) <sup>a</sup>	$V^b$ ( $\text{cm}^3 \text{mol}^{-1}$ )	$\delta^c$ [( $\text{cal cm}^{-3}$ ) <sup>1/2</sup> ]
DB1 (100% dimethyl-)	98.49	6.18
DB5 (5% phenyl-, 95% dimethyl-)	100.67	6.27
DB17 (50% phenyl-, 50% methyl-)	120.25	7.15
DB225 (50% methylcyanopropyl, 50% methylphenyl-)	139.00	8.34

<sup>a</sup> Composition taken from column supplier catalogues.  $V$  and  $\Delta H$  values of mixed phases were estimated from the percentage contributions of the  $V$  and  $\Delta H$  values of the single component phases.

<sup>b</sup> Estimated from liquid densities of corresponding silanes, obtained from Ref. [16].

<sup>c</sup> Calculated according to Eq. 1 from  $V$  and  $\Delta H$  values estimated by Eq. 4 from boiling point temperatures of corresponding silanes, obtained from Ref. [16].



This approximation is equivalent to the assumption that the number of orientations is proportional to the number of configurations of a mixture of free atoms at the lattice site. Note that, in addition to Eq. 6, Eq. 7 introduces systematic differences between PCDFs ( $nO = 1$ ) and PCDDs ( $nO = 2$ ). Moreover,  $A_i$  displays a maximum for PCDD/F at  $nCl = 4$ , whereas no maximum is found for  $A_z$  of  $n$ -alkanes with increasing  $nC = z$ .

### 2.3. Derivation of parameters

In order to derive  $x$  fragment parameters, Eqs. 5 and 6 have to be applied in a (non-)linear multiple regression and multi-response fit of the pertinent constants to experimental data of  $I_{i,s}$ ,  $\Delta H_i$  and  $V_i$ . The  $x$  fragment starting values have to be derived using Eq. 6 in a multilinear fit to experimental data or from fragment values obtained from previous calculations. Starting values for  $\Delta X$  and  $c$  constants have to be obtained from theoretical considerations or from previous results.  $X$  starting values, e.g., correspond to Flory–Huggins contributions of  $\pm 0.3$ ,  $c_1 = c_2 = 1$  holds for a simple Scatchard–Hildebrand solubility parameter model and  $c_3$  has to be in the range of  $-1$  to  $+1$ . Starting values of  $a$  and  $b$  constants may be obtained from experimental  $P_i$  and  $\Delta H_i$  data or from previous results. If the starting values of the  $x$  fragment parameters are sufficiently close to their final values, these parameters can be fitted simultaneously with the  $\Delta X$ ,  $a$ ,  $b$  and  $c$  constants.

### 2.4. Validation of the method

Once the  $x$  fragment parameters have been obtained, they can be used in Eq. 2 in order to calculate  $\ln RRT_{i,s}$  values. To this end the  $X$ ,  $a$ ,  $b$  and  $c$  parameters of this equation have to be fitted by a nonlinear regression procedure to experimental data of  $\ln RRT_{i,s}$ . (Starting) values of  $b$  and  $c$  constants can be taken from the foregoing  $x$  parameter derivation, whereas starting values of  $a_{1,1}$ ,  $a_{2,1}$  and  $a_{0,1}$  [ $+\ln(298.15R/M_s) - \ln V_{g,r}$ ] have to be found by trial and error. This type of calculation implies a validation of

the  $x$  parameters derived and the model equations.

### 2.5. Statistics

All multilinear regression calculations were carried out by the MLINREG procedure of the STATPAK program (North-West Analytical, Portland, OR, USA). All nonlinear multiple, multi-response, regression calculations were carried out by the SOFA program, developed previously [2]. This program is based on Simplex optimization with weighing of each type of property ( $t$ ) by a factor of  $w_t$ , which is assumed to be inversely proportional to some measure for the experimental error ( $e_t$ ). Using a pseudolinear approximation, the 95% confidence limits of the derived  $x$  parameters and constants can be calculated. The additional statistical data are the mean deviation ( $\langle \sigma_t \rangle$ ) of calculated from the  $N_t$  experimental values for each type of property, the corresponding correlation coefficient ( $r_t$ ), not corrected for the number of parameters. All calculations can be carried out on a personal computer (minimum speed equivalent to a 486 Intel microprocessor with mathematical coprocessor).

### 2.6. Numerical example

A numerical example of the calculation of  $I$  of OCDF (after derivation of  $x$  parameters and  $a$ ,  $b$ ,  $c$ ,  $X$  constants) is given in the Appendix.

## 3. Results

### 3.1. Derivation of $x$ parameters

The  $x$  parameter derivation was performed using experimental values of heats of vaporization ( $N_t = 16$ ), molar volumes ( $N_t = 11$ ) (see Table 3), Kovats retention indices of PCDFs at a mean temperature of 510.65 K ( $N_t = 115$ ) [5] and of PCDDs at a mean temperature of 528.15 K ( $N_t = 41$ ) [6], both determined on a DB5 column with characteristics given in Table 1. Weights ( $w_t$ ) were derived from various measures for

experimental inaccuracies and uncertainties ( $e_i$ ) as reported in the literature. The latter were also reported for  $I$  ( $e = 7$ ) by Robbat and Kalogeropoulos [9]. The results of this derivation are summarized in Tables 2, 3 and 4.

Table 2 shows the  $x$  parameters derived and their 95% confidence limits. It can be seen that all 42 parameters, except for  $h_{\text{ClCl}_6}$ ,  $h_{\text{ClCl}_m}$ ,  $v_{\text{ClCl}_6}$  and  $v_{\text{ClCl}_2}$ , are statistically significant, in spite of their large number. With the help of Eqs. 6 and 1 all 212  $\Delta H$ ,  $V$  and  $\delta$  values were calculated. Some results are included in Table 3 together with their deviation of (semi-)empirical data and other statistics. Inaccuracies in calculations turn out to be equal to or less than experimental inaccuracies. The differences between PCDF and PCDD congeners with identical chlorine substitution pattern, as shown in Tables 2 and 3, are evident and explain their different chromatographic behaviour.

Table 2

Heat of vaporization ( $h$ ) and molar volume ( $v$ ) parameters for PCDD/Fs derived using model Eqs. 5 and 6 in a nonlinear fit to 183 experimental data

	$n_{\dots}$ OCDF <sup>a</sup>	$n_{\dots}$ OCDD <sup>a</sup>	$h$ fragment (cal mol <sup>-1</sup> )	$v$ fragment (cm <sup>3</sup> mol <sup>-1</sup> )
$x_{0_{\text{DF}}}$	1	0	15558 (10)	140.40 (0.10)
$x_{0_{\text{DD}}}$	0	1	17772 (44)	146.96 (0.20)
$x_{\text{Cl}}$	8	8	1854 (92)	15.76 (0.08)
$x_{\text{ClCl}_6}$	6	6	-5 (8) <sup>b</sup>	3.44 (0.11)
$x_{\text{ClCl}_m}$	4	4	-358 (10)	-0.52 (0.12)
$x_{\text{ClCl}_p}$	2	2	-296 (15)	-0.70 (0.17)
$x_{\text{ClCl}_6}$	2	0	-442 (62)	0.00 (0.14) <sup>b</sup>
$x_{\text{ClCl}_m}$	4	0	241 (111)	-4.50 (0.15)
$x_{\text{ClCl}_p}$	2	0	-117 (60)	-3.84 (0.14)
$x_{\text{ClCl}_6}$	2	4	-332 (59)	-0.66 (0.12)
$x_{\text{ClCl}_m}$	4	8	44 (112) <sup>b</sup>	-5.96 (0.13)
$x_{\text{ClCl}_p}$	2	4	-365 (58)	-3.66 (0.12)
$x_{\text{ClCl}_{11}}$	0	2	273 (18)	-4.77 (0.19)
$x_{\text{ClCl}_{12}}$	1	0	778 (20)	-0.05 (0.23) <sup>b</sup>
$x_{\text{ClCl}_{13}}$	1	0	-29 (18)	-3.95 (0.21)
$x_{\text{ClCl}_{14}}$	2	4	-163 (11)	0.57 (0.14)
$x_{\text{ClCl}_{15}}$	2	0	80 (14)	-2.71 (0.17)
$x_{\text{ClCl}_{16}}$	4	4	-216 (9)	0.93 (0.13)
$x_{\text{ClCl}_{17}}$	2	2	-211 (13)	-0.20 (0.15)
$x_{\text{ClCl}_{18}}$	2	2	-169 (12)	1.40 (0.14)
$x_{\text{ClCl}_{19}}$	2	2	-323 (12)	3.58 (0.15)

<sup>a</sup> Identifiers of Eq. 6 for octachloro-DF/DD (OCDF/D) as an example.

<sup>b</sup> Parameter statistically not significant.

Values in parentheses represent the 95% confidence limits.

Table 4 summarizes the derived class and class-solvent constants. They turn out to be statistically significant without exception. Thus the introduction of molecular orientational exchange entropy, as shown by the  $c_3$  values, substantially improved the prediction.

Additional statistical results are included in Table 6. Fig. 2 shows the excellent correspondence between calculated and experimental  $I$  data.

### 3.2. Validation of the method

In order to validate the  $x$  parameters derived, Eq. 2 was used in a multiple nonlinear fit of the pertinent  $X$ ,  $a$  and  $c$  constants to experimental ln RRT data of all ( $N_t = 38$ ) tetrachlorobenzofurans (TCDFs) on four columns of different polarity (DB1, DB5, DB17, DB225) [7]. Column properties were those of Table 1, showing increasing

Table 3  
 Predicted values of heat of vaporization ( $\Delta H$ ), molar liquid volumes ( $V$ ) and solubility parameters ( $\delta$ ) at 298.15 K, of PCDF/D, together with their deviations (exp. – calc.) from experimental data (given in parentheses)

Congener	$\Delta H^a$ (cal mol <sup>-1</sup> )	$V^b$ (cm <sup>3</sup> mol <sup>-1</sup> )	$\delta^c$ (cal cm <sup>-3</sup> ) <sup>1/2</sup>
DF	15558 (872)	140.40 (1.22)	10.325 (0.250)
36-	18939 (78)	157.53	10.792
248-	20038 (449)	168.01	10.758
2378-	21586 (232) <sup>d</sup>	184.35 (0.27) <sup>d</sup>	10.671 (0.051)
12346789-	25277 (-737)	230.50 (-1.63) <sup>d</sup>	10.348 (-0.119)
DD	17772 (-163)	146.96 (-4.10)	10.812 (0.102)
1-	19338 (-92)	156.10 (2.66)	10.959 (-0.119)
2-	19305 (180)	153.09 (2.46)	11.056 (-0.035)
23-	20833 (-444)	162.67	11.155
27-	20515 (137)	162.81 (0.92)	11.062 (0.007)
28-	20669 (1063)	160.63 (7.26)	11.180 (0.041)
124-	21778 (-386)	173.60	11.047
137-	21661 (595)	170.18	11.127
1234-	22943 (-365)	186.10	10.959
2378-	22910 (-173)	188.34 (-2.47)	10.886 (0.029)
234678-	24831	210.70 (-4.45)	10.726
12346789-	25738 (-1051)	231.27 (-1.15)	10.427 (-0.194)
$r$	0.982	0.995	0.926
$\langle\sigma\rangle$	439	2.60	0.095
$e$	375	3.00	0.176
$N$	16	11	10

<sup>a</sup> (Experimental) data inferred from Ref. [17] using an empirical  $d\Delta H/dT = -13$  cal mol<sup>-1</sup> K<sup>-1</sup> value.

<sup>b</sup> Semi-empirical data calculated from the crystalline molar volume ( $V_c$ ) according to  $V = 13.05 + 0.98063V_c$  [18].  $V_c$  obtained from crystalline densities from Refs. [19–25].

<sup>c</sup> Calculated by Eq. 1.

<sup>d</sup> Deviation from semi-empirical value estimated from (semi-)empirical values of DF, DD, 2378-D and 1234678-DD.

values of  $\delta_s$  or increasing polarity;  $b_1$  and  $c_{3,1,5}$  (PCDF) values were identical to those of Table 4. The experimental data were obtained applying different temperature programs from Ryan et al. [7], which were simulated by Eqs. 3 and 4. Experimental uncertainties were not reported by these authors; a value of  $e = 0.001$  for ln RRT was inferred from their data. The results are included in Tables 5 and 6 and in Fig. 3.

DB1, DB5 and DB17 results are similar, DB225 (the polar cyanopropyl column) results showing clear deviation from these. The best results are obtained for DB5, the column which was also used for the derivation of  $x$  parameters, and are relatively poor for the polar DB225 column. Several  $a_1$  and  $a_2$  contributions are not significant from a statistical point of view. These

results are in accordance with the additional statistical data of Table 6 and the scatter diagrams of Fig. 3.

#### 4. Discussion and conclusions

The nonlinear SOFA model has a thermodynamic basis extended with a relatively large number of extra-thermodynamic heat of vaporization and molar volume fragment parameters and with compound class and class-solvent constants. Temperature dependence of properties is included via empirical relationships. According to these characteristics the model allowed for the prediction of Kovats retention index and relative retention times of PCDF/Ds at different tem-

Table 4

Compound class and class-solvent constants derived using model Eqs. 5 and 6 in a nonlinear regression to 183 experimental data

Constant	$I(\text{PCDFs})$	$I(\text{PCDDs})$
$a_1 + \Delta X_{1,z,s}$	13.383 (0.210)	14.558 (0.274)
$b_1$	0.8162 <sup>a</sup>	0.8162 <sup>a</sup>
$c_{1,1,s}$	1.045 (0.110)	1.237 (0.161)
$c_{2,1,s}$	0.438 (0.018)	0.406 (0.021)
$c_{3,1,s}$	-0.142 (0.024)	-0.164 (0.032)
$c_{1,z,s}$	0.607 (0.168) <sup>b</sup>	0.607 (0.68) <sup>b</sup>
$c_{2,z,s}$	0.781 (0.154) <sup>b</sup>	0.781 (0.154) <sup>b</sup>
$c_{3,z,s}$	0.15 (0.07) <sup>b</sup>	0.15 (0.07) <sup>b</sup>

<sup>a</sup> Not varied, but derived by monolinear fit of experimental  $\Delta H_i$  data to experimental  $P_i$  data [17] via  $\ln P_i = a_1 - bI\Delta H_i$ .

<sup>b</sup> Values for  $I(\text{PCDFs})$  and  $I(\text{PCDDs})$  forced to be identical. 95% Confidence limits are in parentheses; non-significant additional decimal figures are given in order to avoid rounding errors of data used in the Appendix.

peratures and, though less complete, on four columns of different polarity. In this way the SOFA model can assist in the choice of stationary phases and the identification of unknown compounds provided that sufficient data of the stationary phase are available in order to estimate its approximate molar volume and solubility parameter. In addition, heat of vaporization, (sub-cooled) molar liquid volume and solubility parameter were predicted (Table 3), which

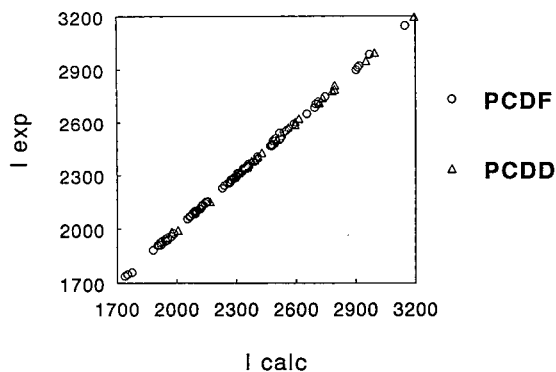


Fig. 2. Correlations between calculated (Eq. 2) and experimental data for Kovats retention indices ( $I$ ) of polychlorodibenzofurans (510.65 K) and polychlorodibenzo[*p*]dioxins (528.15 K) on DB5 columns.

was a main objective of this study. The different behaviour of PCDF and PCDD could be attributed to the presence of partly differing fragment parameters and maximum number of orientations on a lattice site in the two types of congeneric molecules. Moreover, though not shown here, values were obtained for the various enthalpic and entropic contributions to these properties (cf. Ref. [2]) and for boiling point temperatures (using Eq. 4). Table 6 shows that all predictions, with the exception of relative retention times on polar columns, are of the same order of accuracy as the experimental data. This accuracy allows for the physical discrimination of both isomer groups from each other and isomers within a group.

Other models have been used for the predictions of separate chromatographic properties of PCDFs and PCDDs. Their performance is summarized in Table 6 as well. Fragment models [6,8] dissect the retention property directly into contributions of molecular fragments (cf. the  $x$  parameters in the SOFA model, which dissect  $\Delta H$  and  $V$ ), turn out to be of equal accuracy compared to SOFA and require only simple mathematics and computer programs. The pertinent fragment parameters and their values, however, vary with type of property, compound series, column and temperature program. In addition, they do not provide much information on the chromatographic partitioning process.

Molecular connectivity [9] and mixed fragment-connectivity models [10] turn out to be of either equal or lower accuracy compared to SOFA. They have drawbacks similar to those of fragment models.

Models using molecular properties such as van der Waals surface [11], polarizability, ionization potential and dipole moment [12] do have, in contrast to the fragment and molecular connectivity models, a partly physical basis. The application of these molecular descriptors also has a scope more general than the latter. With respect to this they are similar to SOFA, though less complete. As they are of a computational simplicity intermediate to the fragment plus connectivity models and SOFA, they might have good perspectives for use. Currently, however, their

Table 5  
Compound class and class-solvent constants as found by Eq. 2 for TCDFs on DB1, DB5, DB17 and DB225 columns

Constant	DB1	DB5	DB17	DB225
$-X_{1,s} \dots^a$	3.83 (3.14)	4.09 (2.05)	5.32 (4.17)	11.97 (0.80)
$c_{1,1,s}$	0.59 (0.01)	0.61 (0.01)	0.64 (0.02)	0.82 (0.05)
$c_{2,1,s}$	1.94 (0.06)	1.73 (0.06)	1.75 (0.29)	1.28 (0.28)
$a_{1,1}$	-0.01 (0.03) <sup>b</sup>	-0.01 (0.02) <sup>b</sup>	-0.03 (0.04) <sup>b</sup>	-0.045 (0.021)
$a_{2,1} \cdot 10^5$	9.28 (7.10)	6.93 (5.53)	-2.54 (10.6) <sup>b</sup>	-6.74 (5.42)

<sup>a</sup>  $-X_{1,s} - a_{0,1} + \ln(298.15R/M_s) - \ln V_{g,r}$  was fitted as a sum.

<sup>b</sup> Contribution statistically not significant.

95% Confidence limits are in parentheses.

accuracy is very poor compared to all other models.

Finally, UNIQUAC and UNIFAC models have been used for the prediction of partition constants [26,27]. In order to solve the problem of finding values of intermolecular interactions each time a new molecule is introduced, in UNIFAC molecular interactions were composed out of interactions between functional groups of the pertinent molecules. In this thermodynamic

model isomer differences are treated incompletely, however. Differences between *o*-, *m*- and *p*-substitution on ring systems are, e.g., not accounted for. In its current version UNIFAC, therefore, is not useful for chromatographic purposes requiring high accuracy. It has, however, to be mentioned that some common basis exists between the UNIQUAC model, underlying UNIFAC, and our SOFA model [2].

It would be useful to develop a method with a

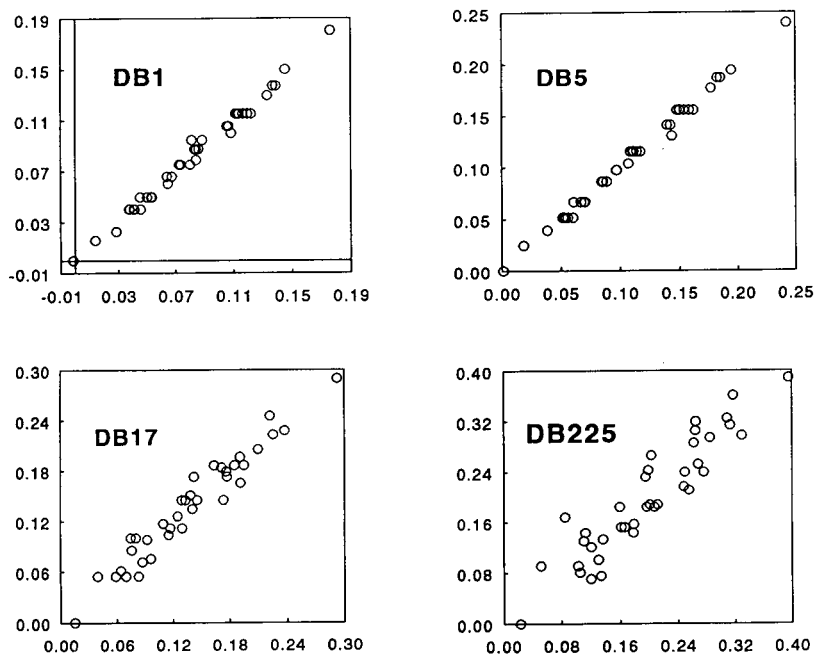


Fig. 3. Correlations between calculated (Eq. 3) values (on the horizontal axes) and experimental  $\ln RRT$  data (on the vertical axes) for 38 TCDFs on DB1, DB5, DB17 and DB225 stationary phases.

Table 6

Comparison of statistical results obtained by the SOFA model and other prediction models for chromatographic retention of PCDF/Ds

Model	Property	Compounds	<i>N</i>	<i>r</i>	$\langle \sigma \rangle$	<i>e</i>
SOFA-Eq.5	<i>I</i>	PCDF	115 <sup>c</sup>	0.9997	5.0	5.0
SOFA-Eq.5	<i>I</i>	PCDD	41 <sup>a</sup>	0.9997	4.8	5.0
SOFA-Eq.2	ln RRT-DB1	TCDF	38 <sup>b</sup>	0.994	0.003	0.001
SOFA-Eq.2	ln RRT-DB5	TCDF	38 <sup>b</sup>	0.997	0.003	0.001
SOFA-Eq.2	ln RRT-DB17	TCDF	38 <sup>b</sup>	0.970	0.012	0.001
SOFA-Eq.2	ln RRT-DB225	TCDF	38 <sup>b</sup>	0.928	0.028	0.001
Fragment <sup>a</sup>	<i>I</i>	PCDD	41 <sup>a</sup>	0.9998	3.5 <sup>k</sup>	
Fragment <sup>b</sup>	<i>I</i> <sup>b</sup>	PCDF	110 <sup>c</sup>	0.999	4.8 <sup>k</sup>	
MC <sup>d</sup>	<i>I</i>	PCDF	115 <sup>c</sup>	0.9944	16.0 <sup>k</sup>	
MC/Fragment <sup>e</sup>	<i>I</i>	PCDD	34 <sup>a,c</sup>	>0.9995	1.8	
SA <sup>f</sup>	<i>I</i>	PCDF	115 <sup>c</sup>	0.984	30? <sup>f,k</sup>	
QC <sup>g</sup>	<i>I</i>	PCDF	69 <sup>c,g</sup>	0.963	43 <sup>k</sup>	
QC <sup>g</sup>	<i>I</i>	PCDD	37 <sup>c,g</sup>	0.990	25 <sup>k</sup>	

<sup>a</sup> Ref. [6]. Multilinear regression dissecting *I* into 11 fragment parameters.

<sup>b</sup> Ref. [8]. Multilinear regression dissecting *I* into 17 fragment parameters. Non-logarithmic *I*-index definition used.

<sup>c</sup> Ref. [5].

<sup>d</sup> Ref. [9]. Multilinear regression using 6 molecular connectivity (MC) indices.

<sup>e</sup> Ref. [10]. Multilinear regression using one molecular connectivity index and 6 fragment parameters. Selective use of experimental data.

<sup>f</sup> Ref. [11]. Monolinear regression using the molecular surface area (SA) as parameter. The reported error of 0.98 cannot be correct in view of other errors reported and the low correlation coefficient. The correct value is estimated to be about 30 retention index units.

<sup>g</sup> Ref. [12]. Multilinear regression using molecular polarizability, ionization potential and squared dipole moment as quantum chemical (QC) parameters. Selective use of experimental data.

<sup>h</sup> Ref. [7]. Only TCDF data selected, see text.

<sup>k</sup> If standard errors of regression were reported, the latter were divided by 1.3 in order to roughly estimate the mean error.

sound physical basis such as SOFA and with an equal accuracy, but using a reduced number of *x* fragment parameters or even without the latter. Work on this objective is in progress, in which  $\Delta H$  and *V* are calculated from intermolecular interactions using the atom–atom pair potential approximation [28]. By this, it is simultaneously aimed at the improvement of the calculation of the interactions between solute and solvent molecules (the effect of column polarity).

## 5. Note

The calculated values of  $\Delta H$ , *V*,  $\delta$ , *T*<sub>bp</sub> and *I* of all 212 PCDF/Ds and the calculated values of ln RRT (DB1, DB5, DB17, DB225) of all 38 TCDFs are available from the authors on request.

## Appendix: calculation of *I* (OCDF)

As an example of a detailed calculation, performed by computer in SOFA, the calculation of the Kovats retention index of octachlorodibenzofuran (OCDF) on a DB5 column at a mean temperature of 510.65 K (237.5°C) is given.

Molecular identifiers, *n* . . . , and fragment contributions, *h* . . . and *v* . . . , of OCDF are found in Table 2. After application of Eq. 6 one obtains:  $\Delta H$  (298.15 K, OCDF) = 25277 cal mol<sup>-1</sup> and *V* (298.15 K, OCDF) = 230.50 cm<sup>3</sup> mol<sup>-1</sup>. Using Eq. 1 the solubility parameter is obtained:  $\delta$  (298.15 K, OCDF) = 10.348 [cal cm<sup>-3</sup>]<sup>1/2</sup>. For the calculation of combinatorial entropy effects an approximated volume *V*<sup>co</sup> (298.15 K, OCDF) = *v*<sub>o</sub> + 8*v*<sub>C1</sub> = 140.40 + 8 × 15.76 = 266.48 cm<sup>3</sup> mol<sup>-1</sup> was used in order to

account for the non-isomer specific behaviour of  $S^{\text{co}}$  (see Ref. [2]).

Heat vaporization, molar liquid volume and solubility parameter of the stationary phase (DB5) at 298.15 K were obtained from model compounds (see also Table 1). DB5 is approximated by a mixture of 5% phenyl- and 95% dimethyl-silane and the corresponding parameters were found from the percentage contribution of the pure model compounds:  $\Delta H$  (298.15 K, DB5) = 4550 cal mol<sup>-1</sup>,  $V$  (298.15 K, DB5) = 100.67 cm<sup>3</sup> mol<sup>-1</sup> and (via Eq. 1):  $\delta$  (298.15K, DB5) = 6.27 [cal cm<sup>3</sup>]<sup>1/2</sup>. The use of model compounds may lead to deviation of  $\delta$  values presented elsewhere.

The  $z$  and  $z + 1$  values of the corresponding  $n$ -alkanes, found by optimization in SOFA, turned out to be 31 and 32, respectively. The  $\Delta H$  and  $V$  values of  $n$ -alkanes at 298.15 K are obtained from the empirical equation given in Table 3 of Ref [2]:  $\Delta H$  (298.15 K,  $z = 31$ ) = 25059 cal mol<sup>-1</sup>,  $\Delta H$  (298.15 K,  $z = 32$ ) = 25516 cal mol<sup>-1</sup>,  $V$  (298.15 K,  $z = 31$ ) = 545.34 cm<sup>3</sup> mol<sup>-1</sup>,  $V$  (298.15 K,  $z = 32$ ) = 562.84 cm<sup>3</sup> mol<sup>-1</sup>. Via Eq. 1 we find:  $\delta$  (298.15 K,  $z = 31$ ) = 6.598 [cal cm<sup>-3</sup>]<sup>1/2</sup>,  $\delta$  (298.15 K,  $z = 32$ ) = 6.551 [cal cm<sup>-3</sup>]<sup>1/2</sup>.

Parameters at 510.65 K are obtained from values at 298.15 according the expressions  $\Delta H(T) = \Delta H$  (298.15 K) - 13 (T - 298.15) and  $V(T) = V$  (298.15 K) [1 + 0.001237(T - 298.15)] (see Ref. [2]):  $\Delta H$  (510.65 K, OCDF) = 22515 cal mol<sup>-1</sup>,  $\Delta H$  (510.65 K, DB5) = 1788 cal mol<sup>-1</sup>,  $\Delta H$  (510.65 K,  $z = 31$ ) = 22297 cal mol<sup>-1</sup>,  $\Delta H$  (510.65 K,  $z = 32$ ) = 22753 cal mol<sup>-1</sup>,  $V$  (510.65 K, OCDF) = 291.09 cm<sup>3</sup> mol<sup>-1</sup>,  $V^{\text{co}}$  (510.65 K, OCDF) = 336.53 cm<sup>3</sup> mol<sup>-1</sup>,  $V$  (510.65 K, DB5) = 127.13 cm<sup>3</sup> mol<sup>-1</sup>,  $V$  (510.65 K,  $z = 31$ ) = 688.69 cm<sup>3</sup> mol<sup>-1</sup>,  $V$  (510.65 K,  $z = 32$ ) = 710.79 cm<sup>3</sup> mol<sup>-1</sup>. From these result via Eq. 1:  $\delta$  (510.65 K, OCDF) = 8.594 (cal cm<sup>-3</sup>)<sup>1/2</sup>,  $\delta$  (510.65 K, DB5) = 2.466 (cal cm<sup>-3</sup>)<sup>1/2</sup>,  $\delta$  (510.65 K,  $z = 31$ ) = 5.559 (cal cm<sup>-3</sup>)<sup>1/2</sup> and  $\delta$  (510.65 K,  $z = 32$ ) = 5.530 (cal cm<sup>-3</sup>)<sup>1/2</sup>.

The logarithm of the temperature independent orientational entropy descriptors,  $A$ , are obtained from Eq. 7 in a numerical approximation of  $\ln A(n\text{Cl}) = -19.1131 + 0.26419(n_{\text{Cl}} - 4)^2$  for

OCDF and  $\ln A(z) = -0.782 - 1.910 z$  for  $n$ -alkanes leading to  $\ln A(\text{OCDF}) = -14.879$ ,  $\ln A(z = 31) = -59.996$  and  $\ln A(z = 32) = -61.906$ .

The temperature independent class constants  $a_1 + \Delta X_{1,z,s} = 13.383$ ,  $b_1 = 0.8162$ ,  $c_{1,1,s} = 1.045$ ,  $c_{2,1,s} = 0.438$ ,  $c_{3,1,s} = 0.142$ ,  $c_{1,z,s} = 0.607$ ,  $c_{2,z,s} = 0.781$ ,  $c_{3,z,s} = 0.148$  obtained after derivation are given in Table 4. The temperature independent constants  $a_z = 12.764$  and  $b_z = 0.62335$  are obtained from experimental  $n$ -alkane data (See Ref. [2]).

Substitution of the appropriate data mentioned above into Eq. 5 leads to  $I(\text{calc}) = 3150$ , whereas the experimental value  $I(\text{exp}) = 3147$ .

## References

- [1] W.E. Hammers, G.J. Meurs and C.L. De Ligny, J. Chromatogr., 247 (1982) 1–13.
- [2] H.A.J. Govers, J. Chem. Soc. Faraday Trans., 89 (1993) 3751–3759.
- [3] J.H. Hildebrand and R.L. Scott, The Solubility of Nonelectrolytes, Reinhold, New York, NY, 1950, pp. 119–134.
- [4] H. Loonen, Bioavailability of Chlorinated Dioxins and Furans in The Aquatic Environment, Thesis, University of Amsterdam, 1994, pp. 135–163.
- [5] M.D. Hale, F.D. Hileman, T. Mazer, T.L. Shell, R.W. Noble and J.J. Rook, Anal. Chem., 57 (1985) 640–648.
- [6] J.R. Donnelley, W.D. Munslow, R.K. Mitchum and G.W. Sovocool, J. Chromatogr., 392 (1987) 51–63.
- [7] J.J. Ryan, H.B.S. Conacher, L.G. Panopio, B.P.-Y. Lau and J.A. Hardy, J. Chromatogr., 541 (1991) 131–183.
- [8] F.D. Hileman, M.D. Hale, T. Nazer and R.W. Noble, Chemosphere, 14 (1985) 601–608.
- [9] A. Robbat and C. Kalogeropoulos, Anal. Chem., 62 (1990) 2684–2688.
- [10] S. Sekusak and A. Sabljic, J. Chromatogr., 628 (1993) 69–79.
- [11] W.J. Dunn III, M. Koehler, D.L. Stalling and T.R. Schwartz, Anal. Chem., 58 (1986) 1835–1838.
- [12] V.S. Ong and R.A. Hites, Anal. Chem., 63 (1991) 2829–2834.
- [13] H.A.J. Govers, J. Chem. Phys., 67 (1977) 4199–4205.
- [14] J. Novak, in J.A. Jonsson (Editor), Chromatographic Theory and Basic Principles, Marcel Dekker, New York, NY, 1987, pp. 103–156.
- [15] A.F.M. Barton, Chem. Rev., 75 (1975) 731–753.
- [16] D.R. Lide (Editor), Handbook of Chemistry and Physics, 72nd edition 1991–1992, CRC Press, Boca Raton, FL, 1991.
- [17] B.F. Rordorf, Chemosphere, 18 (1989) 783–788.

- [18] H.A.J. Govers, in preparation.
- [19] A. Banerjee, *Acta Cryst.*, B28 (1973) 2984–2991.
- [20] A.W. Cordes and C.K. Fair, *Acta Cryst.*, B30 (1974) 1621–1623.
- [21] J.S. Cantrell, D.W. Tomlin and T.A. Beiter, *Chemosphere*, 19 (1989) 183–188.
- [22] J.S. Cantrell, N.C. Webb and A.J. Mabis, *Acta Cryst.*, B25 (1969) 150–156.
- [23] F.P. Boer, M.A. Neuman, F.P. van Remoortere, P.P. North and H.W. Rinn, *Adv. Chem.*, 120 (1973) 14–25.
- [24] F.P. Boer, F.P. van Remoortere and W.W. Muelder, *J. Am. Chem. Soc.*, 94 (1972) 1006–1007.
- [25] C.J. Koester, J.C. Huffman and R.A. Hites, *Chemosphere*, 17 (1988) 2419–2422.
- [26] D.S. Abrams and J.M. Prausnitz, *AIChE J.*, 21 (1975) 116–128.
- [27] A. Fredenslund, R.L. Jones and J.M. Prausnitz, *AIChE J.*, 21 (1975) 1086–1099.
- [28] H.A.J. Govers, *Calculation of Lattices Energies of Unitary and Binary Molecular Crystals by The Atom-Atom Approximation*, Thesis, University of Utrecht, 1974.



# Repetitive liquid injection system for inverse gas chromatography

S. Panda, Q. Bu, K.S. Yun, J.F. Parcher\*

*Chemistry Department, University of Mississippi, University, MS 38677, USA*

First received 16 January 1995; revised manuscript received 1 June 1995; accepted 1 June 1995

---

## Abstract

A hybrid injection system composed of a closed-loop vaporization chamber with a gas sampling valve is described. The system allows liquid injection into the vaporization loop with subsequent multiple injections of the vaporized solute(s) via the gas sampling valve (GSV). Very small amounts of probe solutes can be injected without a dilution solvent, and the vaporization loop acts as a “retention gap” for capillary columns. The use of a pneumatically controlled valve injector provides very accurate and reproducible injection volumes at precise time intervals. Combination of precisely timed injections with temperature programming of the column oven produces continuous chromatograms and retention data at controlled temperature increments. The proposed injection system eliminates the need for split injectors; it is cleaner than normal in-line injectors because nonvolatile samples cannot reach the column; and the instrumentation is easily automated. The major disadvantages are the restriction that the samples must be volatile at temperatures lower than the upper temperature limit of the valve rotor; the GSV is susceptible to both contamination and mechanical failure; the sample can be exposed to metal components of the valve; and initial distribution of the sample throughout the closed-loop vaporization chamber may be slow.

---

## 1. Introduction

Inverse gas chromatography (IGC) is an established method for the investigation of surfaces and interfaces, as well as the study of polymer structures, interactions, and phase transitions [1]. The technique is based on the measurement of the retention behavior of one or more well-characterized probe solutes to determine some physical or chemical properties of nonvolatile stationary phase materials, such as polymers, solid adsorbents, or mixtures of materials. The usual experimentation involves the measurements of the retention volumes of the probe

solutes over a range of temperatures. Thermodynamic parameters can be calculated directly from the retention data, and phase changes can often be detected from discontinuities in a van't Hoff-type plot of the logarithm of the retention volume versus the reciprocal temperature [2–6].

The experimental technique of IGC is very appealing because the material to be examined can be coated on a solid support (to provide a thin film) in a packed column or coated on the walls of an open tubular capillary column (to avoid the possibility of adsorption on a solid support). The experiments can be performed isothermally or in a temperature-programmed mode similar to differential scanning calorimetry (DSC) methodology. The samples can be in-

---

\* Corresponding author.

jected as vapors via a gas sampling valve (GSV) or by liquid syringe injections. The experiments are simple, fast, and require no specialized instrumentation. These are particularly significant advantages when compared to such alternative techniques as DSC. A variety of solutes can be used as probes to study different types of molecular interactions in a low-energy regime that is difficult to investigate by classical experimental techniques. Finally, the technique can be applied to systems not amenable to other experimental approaches. For example, IGC can be used to study phase transitions in polymers in contact with sorbable vapors or supercritical fluids at high pressures.

Nevertheless, there are some problems associated with the technique of inverse gas chromatography. Most of the difficulties arise from the complexity of retention mechanisms typically observed with IGC systems. Solute adsorption on polymeric surfaces is usually prevalent, and concurrent bulk partition mechanisms are often observed, the relative significance of which may depend upon the temperature and the state of the stationary phase. Adsorption mechanisms are usually complicated, resulting in nonlinear isotherms especially at low temperatures, and both adsorption and partition (diffusion) kinetics may be slow on a chromatographic time scale. As a result of these problems, elution peaks for the probe solutes are often asymmetric and retention volumes may consequently vary with sample size, film thickness, and often with flow-rate as well. These phenomena are usually observed with polymeric materials at temperatures close to the glass transition temperature,  $T_g$ , of the stationary phase.

Another problem is often encountered in the interpretation of the van't Hoff plots used to determine phase transition temperatures. Such interpretation is complicated by nonequilibrium conditions observed when the stationary phase undergoes a phase transition. Under these conditions, solute retention mechanisms almost always include both adsorption and partition, which may be influenced by slow diffusion kinetics. Thus, the flow-rate of the carrier gas, which

determines the contact time of a solute with the stationary phase, becomes a critical parameter. Some authors have suggested extrapolation of the retention volumes at a fixed temperature to zero flow-rate to measure (equilibrium) partition and adsorption [5,6]; whereas others [3] have proposed the opposite extrapolation to infinite flow-rate to eliminate retention contributions from partition mechanisms. Determination of transition temperatures from van't Hoff plots is further complicated by the assignment of such transition temperatures to local maxima, i.e., the first deviation from linearity with decreasing temperature, in some systems (liquid crystalline polymers [2], for example). In other cases, local minima, i.e., the first deviation from linearity with increasing temperature, are used to locate the transition temperature(s) (polystyrene [5,6] is an example).

Investigation and resolution of these problems are critically dependent upon reliable experimental data from IGC experiments. In turn, the integrity of the experimental technique is dependent upon an accurate delivery system for the probe solute(s). The injection system must provide multiple injections of equal amounts of the same sample at precisely controlled time intervals. The injected volumes must be small to ensure infinite dilution conditions; however, any solvent, such as those commonly used to dilute analytical samples, is undesirable because a large solvent peak could limit the cycle time for repetitive injections and/or obscure early eluting solutes. Syringe injections of liquid solutes (with and without solvent) have been used for IGC studies; vapor injection has also been used and is an excellent injection method but limited to volatile solutes; and automatic liquid samplers (ALSs) [8] as well as head-space injectors [2,4] have all been used for IGC studies. Syringe injections of liquids or vapors, whether manual or with an ALS, are seldom adequately reproducible, especially with split injector systems. Head-space injectors and GSVs are more reproducible but limited to volatile solutes. None of these injection methods is entirely satisfactory. Thus, in an attempt to alleviate at least

some of these problems, a hybrid injector system involving injection of vaporized liquid samples via a gas sampling valve is described herein.

## 2. Experimental

The proposed injection system is illustrated schematically in Fig. 1. The packed-column injector, gas sampling valve, and isolation valve must all be maintained at a temperature sufficient to assure complete vaporization of all probe solutes but below the upper temperature limit of the GSV rotor (typically 350°C). In Fig. 1, the sampling valve is shown in a dual-injection mode because this configuration allows the maximum number of injections from an event table in a typical GC–MS system. However, a normal six-port valve with a single injection loop would work as well. In an injection sequence, the isolation valve would be set in the position shown in Fig. 1 to form a closed loop (shown in bold) with the injection port and GSV. A liquid

sample can be injected into the packed-column injector and allowed to vaporize and distribute throughout the closed loop. Individual injections into the analytical column are initiated from the sampling valve at fixed time intervals. In this particular instrument, the capillary inlet system was used simply as a splitter in front of the mass specific detector. The capillary column was maintained at a sufficiently high temperature to act merely as a transfer tube rather than a separation column. If this is not feasible, the capillary column can be replaced with an empty fused-silica column. At the completion of an injection sequence, the vaporized sample can be removed from the injector by actuating the isolation valve to allow a sweep gas to flush out the analytical sample.

In this investigation a mass specific detector was used as the detection device, although any GC detector would be acceptable. The advantage of a mass specific detector for IGC experiments is the ability of this detector to distinguish individual probe species even if they are not chromatographically resolved from other species or a solvent peak.

## 3. Results and discussion

Typical IGC data collected with the injector system described previously are shown in Fig. 2. In this example, the polymer was polymethylmethacrylate (PMMA) and the probe solute was xylene. The literature value [9] for the glass transition temperature,  $T_g$ , of PMMA is about 105°C. The column temperature was programmed from 50 to 220°C at 1°C/min during the course of the experiment. The valve injector was programmed for repetitive injections at 10-min intervals. This sequence produced elution peaks at approximately 10°C intervals. The period is not precise because the retention times of the probe solutes varied significantly with temperature and the physical state of the polymer.

The measured retention volume data for xylene with PMMA are shown in Fig. 3 in the

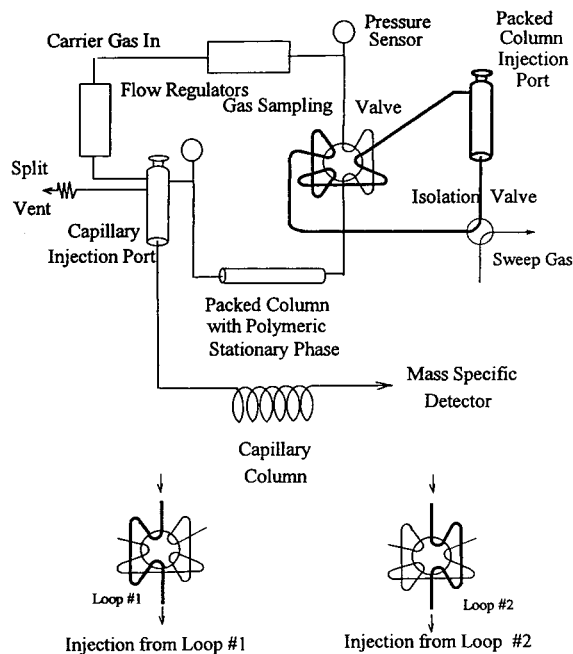


Fig. 1. Schematic diagram of the off-line IGC injection system.

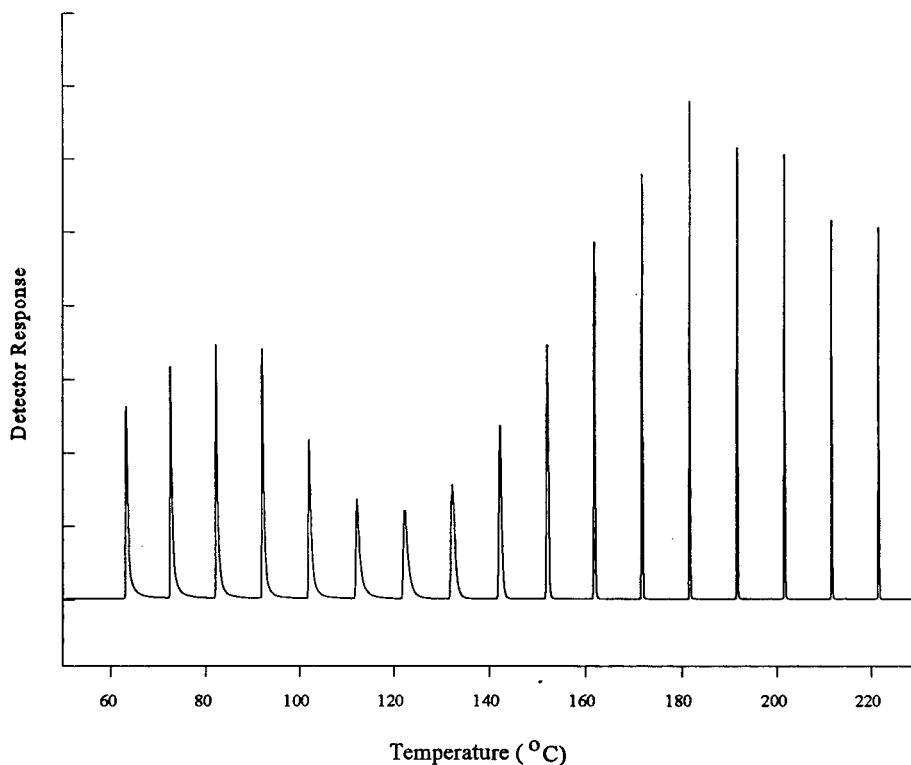


Fig. 2. Chromatogram of xylene on PMMA with the column temperature programmed from 50 to 220°C at 1°C/min.

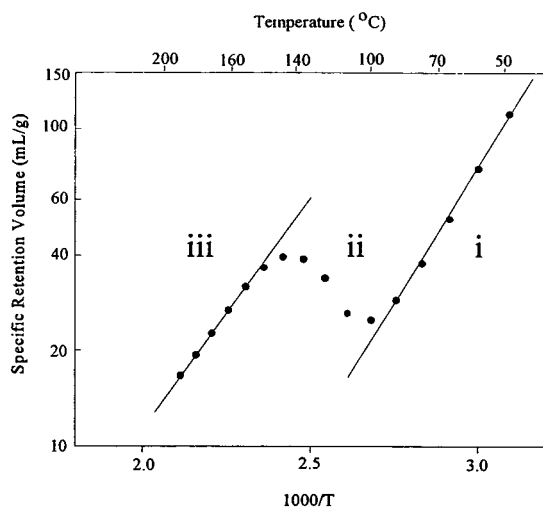


Fig. 3. Van't Hoff plot for xylene with PMMA polymer.

form of a classical van't Hoff type plot of  $\ln V_g^0$  versus  $1000/T$ . The generally accepted interpretation of such plots involves division of the plot into three distinct regimes. These are (i) the linear region at low temperatures that typifies the glassy phase of the polymer and the slope of the line is proportional to the enthalpy of adsorption of the probe solute on the surface of the polymer film, (ii) the discontinuity at intermediate temperatures reflecting a nonequilibrium condition in which the retention of the probe depends on the contact time of the probe with the polymer surface, and (iii) the second linear portion at high temperature where the polymer state is rubber and the slope of the line reflects the enthalpy of solution of the probe solute in the bulk polymer. The exact retention mechanism for polymers in a rubber state is

uncertain, and it has been suggested that, even at high temperatures, the primary retention mechanism is surface adsorption [10]. The relative significance of adsorption and absorption mechanisms for polymers above  $T_g$  is probably determined primarily by the nature of the probe and the polymer and may vary significantly from one system to another.

Determination of  $T_g$  from inverse gas chromatography data such as that illustrated in Fig. 3 is somewhat problematical; however, the most common approach [5,6] is to specify  $T_g$  as the temperature at which the first deviation from linearity is observed in the low-temperature regime. In the example shown in Fig. 3, the  $T_g$  value calculated this way would be 90–100°C. In other cases, the phase transition temperature has been assigned as the temperature at the first point of deviation from linearity of the high-temperature region. Thus,  $T_g$  would be 140–150°C in the example shown in Fig. 3. Differential scanning calorimetric results, on the other hand, clearly show that there is a phase transition in the temperature range of 90–100°C, which shows that  $T_g$  should be determined from the point of deviation from linearity in the low-temperature range in this particular case.

### 3.1. Sample discrimination

The upper limit on molecular mass of the samples depends upon the temperature of the closed-loop injector. The upper temperature limit is usually set by the rotor of the GSV, and 350°C is a typical value. Thus, the proposed injection system is limited to solutes that have a reasonable vapor pressure at 300–350°C. This is a significant limitation for its use as a general injection system; however, most solutes used as IGC probes easily meet this requirement.

### 3.2. Dilution effects

The injection system is a closed loop, and the sample loop of the GSV is filled with carrier gas at the end of an injection cycle. Thus, a fixed volume of sample is lost with each injection and a similar volume of carrier gas is introduced into

the closed-loop injection system. This results in a decrease in peak area with each successive sampling valve injection. A logarithmic plot of the normalized peak area versus injection number is shown in Fig. 4 for three commonly used IGC probe solutes. The slope of the regression line, which is equal to the log of the fraction of sample remaining in the closed-loop injector after each valve injection, was  $-0.014$ . Thus, a loss of about 3% of the sample per injection was observed for this particular system. The percentage loss will vary with the design of the systems and the volume of the sample loops in relation to the total volume of the closed-loop injector. Nevertheless, the loss of 3% per injection allows about 75 repetitive injections before the sample size is reduced to 10% of the original liquid sample injected into the packed column inlet. The relative standard deviation of the data shown in Fig. 4 was approximately 1.8%. This uncertainty included the variance due to the injector valve as well as the uncertainty in the integration measurements.

### 3.3. Peak shape analysis

The dilution effect described above produced elution peaks of decreasing peak area and, presumably, the peak heights should decrease

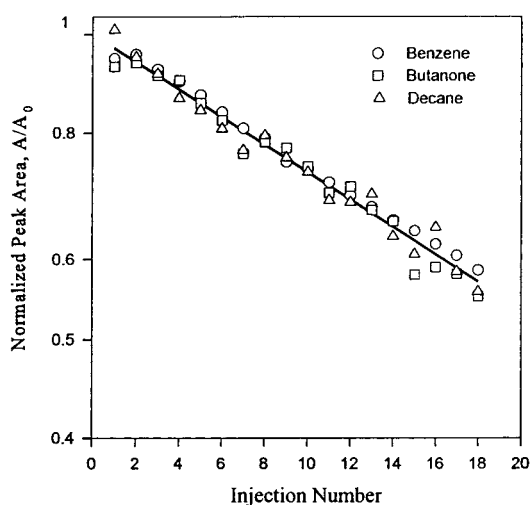


Fig. 4. Dilution effect caused by the gas sampling valve.

with an increasing number of injections. In fact, the chromatogram displayed in Fig. 2 shows that no such simple pattern is observed. Instead, a complex series of maxima and minima is evident throughout the chromatogram. This phenomenon is caused by an interdependent set of factors that each influence the shape of the elution peaks. These factors and their possible consequences are:

(1) The PMMA polymer undergoes a phase change from glass  $\rightarrow$  rubber in the range of 90 to 100°C. As a result, the retention mechanism changes from predominately adsorption for the glassy polymer to primarily absorption in the rubbery or liquid polymer at high temperatures. Adsorption mechanisms usually produce asymmetric peaks, whereas absorption mechanisms produce Gaussian peaks if diffusion of the probe solute in the polymer is fast on the chromatographic time scale.

(2) The column temperature was programmed up with each successive injection. Such a temperature increase would normally produce increasingly sharp elution peaks with increasing height due to more efficient mass transfer kinetics in the polymer at high temperatures.

(3) The dilution effect causes the peak area to decrease with each successive injection. This would normally produce a concomitant decrease in peak height.

These factors, viz., temperature, phase change, dilution, absorption, adsorption, and diffusion, all affect the shape of the elution peaks shown in Fig. 2. Asymmetric peaks were observed below 120–130°C, whereas above 130°C the elution peaks were Gaussian (symmetric) with increasingly smaller band widths. In the temperature range 90–120°C, which encompasses the glass transition temperature, the peaks became increasingly broad with increasing temperature. This is an anomalous phenomenon rarely observed in chromatographic systems. The dispersion process (peak broadening) is enhanced due to the change in phase and slow mass transport in the rubber polymer at temperatures slightly above  $T_g$ . This pattern of peak shapes has been observed previously [7,11], and the explanation given above (excluding the dilution

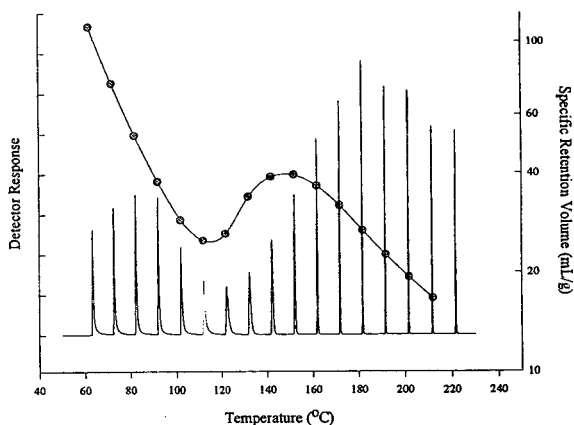


Fig. 5. Superposition of the chromatogram and specific retention volumes of xylene with PMMA.

effect) is derived in part from the discussion therein. The relationship between retention, peak shape, and temperature is shown in Fig. 5, in which the logarithm of the specific retention volume of xylene is plotted versus the elution temperature of each peak. Superposition of the chromatogram (Fig. 2) and specific retention volume data (Fig. 3) illustrates the close correlation of the minimum in the pseudo-van't Hoff plot and the maximum peak spreading (minimum peak height) in the chromatogram. Continuous, precisely timed injections coupled with temperature programming of the column temperature are required for this type of investigation.

### 3.4. Potential advantages of the injection system

The proposed system eliminates the need for flow splitting and retention gaps for capillary GC. Because the vaporization process occurs off-line, there are no flow or pressure disturbances and the cooling effect of the solvent vaporization does not influence the injections. The off-line injection system is cleaner and less susceptible to septum bleed or leaks than common in-line injectors. Nonvolatile sample components cannot contaminate the column but remain mostly in the liner of the packed-column injection port. Finally, the entire system is easily automated and very simple to operate.

### 3.5. Potential disadvantages

The system will be ineffective for very high boiling compounds because of the upper temperature limit of the gas sampling valve components. Because the GSV is a mechanical apparatus, it is subject to contamination, mechanical failure, and could cause catalytic reactions of some solutes. The device does not deliver a constant amount of sample due to dilution of the original sample with carrier gas by the GSV. Because the liquid sample is injected at only one point in the closed-loop system, a finite amount of time is required to achieve uniform distribution of the sample throughout the system. This time requirement varies with the design of the system as well as the type of sample.

### 4. Conclusions

While the proposed injection system is not a universal injector, it is an excellent device for repetitive injection of simple solute mixtures. Thermodynamic studies and inverse GC provide two examples of experimental techniques requiring such injection sequences. The system is simple, accurate, and easily automated. It requires computer control and remotely actuated valves; however, it can sometimes be used to replace split-flow injectors, eliminate septum purge flows, and retention gap technology.

### Acknowledgements

Acknowledgement is made to the National Science Foundation and to the donors of the Petroleum Research Fund, administered by the American Chemical Society, for support of this research.

### References

- [1] D.R. Lloyd et al. (Editors), *Inverse Gas Chromatography: Characterization of Polymers and Other Materials*, ACS Symp. Ser. No. 391, American Chemical Society, Washington, DC, 1989.
- [2] M. Romansky and J.E. Guillet, *Polymer*, 35 (1994) 584–589.
- [3] P. Mukhopadhyay and H.P. Schreiber, *Macromolecules*, 26 (1993) 6391–6396.
- [4] L.Q. Xie, *Polymer*, 34 (1993) 4579–4584.
- [5] J.M. Braun and J.E. Guillet, *Macromolecules*, 9 (1976) 617–621.
- [6] J.M. Braun and J.E. Guillet, *Macromolecules*, 6 (1975) 882–888.
- [7] G.J. Courval and D.G. Gray, *Macromolecules*, 8 (1975) 916–920.
- [8] J.E. Guillet, *Proc. ACS Divis. Polym. Mater.*, 58 (1988) 645.
- [9] P.D. Condo, I.C. Sanchez, C.G. Panayiotou and K.P. Johnston, *Macromolecules*, 25 (1992) 6119–6127.
- [10] R.-Y. Qin and H.P. Schreiber, *Langmuir*, 10 (1994) 4153–4156.
- [11] D.G. Gray and J.E. Guillet, *Macromolecules*, 7 (1974) 244–247.





# Assessment of some possibilities for improving the performance of gas chromatographic thermal conductivity detectors with hot-wire sensitive elements

Ilia P. Mitov<sup>a,\*</sup>, Luchezar A. Petrov<sup>b</sup>

<sup>a</sup>Central Laboratory of Biomedical Engineering, Bulgarian Academy of Sciences, Acad. G. Bonchev Str., bl. 105, 1113 Sofia, Bulgaria

<sup>b</sup>Institute of Catalysis, Bulgarian Academy of Sciences, Acad. G. Bonchev Str., bl. 11, 1113 Sofia, Bulgaria

First received 16 March 1994; revised manuscript received 18 April 1995; accepted 19 May 1995

## Abstract

The possibilities for improving the performance of gas chromatographic thermal conductivity detectors (TCD) by using hot-wire sensitive elements with appropriate design and increased resistance were studied. It is shown that the design of the traditional TCD with one-way heat conduction, and also the new kind of sensitive element design with two-way heat conduction, in which one of the filament leads is assembled inside the coil along its axis, can be optimized. The best TCD performance can be achieved if the sensitive element spiral pitch is minimal and the spiral radius is equal to  $r_c/e$  in the case of one-way heat conduction and to the mean radius  $(r_c + r_1)/2$  in the case of two-way heat conduction, where  $r_c$  and  $r_1$  are the radii of the gas cavity and of the central filament lead, and  $e \approx 2.7$  is the Napierian number. Further, the optimization of the sensitive element design provides an increase in its resistance, which additionally improves the TCD performance. Following this approach and taking into account the ultimate capabilities of modern electronics, two new optimized designs of the sensitive elements with about 650  $\Omega$  resistance at 0°C, that after the numerical estimations presented could improve the TCD performance more than tenfold, are developed and proposed for further experimental studies.

## 1. Introduction

The principle of operation and the factors affecting thermal conductivity detector (TCD) output signals have been treated in many publications and are summarized in several books [1,2]. It has been shown that the performance of the TCD with four hot-wire sensitive elements can be improved if the Wheatstone bridge is supplied from a d.c. source with constant-current

control [3] (Fig. 1) and if the filament resistance at 0°C,  $R_0$ , is increased to 100  $\Omega$  [4,5]. The latter limitation is due to the traditional design of the sensitive elements and of the d.c. sources currently used in commercial gas chromatographs. Since the restrictions concerning the d.c. sources are not crucial for modern electronics, the problem of designing hot-wire sensitive elements with  $R_0 = 500\text{--}700 \Omega$  becomes important. The theoretical and some practical aspects of this problem are treated in this paper. The dependence of TCD operation on the design and the resistance

\* Corresponding author.

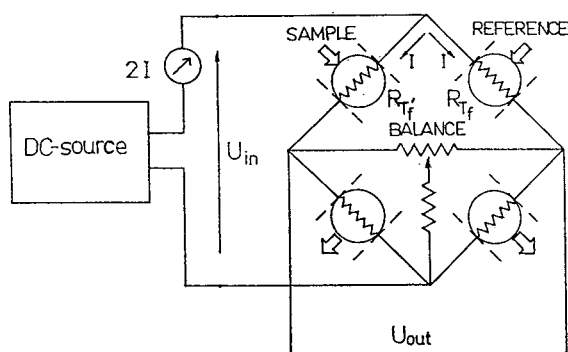


Fig. 1. TCD with four hot-wire sensitive elements in a Wheatstone bridge supplied from a d.c. source with constant current control.

of its sensitive elements was studied with the intention of developing and proposing new types of high-resistance hot-wire sensitive elements that could substantially improve the TCD performance.

## 2. Theoretical

The output signal of the TCD shown in Fig. 1 is due to the difference between the temperatures  $T'_f$  and  $T_f$  ( $^{\circ}\text{C}$ ) of the filaments in the TCD sample and reference cavities due to the sample components entering the detector as a mixture with the carrier gas. Taking into account the temperature dependence  $R_{Tf} = R_0(1 + \alpha T_f)$  of the filament resistance, the TCD output signal is

$$U_{\text{out}} = I(R_{Tf'} - R_{Tf}) = IR_0\alpha(T'_f - T_f) \quad (1)$$

where  $I$  (A) is the current heating the sensitive elements,  $R_0 = \rho_0 l_f / S_f$  ( $\Omega$ ) is the resistance of the filaments at  $0^{\circ}\text{C}$  and  $\alpha$  ( $^{\circ}\text{C}^{-1}$ ) is the coefficient of resistance of the material with resistivity  $\rho_0$  ( $\Omega$  cm), from which the filaments with length  $l_f$  (cm) and cross-section  $S_f = \pi r_f^2$  ( $\text{cm}^2$ ) are made.

While the temperature  $T_c$  ( $^{\circ}\text{C}$ ) of the TCD block is kept constant, the filament temperature is determined from the heat balance established between the filament heat flux and the heat

losses through the thermal conductivity and the heat capacity of the gas mixture in the cavity considered, the heat conduction in the hot wire support, the convection and the radiation.

If the sum of the last three types of heat losses is denoted by  $S$ , then the heat balance in the TCD reference cavity is

$$I^2 R_0 (1 + \alpha T_f) / J \\ = G\lambda(T_f - T_c) + V_{\mu} C_p (T_g - T_c) + S \quad (2)$$

where  $J = 4.19$  J/cal is the Joule equivalent,  $G$  (cm) is the TCD cell factor,  $\lambda$  ( $\text{cal}/\text{cm} \cdot \text{s} \cdot ^{\circ}\text{C}$ ) is the thermal conductivity of the carrier gas,  $V_{\mu} = 273 V_{\text{vol}} / 22420 (273 + T_m)$  (mol/s) is the molar flow-rate of the gas through the cavity, calculated from the volume flow-rate  $V_{\text{vol}}$  (ml/s) and the temperature  $T_m$  ( $^{\circ}\text{C}$ ) of the measuring device,  $C_p$  ( $\text{cal}/\text{mol} \cdot ^{\circ}\text{C}$ ) is the molar heat capacity of the carrier gas at constant pressure and  $T_g$  ( $^{\circ}\text{C}$ ) is the average temperature of the gas leaving the TCD reference cavity.

Since the calculation of  $G$  and  $T_g$ , needed for solving the TCD main Eq. 2, requires information about the sensitive element design and the temperature distribution in the gas cavity, some supplementary assumptions are made. The common features of the considered sensitive element designs are that the filament is coiled in a spiral of length  $l_s$ , coaxially situated in the TCD gas cavity (Fig. 2), and that the radius of

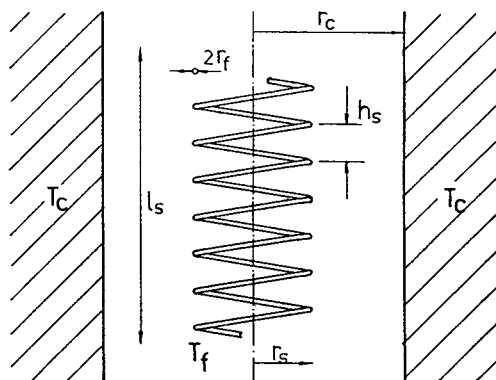


Fig. 2. TCD temperatures and sensitive element design parameters.

the spiral  $r_s$  exceeds its pitch  $h_s$ , ensuring practically acceptable values of  $l_s$  even if the high-resistance filament is up to 1 m long. The supplementary assumption about the temperature distribution in the gas cavity is that all the points of the cylindrical surface formed by the coil are at the same temperature  $T_f$ , if the spiral pitch  $h_s$  is small enough in comparison with the radiuses of the sensitive element  $r_s$  and of the TCD gas cavity  $r_c$ . Then the temperature distribution between the coil and the wall of the cavity is

$$T_{\text{out}}(r) = \frac{T_f \ln(r_c/r) + T_c \ln(r/r_s)}{\ln(r_c/r_s)}, \quad r_s \leq r \leq r_c \quad (3)$$

and if the region inside the coil is filled with gas only, its temperature at the above assumption has to be  $T_f$ , as shown in Fig. 3a.

In this case with one-way heat conduction (outwards to the cavity wall), the TCD cell factor is  $G_1 = 2\pi l_s / \ln(r_c/r_s)$ , the average temperature of the gas departing the TCD reference cavity is

$$\begin{aligned} T_g &= \frac{1}{r_c^2} \left[ \int_0^{r_s} T_f d(r^2) + \int_{r_s}^{r_c} T_{\text{out}}(r) d(r^2) \right] \\ &= T_c + \frac{T_f - T_c}{2r_c^2} \cdot \frac{r_c^2 - r_s^2}{\ln(r_c/r_s)} \end{aligned}$$

and the filament temperature  $T_f$  derived from the TCD main Eq. 2 is

$$T_f = T_c + \frac{I^2 R_0 (1 + \alpha T_c) / J - S}{G_1 \lambda + V_\mu C_p (r_c^2 - r_s^2) / 2r_c^2 \ln(r_c/r_s) - \alpha I^2 R_0 / J} \quad (4)$$

In view of the fact that the heat losses denoted by  $S$  are virtually independent of the gas composition and their percentage in the total sum of losses is relatively small, in the following analysis the term  $S$  is ignored and Eq. 4 is transformed into

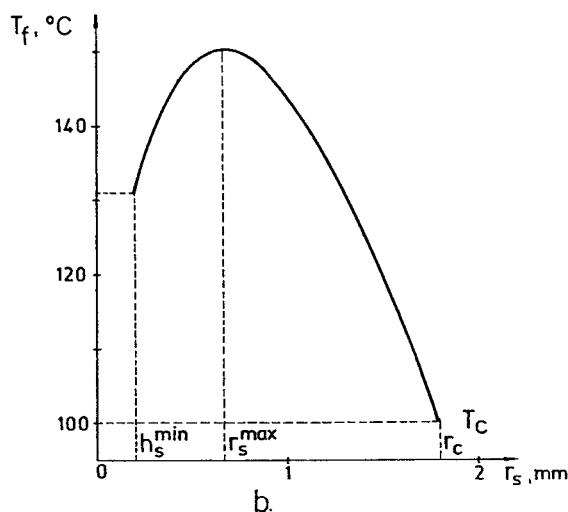
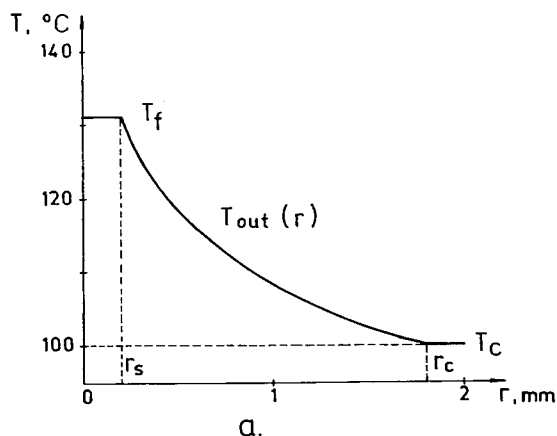


Fig. 3. TCD with one-way heat conduction: (a) temperature distribution; (b) filament temperature. Conditions assumed in the numerical calculations: carrier gas, helium at a flow-rate of 60 ml/min measured at 20°C; tungsten filaments of  $r_f = 5.7 \mu\text{m}$  coiled in spirals with  $r_s$  (mm),  $R_0 = 300 r_s$  ( $\Omega$ ),  $h_s = 200 \mu\text{m}$  and  $l_s = 18$  mm; heating current  $I = 50$  mA corresponding to  $x_{\text{max}} = 5$  mol-% for the design version 2 in Fig. 5.

$$T_f = T_c + (1/\alpha + T_c) \frac{A}{1 + BC_p - A} \quad (5)$$

using for simplifying the equations the symbols  $A$  and  $B$  instead of the expressions  $\alpha I^2 R_0 / J G_1 \lambda$  and  $V_\mu (r_c^2 - r_s^2) / 4\pi l_s \lambda r_c^2$ , respectively.

The TCD output signal, derived from Eq. 1 using Eq. 5, is

$$U_{\text{out}} = IR_0(1 + \alpha T_c) \frac{A}{1 + BC_p - A} \cdot \frac{1 - \lambda'/\lambda + B(C_p - C'_p)}{\lambda'/\lambda + BC'_p - A} \quad (6)$$

where  $\lambda'$  and  $C'_p$  refer to the gas mixture in the sample cavities.

The last term of Eq. 6 can be expressed as a function  $f(x)$  of the molar concentration  $x$  of the sample component  $i$  entering the TCD as a mixture with the carrier gas, using the well known relationship  $1/\lambda' = 1/\lambda + (1/\lambda_i - 1/\lambda)x$ , which is valid at component concentrations  $x \leq 10$  mol-%, the assumption  $C'_p = C_p + (C_{p,i} - C_p)x$  and the symbols  $L = \lambda/\lambda_i - 1$ ,  $M = A - BC_p$  and  $N = B(C_{p,i} - C_p)$  for simplifying the equations. Then,

$$f(x) = \frac{(L - N)x - LNx^2}{(1 - M) - (LM - N)x + LNx^2} \quad (7)$$

and since  $L \gg N$  owing to the great thermal conductivity of the carrier gases commonly used, the TCD response is positive. Regardless of the non-linearity of  $f(x)$ , Eq. 7, if the component concentrations are small enough, then the TCD operation can be assumed to be linear with a coefficient of sensitivity

$$K = \left. \frac{dU_{\text{out}}}{dx} \right|_{x=0} = IR_0(1 + \alpha T_c) \frac{(L - N)A}{(1 - M)^2} \quad (8)$$

which in the traditional analysis of the TCD performance is the main subject of theoretical estimations, whereas the detection level and even the TCD linear range are determined experimentally. However, the knowledge of  $U_{\text{out}}$  provides a wider estimation of TCD performance including not only  $T_f$  and  $K$ , but also the upper limit  $x_{\text{max}}$  (mol-%) of the TCD linear range, the corresponding maximum output signal  $U_{\text{max}} = Kx_{\text{max}}$  and the d.c. source voltage  $U_{\text{in}} = 2IR_0(1 + \alpha T_f)$  (V) and the power  $P = 2IU_{\text{in}}$  (W) required for supplying the Wheatstone bridge with the necessary constant current.

Since  $x_{\text{max}}$  is defined by

$$\left| \frac{U_{\text{out}} - Kx}{Kx} \right| = \delta$$

if the deviations from the linearity are restricted to  $\delta = 3\%$ , then using Eqs. 6, 7 and 8 the actual equation for calculating the upper limit of the TCD linear range is

$$\left| \frac{\left( \frac{L - N}{1 - M} - \frac{L^2}{L - N} \right) x - \frac{LN}{1 - M} \cdot x^2}{1 - \left( \frac{L - N}{1 - M} - L \right) x + \frac{LN}{1 - M} \cdot x^2} \right| = 0.03 \quad (9)$$

### 3. Results and discussion

The results presented below can be explained more consistently if the small terms involving the heat capacities in the relationships used for the TCD performance estimation are discarded, giving

$$\Delta T = T_f - T_c \approx (1/\alpha + T_c) \frac{A}{1 - A}$$

$$K \approx L(1 + \alpha T_c)R_0 \cdot \frac{AI}{(1 - A)^2}$$

$$x_{\text{max}} \approx \frac{2.9}{L} \cdot \frac{1 - A}{A}$$

$$U_{\text{max}} \approx 0.029(1 + \alpha T_c)R_0 \cdot \frac{I}{1 - A}$$

$$U_{\text{in}} \approx 2(1 + \alpha T_c)R_0 \cdot \frac{I}{1 - A} \approx 69 U_{\text{max}}$$

$$P \approx 4(1 + \alpha T_c)R_0 \cdot \frac{I^2}{1 - A} \approx 137 IU_{\text{max}} \quad (10)$$

Taking into account the form of the expression  $A$  introduced above, the relationships (10) show that:

(a) the main factor affecting the TCD performance is the filament heating current  $I$ , but only the increase in TCD block temperature  $T_c$  improves the performance parameters  $\Delta T$ ,  $K$  and  $U_{\text{max}}$  without a degradation of the upper limit  $x_{\text{max}}$  of the TCD linear range;

(b) the temperature difference  $\Delta T$  is inversely proportional to  $x_{\text{max}}$  with a coefficient that depends on  $L$ ,  $\alpha$  and  $T_c$  only;

(c) the improvement of the maximum output signal  $U_{\text{max}}$  generated in the TCD linear range

requires a proportional increase of the d.c. source voltage  $V_{in}$  and power  $P$  (which is proportional to  $I$  again);

(d) the increase in the filament resistance  $R_0$  is a favourable factor for improving the TCD performance, but its clarification needs a further analysis of the expression  $A$ , which comprises all the others sensitive element design parameters.

The detailed study of the expression  $A$  reveals that it is not influenced by the value of the filament resistance  $R_0$  taken alone, but by the dimensions of the sensitive element, for some of which an optimum proportion exists. These conclusions follow from the known relationship  $l_f = l_s[(2\pi r_s/h_s)^2 + 1]^{1/2}$ , which for  $r_s \geq h_s$  can be approximated as  $l_f = 2\pi l_s r_s/h_s$ . Then, concerning sensitive elements coiled from filaments of a given material and cross-section, the correct form of the expression  $A$  is

$$A = \frac{\alpha I^2 \rho_0}{J \lambda S_f} \cdot \frac{r_s}{h_s} \ln(r_c/r_s) \quad (11)$$

The possibilities of increasing  $A$  by varying  $r_s$  and  $h_s$  depend on the supplementary requirements imposed. When both the detector volume  $V_d = \pi r_c^2 l_s$  and  $R_0$  are predetermined, then the  $r_s/h_s$  ratio is also predefined, but the value of  $A$  can be increased by minimizing to the practically acceptable limits both  $r_s$  and  $h_s$  in the same proportion. For example, consider a “classical” TCD with  $r_c = 1.8$  mm and  $V_d \approx 200$   $\mu$ l, whose sensitive elements are coiled from tungsten filaments of  $r_f = 5.7$   $\mu$ m in spirals with  $R_0 = 60$   $\Omega$ ,  $l_s = 18$  mm and  $r_s = h_s = 400$   $\mu$ m. This TCD is used in the present work for comparison purposes regardless of the fact that most of the sensitive elements currently available have lower performance because their spirals are not coaxially placed in the TCD gas cavities and are of lower resistance. However, the performance assessments  $\Delta T$  and  $K$  of the considered “classical” TCD can be improved with more than 50% by increasing  $\ln(1800/200)/\ln(1800/400) = 1.46$  times the value of  $A$  in Eq. 11 through a decrease in both  $r_s$  and  $h_s$  to 200  $\mu$ m, while keeping all the other design parameters and operational conditions unchanged.

When only the detector volume  $V_d$  is predetermined, but the filament resistance  $R_0$  is allowed to vary, the sensitive element spiral radius  $r_s$  and pitch  $h_s$  are independent. Since the expression  $A$  depends inversely on  $h_s$ , it can be increased by reducing  $h_s$  to the practically acceptable limit. Then, by means of the spiral radius the value of  $A$  can be increased still further and even maximized, since Eq. 11 as a function of  $r_s \in [h_s^{\min}, r_c]$  has a maximum at  $r_s^{\max} = r_c/e$ , where  $e \approx 2.7$  is the Napierian number. In view of the fact that the existence of such a maximum is essential for TCD design optimization and performance improvement, the direct influence of  $r_s$  on the filament temperature  $T_f$  according to Eq. 5 is quantitatively evaluated. The supposed common TCD operational conditions and the design parameters used are explained in Fig. 3, where the increase in  $R_0$  proportionally to  $r_s$  is also described. The relationship presented in Fig. 3b shows that since the “heat capacity effect” involved in Eq. 5 by the term  $BC_p$  is almost negligible, the filament temperature  $T_f$  as a function of  $r_s$  follows the course of the expression  $A$  and has a marked maximum at a sensitive element spiral radius very close to  $r_s^{\max}$ . Further, it is important to note that in addition to a maximum value of the expression  $A$ , the optimization of the sensitive element design by using  $h_s^{\min}$  and  $r_s^{\max}$  provides a higher resistance  $R_0$  than of the “classical” TCD, because  $r_s^{\max}$  as a  $1/e$  part of the gas cavity radius is relatively large. Therefore, the optimization of sensitive element design is an important approach for TCD performance improvement, because in accordance with Eq. 10 such sensitive elements not only have high values of  $\Delta T$  (and lower values of  $x_{\max}$ , which is inversely proportional to  $\Delta T$ ), but also, owing to the increased  $R_0$ , they have additionally improved coefficients of sensitivity  $K$  and higher values of the maximum output signals  $U_{\max}$  generated in the TCD linear range.

The next possibility for TCD performance improvement involves a new kind of sensitive element design, based on the fact that if the spiral radius  $r_s$  is large enough, one of the filament leads with temperature  $T_c$  can be assem-

bled inside the coil along its axis. Then the temperature distribution between the spiral and the cavity wall is  $T_{\text{out}}(r)$  from Eq. 3, but between the central lead with radius  $r_1$  and the coil the temperature distribution is

$$T_{\text{in}}(r) = \frac{T_f \ln(r/r_1) + T_c \ln(r_s/r)}{\ln(r_s/r_1)}, \quad r_1 \leq r \leq r_s$$

as it is shown in Fig. 4a.

In this case of two-way heat conduction (outwards to the cavity wall and inwards to the central lead), the TCD cell factor is  $G_2 = 2\pi l_s \ln(r_c/r_1) / \ln(r_c/r_s) \ln(r_s/r_1)$ , the average temperature of the gas leaving the TCD reference cavity is

$$\begin{aligned} T_g &= \frac{1}{r_c^2 - r_1^2} \left[ \int_{r_1}^{r_s} T_{\text{in}}(r) d(r^2) + \int_{r_s}^{r_c} T_{\text{out}}(r) d(r^2) \right] \\ &= T_c + \frac{T_f - T_c}{2(r_c^2 - r_1^2)} \left[ \frac{r_c^2 - r_s^2}{\ln(r_c/r_s)} - \frac{r_s^2 - r_1^2}{\ln(r_s/r_1)} \right] \end{aligned}$$

and the filament temperature is represented by Eq. 5 with  $A = \alpha I^2 R_0 / JG_2 \lambda$  and

$$B = \frac{V_\mu}{4\pi l_s \lambda} \left[ \frac{r_c^2 - r_s^2}{r_s^2 - r_1^2} - \frac{\ln(r_c/r_s)}{\ln(r_c/r_1)} \right]$$

The possibilities for TCD performance improvement by means of the new kind of sensitive element design are studied using the correct form of the expression  $A$  for the case of two-way heat conduction:

$$A = \frac{\alpha I^2 \rho_0}{J \lambda S_f} \cdot \frac{r_s}{h_s} \cdot \frac{\ln(r_s/r_1) \ln(r_c/r_s)}{\ln(r_c/r_1)} \quad (12)$$

and following the same approach as above in the last case of one-way heat conduction. The results obtained are similar to the aforesaid also, because in Eq. 12  $A$  as a function of  $r_s \in [r_1, r_c]$  has a maximum at  $r_s^{\text{max}} = (r_1 r_c)^{1/2} \exp\{[\ln^2(r_c/r_1) / 4 + 1]^{1/2} - 1\}$  and the filament temperature  $T_f$  evaluated quantitatively as a function of  $r_s$  according to Eq. 5 has a marked maximum at a spiral radius very close to  $r_s^{\text{max}}$ , as is shown in Fig. 4b. Further, owing to the almost doubled heat flux in the new kind of sensitive elements, the maximum values of the expression  $A$  and the filament temperature  $T_f$  are lower than in the

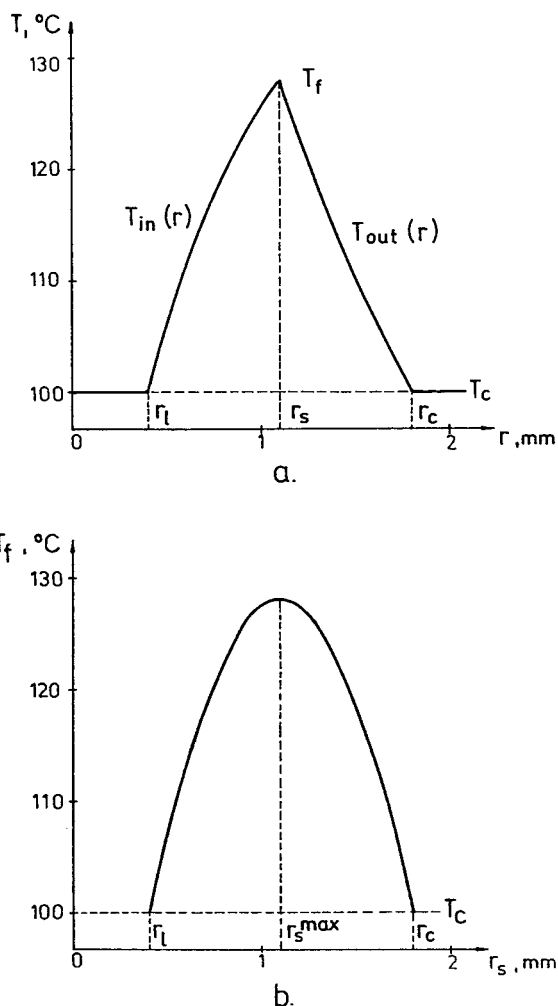


Fig. 4. TCD with two-way heat conduction: (a) temperature distribution; (b) filament temperature. Conditions assumed in the numerical calculations: carrier gas, filament and spirals as in Fig. 3; heating current  $I = 52$  mA corresponding to  $x_{\text{max}} = 5$  mol-% for the design version 4 in Fig. 5.

TCD with one-way heat conduction and optimized design, whereas in the considered domain of  $r_1$  and  $r_c$  the optimum value  $r_s^{\text{max}}$  for the case of two-way heat conduction can be approximated with the mean radius  $(r_1 + r_c)/2$  and is greater than  $r_c/e$ . Therefore, the optimization of the new kind of sensitive element design by using  $h_s^{\text{min}}$  and  $r_s^{\text{max}}$  in addition to a sufficiently high value of the expression  $A$  in Eq. 12 provides a significant increase in filament resistance  $R_0$  with

a corresponding improvement of the TCD coefficient of sensitivity  $K$  and of the maximum output signal  $U_{\max}$  generated in the TCD linear range.

The performance assessments of the considered TCD are evaluated quantitatively designating  $x_{\max}$  as an argument with a range from 1 to 10 mol-% and solving Eq. 9 for the quantity  $M$  introduced above. The solution is

$$M = \frac{3 + \left(2.03 + \frac{N}{L-N} + 0.0103Lx_{\max}\right)Nx_{\max}}{3 + \left(1.03 + \frac{N}{L-N}\right)Lx_{\max}}$$

and through it the expression  $A$ , the filament heating current  $I$  necessary for the TCD operation in the  $[0, x_{\max}]$  linear range and  $T_f$ ,  $K$ ,  $U_{\max}$ ,  $U_{\text{in}}$  and  $P$  are evaluated according to the complete equations given above.

The numerical estimations thus obtained for

the four sensitive element design versions discussed above under assumed common TCD operational conditions are presented in Fig. 5 in a traditional manner, using as an independent variable the constant current needed for supplying the Wheatstone bridge and ignoring as unimportant the assessments of the required d.c. source voltage and power. Since the relationships in Fig. 5 corroborate the possibility of TCD performance improvement by means of sensitive element design optimization and filament resistance increase, two new types of TCD hot-wire sensitive elements with  $R_0 \approx 650 \Omega$  and detector volumes  $V_d \approx 200 \mu\text{m}$  are evaluated and proposed for development and further experimental study.

The first new sensitive element is of optimized one-way heat conduction design and its resistance  $R_0 = 640 \Omega$  is achieved by increasing the

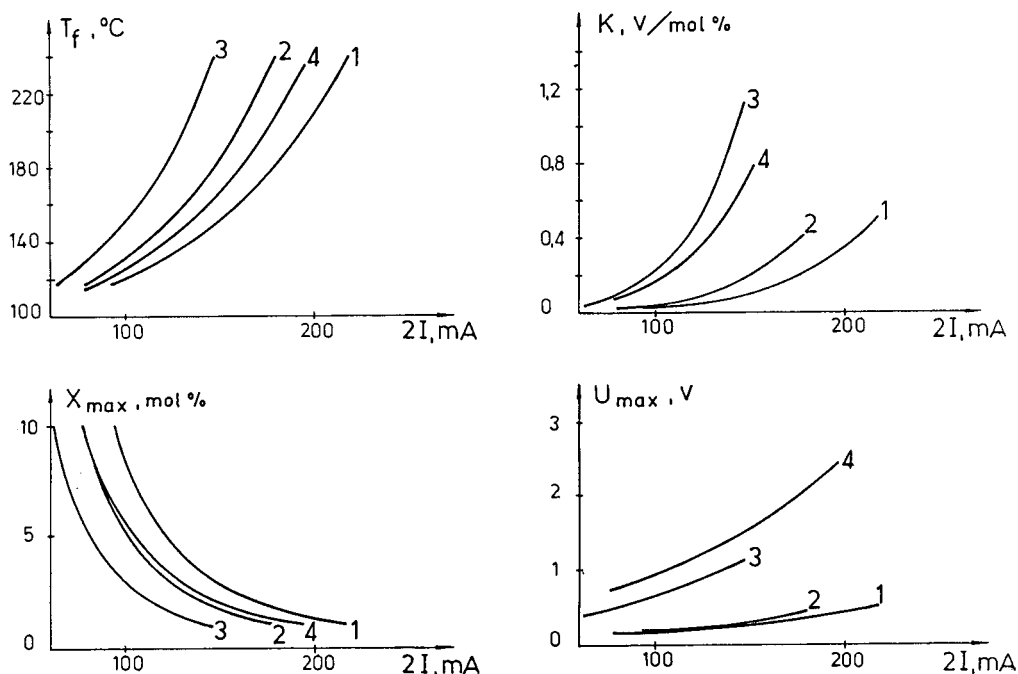


Fig. 5. TCD performance. Conditions assumed in the numerical calculations: TCD block temperature,  $100^\circ\text{C}$ ; component, propane in the same carrier gas as in Fig. 3; filament as in Fig. 3 coiled in spirals with  $r_s$  or  $r_s^{\max}$  for four sensitive element design versions with detector volume  $V_d \approx 200 \mu\text{l}$  ( $r_1 = 0$  represents the TCD with one-way heat conduction): (1)  $r_c = 1.8 \text{ mm}$ ,  $r_1 = 0$ ,  $r_s = 400 \mu\text{m}$ ,  $R_0 = 60 \Omega$ ,  $h_s = 400 \mu\text{m}$ ,  $l_s = 18 \text{ mm}$ ; (2)  $r_c = 1.8 \text{ mm}$ ,  $r_1 = 0$ ,  $r_s = 200 \mu\text{m}$ ,  $R_0 = 60 \Omega$ ,  $h_s = 200 \mu\text{m}$ ,  $l_s = 18 \text{ mm}$ ; (3)  $r_c = 1.8 \text{ mm}$ ,  $r_1 = 0$ ,  $r_s^{\max} = 660 \mu\text{m}$ ,  $R_0 = 200 \Omega$ ,  $h_s = 200 \mu\text{m}$ ,  $l_s = 18 \text{ mm}$ ; (4)  $r_c = 1.8 \text{ mm}$ ,  $r_1 = 0.4 \text{ mm}$ ,  $r_s^{\max} = 1100 \mu\text{m}$ ,  $R_0 = 330 \Omega$ ,  $h_s = 200 \mu\text{m}$ ,  $l_s = 18 \text{ mm}$ ;

spiral length to  $l_s = 190$  mm, while the detector volume  $V_d = \pi r_c^2 l_s$  is kept restricted by reducing the gas cavity radius to  $r_c = 0.54$  mm. Taking into account the known cell factor  $G = 2\pi l_s / \ln(0.54a/r_s)$  of a gas cavity with square cross-section, the value of  $r_c$  corresponds to a square of side  $a = 1$  mm.

The second new sensitive element is of optimized two-way heat conduction design and its resistance  $R_0 = 660 \Omega$  is achieved by decreasing the spiral pitch to the technologically accessible limit  $h_s^{\min} = 100 \mu\text{m}$ , while all the other parameters of the design version 4 in Fig. 5 are kept unchanged.

The quantitatively assessed complete TCD performance of the two new types of high resistance sensitive elements with optimized designs is presented in Fig. 6 in comparison with the “classical” TCD described above. The evaluated relationships suggest, that in accordance with Eq. 10, all sensitive element types operate in a given linear range at almost the same filament temperature (Fig. 6b) and the values of  $T_f$  are inversely proportional to  $x_{\max}$ . Nevertheless, owing to their inherent high coefficients of sensitivity (Fig. 6c), which become higher with increase in TCD block temperature  $T_c$  in Eq. 8, the maximum output signals generated in the linear ranges of the new types of sensitive elements are 1–5 V (Fig. 6d) without involving additional amplifiers. The well known fact that the output signals generated by most of the TCDs currently used are below 0.1 V, and the ratios 0.477:0.274:0.045 and 2.384:1.371:0.226 between the values of  $K$  and  $U_{\max}$  for the design versions 1, 2, and 3 in Fig. 6 at  $x_{\max} = 5$  mol-% allow the conclusion that the proposed high-resistance hot-wire sensitive elements with optimized designs could improve the TCD performance more than tenfold.

The comparison of the two new designs shows that the former allows a stronger heating current (Fig. 6a) owing to its minimal (equal to  $h_s$ ) spiral radius and provides higher sensitivity and a greater output signal (Fig. 6c and d). However, its requirements for the d.c. source voltage and power necessary for supplying the TCD are

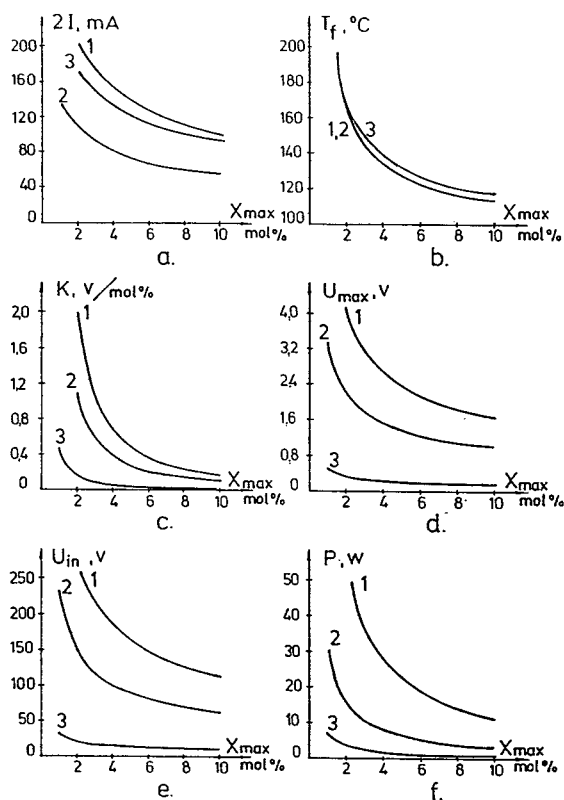


Fig. 6. TCD performance and d.c. source requirements. Two new high-resistance sensitive elements with optimized designs (1 and 2) in comparison with a “classical” TCD (3) the same as design version 1 in Fig. 5. Conditions assumed in the numerical estimations as in Fig. 5. (1)  $r_c = 0.54$  mm,  $r_1 = 0$ ,  $r_s^{\max} = 200 \mu\text{m}$ ,  $R_0 = 640 \Omega$ ,  $h_s = 200 \mu\text{m}$ ,  $l_s = 190$  mm; (2)  $r_c = 1.8$  mm,  $r_1 = 0.4$  mm,  $r_s^{\max} = 1100 \mu\text{m}$ ,  $R_0 = 660 \Omega$ ,  $h_s = 100 \mu\text{m}$ ,  $l_s = 18$  mm; (3)  $r_c = 1.8$  mm,  $r_1 = 0$ ,  $r_s = 400 \mu\text{m}$ ,  $R_0 = 60 \Omega$ ,  $h_s = 400 \mu\text{m}$ ,  $l_s = 18$  mm.

severe (Fig. 6e and f) and with increase in TCD block temperature become rigorous ( $U_{in} = 290$  V and  $P = 40$  W for  $x_{\max} = 5$  mol-% at  $T_c = 300^\circ\text{C}$  after a supplementary calculation), but still accessible for the ultimate capabilities of modern electronics.

The final results of this work is the development of two practical designs of high-resistance sensitive elements, which implement the best possibilities for TCD performance improvement



obtained above for both cases of heat conduction.

In the first design developed, which corresponds to version 1 in Fig. 6 and is shown in Figs. 7 and 8, the coil 1 of length 190 mm is situated in the ten channels 2 with cross-section  $1 \times 1 \text{ mm}^2$  of the element body 3 and is bent between the adjacent channels through the helical grooves 5 on the insulating pegs 4. The body 3 is coupled in the element base 6 and is fastened by the nut 7, while the leads 8 of the coil are hermetically embedded in the perforations 9 by the insulators 10. The assembled sensitive elements are placed in the nests 11 of the TCD block 12, whose channels 13 split the gas flows among the relevant sensitive elements. Thus the

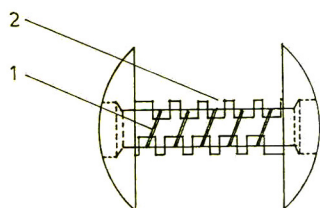
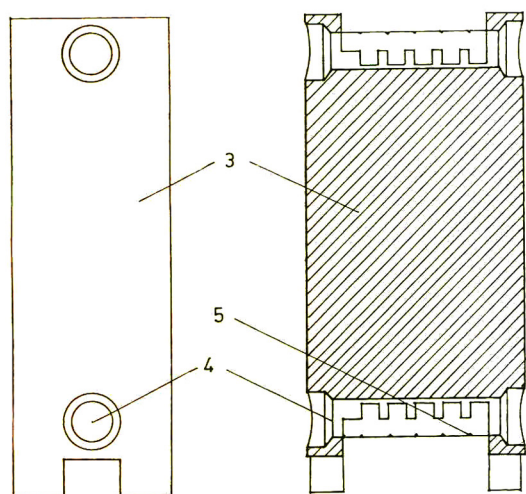


Fig. 7. First new sensitive element design: 1 = coil; 2 = channels for gas cavities; 3 = body; 4 = insulating pegs; 5 = helical grooves.

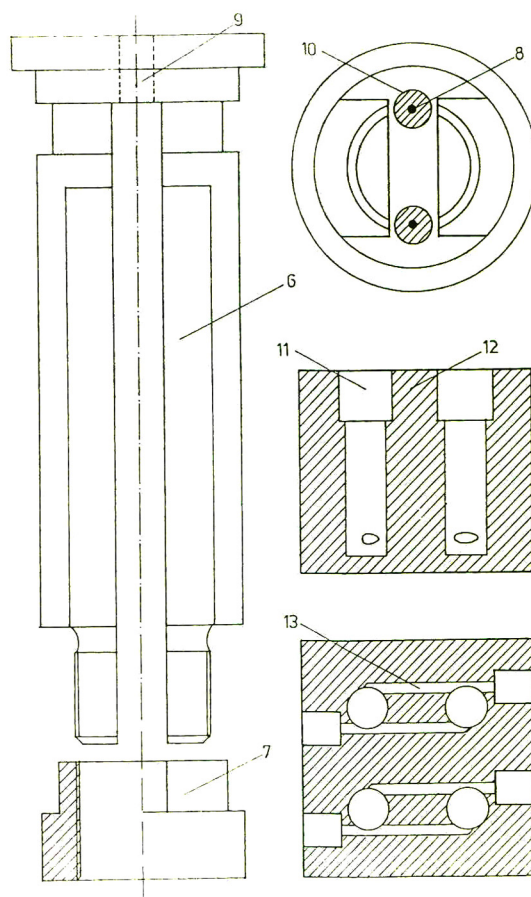


Fig. 8. First new sensitive elements design (continued): 6 = base; 7 = nut; 8 = leads; 9 = perforations; 10 = insulators; 11 = nests for sensitive elements; 12 = TCD block; 13 = channels for gas flows.

adverse "heat capacity effect" is decreased, while the additional inherent split among the channels 2 improves the TCD response time.

In the second TCD sensitive element design developed, which corresponds to version 2 in Fig. 6 and is shown in Fig. 9, coil 1 of radius 1.1 mm is situated around the central lead 3 of radius 0.4 mm including a 0.1 mm thickness of the insulator 2. Sagging and vibrations of the coil can be prevented through the three PTFE holders 4, by applying PTFE to the whole filament 5 or by coiling in the manner shown in Fig.

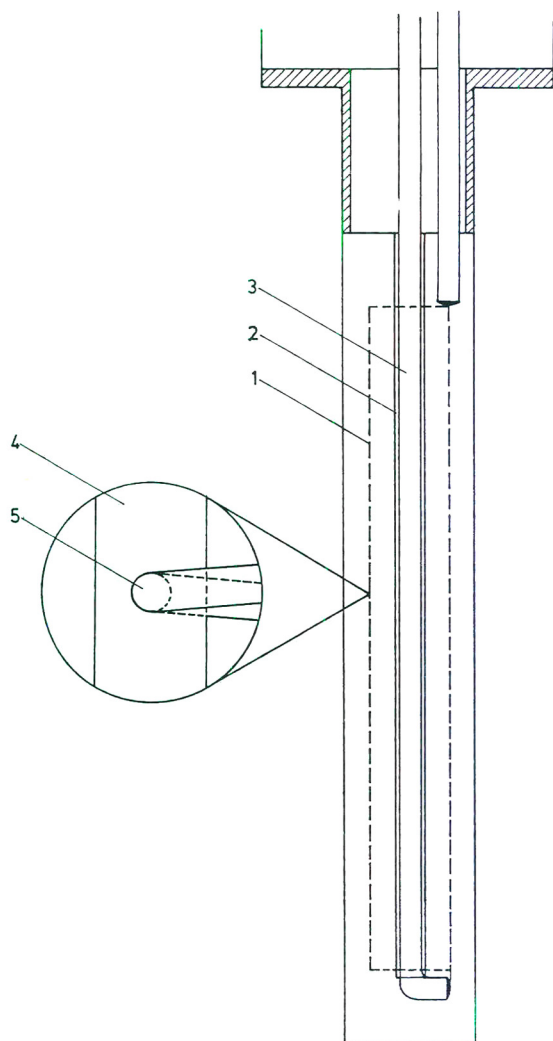


Fig. 9. Second new sensitive element design: 1 = coil; 2 = insulator; 3 = central lead; 4 = PTFE holders; 5 = filament.

10, where the primary spiral is of  $r_s = 200 \mu\text{m}$  and  $h_s = 125 \mu\text{m}$ , which parameters are technologically accessible and practically suitable, while the secondary sensitive element spiral is of  $r_s^{\text{max}} = 1.1 \text{ mm}$  and  $h_s = 1 \text{ mm}$ .

#### 4. Conclusions

The analytical and numerical estimations presented allow the conclusion that in both one-

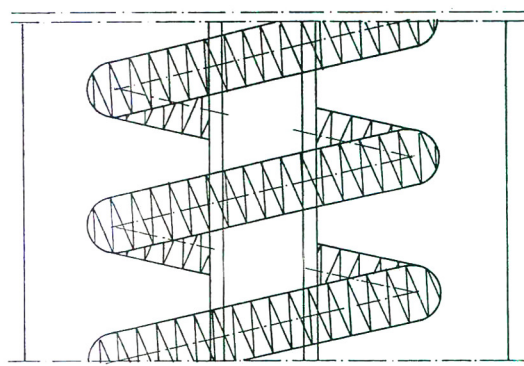


Fig. 10. Second new sensitive element design with a twice-coiled filament.

and two-way heat conduction the TCD sensitive element design can be optimized by using the appropriate spiral pitches and radiuses obtained. The positive effect of the hot-wire sensitive element design optimization on the TCD performance is additionally enhanced by the significant increase in the filament resistance provided. Further, the quantitative estimations show that the filament resistance at  $0^\circ\text{C}$  can be increased to  $500\text{--}700 \Omega$  if the ultimate capabilities of modern electronics are utilized in the d.c. sources needed for a TCD. Finally, the practical problems of the TCD performance improvement presented can be solved by the development of new optimized designs of high-resistance hot-wire sensitive elements, which could improve more than tenfold

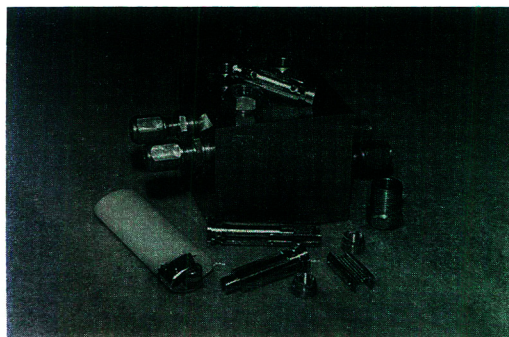


Fig. 11. Photograph of first new design developed after the schematic drawings shown.

the performance of the “classical” TCD used in gas chromatography and in the other methods employing thermal conductivity phenomena for the measurement, analysis and control of volatile substances.

Fig. 11 shows the first new design developed.

## References

[1] S. Dal Nogare and R.S. Juvet, Jr., *Gas-Liquid Chromatography*, Interscience, New York, 1962.

- [2] D.J. David, *Gas Chromatographic Detectors*, Wiley, New York, 1974.
- [3] J.E. Baudean, L.S. Ettre, M.J. Hartigan, H. Hoberecht, E.W. March, R. Pigliucci, J.E. Purcell and B. Melton, *Am. Lab.*, May (1977) 17–24.
- [4] H.M. McNair and E.J. Bonelli, *Basic Gas Chromatography*, Consolidated Printers, Oakland, CA, 1967.
- [5] Shimadzu Gas Chromatograph GC-8A Catalog, Shimadzu, Tokyo, 1987.



# Thermodynamic consideration of the retention mechanism in a poly(perfluoroalkyl ether) gas chromatographic stationary phase used in packed columns

Reynaldo C. Castells<sup>a,b,\*</sup>, Lilian M. Romero<sup>b</sup>, Angel M. Nardillo<sup>a,b</sup>

<sup>a</sup>*CIDEPINT, 52 e/ 121 y 122, 1900 La Plata, Argentina*

<sup>b</sup>*División de Química Analítica, Facultad de Ciencias Exactas, Universidad Nacional de La Plata, 1900 La Plata, Argentina*

First received 7 February 1995; revised manuscript received 19 May 1995; accepted 23 May 1995

## Abstract

Retention volumes of fifteen hydrocarbons were measured in columns containing several concentrations of a commercial poly(perfluoroalkyl ether), Fomblin Y HVAC 140/13, as the stationary phase. Two different types of packing were studied: one of them employed pre-silylated Chromosorb P AW DMCS as the solid support and the other type was prepared by coating the stationary phase on Chromosorb P AW and silylating on-column. On-column silylated columns showed unequivocal symptoms of partial deactivation; retention volumes changed regularly with the content of stationary phase in pre-silylated columns. Analysis of retention in pre-silylated columns indicates that a mixed mechanism (partition and adsorption onto the gas–liquid interface) is operative. The systems hydrocarbon–perfluorocompound show pronounced positive deviations from the ideal behaviour that can be attributed to repulsion between the hydrocarbon and the perfluorocompound segments.

## 1. Introduction

Perfluorinated substances have been sporadically employed as stationary phases in gas chromatography, and this mostly for the separation of substances of high chemical reactivity or perfluorocompounds and freons. Excellent review articles have been written by Pomaville and Poole [1] and by O'Mahony et al. [2].

Highly fluorinated fluids are characterized by their chemical inertia and by very weak molecular interactions, both in the pure state and in mixtures with other substances. Cohesive energy densities of perfluoroalkanes and perfluoro-

cycloalkanes are much lower than those of the corresponding hydrocarbons [3], and although fluorocarbons and hydrocarbons are individually highly non-polar, their mixtures show important deviations from Raoult's law [3–5]. These properties have two important consequences in relation with their use as gas chromatographic stationary phases. On the one hand, as pointed out by Poole and co-workers [1,6,7], retention times in highly fluorinated stationary phases will be shorter than in conventional phases, thus enabling the separation of low-volatility or thermally labile substances. On the other hand, weak interactions with the solid support or the capillary wall result in insufficient surface deactivation, uneven distribution and poor film stability,

\* Corresponding author.

reflected in peak asymmetry, low efficiency and retention time variations; all of these deleterious symptoms are very markedly displayed when using perfluoroparaffins.

Drastic improvements in the chromatographic behaviour are obtained by incorporating polar groups in the stationary phase molecules. The poly(perfluoroalkyl ether) phase Fomblin YR,

$[(OCFCF_3CF_2)_n-(OCF_2)_m]$ , was introduced in 1983 by Dhaneesar and Poole [6,7]; paraffinic and olefinic hydrocarbons, injected at temperatures markedly lower than their boiling points, elute from these columns with short retention times, with very good peak shapes, but asymmetric peaks are obtained for solutes of higher polarity. Furthermore, the authors found that packings prepared by coating previously silylated supports (Gas-Chrom Q) gave symmetrical peaks when tested at low temperatures, but after heating to above 100°C and returning to low temperatures for re-testing, shorter retention times and asymmetric peaks were obtained, a behaviour that the authors attribute to film contraction, which results in bare-surface exposition and liquid lenses. Columns stable at temperatures higher than 200°C and with efficiencies similar to those obtained for conventional phases were obtained by coating Chromosorb P, packing the columns with coated support, and on-column silylating by injection of Silyl-8 or bis(trimethylsilyl)trifluoroacetamide (BSTFA) [6,7].

Mixtures of fluorocarbon compounds and aliphatic or alicyclic hydrocarbons are the only known examples of systems with large positive excess functions where none of the components is polar; as such, they have been the subject of many studies since the 1950s [8,9]. Although these trends are qualitatively consistent with the large differences in cohesive energy densities of fluorocarbons and hydrocarbons, the solubility parameter approach does not give a satisfactory quantitative explanation [3]. Plots of surface tension against composition also show pronounced deviations from the ideal behaviour [10,11]. The objective of the present paper is to obtain thermodynamic data for the processes of solution and adsorption on the gas-liquid interface for a group of hydrocarbons at infinite

dilution in a highly fluorinated stationary phase near room temperature. A high-molecular-mass perfluoroalkane was supposed to be used as the solvent, according with the original plan; the poor performance of these substances as stationary phases compelled us to modify the project. Fomblin was then chosen because of its characteristics and to profit from the experience collected by Poole and co-workers on this stationary phase.

## 2. Experimental

### 2.1. Materials and columns

Fomblin Y HVAC 140/13 (weight average molecular mass 6500) and 1,1,2-trichlorotrifluoroethane (Freon 113) were purchased from Aldrich; BSTFA was obtained from Supelco. Hydrocarbon solutes of different origins, all of them more than 99% pure, were used as received. Column packings were prepared in a rotary evaporator, using Freon 113 as solvent. Coated supports were packed into 1.0 m × 0.53 cm I.D. stainless-steel tubes with the aid of vacuum suction and gentle tapping. Two sets of columns were prepared:

(a) On-column silylated columns: a packing containing 5.67% by weight of Fomblin on Chromosorb P AW 60/80 was prepared by the above-mentioned method. A 1.80 m × 0.4 cm I.D. glass column containing this packing was installed in a Konik gas chromatograph (see later) with a glass-lined injector; the injector and the column oven were set to 100 and 150°C, respectively, and on-column silylation was performed by slowly injecting 100 μl of BSTFA with a nitrogen flow-rate of 5 ml/min. The column was held at 150°C for several hours, and the silylating treatment was then repeated after reversing the column end connections. The column was carefully emptied and its content was used as starting material to prepare packings with higher stationary-phase concentrations, by successively adding Fomblin by the above-mentioned coating technique. By this method four columns containing 5.67, 8.30,

13.36 and 22.05 weight percentage (*w*) of Fomblin on the same lot of solid support were prepared, with the objective of minimizing unpredictable effects associated with the silylating process.

(b) Pre-silylated columns, containing 4.29, 5.56, 7.50, 10.89, 15.52 and 19.40% by weight of Fomblin were prepared using Chromosorb P AW DMCS 60/80 as the solid support.

## 2.2. Apparatus and procedure

The study of thermal stability of packings was performed in a Konik 3000 gas chromatograph, equipped with a flame ionization detector (FID) and a Spectra Physics Datajet Integrator, using 1.50 × 2 mm I.D. glass columns.

A home-assembled apparatus, in which column temperature was controlled to better than ± 0.05°C by immersion in a water bath, was used for the remaining measurements. Nitrogen, successively passed through a molecular sieves trap (Davidson 5A), a Brooks 8606 pressure regulator, a Brooks 8743 flow controller and a 2 m × 1/8 in. O.D. coiled copper tube immersed in the column bath, was used as the carrier gas. Inlet pressures were measured by means of a mercury manometer at a point between the copper coil and a Swagelok 1/4 in. s.s. "T"; one branch of the latter was provided with a septum, and the columns were connected to the remaining branch. Solute vapours were on-column injected by using Hamilton syringes. Eluates were detected with a Hewlett-Packard 5750 FID and electrometer signals were fed to a Hewlett-Packard 3396A integrator. Flow-rates ranging between 15 and 30 ml/min were measured by means of a water jacketed soap film flow meter.

Sample sizes of the order of 10<sup>-2</sup> μmol resulted in symmetrical peaks for all the studied solutes, thus warranting Henry's law conditions for all the retention mechanisms. Aromatic hydrocarbons, whose peaks displayed a slight asymmetry that persisted at the smallest sample sizes compatible with instrumental noise, were excluded from this study. Solute vapours and a small methane sample were simultaneously in-

jected; net retention times were measured to 10<sup>-3</sup> min between the maxima of the solute and the methane peaks. Specific retention volumes (*V<sub>g</sub><sup>0</sup>*) and net retention volumes per gram of packing (*V<sub>N</sub>*) were calculated from values of the operating parameters in the usual form [12]. Values at each temperature were means of no less than four injections; retentions were measured for groups of three to four solutes at five temperatures equally spaced within the range 22–35°C, and the measurements for the same group of solutes were repeated after two to three weeks.

Densities of Fomblin were measured at twelve temperatures between 19 and 41°C with a 3-ml pycnometer that had been carefully calibrated through the same temperature interval, and were least-squares fitted to the following polynomial:

$$\rho_2(T/^\circ\text{C}) = 1.94429 - 1.2808 \cdot 10^{-3}t - 1.30 \cdot 10^{-5}t^2 + 10^{-7}t^3 \quad (1)$$

The thermal expansion coefficient, as calculated from Eq. 1, is  $\alpha_2 = 9.15 \cdot 10^{-4} \text{ K}^{-1}$  at 25°C.

## 3. Results and discussion

### 3.1. Comparing pre-silylated and on-column silylated packings

The pattern displayed in Fig. 1 for four representative cases is common for all the solutes. *V<sub>N</sub>* increases in a satisfactory linear fashion with percentage Fomblin in the pre-silylated Chromosorb P phases. An important decrease in *V<sub>N</sub>* occurs, particularly with unsaturated solutes, when the Fomblin proportion increases above 5.7%, on post-silylated packings.

A series of alternative suggestions could be made to explain the behaviour observed in on-column silylated packings. Identification of the retention mechanisms that operate in these columns and discriminating between their respective contributions to the total retention would be a difficult task, with dubious results. Pre-silylated packings represent a more attractive option



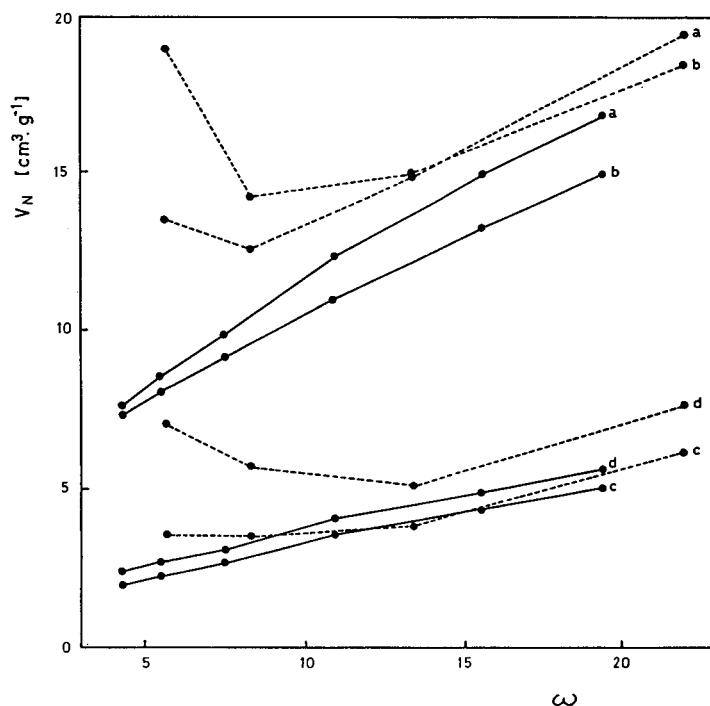


Fig. 1. Retention volume per gram of packing at 25°C ( $V_N$ ) against percentage by weight of stationary phase ( $w$ ). Dashed lines: on-column silylated packings. Solid lines: pre-silylated packings. Solutes: (a) *n*-octane; (b) 1-octene; (c) cyclohexane; (d) cyclohexene.

when the objective is to isolate the effects of the liquid phase from those of the solid support.

The physical meaning of retention volumes measured in pre-silylated columns, on the other hand, could be questioned in terms of the thermal instability of these packings. Therefore, and although the retention volumes demonstrated excellent reproducibility in the 22–35°C temperature range, a test addressed to check the stability of pre-silylated packings under conditions considerably more stringent than those prevailing during the thermodynamic measurements was performed. *n*-Nonane and *n*-decane retention volumes were measured at six temperatures between 40 and 75°C in columns containing 10.89 and 19.40% packings; the columns were then slowly heated to 120°C and kept for 1.5 h at this temperature, spontaneously cooled down to room temperature, and heated again to 120°C for 1.5 h; retention volumes were then re-measured in the 40–75°C interval. The results of this

experiment are summarized in Table 1, and show not only that the retention volumes measured before and after heating are coincident, but also that the slopes of the plots of  $\ln V_g^0$  versus  $1/T$  remain constant. The efficiency of both columns is poor and heating seems to produce a drop in the number of theoretical plates of the column containing the 10.89% packing. Summarizing, there are no counter-indications for the employment of these columns in the measurement of thermodynamic properties, where column efficiency is a desirable but not an essential parameter.

Only results obtained using pre-silylated packings are referred to in the following sections.

### 3.2. Obtaining the thermodynamic results

Experimental results obtained on each column were fitted to the equation



Table 1

Effect of thermal treatment on specific retention volumes, their temperature dependence and the efficiency of columns packed with Fomblin coated on Chromosorb P AW DMCS

	<i>n</i> -Decane		<i>n</i> -Nonane	
	Pre <sup>a</sup>	Post <sup>a</sup>	Pre <sup>a</sup>	Post <sup>a</sup>
<i>w</i> = 10.89%				
$V_g^0$ , 45°C	193.7	192.7	93.75	94.00
$V_g^0$ , 55°C	129.9	129.2	65.32	65.64
$V_g^0$ , 70°C	67.56	67.37	36.53	36.63
$B^b$	4626	4663	4149	4170
<i>N</i> , 50°C <sup>c</sup>	1670	1450	1450	1200
<i>N</i> , 70°C <sup>c</sup>	1400	990	875	810
<i>w</i> = 19.40%				
$V_g^0$ , 50°C	115.5	113.4		
$V_g^0$ , 62°C	70.82	70.00		
$V_g^0$ , 74°C	44.64	44.82		
$B^b$	4506	4409		
<i>N</i> , 50°C <sup>c</sup>	1260	1320		
<i>N</i> , 74°C <sup>c</sup>	1300	1260		

<sup>a</sup> Results before and after the thermal treatment (details in the text).

<sup>b</sup> Least-squares slopes for the fit to the equation  $\ln V_g^0 = B/T + \text{constant}$ .

<sup>c</sup> Number of theoretical plates.

$$\ln V_g^0 = -\Delta H_s^0/RT + \text{constant} \quad (2)$$

where  $\Delta H_s^0$ , the heat of sorption, corresponds to the transfer of one mole of solute from an ideal vapour phase at a partial pressure of 1 atm to a stationary phase of yet undefined characteristics. Regression analysis of the results obtained in a given column showed that: (a) values of percent standard deviation of the heats of sorption,  $100\sigma(\Delta H_s^0)/\Delta H_s^0$ , were smaller than 1.5% for all the solutes; (b) retention volumes obtained in a just conditioned column differed by less than 0.8% from those obtained under identical conditions after two or more weeks of column use, and the differences between the corresponding heats of sorption were smaller than 4%.

In Figs. 2 and 3  $V_g^0$  values at 25°C and heats of sorption, respectively, have been plotted against *w* for a group of representative solutes. The existence of a mixed retention mechanism is made evident by both plots, since straight lines parallel to the horizontal axis should be obtained for a pure partitioning process; furthermore, it

can be deduced from Fig. 3 that the adsorptive component is markedly more exothermic than its solution counterpart [13]. Several years ago Conder et al. [14] proposed the following equation to express the retention volume per gram of packing when mixed mechanisms are operative:

$$V_N = K_L V_L + K_A A_L + K_S A_S \quad (3)$$

where  $K_L$  is the liquid–gas partition coefficient,  $K_A$  and  $K_S$  are the adsorption coefficients at the gas–liquid and at the liquid–solid interfaces, respectively, and  $V_L$ ,  $A_L$  and  $A_S$  represent the liquid volume, the gas–liquid interfacial area and the liquid–solid interfacial area, all of them expressed per gram of packing; adsorption on bare portions of the support is not considered in Eq. 3, which seems reasonable for packings containing more than 3–4% by weight of stationary phase on Chromosorb P. Models endeavouring more detailed descriptions, involving equations with larger number of terms and, as such, of more difficult and dubious applicability to real data, have been more recently proposed [15].

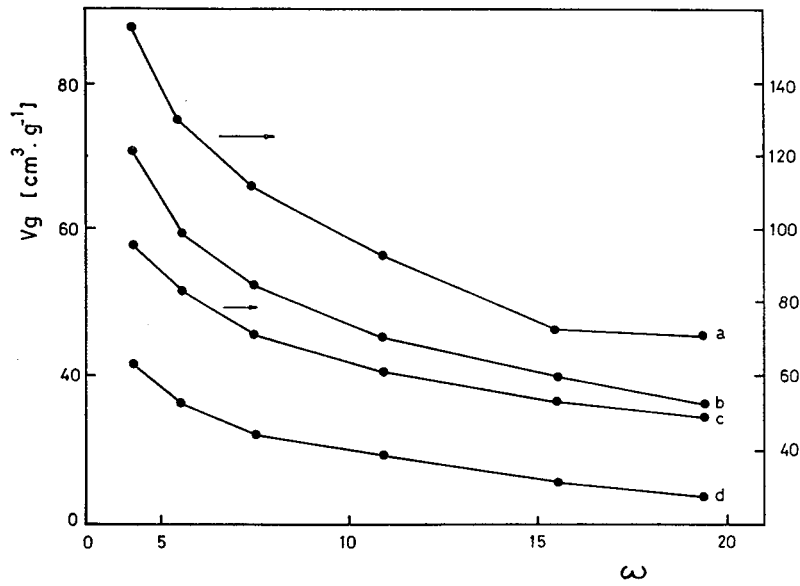


Fig. 2. Specific retention volumes at 25°C ( $V_g^0$ ) against percentage by weight of stationary phase ( $w$ ). Solutes: (a) 1-octene; (b) *n*-heptane; (c) 2,2-dimethylhexane; (d) cyclohexene.

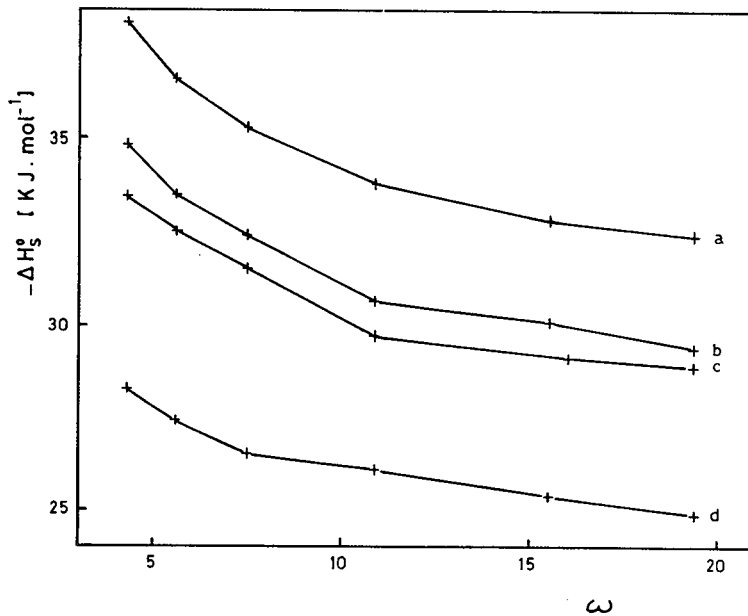


Fig. 3. Heats of sorption ( $\Delta H_s^0$ ) against percentage by weight of stationary phase ( $w$ ). Solute symbols as in Fig. 2.

The values of  $A_L$  necessary to fit experimental results to Eq. 3 were calculated by following the proposal of Martire et al. [16], taking into consideration the large difference between the densities of  $\beta, \beta'$ -thiodipropionitrile and Fomblin [17].

Multiple linear regression to Eq. 3, assigning to  $A_S$  values calculated from the specific surface area of the support, was unsuccessfully attempted in the first place; the fit was insensible to very large changes in the values assigned to  $A_S$ , the coefficients had no statistical significance and, furthermore, it was found that Eq. 3 was over-parameterized, as evidenced by dependencies larger than 0.9999. On the other hand, there was a good linear relationship between the variables  $V_N/V_L$  and  $A_L/V_L$ , as indicated by correlation coefficients higher than 0.997 and by the small coefficients of variation of both the intercepts and the slopes (see second and fifth column in Table 2, respectively). In terms of Eq. 3, since  $V_L$  increases almost five times and  $A_L$  decreases by about 60% between the lower and the higher stationary phase loading, it is reasonable to conclude that  $K_S$  is negligible under the present circumstances. In other words, within the experimental errors of our measurements, the

intercepts and the slopes obtained by means of the linear regression can be identified with the coefficients  $K_L$  and  $K_A$ , respectively.

These results indicate that hydrocarbon retention in columns containing Fomblin coated on Chromosorb P AW DMCS can be attributed to partition and adsorption on the gas–liquid interface. Depending on the solute, the contribution of adsorption to the total retention ranges between 50–60% at the lower loading and between 10–15% in the column with higher concentration of stationary phase, as calculated by using the  $K_L$  and  $K_A$  results obtained as indicated in the former paragraph together with the  $V_L$  and  $A_L$  values characteristic of each column.

Standard enthalpies of solution, corresponding to the transfer of one mole of solute from an ideal vapour phase at a pressure of 1 atm to an hypothetical solution at unitary weight fraction, with behaviour extrapolated from infinite dilution, were calculated by means of the equation [18]

$$\Delta H_L^0 = -R[\partial \ln K_L / \partial (1/T)] - RT(1 - \alpha_2 T) \quad (4)$$

The assumption of ideal vapour behaviour implied in Eq. 4 is justified by a rapid calculation

Table 2  
Thermodynamic functions of partition and adsorption of vapours at infinite dilution in Fomblin at 25°C

Solute	$K_L \pm \sigma(K_L)$	$-\Delta H_L^0$ (kJ/mol)	$\chi^*(\text{int})$	$K_A \pm \sigma(K_A)$ ( $\times 10^4$ cm)	$-\Delta H_A^0$ (kJ/mol)	$-\Delta H_C^0$ (kJ/mol)
<i>n</i> -Hexane	29.21 $\pm$ 1.12	24.7 $\pm$ 3.2	2.462	0.573 $\pm$ 0.031	30.5 $\pm$ 5.4	31.6
<i>n</i> -Heptane	65.33 $\pm$ 1.64	28.1 $\pm$ 2.8	2.761	1.239 $\pm$ 0.042	36.4 $\pm$ 4.4	36.6
2-Methylhexane	53.21 $\pm$ 1.31	26.2 $\pm$ 2.8	2.605	0.998 $\pm$ 0.033	35.7 $\pm$ 4.5	34.8
2,3-Dimethylpentane	60.12 $\pm$ 1.71	26.1 $\pm$ 2.7	2.472	0.949 $\pm$ 0.044	35.4 $\pm$ 5.5	34.2
<i>n</i> -Octane	145.1 $\pm$ 6.95	31.1 $\pm$ 4.9	3.058	2.970 $\pm$ 0.177	42.7 $\pm$ 8.2	41.5
2-Methylheptane	117.5 $\pm$ 6.04	30.7 $\pm$ 4.9	2.883	2.337 $\pm$ 0.154	40.4 $\pm$ 8.4	39.7
2,2-Dimethylhexane	88.90 $\pm$ 2.28	28.4 $\pm$ 2.8	2.646	1.681 $\pm$ 0.058	38.7 $\pm$ 4.7	37.3
2,2,4-Trimethylpentane	77.93 $\pm$ 3.10	26.4 $\pm$ 3.7	2.406	1.353 $\pm$ 0.079	38.0 $\pm$ 7.3	35.1
<i>n</i> -Nonane	325.5 $\pm$ 15.7	36.0 $\pm$ 5.6	3.340	6.906 $\pm$ 0.400	45.8 $\pm$ 8.6	46.4
1-Heptene	55.7 $\pm$ 2.13	26.2 $\pm$ 3.8	2.764	1.287 $\pm$ 0.054	36.6 $\pm$ 5.6	36.1
1-Octene	122.9 $\pm$ 3.82	30.6 $\pm$ 3.4	3.057	3.090 $\pm$ 0.097	40.9 $\pm$ 4.6	40.8
Cyclohexane	45.68 $\pm$ 2.03	25.3 $\pm$ 3.4	2.671	0.621 $\pm$ 0.052	30.5 $\pm$ 7.7	33.0
Cyclohexene	48.73 $\pm$ 2.41	26.9 $\pm$ 4.5	2.758	0.872 $\pm$ 0.061	28.8 $\pm$ 6.9	33.3
Methylcyclohexane	79.24 $\pm$ 3.68	27.6 $\pm$ 4.1	2.713	1.165 $\pm$ 0.094	35.1 $\pm$ 8.8	35.4
Ethylcyclohexane	191.1 $\pm$ 9.16	31.0 $\pm$ 4.6	3.020	2.808 $\pm$ 0.233	40.5 $\pm$ 10.2	40.5

[12] which indicates that the non-ideality correction in the case of the most volatile solute at the higher experimental temperature (*n*-hexane at 35°C) amounts to about 0.3% of  $K_L$ , a value below our estimation of the experimental error.

Enthalpies of adsorption were computed from the expression

$$\Delta H_A^0 = -R[\partial \ln K_A / \partial (1/T)] \quad (5)$$

and can be shown [19] to correspond to the transfer of one mole of solute from an ideal vapour phase at 1 atm to an ideal adsorbed state in which the molecules of the adsorbate interact with the surface only. In as much as adsorbate–adsorbate interactions are absent, the value of the adsorption enthalpy does not depend on the definition of the adsorbed state; this statement obviously does not apply to the adsorption free energy and entropy.

Solution and adsorption properties have been gathered in Table 2. As already mentioned, the uncertainties assigned to  $K_L$  and  $K_A$  values are the standard deviations for the intercept and the slope, respectively, obtained in the regression of  $V_N/V_L$  against  $A_L/V_L$ . The confidence ranges for  $\Delta H_L^0$  and  $\Delta H_A^0$  at the 95% level were estimated by following a method proposed some years ago [13], which takes into consideration that two successive regressions are necessary to obtain the enthalpy values. The latent heats of condensation,  $\Delta H_C^0$  [20], were included in Table 2 for comparison.

The results shown in the table change very regularly with the molecular structure of the solutes. Thus the plots of  $\ln K_L$  for *n*-alkanes against their carbon number, *N*, are straight lines with correlation coefficients  $r = 0.99997$ , and those of  $\ln K_A$  against *N* result in  $r = 0.9997$ . Both  $K_L$  and  $K_A$  are smaller for branched than for normal alkanes with the same *N*, and (except for the  $K_L$  result for 2,3-dimethylpentane) both values decrease as branching increases. The partition coefficients of the alkenes are smaller than those of the corresponding alkanes, while the opposite trend is observed for the adsorption coefficients. Partition coefficients of cycloalkanes are larger than those of the alkanes with the

same carbon number, but the adsorption coefficients of both groups of substances are coincident within experimental error.

As could be expected, less regularity is found when the enthalpies are compared: plots of  $\Delta H_L^0$  and of  $\Delta H_A^0$  against *N* for *n*-alkanes are well represented by straight lines, but their correlation coefficients drop to 0.994 and 0.991, respectively. In general terms, branched alkanes and alkenes show less negative  $\Delta H_L^0$  and  $\Delta H_A^0$  values than normal alkanes with the same *N*.

Figs. 4 and 5 show that there is a strong correlation between  $K_A$  and  $K_L$  on the one hand, and between  $\Delta H_A^0$  and  $\Delta H_L^0$  on the other. It can be concluded from this behaviour that solution and adsorption are ruled by the same physical factors, either energetic or statistical. However, when the enthalpies of adsorption and of solution are compared with the latent heats of condensation it is found that:

- the differences  $\Delta H_A^0 - \Delta H_C^0$  are zero within experimental error, indicating that the liquid–gas interface of Fomblin is a low-energy surface on which the hydrocarbon molecules adsorb without experiencing the influence of large repulsion or attraction forces, and
- the differences  $\Delta H_L^0 - \Delta H_C^0$ , rough estimators of infinite dilution excess enthalpies, range between 7 and 10 kJ/mol, indicating that the solute molecules are repelled from the bulk liquid and require the absorption of important quantities of energy in order to penetrate it.

Deviations from the ideal behaviour are more important in bulk mixtures than on surfaces, a fact already detected by Handa and Mukerjee [10], who attributed it to the lower number of nearest neighbours that a molecule has on a surface compared to the situation in bulk solution. These authors semiquantitatively explained the surface properties of *n*-alkane–perfluoroalkane mixtures by assuming unitary surface activity coefficients and modelling the bulk activity coefficients by means of the regular solution and the Flory–Huggins approaches.

Flory–Huggins interaction parameters,  $\chi^*$ , were calculated with the equation [21]

$$\chi^* = \ln(RT\rho_2/K_L D_1^0 M_1) - \ln(v_1^*/v_2^*) - 1 + (M_1 v_1^*/M_2 V_2^*) \quad (6)$$

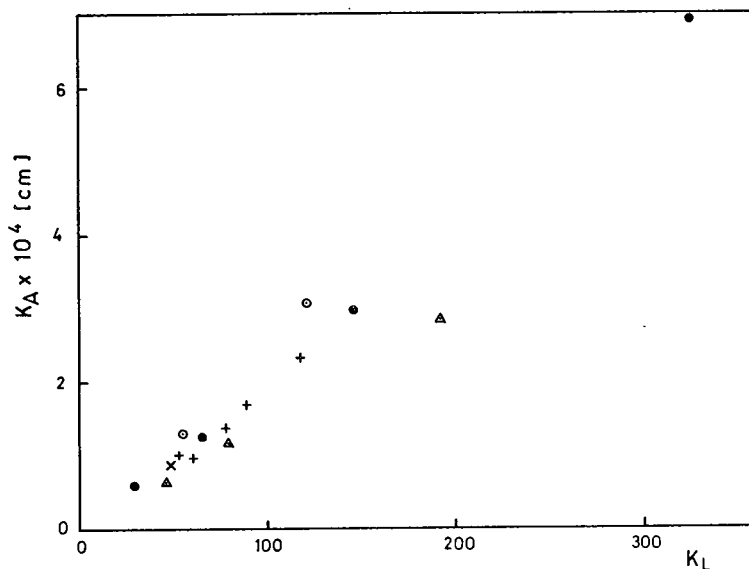


Fig. 4. Adsorption coefficients ( $K_A$ ) against partition coefficients ( $K_L$ ) at 25°C. Solutes: (●) *n*-alkanes; (+) branched alkanes; (○) alkenes; (△) cycloalkanes; (×) cyclohexene.

where  $M_1$  and  $p_1^0$  represent the solute molecular mass and vapour pressure at the column temperature, respectively,  $M_2$  is the polymer number averaged molecular mass and  $v_1^*$  and  $v_2^*$  are

the solute and the polymer specific “hard core” volumes, calculated by means of the Flory state equation [22] using experimental thermal expansion coefficients. The interaction parameter is a non-dimensional free energy term that includes all the non-combinatorial contributions to excess free energy; Eichinger and Flory [22] express  $\chi^*$  as a sum of two contributions:

$$\chi^* = \chi^*(fv) + \chi^*(int) \quad (7)$$

where  $\chi^*(fv)$  is the free volume contribution, and  $\chi^*(int)$  results from contact interactions.

Unusually high  $\chi^*$  values, ranging between 2.4 and 3.4, are obtained for the systems studied in the present paper. With as only exception *n*-hexane, free volume effects contribute less than 2.5% to the total interaction parameter. The highly positive non-ideality of these mixtures results from very large differences between the force fields surrounding the hydrocarbon and the perfluorocarbon segments.

Values of  $\chi^*(int)$  can be found in the fourth column of Table 2; they were fitted by a non-linear regression method to the equation

$$\chi^*(int) = (V_1^*/RT)(\delta_1 - \delta_2)^2 \quad (8)$$

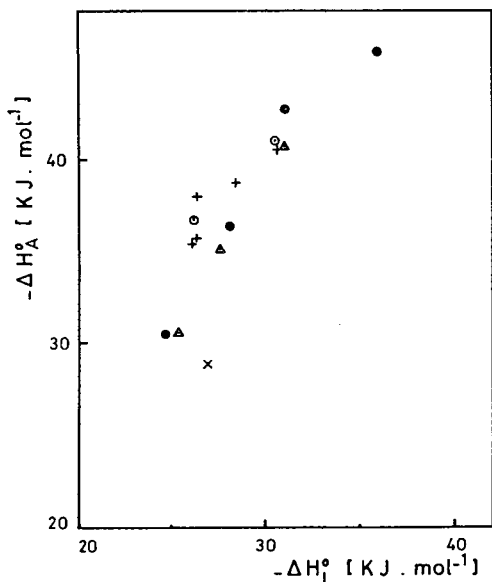


Fig. 5. Enthalpy of adsorption ( $\Delta H_A^0$ ) against enthalpy of solution ( $\Delta H_L^0$ ). Symbols as in Fig. 4.

where  $V_1^* = M_1 v_1^*$ ,  $\delta_1$  is the solute solubility parameter [23], and  $\delta_2$ , the polymer solubility parameter, was the fitting parameter. A value  $\delta_2 = 7.65 \text{ J}^{1/2} \text{ cm}^{-3/2}$  is thus obtained; the standard deviation obtained for  $\delta_2$  is only  $0.084 \text{ J}^{1/2} \text{ cm}^{-3/2}$ , indicating that the experimental results fit nicely to Eq. 8. However, the value returned for  $\delta_2$  is unusually low and, from our point of view, its physical meaning is not clear. This is by no means a novelty in dealing with polymer solubility parameters.

### Acknowledgements

This work was sponsored by CONICET (Consejo Nacional de Investigaciones Científicas y Tecnológicas) through PID-BID 1121, and by CICPBA (Comisión de Investigaciones Científicas de la Provincia de Buenos Aires).

### References

- [1] R.M. Pomaville and C.F. Poole, *Anal. Chim. Acta*, 200 (1987) 151.
- [2] T.K.P. O'Mahony, A.P. Cox and D.J. Roberts, *J. Chromatogr.*, 637 (1993) 1.
- [3] J.H. Hildebrand, J.M. Prausnitz and R.L. Scott, *Regular and Related Solutions*, Van Nostrand-Reinhold, New York, 1970.
- [4] R.G. Bedford and R.D. Dunlap, *J. Am. Chem. Soc.*, 80 (1958) 282.
- [5] R.D. Dunlap, R.G. Bedford, J.C. Woodbrey and S.D. Furrow, *J. Am. Chem. Soc.*, 81 (1959) 2927.
- [6] S.C. Dhanesar and C.F. Poole, *J. Chromatogr.*, 267 (1983) 388.
- [7] S.C. Dhanesar and C.F. Poole, *Anal. Chem.*, 55 (1983) 1462.
- [8] R.L. Scott, *J. Phys. Chem.*, 62 (1958) 136.
- [9] F.L. Swinton, in M.L. McGlashan (Editor), *Chemical Thermodynamics, Specialist Periodical Reports*, Vol. 2, Chemical Society, London, 1978, p. 147.
- [10] T. Handa and P. Mukerjee, *J. Phys. Chem.*, 85 (1981) 3916.
- [11] P. Mukerjee, *Colloid Surface A*, 84 (1994) 1.
- [12] J.R. Conder and C.L. Young, *Physicochemical Measurements by Gas Chromatography*, Wiley, New York, 1979, Ch. 2.
- [13] R.C. Castells, *J. Chromatogr.*, 111 (1975) 1.
- [14] J.R. Conder, D.C. Locke and J.H. Purnell, *J. Phys. Chem.*, 73 (1969) 700.
- [15] R. Nikolov, *J. Chromatogr.*, 241 (1982) 237.
- [16] D.E. Martire, R.L. Pecsok and J.H. Purnell, *Trans. Faraday Soc.*, 61 (1965) 2496.
- [17] R.L. Martin, *Anal. Chem.*, 33 (1961) 347.
- [18] R.C. Castells, *J. Chromatogr.*, 350 (1985) 339.
- [19] E.F. Meyer, *J. Chem. Educ.*, 57 (1980) 120.
- [20] R.R. Dreisbach, *Adv. Chem. Ser.*, 15 (1955); 22 (1959).
- [21] D. Patterson, Y.B. Tewari, H.P. Schreiber and J.E. Guillet, *Macromolecules*, 4 (1971) 356.
- [22] B.E. Eichinger and P.J. Flory, *Trans. Faraday Soc.*, 64 (1968) 2035.
- [23] A.F.M. Barton, *Handbook of Solubility Parameters*, CRC Press, Boca Raton, FL, 1983.



ELSEVIER

Journal of Chromatography A, 715 (1995) 309–315

JOURNAL OF  
CHROMATOGRAPHY A

# Glycerol as a new dissolution medium for $\alpha$ -, $\beta$ - and $\gamma$ -cyclodextrins for preparing stereoselective stationary phases for gas–liquid chromatography

D. Sybilska\*, M. Asztemborska, D.R. Zook, J. Goronowicz

*Institute of Physical Chemistry of the Polish Academy of Sciences, Kasprzaka 44/52, 01-224 Warsaw, Poland*

First received 24 March 1995; revised manuscript received 19 May 1995; accepted 19 May 1995

## Abstract

Glycerol was applied as the dissolution medium for  $\alpha$ ,  $\beta$ - and  $\gamma$ -cyclodextrins and its gas–liquid chromatographic performance was compared with that of formamide. Various stationary glycerol-based chiral phases for classical gas–liquid chromatography were examined. The columns containing glycerol appeared relatively stable in comparison with those prepared with formamide. Glycerol-based phases functioned over the temperature ranged 80–100°C for about 400 h without any changes indicating losses of glycerol or activity. Owing to the lower stability of cyclodextrin complexes in glycerol medium relative to those in formamide, and the fact that glycerol-based columns allow operation ca. 40°C higher, many separations which were previously unreported at higher temperatures were achieved. The model compounds tested were (+/-)- $\alpha$ -pinene, *cis/trans*-decalin, *cis/trans*-anethole, *cis-trans*-isofafrol, *cis-trans*-isoeugenol, (+/-)-camphor, (+/-)-fenchone, (+/-)-isomenthone, (+/-)-isopinocampheol, (+/-)-borneol and (+/-)-isoborneol.

## 1. Introduction

Cyclodextrins (CDs) are known to form stereoselective inclusion complexes with a variety of substances of either an acidic, basic or neutral nature [1]. This property has been used to advantage in gas chromatography, especially during recent years as they have appeared on the market as commercial products. To date hundreds of publications, reviews [2,3] and a monograph [4] have appeared demonstrating their utility in many fields of fundamental and applied research.

For a long time it was generally believed that

CDs form inclusion complexes only in pure aqueous solutions [5,6]. For that reason, many attempts to modify gas chromatographic systems by free cyclodextrins for analytical purposes failed, mainly because the partition gas chromatographic mode (gas–liquid chromatography) remained unachievable.

In the early 1980s we obtained a satisfactory gas–liquid chromatographic system by successful application of a formamide medium with dissolved  $\beta$ -cyclodextrin[7],  $\gamma$ -cyclodextrin and  $\alpha$ -cyclodextrin[8], the last solution after addition of some auxiliary compound ( $\text{LiNO}_3$ ) [9].

It appeared that  $\beta$ -CD permits highly selective separations of structural and geometrical isomers whereas  $\alpha$ -CD is especially useful for the chiral

\* Corresponding author.

recognition of terpenic compounds (see Ref. [6] and references cited therein). However, owing to the physical properties of formamide, i.e. its very polar nature and relatively low boiling point, the area of applications of this method mainly involved lower hydrocarbons, i.e., volatile hydrophobic compounds.

It has become clear that, despite the remarkably high separation factors achieved with packed columns with CDs dissolved in formamide stationary phase, the efficiency of packed columns is poor. Some other limitations should also be mentioned, primarily the short lifetime of the columns and the fact that the method could not be adapted for work using capillary columns. Further, the analysis of higher molecular mass hydrocarbons or more polar compounds, which are more easily dissolved in formamide medium, requires another matrix solvent of higher boiling point and lower polarity. We have found that such requirements, to a limited extent at least, are met by glycerol, which has a boiling point of 290°C and a dielectric constant of 42.98 in comparison with the 210°C and 109.5, respectively, for formamide.

This paper presents our first results obtained using packed-column systems with glycerol in place of formamide as the CD-dissolving stationary phase. Finally, it is noted that improved analysis performance was achieved by König and

co-workers [10,11] and subsequently by Armstrong et al. [12] by the introduction CD derivatives, which are liquid or waxy at relatively low temperatures, as the stationary phases in capillary columns. CD derivatives used in capillary GC are characterized by a relatively poorer enantioselectivity but a higher efficiency of the columns than obtained with packed CD columns. Both capillary and packed approaches are still undergoing refinement and development. An additional alternative, approached by Schurig and co-workers [13,14] uses high-melting cyclodextrin derivatives dissolved or suspended in polysiloxane stationary phases, while Smolkova-Keulemansova et al. [5] adapted formamide modified with  $\beta$ -cyclodextrin to micropacked columns.

## 2. Experimental

### 2.1. Chemicals

$\alpha$ -,  $\beta$ - and  $\gamma$ -cyclodextrins were supplied by Chinoin (Budapest, Hungary). Chromosorb W NAW (0.18–0.25 mm) for GC was a product of Johns-Manville (Litho, USA). All other substances were of analytical-reagent grade and were used without further purification.

Table 1  
Column characteristics

Column code	Cyclodextrin	Concentration of CD in stationary phase (m) <sup>a</sup>	Stationary phase
M	–	0.000	Glycerol
A1	$\alpha$ -CD	0.041	Glycerol
A2	$\alpha$ -CD	0.082	Glycerol
A3	$\alpha$ -CD	0.163	Glycerol
A4	$\alpha$ -CD	0.163	Formamide
B1	$\beta$ -CD	0.070	Glycerol
B2	$\beta$ -CD	0.175	Glycerol
B3	$\beta$ -CD	0.175	Formamide
G1	$\gamma$ -CD	0.082	Glycerol
G2	$\gamma$ -CD	0.184	Glycerol

<sup>a</sup> m = Molal.



## 2.2. Apparatus and procedures

Chromatographic studies were performed using a Hewlett-Packard (Waldbronn, Germany) Model 5890 series II gas chromatograph equipped with dual flame ionization detectors. The peak areas and retention times were measured by means of a Hewlett-Packard Model 3396 series II integrator.

## 2.3. Columns

Glass columns with dimensions 2 m × 4 mm I.D. (2 m × 2 mm I.D. in the case of a semi-micropacked column) were filled with Chromosorb W NAW, which was coated with either  $\alpha$ -,  $\beta$ -, or  $\gamma$ -CD dissolved in either glycerol or formamide as shown in Table 1.

## 2.4. Procedures

The stabilities of CD complexes were compared using the following simplified equations [6,7]:

$$t'_{R(\text{CD,Gly})} = t'_{R(\text{Gly})}(1 + K_G[\text{CD}]) \quad (1)$$

where  $t'_{R(\text{CD,Gly})}$  and  $t'_{R(\text{Gly})}$  are the adjusted retention times of a solute on the column containing a given CD in glycerol and of the solute on the control column containing glycerol alone, respectively,  $K_G(\text{m}^{-1})$  is the stability constant of the complex and  $[\text{CD}]$  is the molal concentration of a given CD in glycerol:

$$K_G = \frac{[\text{G} \cdot \text{CD}]}{[\text{G}][\text{CD}]} \quad (2)$$

Thus Eq. 1 is true only if a CD complex of 1:1 stoichiometry is formed, and under comparable conditions when the only varying parameter is the CD concentration. For this reason, a constant inlet pressure ( $2.75 \pm 0.05$  atm) and helium flow-rate ( $40 \pm 0.5$  ml/min) were carefully maintained. Under these conditions, it was possible to compare the stability constants of various CD · G complexes although their exact values could not be determined [16,17]. More general equations

taking into account complexes of 1:1 and 1:2 stoichiometry are being formulated.

## 3. Results and discussion

The main topic of this study was to expand the area of application of cyclodextrins in gas-liquid chromatography by using glycerol instead of formamide as the dissolution medium. Gas-liquid chromatography is characterized by high reversibility and a large range of linear isotherms that allows recognition of the regio- and stereoselectivity imparted to the liquid stationary phase by complexation with CDs. However, the use of this approach requires the influence of the solvent matrix-medium to first be considered.

Examination of Eq. 1 leads to the conclusions that the dissolution medium plays a predominant role. In fact, it dictates the initial parameters of the system under investigation, and subsequently influences the inclusion processes between the CD and analyte molecules.

### 3.1. Comparison of formamide and glycerol behaviour

#### Solubility

The physical properties of glycerol differ substantially from those of formamide. Their polarities and boiling points were given above. The more limited working temperature range possible with formamide versus glycerol was also discussed in the Introduction. The relative solubility of glycerol and formamide will be considered next.

In a preliminary study, we found that various cyclodextrin species exhibit differing solubility in the solvents considered in the study, formamide, glycerol and water, namely  $\alpha$ -CD is relatively soluble in water but is almost insoluble in either formamide or glycerol,  $\beta$ -CD is very soluble in formamide (like sugar in water), whereas its solubility in either water or glycerol is very limited, and  $\gamma$ -CD exhibits moderate solubility in all three solvents. Hence to prepare  $\beta$ -CD-glycerol,  $\alpha$ -CD-formamide and  $\alpha$ -CD-glycerol columns the use of some solubilizers was necessary.

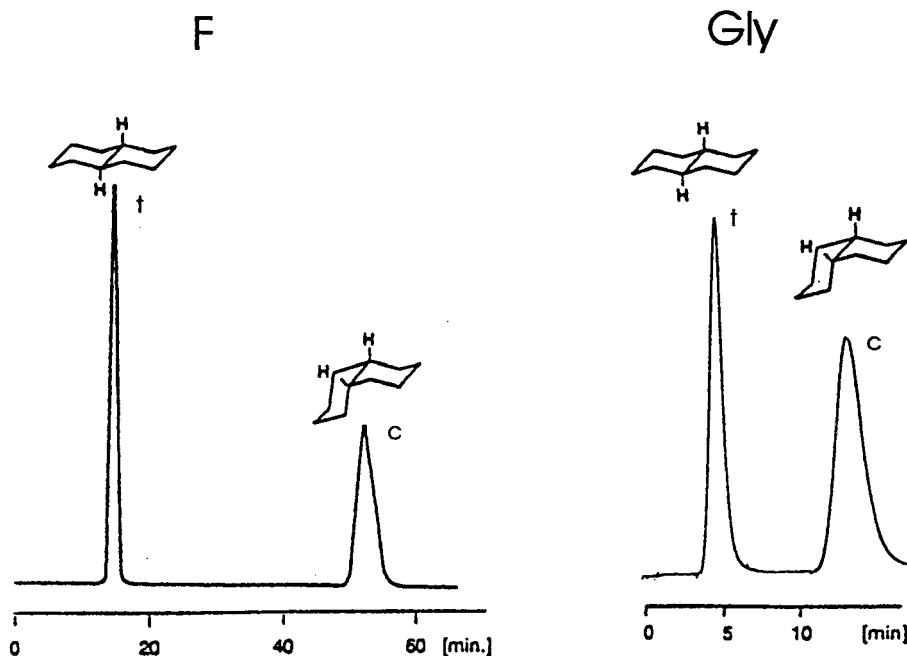


Fig. 1. Separations of decalins obtained on formamide B3 (F) and glycerol B2 (Gly) columns modified with  $\beta$ -CD. Temperature, 70°C; flow-rate, 60 ml/min.

The best appeared to be  $\text{H}_2\text{O}$  and  $\text{LiNO}_3$  for  $\alpha$ -CD and urea for  $\beta$ -CD. The respective roles of  $\text{H}_2\text{O}$ ,  $\text{LiNO}_3$  and urea have not yet been

clarified, but may involve structural changes in  $\alpha$ - and  $\beta$ -CD molecules, or may involve simple solubilization processes. In the  $\alpha$ -CD-form-

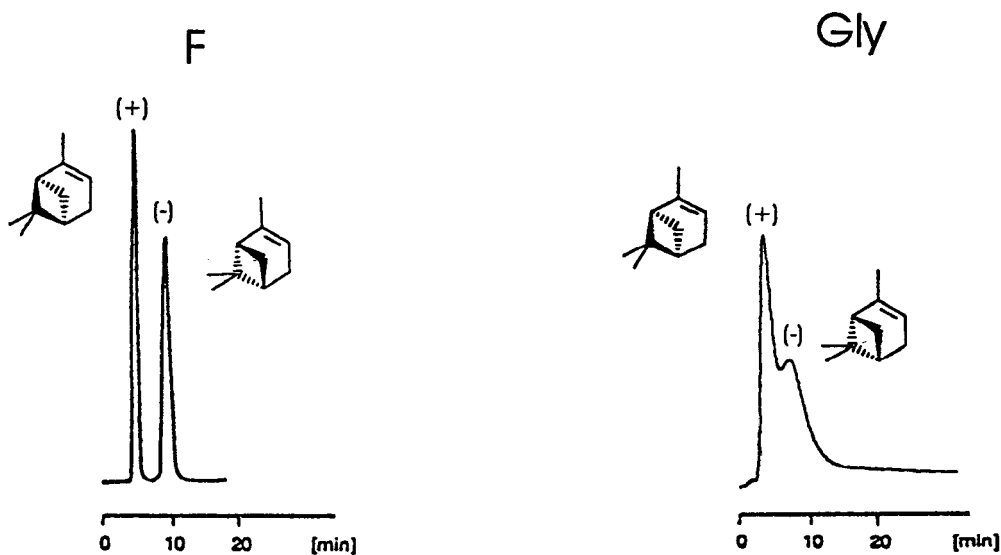


Fig. 2. Separations of (+/-)- $\alpha$ -pinenes obtained on formamide A4 (F) and glycerol A3 (Gly) columns modified with  $\alpha$ -CD. Temperature, 40°C; flow-rate, 40 ml/min.

amide system we used  $\text{LiNO}_3$  for stabilization the column, whereas Lindström et al. [18] successfully applied a wetting procedure of the carrier gas.

#### Durability

We found that the columns prepared with glycerol are relatively durable in comparison with those prepared with formamide. The glycerol columns were operated at temperature from 80 to 100°C for about 400 h without any changes indicating losses in either glycerol or column activity.

#### Chromatographic properties of $\beta$ - and $\alpha$ -CD dissolved in glycerol and formamide media

The model compounds examined were *cis-trans*-decalins and (+/-)- $\alpha$ -pinenes. They were chosen for this investigation since it has been found previously that  $\beta$ -CD is a very efficient selector for decalins, and  $\alpha$ -CD is known to be remarkably enantioselective towards (+/-)- $\alpha$ -pinenes. These two compounds allow the experiments to be carried out under very similar conditions. In practice, a 70–75°C temperature range is the upper limit possible for formamide, and at the same time it is very close to the lower limit for the convenient use of glycerol.

As can be seen from Fig. 1, which shows separations of decalins, using  $\beta$ -CD the selectivity factors  $\alpha_{(cis/trans)}$  are very similar on both glycerol and formamide modified with  $\beta$ -CD, i.e., ca. 3. In contrast the retention data (adjusted retention times,  $t'$ ) differ substantially, indicating that the stabilities of  $\beta$ -CD complexes with decalins in glycerol are about three times lower than those in formamide. This behaviour agrees with theory, since the expected stability of the complexes should increase with increasing polarity of the matrix-solvent.

The results for  $\alpha$ -pinenes are shown in Fig. 2; it seems that the stabilities of  $\alpha$ -CD complexes with  $\alpha$ -pinenes at temperatures from 75 to 80°C are too low to give evidence of the true enantioselectivity of the column. For this reason the separations shown in Fig. 2 were performed at a lower temperature, 40°C, which is far below that recommended for glycerol media. Nevertheless,

the same tendency has been confirmed, the separation factors by  $\alpha_{(-/+)}$  are very similar and the retention times of pinenes on glycerol modified with  $\alpha$ -CD are shorter than those observed on formamide. The low-temperature experiment demonstrates the low efficiency of glycerol columns when working at 40°C.

#### 3.2. Examples of resolution

##### Geometrical isomers

The examples given below related to various separations achievable only on the glycerol column.

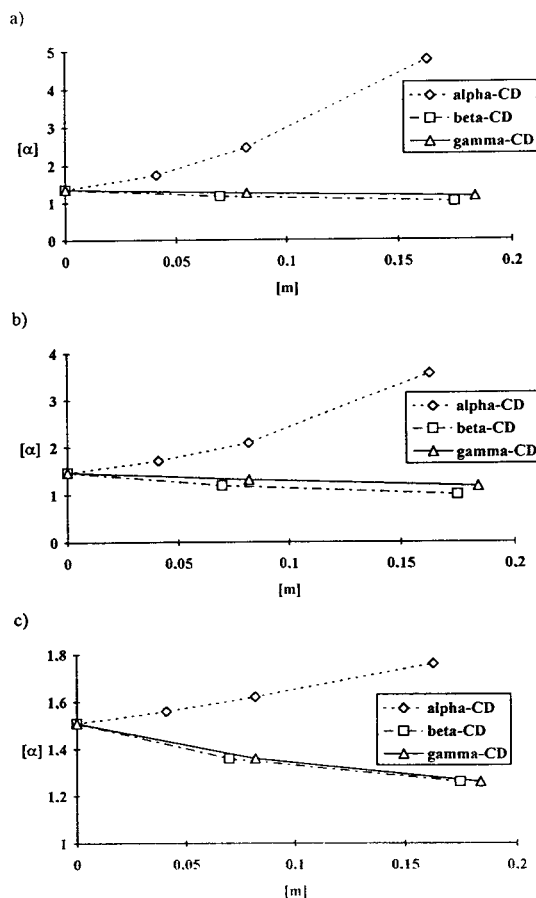


Fig. 3. Separation factor  $\alpha$  for (a) *cis-trans*-anethole, (b) isosafrol and (c) isoeugenol versus  $\alpha$ -,  $\beta$ - and  $\gamma$ -CD concentration. Temperature (a) and (b) 80 and (c) 100°C; flow-rate, 40 ml/min.

Fig. 3 presents the separation factor  $\alpha$  for *cis-trans*-anethole, -isosafrinol and -isoeugenol versus  $\alpha$ ,  $\beta$ - and  $\gamma$ -CD concentration. It can be seen that  $\alpha$ -CD exhibits a remarkable stereoselectivity towards *trans-cis* positions. Much more stable complexes are possible with *trans* isomers. The direction of this stereoselectivity follows that of the starting material, i.e., for glycerol ( $\alpha$ -*trans/cis*  $\approx 1.5$ ).

Using  $\alpha$ -CD modifier, a relatively high stereoselectivity ( $\alpha \approx 4$ ) could be reached for anethole and isosafrinol.  $\beta$ -CD and  $\gamma$ -CD behave in a reverse manner; they exhibit moderate stereoselectivity and form more stable complexes with a *cis* configuration. In effect, the overall stereoselectivity decreases as the  $\beta$ - or  $\gamma$ -CD concentration increases and under the same conditions one process is nullified by the other ( $\alpha \approx 1.00$ ).

The similar observed complexation of *trans-cis* isomers by CDs (especially by  $\alpha$ -CD) may suggest that the insertion of a  $-\text{CH}=\text{CHCH}_3$  group in the CD cavity is a major factor in the stereospecific recognition of these geometrical isomers, almost independently of the other dissimilar molecular features between these three compounds. It is noted that the relationship between the separation coefficient and the  $\alpha$ -CD

concentration at 80°C is distinctly non-linear. This may indicate that at higher  $\alpha$ -CD concentration, in addition to complexes of 1:1 stoichiometry, also 1:2 complexes richer in  $\alpha$ -CD are formed.

Isoeugenol was seen to behave differently, maybe because the temperatures of the investigations were higher (by about 20°C) than those applied to anethole and isosafrinol. The temperatures were chosen in order to reach reasonable elution times of isoeugenol from the glycerol-containing columns. Nevertheless, it is seen that the tendencies seen in Fig. 3 are similar to those observed for both anethole and isosafrinol.

#### Enantiomers

Fig. 4 shows the separation obtained for enantiomers of selected terpene ketones, (+/-)-camphor, (+/-)-fenchone and (+/-)-isomenthone, which were obtained on glycerol columns modified with  $\alpha$ -CD.

Fig. 5 shows the separations of enantiomers of selected terpene alcohols, (+/-)-isopinocampheol, (+/-)-borneol and (+/-)-isoborneol, obtained on glycerol columns modified with  $\alpha$ -CD.

As mentioned earlier (see Introduction), there are great difficulties in adapting formamide

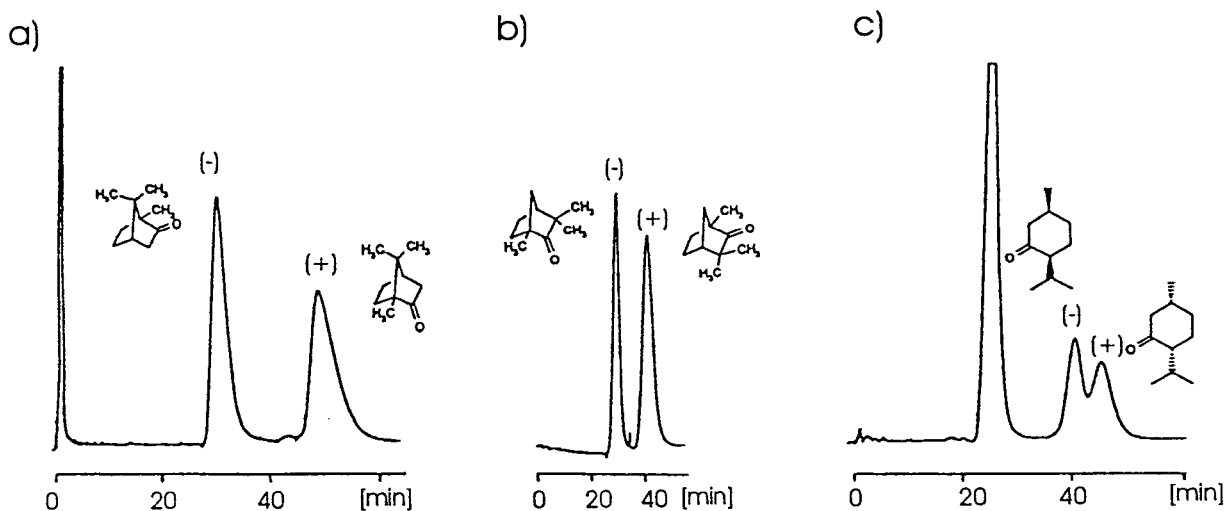


Fig. 4. Separations of enantiomers of terpene ketones: (a) (+/-)-camphor, column A1, 90°C; (b) (+/-)-fenchone, column A1, 60°C; (c) (+/-)-isomenthone, column A2, 60°C. Flow-rate, 40 ml/min.

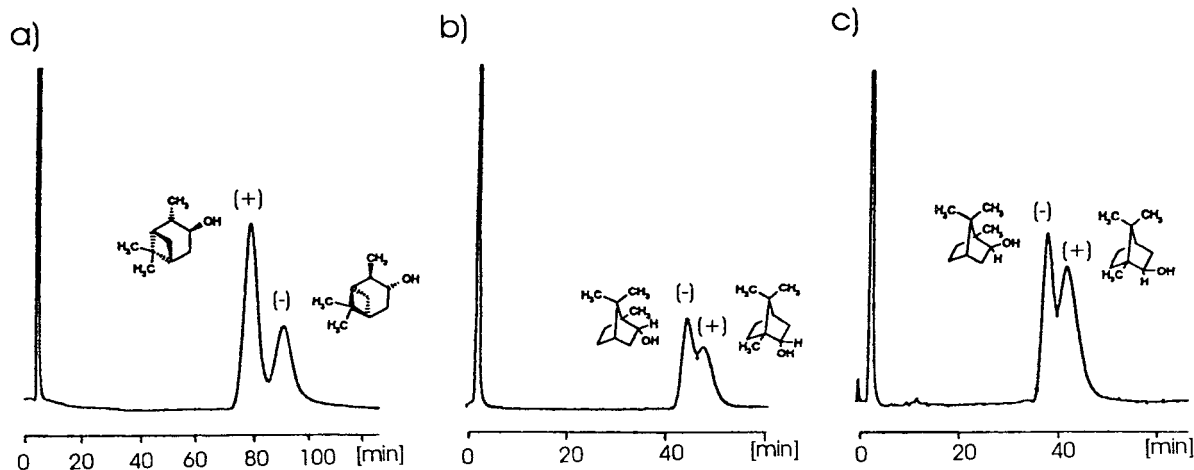


Fig. 5. Separations of enantiomers of terpene alcohols: (a) (+/-)-isopinocampheol, column A3, 80°C; (b) (+/-)-borneol, column A1, 90°C; (c) (+/-)-isoborneol, column A1, 90°C. Flow-rate, 40 ml/min.

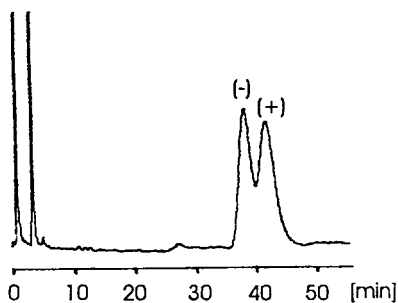


Fig. 6. Separation of (+/-)-isoborneol obtained on a semi-micropacked A1 column. Temperature, 90°C; flow-rate, 15 ml/min.

phases modified by cyclodextrins, especially  $\alpha$ -CD, to work in capillary column techniques, with micropacked columns and semi-micropacked (2 mm I.D.) columns. Our latest results for a preliminary investigation, shown in Fig. 6, suggest that the problem with capillary columns also should find some progress through application of glycerol (compare with Fig. 5c).

## References

- [1] J. Szejtli, *Cyclodextrins and Their Inclusion Complexes*, Akadémiai Kiadó, Budapest, 1982.
- [2] V. Schurig and H.P. Novotny, *Angew. Chem., Int. Ed. Engl.*, 29 (1990) 939.
- [3] S. Li and W.C. Purdy, *Chem. Rev.*, 92 (1992) 1457.
- [4] W.A. König, *Gas Chromatographic Separations with Modified Cyclodextrins*, Hüthig, Heidelberg, 1992.
- [5] J.L. Lach and T.-F. Chin, *J. Pharm. Sci.*, 53 (1964) 69.
- [6] D.W. Griffiths and M.L. Bender, *Adv. Catal.*, 23 (1973) 209.
- [7] D. Sybilska and T. Kościelski, *J. Chromatogr.*, 261 (1989) 957.
- [8] T. Kościelski, D. Sybilska and J. Jurczak, *J. Chromatogr.*, 280 (1983) 131.
- [9] D. Sybilska and J. Jurczak, *Carbohydr. Res.*, 192 (1989) 243.
- [10] W.A. König, S. Lutz and G. Wenz, *Angew. Chem., Intn. Ed. Engl.*, 27 (1988) 979.
- [11] W.A. König, R. Krebber, P. Evers and G. Bruhn, *J. High Resolut. Chromatogr.*, 13 (1990) 328.
- [12] D.W. Armstrong, W. Li and J. Pitha, *Anal. Chem.*, 62 (1990) 217.
- [13] H.P. Novotny, D. Schmalzing, D. Wistuba and V. Schurig, *J. High Resolut. Chromatogr.*, 12 (1989) 383.
- [14] V. Schurig and H.P. Novotny, *J. Chromatogr.*, 441 (1988) 156.
- [15] E. Smolkova-Keulemansova, S. Pokorna, L. Feltl and K. Tesarik, *J. High Resolut. Chromatogr. Chromatogr. Commun.*, 11 (1988) 67.
- [16] J.H. Purnell, in A.B. Littlewood (Editor), *Gas Chromatography*, Institute of Petroleum, London, 1966, p. 3.
- [17] C. Econ, C. Pommier and G. Guiochon, *J. Phys. Chem.*, 75 (1971) 2632.
- [18] M. Lindström, T. Norin and J. Roeraade, *J. Chromatogr.*, 513 (1990) 315.





ELSEVIER

Journal of Chromatography A, 715 (1995) 317–324

JOURNAL OF  
CHROMATOGRAPHY A

# Gas chromatographic–mass spectrometric characterization of some fatty acids from white and interior spruce<sup>☆</sup>

Danielle-Julie Carrier, James E. Cunningham, Lawrence R. Hogge,  
David C. Taylor, David I. Dunstan\*

Plant Biotechnology Institute, National Research Council of Canada, 110 Gymnasium Place, Saskatoon, Sask. S7N 0W9,  
Canada

First received 28 March 1995; revised manuscript received 19 May 1995; accepted 19 May 1995

## Abstract

The objective of this work was to determine the fatty acid composition of white and interior spruce seeds. Fatty acid methyl ester derivatives obtained from the seed oils were analyzed by gas chromatography. Elution times for some of the spruce fatty acid methyl ester derivatives did not correspond to those of available standards. Diethylamide derivatives were prepared and analyzed by gas chromatography–mass spectrometry. The electron-impact mass spectral fragmentation patterns of the fatty acids of interest indicated *cis*-11-18:1, *cis*-5,*cis*-9-18:2 and *cis*-5,*cis*-9,*cis*-12-18:3.

## 1. Introduction

Interior spruce (*Picea glauca engelmannii* complex) is a natural hybrid between white (*Picea glauca*) and Engelmann (*Picea engelmannii*) spruces that occurs where their ranges overlap. It is an economically important species in British Columbia where 80 million interior spruce seedlings are planted annually. Our goal is to facilitate the production of genetically improved spruce through the development of a clonal propagation system by *in vitro* formation of spruce embryos. Synthetic seed production, involving an artificial endosperm (i.e. storage

reserve for the germinating seedling), is a component of this goal. To develop an artificial endosperm, a better understanding of the nutritional requirements of germinating spruce seedlings would provide a useful basis for our investigation.

Spruce seeds contain approximately 30% lipid by weight [1]. This high lipid concentration suggests that lipid metabolism is, as in other gymnosperms [2], important in the supply of energy during germination before the seedling gains autotrophy. As part of our study, we investigated the lipid content and composition of interior spruce seeds. To our knowledge, no study on the fatty acid content of seeds of this species has been reported. In preliminary gas chromatographic (GC) investigations with trans-methylated products from interior spruce oils,

\* Corresponding author.

\* National Research Council of Canada Publication No. 38920.

the second most abundant fatty acid methyl ester (FAME) within the profile was difficult to identify by matching with standards. This peak eluted between *cis-9,cis-12-18:2* and *cis-9,cis-12,cis-15-18:3* FAME derivatives. A preliminary gas chromatographic–mass spectrometric (GC–MS) characterization indicated that the molecular ion of this peak corresponded to that of an 18:3 FAME. In a previous study on the fatty acids contained in the closely related white spruce [1], the second most abundant component was reported to be 5,9-18:2. To clarify and advance the record of spruce seed fatty acid composition, we undertook the identification of the major fatty acids of white and interior spruce seeds.

Many methods are available for characterizing unsaturated aliphatic compounds by GC–MS. Formation of vicinal diols followed by the formation of either acetonides, boronates, as well as silyl and methyl ethers are common procedures for double-bond elucidation [3]. Although the resulting mass spectral data are informative, the use of osmium tetroxide in the reaction is potentially hazardous. The position of double bonds can also be determined by epoxidation with *m*-chloroperbenzoic acid followed by hydrogenation [3]. Although a successful method, the two-step derivatization procedure is time-consuming. The incorporation of a charge-stabilizing group, such as an amide, at the carboxyl group is another useful method in locating or determining the position of double bonds [4]. The location of the double bond can be deduced from the fragmentation patterns of the mass spectra. Pyrrolidine is generally recommended as the amine of choice for mass spectrometric elucidation of fatty acid structure [3]. However, when the fatty acid in question contains no hydroxy, epoxy or other charge retaining groups, a diethylamine derivatization can be utilized [4]. The advantage of this method, over others, is the ease of derivatization and the simplicity of the resulting mass spectrum. This method was successfully used to determine the double-bond positions of unsaturated fatty acids of Norway spruce (*Picea abies*) [5].

We present here the results of our investigation into the identity of the major fatty acids contained in lipid extracts of white and interior

seeds. The lipid extracts were prepared, derivatized into FAMES and analyzed by GC. Further characterization of the fatty acids involved derivatization with diethylamine and GC–MS analysis.

## 2. Experimental

### 2.1. Chemicals

All chemicals were reagent grade. Methanolic HCl (3 M) was purchased from Supelco Canada (Oakville, Ont., Canada). Diethylamine and glacial acetic acid were obtained from Aldrich (Milwaukee, WI, USA) and Fisher Scientific (Nepean, Ont., Canada), respectively. *Picea glauca* (white spruce) and *Picea glauca engelmannii* complex (interior spruce) seeds were obtained from Prairie Farm Rehabilitation Administration (Indian Head, Sask., Canada) and British Columbia Research (Vancouver, BC, Canada), respectively. Heptadecanoic acid (C17:0) and other FAME standards were purchased from Nu-Chek-Prep (Elysian, MN, USA).

### 2.2. Methods

#### Initial methyl ester study

Interior spruce seeds were extracted and methylated according to published procedures [6–8]. The fatty acid 17:0 was added as an internal standard. FAMES were analyzed as described previously [8].

#### Gas chromatography–mass spectrometry

All GC–MS analyses were performed using a Fisons 8000 gas chromatograph (Fisons Instruments, Manchester, UK) which was fitted with a 60 m × 0.32 mm I.D. DB-23 fused-silica column (J&W Scientific, Folsom, CA, USA) and interfaced to a Fisons Tri 2000 quadrupole mass spectrometer. All samples were injected using the split injection mode. The initial column temperature was 70°C and was ramped at a rate of 20°C per min to 180°C, followed by a programmed increase of 4°C per min to 240°C. The GC interface and source were maintained at



250°C. Repetitive scans were taken every 1.1 s in the mass range of 50 to 510. The electron energy was 70 eV.

#### *Total lipid extraction and diethylamide derivatization*

Isopropanol (1.5 ml) was added to 100 mg of seed and the mixture was homogenized with an Ultra-Turrax (Janke & Kunkel, Germany) for 3 min at maximum speed. The mixture was capped and plunged into a boiling water bath for 5 min. After cooling, 0.75 ml CH<sub>2</sub>Cl<sub>2</sub> was added and the mixture was incubated for 30 min at room temperature with occasional vortexing. Following incubation, 1 ml water and 2 ml CH<sub>2</sub>Cl<sub>2</sub> were added. The mixture was vortexed and centrifuged at 830 g. The organic phase was retained and the aqueous phase re-extracted twice with 2 ml CH<sub>2</sub>Cl<sub>2</sub>. The organic phases were combined and the solvent was evaporated to yield the total lipid extract. To obtain diethylamide derivatives, the protocol devised in Ref. [5] was essentially followed. The total lipid extract was transferred to a 1-ml Pierce Reacti Vial (Rockford, IL, USA), to which 0.8 ml diethylamine and 0.1 ml of glacial acetic acid were added. The vial was purged with N<sub>2</sub>, tightly sealed and placed in a Pierce Reacti-Therm (Rockford, IL, USA) at 105°C for 75 min. Afterwards, the mixture was cooled and transferred to a screw-cap glass test tube. The diethylamine was evaporated under a stream of N<sub>2</sub>. To this tube, 1 ml water and 2 ml CHCl<sub>3</sub> were added, vortexed and centrifuged at 830 g. The organic phase, containing the diethylamide derivatives, was retrieved and evaporated to dryness.

### 3. Results and discussion

#### *3.1. Methyl ester derivatization*

The direct methylation method [6] yielded 150 µg of total lipid fatty acids per mg fresh weight of seed. This method does not always give quantitative recovery of fatty acids from all plant tissues. It works well for leaf tissue, as used originally [6], but not necessarily for other tissues, such as seeds of interior spruce. The total

lipid extraction procedures described by Hara and Radin [7] and Holbrook et al. [8], followed by methylation and GC analysis, yielded amounts in the range of 300 µg of total lipid fatty acids per mg fresh weight of seed. All of the following extractions and transmethyations used the methods described by Holbrook et al. [8].

The results of GC–MS analysis of the total lipid extract of interior spruce seeds are shown in Fig. 1. Peaks 1, 2, 3 and 6 were identified as 16:0, 18:0, 9-18:1 and 9,12-18:2 FAMES, respectively, by comparison to the retention times and mass spectral data of standards. Under the current chromatographic conditions, *trans*-9-18:1 and *trans*-9,*trans*-12-18:2 FAMES eluted about 0.5 min earlier than the corresponding *cis* isomers: *cis*-9-18:1 and *cis*-9,*cis*-12-18:2 FAMES. By combining this with the fact that lipids of plant origin are typically of *cis* configuration, it was inferred that the FAMES detected in this work were also of *cis* configuration. Hence, peaks 3 and 6 of Fig. 1. were identified as *cis*-9-18:1 and *cis*-9,*cis*-12-18:2 FAMES.

Mass spectral data from the second largest component in Fig. 1 (labelled number 7) indicated a molecular ion of 292 which corresponds to an 18:3 FAME. However, the retention time did not correspond to any available standards. Similarly, component number 5 showed a molecular ion of 294, indicating an 18:2 FAME of unknown double-bond positional configuration.

The results of GC–MS analysis of the total lipid extract of white spruce seeds are shown in Fig. 2. Similarity between the FAME profiles of the two species was observed. The molecular ions of peaks D and E were 296 and 294, which indicated 18:1 and 18:2 methyl esters, respectively. Elucidation of the structures of the compounds corresponding to peaks 5 and 7 of Fig. 1 and to peaks D and E of Fig. 2 is presented below.

#### *3.2. Diethylamide derivatization*

Diethylamide derivatization provides the analyte with a charge stabilizing group which retards rearrangement of the molecular ion before fragmentation occurs [3]. This method was first

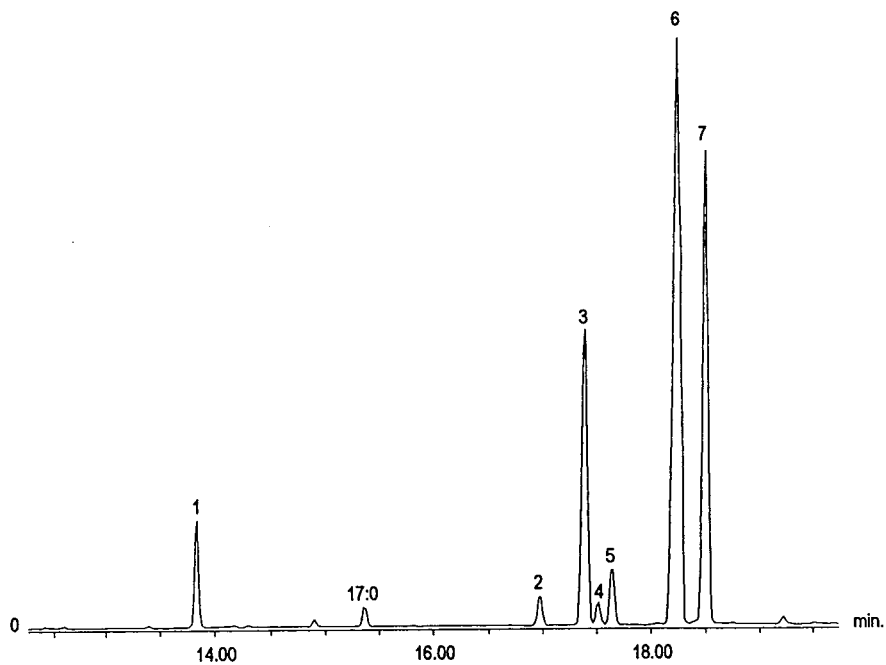


Fig. 1. Mass chromatogram of FAMES obtained from interior spruce oil extract.

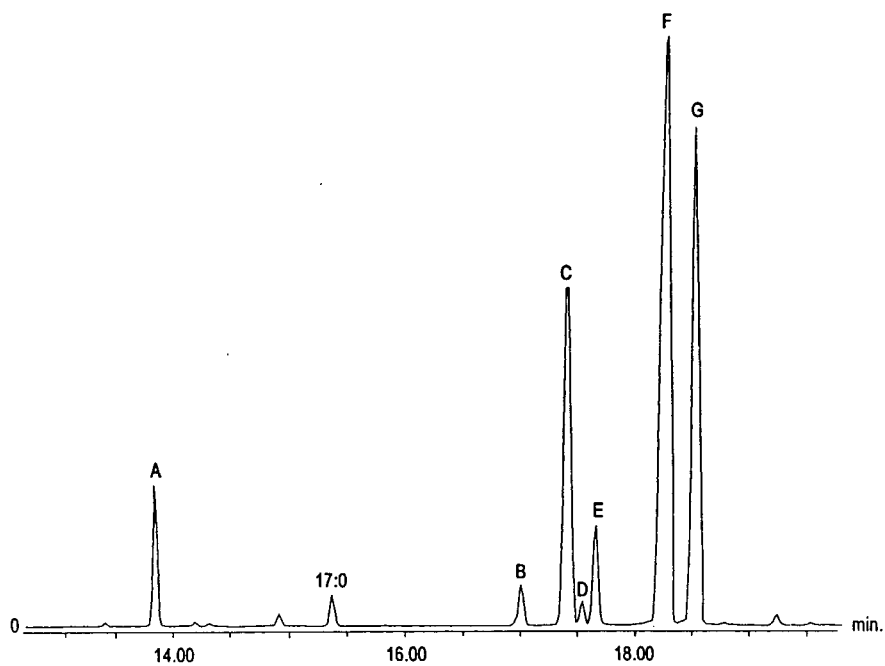


Fig. 2. Mass chromatogram of FAMES obtained from white spruce oil extract.

assessed with a *cis-9,cis-12,cis-15-18:3* ( $\alpha$ -linolenic acid) as a reference compound. The resulting mass spectrum was interpreted using the rules presented in Ref. [5], where saturated bonds are represented by fragments separated by 14 mass units. Fragments separated by 12 mass units between carbons  $n$  and  $n + 1$  indicate the presence of a double bond between carbons  $n + 1$  and  $n + 2$ . The mass spectrum of the diethylamide derivative of *cis-9,cis-12,cis-15-18:3* was readily interpreted using these rules. This mass spectrum was similar to that reported in Ref. [5].

The electron-impact mass spectral fragmentation patterns of diethylamide derivatives of the compounds, corresponding to peaks 6 and 7 of Fig. 1, are shown in Figs. 3A and B, respectively. The mass spectrum shown in Fig. 3A displays a molecular ion of 335 mass units, corresponding to a diethylamide derivative of 18:2. Differences of 12 mass units between fragments  $m/z$  198–210 and  $m/z$  238–250, ascribed double-bond locations to carbons 9–10 and 12–13, respectively, identifying the compound as *cis-9,cis-12-18:2*, as reported in Ref. [5]. The mass spectrum of the diethylamide derivative of the second most abundant fatty acid is shown in Fig. 3B. This compound appeared to have a molecular ion of 333 mass units, indicating a diethylamide derivative of 18:3. Differences of 12 mass units were observed between the fragment ions at  $m/z$  142–154, 196–208 and 236–248, indicating double bonds in the 5, 9 and 12 positions. Taking into consideration that, in spruce, 9,12-18:2 was of *cis* configuration, the compound was identified as *cis-5,cis-9,cis-12-18:3*.

The electron-impact mass spectral fragmentation pattern of the diethylamide derivative of the compound corresponding to peak 5 of Fig. 1 was not sufficiently intense to assign double-bond locations. However, the mass spectral fragmentation pattern of the white spruce diethylamide derivative corresponding to peak E of Fig. 2 was sufficiently intense that double-bond locations could be identified. Results are presented in Fig. 4A, where a molecular ion of 335 mass units, indicating a diethylamide derivative of 18:2, was observed. The fragmentation pattern indicated double bonds in the 5 and 9

position, identifying the compound as *cis-5,cis-9-18:2*. Fig. 4B shows the diethylamide derivative fragment spectrum of the compound, corresponding to peak D of Fig. 2. The molecular ion of 337 mass units corresponded to that of an 18:1 diethylamide derivative. Although less clear, the mass spectrum of this compound showed a 12 mass unit gap between masses 226–238; indicating the double bond to be on carbons 11 and 12. This compound was tentatively identified as *cis-11-18:1*.

In comparing the retention times of FAMES obtained from white spruce to those of interior spruce, it was inferred that peak 5 of Fig. 1 and peak E of Fig. 2 were equivalent (i.e. both are believed to be *cis-5,cis-9-18:2*). Similarly, it was observed that peak D of Fig. 2 and peak 4 shown in Fig. 1 had similar retention times. Hence, they were both tentatively identified as *cis-11-18:1*.

The FAMES corresponding to peaks A, B, C, D, E, F and G of Fig. 2 were identified as 16:0, 18:0, *cis-9-18:1*, *cis-11-18:1*, *cis-5,cis-9-18:2*, *cis-9,cis-12-18:2* and *cis-5,cis-9,cis-12-18:3*. The distribution of these fatty acids, found in white and interior spruce seeds, is shown in Table 1. White and interior spruce seed lipid contents were  $49 \pm 5\%$  and  $41 \pm 1\%$  lipid by fresh weight, respectively.

The spectra of the *cis-5,cis-9-18:2* and *cis-5,cis-9,cis-12-18:3* diethylamide derivatives each have an intense ion at  $m/z$  182 (relative to the other aliphatic chain cleavage ions). The intensity of this ion is likely due to the allylic fragments formed when there are two methylene groups separating the double bonds. The intensity of this ion makes it diagnostically useful in determining this unusual double-bond configuration. This postulation is borne out by examining the spectra of the fatty acid derivatives shown in Figs. 3B and 4A. The spectra shown in Figs. 3A and 4B do not display an intense ion at  $m/z$  182.

The fatty acid *cis-5,cis-9,cis-12-18:3* was detected in *P. abies* [5,9,11] and in *P. engelmannii*, *mariana*, *obovata*, *orientalis* and *sitchensis* [10]. Our results confirm this finding for *P. glauca* and *P. glauca engelmannii* complex. Other workers [1,12] reported the second most abundant fatty acid in *P. glauca* to be *cis-5,cis-9-18:2*. The *P.*

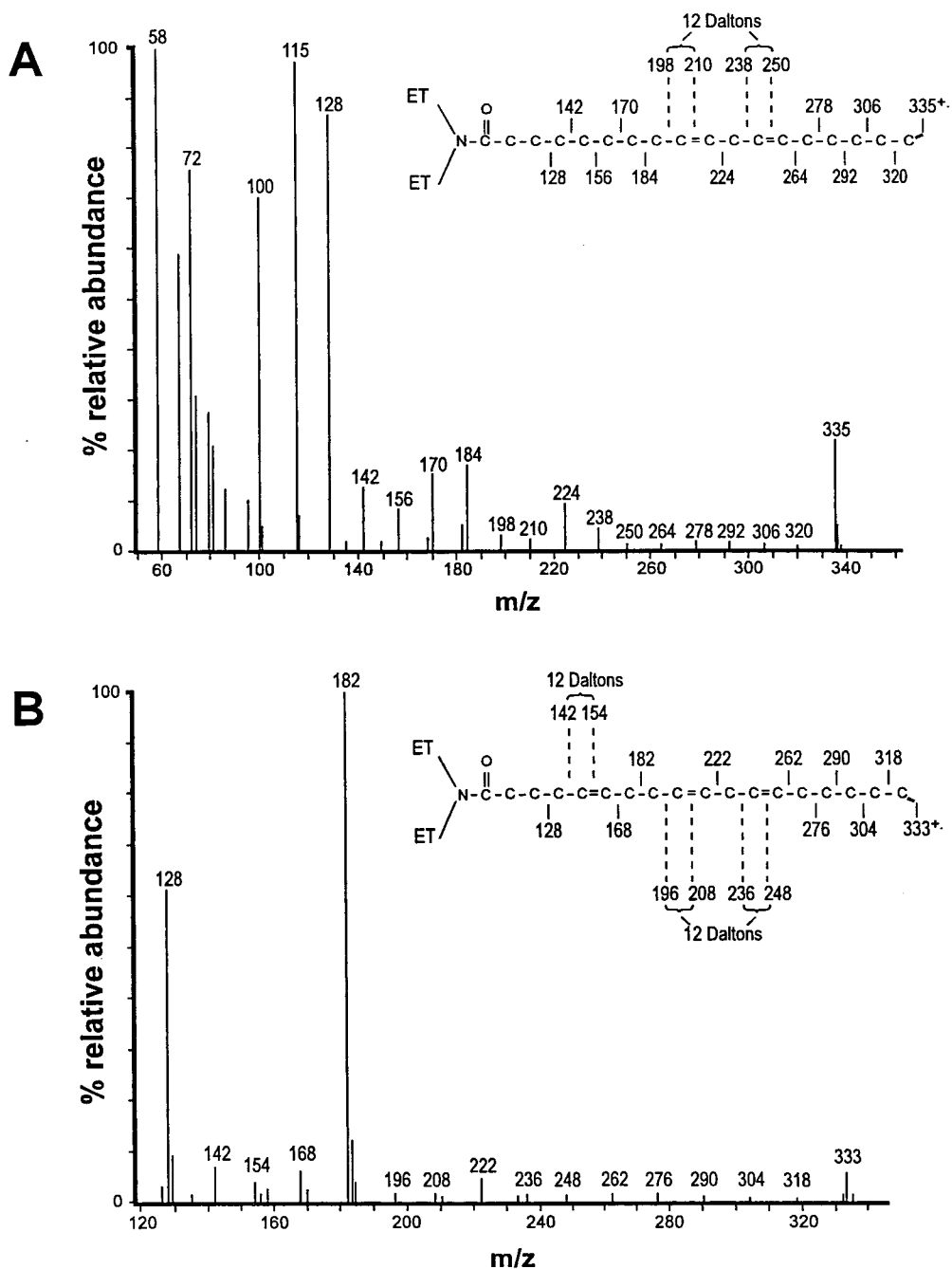


Fig. 3. Mass spectrum of diethylamide derivatives of interior spruce. (A) Mass spectrum of *cis-9,cis-12-18:2*. (B) Mass spectrum of *cis-5,cis-9,cis-12-18:3*. The compounds used to obtain these diethylamide derivatives are identical to the ones used to obtain the FAME derivatives corresponding to peaks 5 and 6, respectively, presented in Fig. 1.

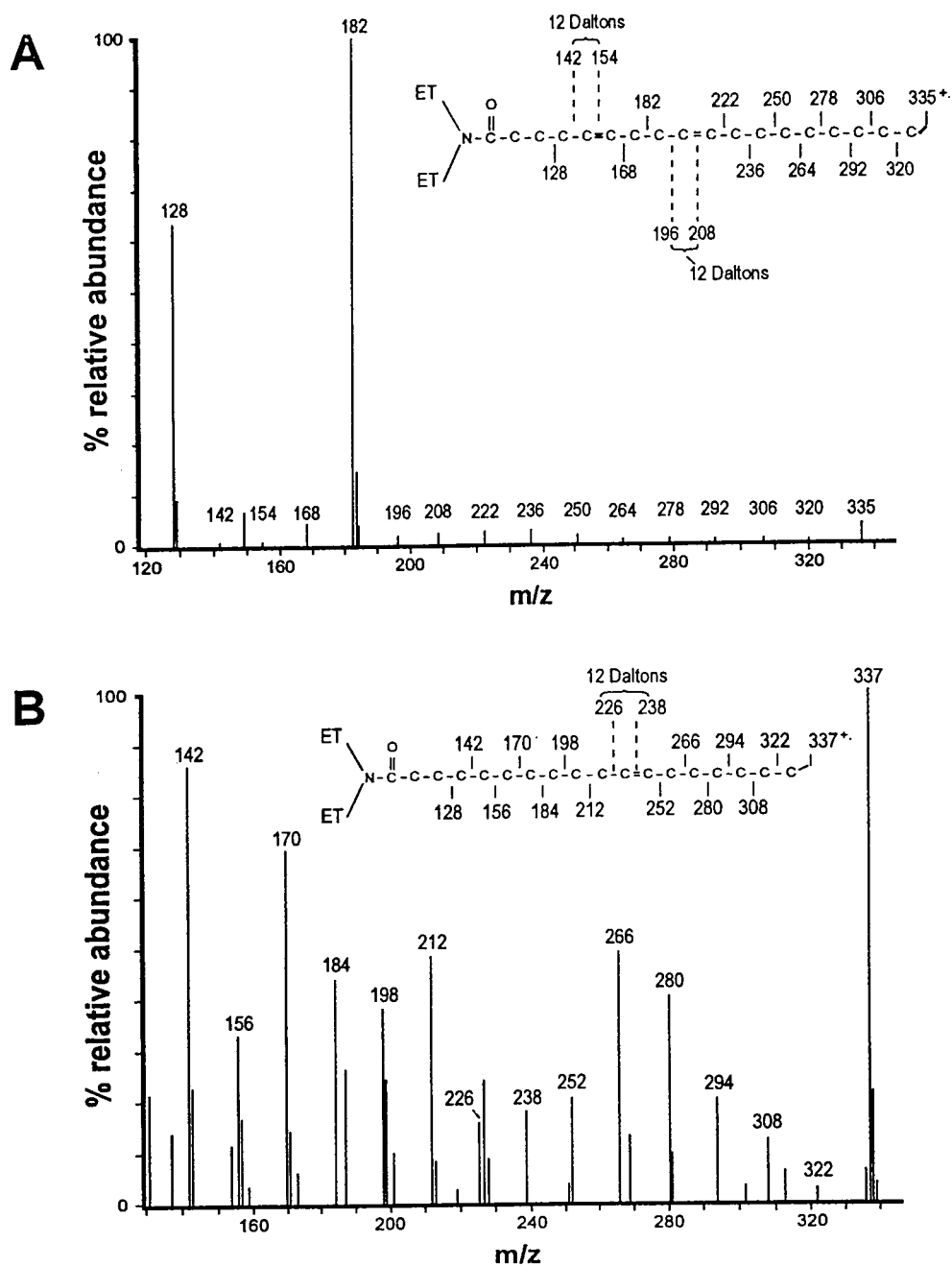


Fig. 4. Mass spectrum of diethylamide derivatives of white spruce. (A) Mass spectrum of *cis-5,cis-9-18:2*. (B) Mass spectrum of *cis-11-18:1*. The compounds used to obtain these diethylamide derivatives are identical to the ones used to obtain the FAME derivatives corresponding to peaks E and D, respectively, presented in Fig. 2.

Table 1

Distribution of 16:0, 18:0, *cis*-9-18:1, *cis*-11-18:1, *cis*-5,*cis*-9-18:2, *cis*-9,*cis*-12-18:2 and *cis*-5,*cis*-9,*cis*-12-18:3 methyl esters in white and interior spruce expressed in  $\mu\text{g}$  per mg of tissue and in percentage of oil content

Seed type	16:0	18:0	9-18:1	11-18:1	5,9-18:2	9,12-18:2	5,9,12-18:3
<i>White spruce</i>							
$\mu\text{g}/\text{mg}$	12 $\pm$ 2	6 $\pm$ 1	74 $\pm$ 13	5 $\pm$ 1	15 $\pm$ 2	209 $\pm$ 33	103 $\pm$ 21
% of oil content	3	2	17	1	4	49	24
<i>Interior spruce</i>							
$\mu\text{g}/\text{mg}$	10 $\pm$ 1	7 $\pm$ 1	74 $\pm$ 11	6 $\pm$ 1	13 $\pm$ 3	196 $\pm$ 23	108 $\pm$ 12
% of oil content	3	2	18	1	3	47	26

*glauca* seeds extracted in our laboratory did contain this fatty acid. However, it was determined to be a minor component of the oil, as shown in Table 1.

### Acknowledgements

We thank British Columbia Research (Vancouver, BC, Canada) and Dan Walker of Prairie Farm Rehabilitation Administration (Indian Head, Sask., Canada) for providing us with interior and white spruce seed, respectively. The authors wish to thank Mike Giblin, Darwin Reed and Douglas Olson for expert technical assistance. This work has been funded by the National Research Council of Canada Agreement, GC103-3-2021, by technology contribution between by the National Research Council of Canada and British Columbia Research.

### References

[1] S.M. Attree, M.K. Pomeroy and L.C. Fowke, *Planta*, 187 (1992) 395.

- [2] T.M. Ching, in T.T. Kozlowski (Editor), *Seed Biology*, Vol. II, Academic Press, New York, 1972, p. 103.
- [3] L. Hogge and J. Millar, in J.C. Giddings et al. (Editors), *Advances in Chromatography*, Vol. 27, Marcel Dekker, New York, 1987, p. 299.
- [4] B.A. Andersson, W.H. Heimermann and R.T. Holman, *Lipids*, 9 (1974) 443.
- [5] R. Nilsson and C. Liljenberg, *Phytochem. Anal.*, 2 (1991) 253.
- [6] J. Browse, P.J. McCourt and C.R. Somerville, *Anal. Biochem.*, 152 (1986) 141.
- [7] A. Hara and N.S. Radin, *Anal. Biochem.*, 90 (1978) 420.
- [8] L.A. Holbrook, J.R. Magus and D.C. Taylor, *Plant Sci.*, 84 (1992) 99.
- [9] R. Ekman, *Phytochemistry*, 19 (1980) 147.
- [10] G.R. Jamieson and E.H. Reid, *Phytochemistry*, 11 (1972) 269.
- [11] M. Olsson, R. Nilsson, P. Norberg, S. von Arnold and C. Liljenberg, *Plant Physiol. Biochem.*, 32 (1994) 225.
- [12] S.M. Attree, M.K. Pomeroy and L.C. Fowke, *Plant Cell Rep.*, 13 (1994) 601.



ELSEVIER

Journal of Chromatography A, 715 (1995) 325–331

JOURNAL OF  
CHROMATOGRAPHY A

## Headspace sampling and gas chromatographic–mass spectrometric determination of amphetamine and methamphetamine in betel

Sheng-Meng Wang<sup>a</sup>, Yong-Chien Ling<sup>a,\*</sup>, Li-Chin Tsai<sup>b</sup>, Yun-Seng Giang<sup>b</sup>

<sup>a</sup>*Department of Chemistry, National Tsing Hua University, Hsinchu 30043, Taiwan*

<sup>b</sup>*Department of Forensic Science, Central Police University, Taoyuan 33334, Taiwan*

First received 2 January 1995; revised manuscript received 23 May 1995; accepted 24 May 1995

### Abstract

A hot headspace sampling (HS) and gas chromatographic–mass spectrometric method (GC–MS) for the determination of amphetamine (AP) and methamphetamine (MA) in betel is described. The method uses potassium carbonate to alkalize the aqueous matrix and to salt-out the analytes prior to HS. The complicated matrices necessitate the separate analysis of betel nut, piper betel, and red slaked lime, which are the three major parts of a finished betel product. Qualitative identification is aided by the mass spectrum provided by the proposed method. The limits of quantitation vary from 0.02 to 1.20  $\mu\text{g}/\text{ml}$ . Precisions calculated for the 5 and 50  $\mu\text{g}/\text{ml}$  concentration range are ca. 20%. The method is simple, rapid, solventless, and requires only a small amount of sample. It may serve as a screening protocol for the determination of AP and MA in betel.

### 1. Introduction

Betel originally grown in Malay is now widely planted in the tropical zone and part of the subtropical area. An edible finished betel product is generally prepared by cutting an unripe betel nut into two halves and sandwiching between the two halves with piper betel and red slaked lime (consisting mostly of oyster shell powder and orange rind). Upon chewing, betel could generate effects such as cooling, cold-protection, and stimulating saliva production [1]. These effects have drawn tens of millions of betel lovers widespread in southeast Asia. In Taiwan, there are about two million betel-chew-

ing people among a population of twenty one million. With the recent increase of drug abuse, the merchants were reportedly resorting to the addition of amphetamine (AP) and methamphetamine (MA) to betel to maintain the loyalty of their customers [2]. The need for analytical methods to detect AP and MA in betel becomes apparent. The headspace sampling (HS) technique has traditionally been used for the analysis of gaseous and volatile analytes [3–7]; however, it has also been reported for the analysis of non-volatile organic compounds [8]. The HS technique is currently being used to determine trace amounts of the semi-volatile compounds AP and MA in urine samples [9–11]. From these studies, HS sampling has shown to be a simple, rapid, solventless, and reliable technique. The

\* Corresponding author.

aim of the present study is to develop a similar HS technique in conjunction with gas chromatography–mass spectrometry (GC–MS) to detect AP and MA in betel. We use MS as the detector to aid qualitative identification, since, from the regulatory point of view, positive confirmation is of prime importance.

## 2. Experimental

### 2.1. Materials

Racemic D,L-amphetamine sulfate (AP- $\text{H}_2\text{SO}_4$ ) and D,L-methamphetamine hydrochloride (MA-HCl) were purchased from Sigma Chemical (St. Louis, MN, USA), benzyl alcohol from Merck Chemical (Darmstadt, Germany), potassium carbonate ( $\text{K}_2\text{CO}_3$ ) from Janssen Chemica (Geel, Belgium), ethyl acetate from Fisher Chemical (Fair Lawn, NJ, USA), and directly used without distillation. A 1 mg/l standard solution was prepared by dissolving 100.0 mg of AP- $\text{H}_2\text{SO}_4$  and 100.0 mg of MA-HCl in 100 ml deionized water. The three components of a finished betel product (betel nut, piper betel, and red slaked lime) used for fortified studies were obtained from a local betel vendor and found to be free of AP and MA. Fortified samples were prepared by soaking each individual component overnight in 20 ml aqueous solution containing an appropriate amount of AP- $\text{H}_2\text{SO}_4$  and MA-HCl. An edible finished betel product was prepared by cutting a betel nut into two halves and sandwiching between the halves with piper betel and red slaked lime. Fortified and real samples were stored in a 4°C refrigerator before analysis.

### 2.2. Headspace sampling

The three components of a finished betel product were analyzed separately. A 1.5-g portion of betel nut (0.3 g piper betel or 0.3 g red slaked lime) was crushed (unnecessary for piper betel and red slaked lime) and placed in a 15-ml HS vial. An appropriate amount (5, 25, 50, 125, or 250  $\mu\text{l}$ ) of standard solution was added. After

5 min, a 3.5-g portion of  $\text{K}_2\text{CO}_3$  was added. The total volume of the vial contents was adjusted to 5 ml by adding deionized water. The vial was sealed with an aluminum hole cap–Teflon-faced septum, then sufficiently shaken, and placed in a 80°C oven for 20 min. Meanwhile, a 1- $\mu\text{l}$  aliquot of 1:50 (v/v) benzyl alcohol in ethyl acetate, used as internal standard (I.S.), was sealed in another empty HS sampling vial. The I.S. vial was also placed in the 80°C oven for 20 min. The I.S. was allowed to vaporize completely using the “full evaporation technique (FET)” [12]. Afterwards, 0.7 ml of the analyte vapor or 0.1 ml of the I.S. vapor was simultaneously injected onto the GC system using a 1.0-ml gas-tight syringe and determined by a mass spectrometer operated in the full scan mode.

### 2.3. Apparatus

GC–MS analyses were carried out using a Hewlett-Packard HP-5890 Series II gas chromatograph coupled to a HP-5971 Series mass selective detector (MSD) operated in full scan mode. The column used was a Hewlett-Packard HP-5 capillary column (25 m  $\times$  0.2 mm I.D., 0.33  $\mu\text{m}$  film thickness). The GC was operated in the splitless mode with the injector temperature at 250°C. Helium was used as the carrier gas at a flow-rate of 1 ml/min. The column temperature was initially held at 60°C for 2 min, then programmed at 10°C/min to 120°C, then at 18°C/min to 250°C, and held for 4.78 min. Effluents from the GC column were transferred via a transfer line held at 280°C and fed into a 70-eV electron impact (EI) ionization source.

The MS analyses were performed using the full scan mode accompanied by extracting ion chromatograms. The  $m/z$  values used for AP, MA, and I.S. were 44, 58, and 108, respectively. The calibration curves were produced by plotting the peak-area ratio (analyte: benzyl alcohol) against the effective concentration (in  $\mu\text{g}/\text{ml}$ , the denominator was the total volume of all materials placed in the HS vial including the added deionized water, i.e., 5 ml) of the appropriate analyte in the fortified samples. The peak-



area ratio used was the mean of three replicate analyses.

### 3. Results and discussion

#### 3.1. Matrix effects and full evaporation technique

A finished betel product consisting of betel nut, piper betel, and red slaked lime fortified with AP and MA is not an ideal solution. Each part would show different and possibly cross-interacting matrix effects on the evaporation of the analytes. Fig. 1 shows the differences in matrix effects when the three parts of a betel were analyzed together (Fig. 1A) and separately (Figs. 1B–D). The peaks at  $t_R$  (retention time) 7.21, 8.74, and 9.48 min in Fig. 1A of the total-ion chromatogram (TIC) of a finished betel product are from the I.S., AP, and MA, respectively. They are further confirmed by the exact match of their mass spectra to those stored in the library. The intense peaks at  $t_R = 9.93$  and 10.64 min are from the matrix and are tentatively assigned as 3-pyridinecarboxylic acid [1] and 5-(2-propenyl)-1,3-benzodioxole, respectively. Comparing Fig. 1A to Figs. 1B–D, it is evident that the former peak comes from the betel nut only and the latter is from both piper betel and red slaked lime. The coherence of the  $t_{R,s}$  of the same analyte in Fig. 1 demonstrates that the method could yield analytically reproducible  $t_{R,s}$ .

The success of this method depends heavily on the use of an appropriate internal standard. We used benzyl alcohol, as suggested in the literature [13]. However, the correlation coefficients of the calibration curves prepared by adding I.S. directly into the HS vials containing betel samples are not satisfactory, i.e., generally less than 0.85. This is because the HS technique used in this study performs best when sampling and analyzing part of the analytes in their vapor phase to achieve the total-amount quantitation. According to Henry's law, the partial vapor pressure of a volatile solute in an ideal solution is equal to the vapor pressure of the pure solute multiplied by its mole fraction in the ideal

solution. Therefore, the analytical results are expressed in units of  $\mu\text{g}/\text{ml}$  rather than the traditional units of  $\mu\text{g}/\text{g}$ . Although similar amounts of I.S. were added into each HS vial, the mole fractions of I.S. in aqueous betel samples were not necessarily the same because of the differences in matrices. Consequently, the partial pressure of I.S. in the headspace of each vial might vary. This problem was solved by using the FET technique to add I.S. into another empty HS sampling vial to achieve complete evaporation. The linearity of the calibration curves was significantly improved, with correlation coefficients generally greater than 0.98. In addition, the similar intensity of the peaks at  $t_R = 7.21$  min in all four TICs shown in Fig. 1 illustrates the appropriateness of the selection of benzyl alcohol as the I.S. and the success of the FET technique.

Table 1 indicates that both AP and MA in the individual betel parts (Figs. 1B–D) show considerably higher intensity than in the finished betel product (Fig. 1A) provided the same amount (50  $\mu\text{l}$  of 1 mg/ml standard solution) of analytes was added. This difference in intensity is ascribed to the slow transfer of AP and MA from the aqueous layer to the headspace due to the competitive transfer of matrix components. The relatively smaller  $r_{AP}$  and  $r_{MA}$  in the finished betel product indicate the presence of a more serious matrix effect in a finished betel. The smaller  $r_{AP}$  and  $r_{MA}$  in the betel nut are presumably due to the adsorption of AP and MA by the cellulose component in betel nut. On the other hand, the largest  $r_{AP}$  and  $r_{MA}$  values—found in the red slaked lime—are tentatively ascribed to the extra alkalizing and salting-out effects generated by the  $\text{Ca}(\text{OH})_2$  in the oyster shell powder which is the major component of the red slaked lime.

#### 3.2. Endogenous alkalizing and salting-out effects of red slaked lime

The red slaked lime was thought to have endogenous alkalizing and salting-out effects on the detection of the concealed AP and MA. To explore this phenomenon, three portions (each

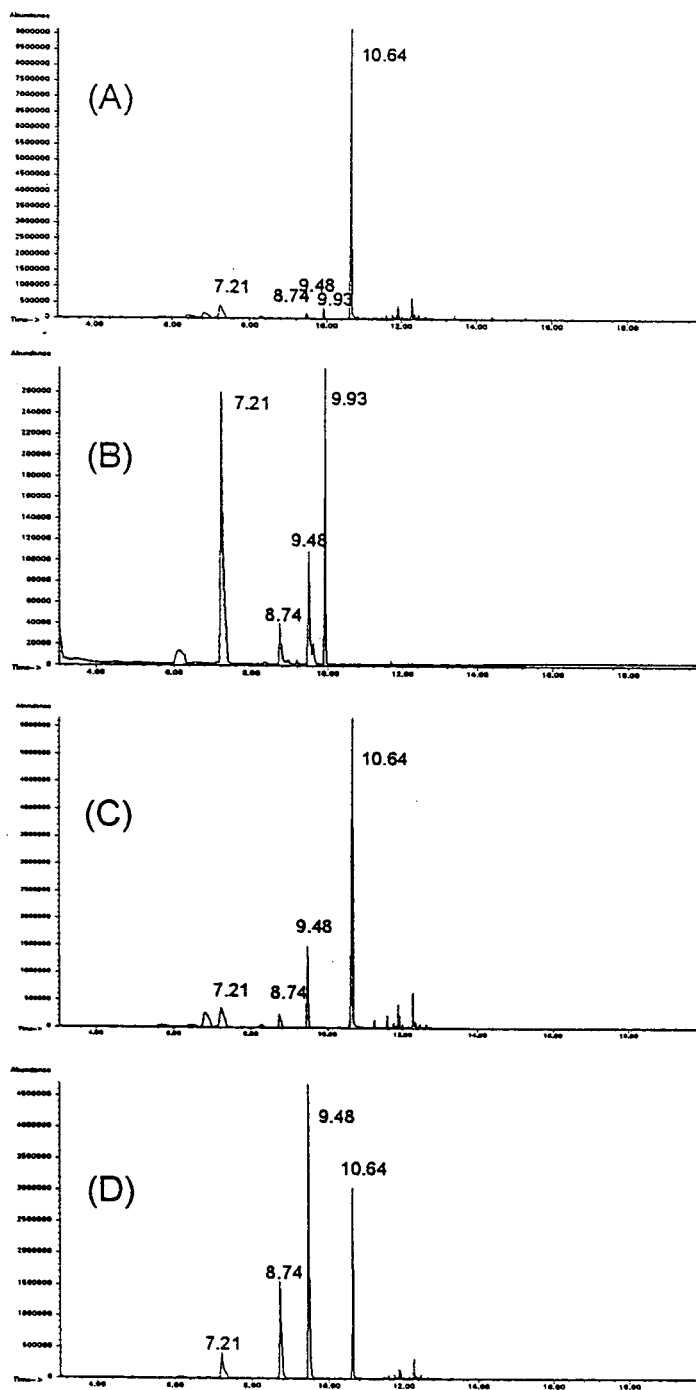


Fig. 1. Total ion chromatograms of samples fortified with amphetamine and methamphetamine: (A) finished betel product, (B) betel nut, (C) piper betel, and (D) red slaked lime.

Table 1  
Matrix effects on the detection of amphetamine and methamphetamine in finished betel product, betel nut, piper betel, and red slaked lime

Matrix	$r_{AP}^a$	$r_{MA}^b$	$r_{M1}^c$	$r_{M2}^d$
Finished betel product	0.02	0.14	0.19	5.74
Betel nut	0.12	0.28	0.44	–
Piper betel	0.36	1.37	–	4.06
Red slaked lime	2.51	5.66	–	2.36

<sup>a</sup> Peak-area ratio of AP/benzyl alcohol (I.S.).

<sup>b</sup> Peak-area ratio of MA/I.S.

<sup>c</sup> Peak-area ratio of matrix peak at  $t_R = 9.93$  min/I.S.

<sup>d</sup> Peak-area ratio of matrix peak at  $t_R = 10.64$  min/I.S.

weighing 0.3 g) of red slaked lime were each mixed with 25  $\mu$ l of 1 mg/ml standard solution. The foregoing HS procedure was followed except that (a) vial A was left at ambient temperature for 20 min with no  $K_2CO_3$  added, (b) vial B was heated in an 80°C oven for 20 min with no  $K_2CO_3$  added, and (c) vial C was heated in an 80°C oven for 20 min with 3.5 g of  $K_2CO_3$  added. The resulting TICs are shown in Fig. 2. Fig. 2A indicates that without an elevated temperature no detectable amounts of the analytes were found in the vapor phase. Fig. 2B indicates that at elevated temperature the endogenous alkalizing and salting-out effects of the red slaked lime give a small amount of the analytes in the vapor phase. Fig. 2C clearly indicates that the added  $K_2CO_3$  assists the conversion of AP- $H_2SO_4$  and MA-HCl into their free state. The corresponding increase in ionic strength generates a stronger salting-out effect. The combined effects lead to a 6.5 and 8.5 times higher peak intensity for AP and MA, respectively. The endogenous alkalizing and salting-out effects caused the matrix peak at  $t_R = 10.64$  min to increase proportionally.

### 3.3. Quantitation

The fortification levels of 1–50  $\mu$ g/ml used in this study were selected because they cover the ranges over which these dopes generate sensational effects [14]. Fig. 3 shows the six calibration curves for AP and MA in the three parts

of betel. The correlation coefficients are better than 0.98. The slopes of the calibration curves of MA are generally larger than those of AP. This higher sensitivity of MA is attributed to its higher volatility and its higher MS response. Of the three matrices, red slaked lime shows the highest sensitivity, benefiting from the extra endogenous alkalizing and salting-out effects; betel nut gives the lowest sensitivity, presumably due to the adsorption of AP and MA by the cellulose component.

The limit of detection, LOD (and of quantitation, LOQ), is defined as the analyte concentration giving a peak in the extracted ion chromatogram with a height equal to the mean +  $N \times$  standard deviation (where  $N = 3$  for the LOD and 10 for the LOQ) [15]. The mean (standard deviation) is the measured average (fluctuations) taken from a baseline region located far away from the analyte peak using the 5 mg/l fortified sample. The LODs and LOQs using fortified betel nut, piper betel, and red slaked lime are summarized in Table 2. The LOQs for AP vary from 0.55  $\mu$ g/ml in red slaked lime to 1.59  $\mu$ g/ml in piper betel, whereas for MA, they vary from 0.02  $\mu$ g/ml in betel nut to 0.04  $\mu$ g/ml in piper betel. The precision is about 20% for the data shown in Fig. 3. Most of this uncertainty is attributed the manual-injection error.

The proposed HS-GC-MS method was applied to the determination of AP and MA in real betel. Among the samples found positive of AP and MA, the AP and MA residues in the betel nut are significantly higher (ranging from 30 to >50  $\mu$ g/ml) as compared to those found in the piper betel and red slaked lime matrices (ranging from 1 to 3  $\mu$ g/ml). This is most likely due to the transfer of analytes from the betel nut to the other matrices.

### 4. Conclusion

The determination of AP and MA in betel can be achieved using the proposed headspace sampling and GC-MS method. The method is simple, rapid, solventless, and requires only a small amount of sample. Qualitative identification is

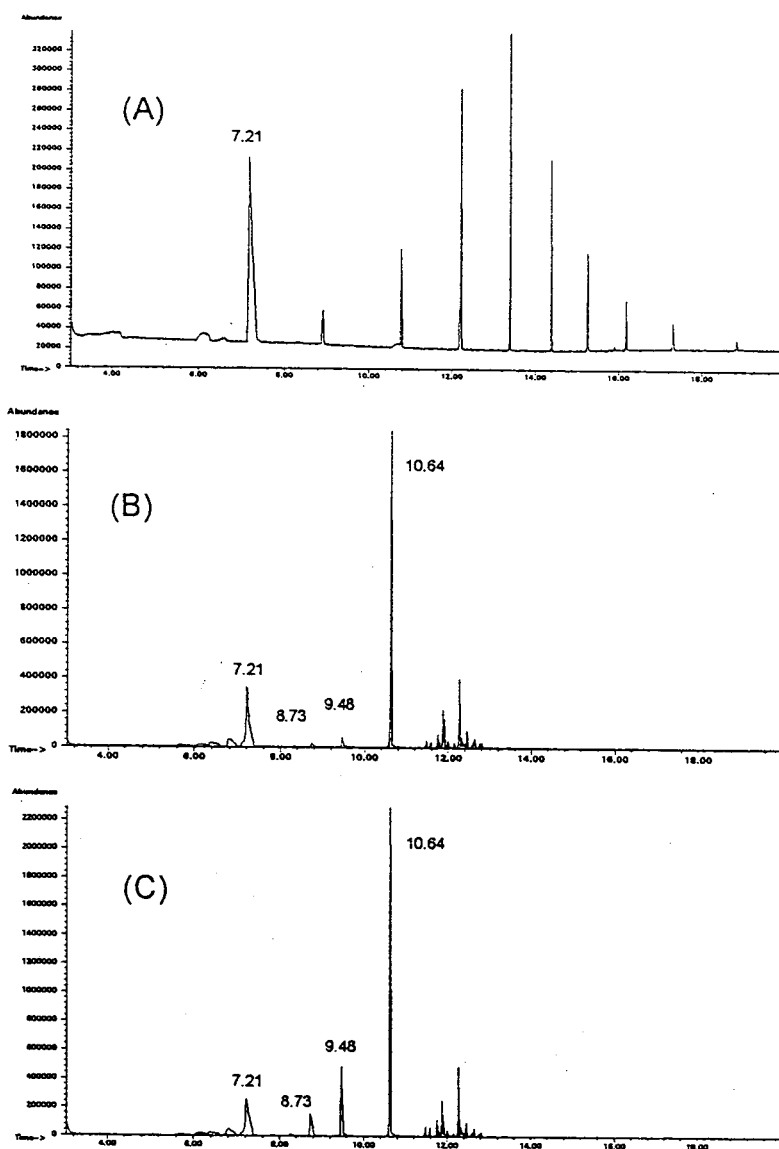


Fig. 2. Total ion chromatograms of 0.3 g red slaked lime containing 25  $\mu\text{g}$  each of AP- $\text{H}_2\text{SO}_4$  and MA-HCl under different HS conditions: (A) at ambient temperature for 20 min with no  $\text{K}_2\text{CO}_3$  added, (B) at 80°C for 20 min with no  $\text{K}_2\text{CO}_3$  added, and (C) at 80°C for 20 min with 3.5 g of  $\text{K}_2\text{CO}_3$  added.

aided by the mass spectrum provided by the proposed method. The limits of quantitation are low enough to detect real samples doped with AP and MA.

#### Acknowledgements

Financial support by the National Science Council of the Republic of China under grant

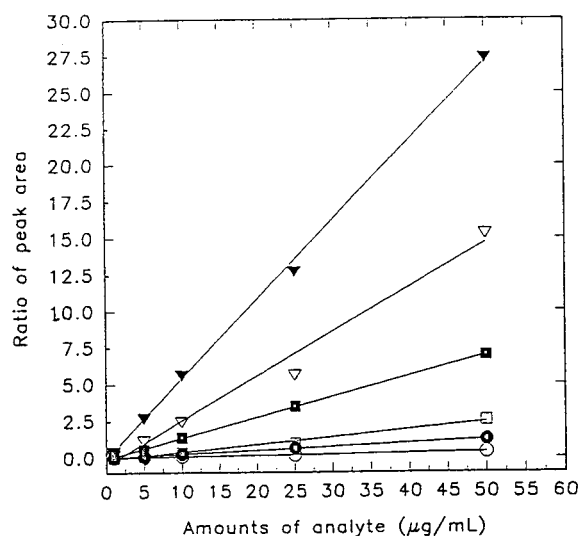


Fig. 3. Calibration curves for AP and MA in the three parts of betel. (○) AP in betel nut, (●) MA in betel nut, (□) AP in piper betel, (■) MA in piper betel, (▽) AP in red slaked lime, (▼) MA in red slaked lime.

Table 2  
Detection limits of amphetamine and methamphetamine in betel nut, piper betel, and red slaked lime

Matrix	Analyte	LOD <sup>a</sup>	LOQ <sup>b</sup>
Betel nut	AP <sup>c</sup>	0.85	1.20
	MA <sup>c</sup>	0.01	0.02
Piper betel	AP	1.13	1.59
	MA	0.02	0.04
Red slaked lime	AP	0.40	0.55
	MA	0.01	0.03

<sup>a</sup> Limit of detection, in µg/ml.

<sup>b</sup> Limit of quantitation, in µg/ml.

<sup>c</sup> AP: amphetamine; MA: methamphetamine.

No. 32245D (to S.-M.W.), NSC84-2113-M-007-040 (to Y.-C.L.), and NSC84-2113-M-015-001 (to Y.-S.G.) is gratefully acknowledged. S.-M.W. thanks the Central Police University for supporting his in-service advanced study.

## References

- [1] J.L. Huang and M.J. McLeish, *J. Chromatogr.*, 475 (1989) 447.
- [2] United Daily News, Taiwan, ROC, February 25, 1994.
- [3] A. Bianchi and M.S. Varney, *Analyst*, 114 (1987) 47.
- [4] B. Kolb and M. Ander, *Fresenius J. Anal. Chem.*, 336 (1990) 291.
- [5] B. Kolb and M. Ander, *Fresenius J. Anal. Chem.*, 336 (1990) 297.
- [6] K. Pekari, M.L. Piekkola and A. Aitio, *J. Chromatogr.*, 491 (1989) 309.
- [7] P. Lansens, C. Meuleman, M. Leermakers and W. Baexens, *Anal. Chim. Acta*, 234 (1990) 417.
- [8] S. Heitefuss, A. Heine and H.S.H. Seifert, *J. Chromatogr.*, 532 (1990) 374.
- [9] H. Tsuchihashi, K. Nakajima and M. Nishikawa, *J. Chromatogr.*, 467 (1989) 227.
- [10] H. Tsuchihashi, K. Nakajima, M. Nishikawa, S. Suzuki, K. Shiomi and S. Takahashi, *Anal. Sci.*, 7 (1991) 19.
- [11] S.-M. Wang, L.-C. Tsai, Y.-S. Giang and Y.-C. Ling, *Chemistry (Chin. Chem. Soc. Taiwan, ROC)*, 51 (1993) 261.
- [12] M. Markelov and J.P. Guzowski, Jr., *Anal. Chim. Acta*, 276 (1993) 235.
- [13] H. Tsuchihashi, K. Nakajima, M. Nishikawa, S. Suzuki, Y. Oka and K. Otsuke, *Forensic Sci. Int.*, 45 (1990) 181.
- [14] T.H. Shih, *Forensic Sci.*, 32 (1991) 45.
- [15] Analytical Methods Committee, *Analyst*, 112 (1987) 199.



# Determination of cholesterol in milk fat by supercritical fluid chromatography

W. Huber, A. Molero, C. Pereyra, E. Martínez de la Ossa\*

*Department of Chemical Engineering, University of Cádiz, Apdo. 40, E-11510 Puerto Real (Cádiz), Spain*

First received 6 December 1994; revised manuscript received 18 May 1995; accepted 19 May 1995

---

## Abstract

A rapid, accurate and precise method for the determination of cholesterol in milk fat using supercritical fluid chromatography (SFC) is described. The accuracy and precision of the developed method are confirmed by analyzing the BCR Reference Material (CRM 164) and by recovery studies of spiked sunflower oil. Furthermore, SFC was compared with gas chromatography (GC). In our case, SFC seems to be more accurate than GC.

---

## 1. Introduction

It is generally accepted that an elevated level of serum cholesterol is an important risk factor of coronary heart disease. Based on studies on this subject, the American Heart Association recommended to reduce the daily intake of fat, especially of saturated fat and cholesterol [1]. For this reason, the food industry is interested in developing new methods to analyze cholesterol in food samples.

Up till now gas chromatography has been the method of choice for the accurate determination of cholesterol in foodstuffs, because it is fast, cheap and well developed [2,3]. However, the development of supercritical fluid chromatography (SFC) as a promising chromatographic technique [4] and the possibility to couple supercritical fluid extraction and SFC has led to the

development of several new methods for the determination of cholesterol and cholesteryl esters by SFC, such as: (i) King [5] analyzed the cholesterol content in a fish-oil capsule by capillary SFC (analysis time, 90 min). However this study did not contain information about the precision of the method. (ii) Ong et al. [6] determined cholesterol in egg yolk and blood serum using capillary SFC (analysis time, 40–45 min). In this paper the conditions for the analysis of cholesterol in egg yolk were given, but no information about sample preparation and precision. (iii) Nomura et al. [7] published a very interesting paper which exactly described the determination of cholesterol and cholesteryl esters in human serum on an ODS-silica gel column, where the analysis took less than 20 min.

In the present work a rapid, accurate and precise method is described for the determination of cholesterol in milk fat by SFC using a simplified sample preparation method. Addition-

---

\* Corresponding author.

ally, a comparison between SFC and gas chromatography (GC) is carried out.

## 2. Experimental

A Lee Scientific supercritical fluid chromatograph (Model 602) from Dionex (Salt Lake City, UT, USA), equipped with a flame-ionization detector (FID), a  $20\text{ m} \times 50\text{ }\mu\text{m}$  I.D. capillary column SB Phenyl 5 with  $0.25\text{ }\mu\text{m}$  film thickness (Dionex) and a  $15\text{ cm} \times 15\text{ }\mu\text{m}$  fused-silica restrictor, is used with a timed-split injection. As carrier gas, carbon dioxide (UN 1013 SFC Grade, Scott Specially Gases, USA) is used.

A Hewlett-Packard gas chromatograph (HP 5890A), equipped with an FID, is used with split injection. The column employed is a fused-silica capillary column ( $30\text{ m} \times 0.25\text{ mm}$  I.D.,  $0.25\text{ }\mu\text{m}$  film thickness), coated with HP-5 (Hewlett-Packard, 19091 J-433). Hydrogen is used as carrier gas.

As reference material anhydrous milk fat (CRM 164) from the Community Bureau of Reference in Brussels, Belgium, is used. For this reference material a cholesterol value of  $273\text{ mg}/100\text{ g}$  ( $\pm 39\text{ mg}/100\text{ g}$ ) is indicated. Cholestane, 98% pure (Aldrich, USA) was used as internal standard.

### 2.1. Sample preparation procedure

The modified sample preparation is based on the method described by Fenton and Sim [3] for the analysis of cholesterol in egg yolk samples. Modifications were made to minimize the sample volume and the preparation time. The sample preparation was performed as follows. A weighted amount ( $0.15\text{ g}$ ) of milk fat was placed into a screw-cap tube ( $100 \times 20\text{ mm}$ ) and  $1.0\text{ ml}$  of the internal standard solution ( $1\text{ mg}$  cholestane/ $1\text{ ml}$  of hexane) was added. Then,  $10\text{ ml}$  of alcoholic KOH solution [ $9.4\text{ ml}$  95% (v/v) ethanol plus  $0.6\text{ ml}$  33% (w/v) KOH] was added. The saponification was carried out in a water bath of  $70^\circ\text{C}$  during  $30\text{ min}$  with occasional shaking. Subsequently, the sample was cooled to room temperature and  $5\text{ ml}$  of deionized water was added.

Extraction of the unsaponifiable constituents was performed with  $10\text{ ml}$  of hexane with permanent shaking for  $1\text{ min}$ . After separation of the layers, the upper hexane layer was removed using a pipette and evaporated at  $35^\circ\text{C}$ . The residue was diluted with  $0.5\text{ ml}$  hexane and then analyzed by SFC and GC.

### 2.2. Supercritical fluid chromatography (SFC)

To analyze cholesterol in milk fat the following method was used: The density of carbon dioxide was held at  $0.2\text{ g/ml}$  for  $2\text{ min}$ , then programmed at  $0.012\text{ (g/ml)}/\text{min}$  to  $0.45\text{ g/ml}$ . The oven temperature was held at  $130^\circ\text{C}$  and the detector temperature (FID) was at  $350^\circ\text{C}$ . The total analysis time was  $25\text{ min}$ . Fig. 1 shows a typical chromatogram of anhydrous milk fat (CRM 164) using SFC (peaks: 1 = cholestane, 2 = cholesterol).

### 2.3. Gas chromatography (GC)

Hydrogen is delivered to the column at a head pressure of  $0.7\text{ bar}$  and at a flow-rate of  $30\text{ ml/min}$ . The injector and the detector temperatures were held at  $300^\circ\text{C}$ . The oven temperature was held at  $260^\circ\text{C}$  for  $1\text{ min}$ , then programmed at a rate of  $4^\circ\text{C}/\text{min}$  to  $300^\circ\text{C}$ . The injection volume was  $1\text{ }\mu\text{l}$  and the total analysis time was  $12\text{ min}$ .

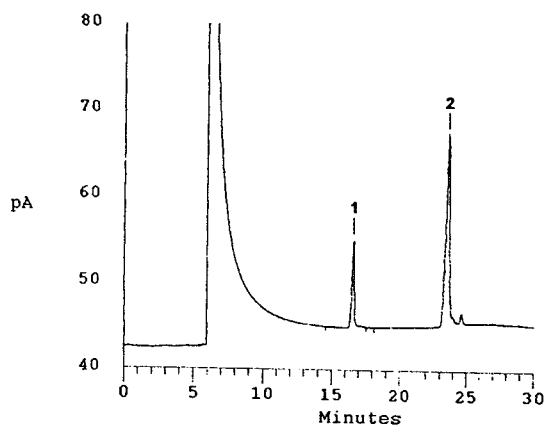


Fig. 1. Supercritical fluid chromatogram of anhydrous milk fat (CRM 164 reference material). Peak: 1 = cholestane, 2 = cholesterol.



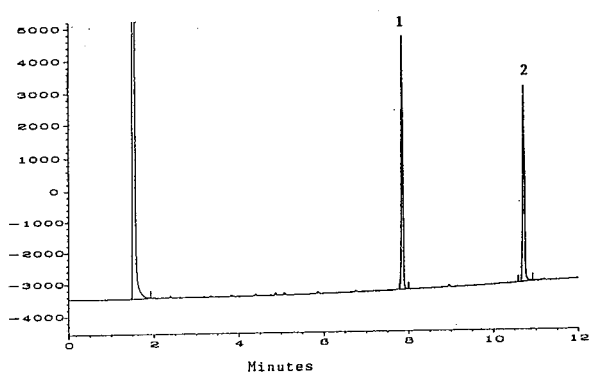


Fig. 2. Gas chromatogram of anhydrous milk fat (CRM 164 reference material). Peaks: 1 = cholestane, 2 = cholesterol.

min. Fig. 2 shows a typical chromatogram of anhydrous milk fat (CRM 164) using GC (peaks: 1 = cholestane, 2 = cholesterol).

### 3. Results and discussion

The relative response factor ( $F$ ) was determined by plotting the mass ratios of cholesterol (CH) over the range 0.2–2.0 mg cholesterol/ml hexane and the internal standard (I.S.) at a level of 1 mg cholestane/ml of hexane versus the ratios of their peak areas (Fig. 3).

Using regression analysis the relative response factor ( $F$ ) and the coefficient of variation (C.V.) were calculated for SFC and GC. In Table 1 the results of the experiments are shown. The cholesterol content ( $C_{MF}$ ) in any milk fat sample (MF) can be determined by using the following equation:

$$C_{MF}(\text{mg/g}) = F \cdot \left( \frac{\text{mg}_{\text{I.S.}}}{\text{g}_{\text{MF}}} \right) \cdot \left( \frac{\text{area}_{\text{CH}}}{\text{area}_{\text{I.S.}}} \right)$$

where  $F$  is the relative response factor,  $\text{mg}_{\text{I.S.}}$  the added amount of the internal standard,  $\text{area}_{\text{CH}}$  and  $\text{area}_{\text{I.S.}}$  are the peak areas of the chromatograms of cholesterol and of the internal standard, respectively.

In order to determine the accuracy and precision of the developed methods two procedures were carried out. First, ten samples of the reference material (CRM 164) were prepared

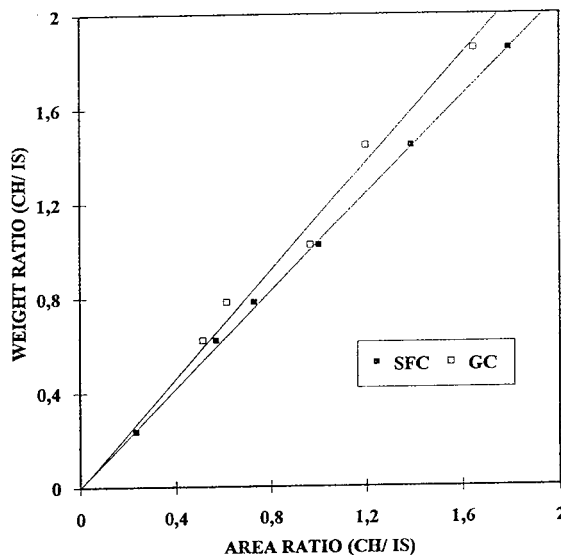


Fig. 3. Mass ratios of cholesterol (CH) and cholestane (I.S.) versus their corresponding area ratios for the determination of the relative response factor ( $F$ ).

Table 1  
Experimental results for the determination of the relative response factors

Method	$F$	C.V. (%)
SFC	1.04	0.04
GC	1.15	6.2

according to the described preparation method. Then, the cholesterol content was analyzed by SFC and GC. Table 2 shows the mean cholesterol content ( $C_{\text{CRM164}}$ ) and the coefficient of variation (C.V.) of these experiments.

For the reference material a cholesterol content of 2.73 mg/g ( $\pm 14.3\%$ ) was found. SFC seems to be more exact in the determination of

Table 2  
Mean cholesterol content and coefficient of variation of the reference material using SFC and GC

Method	$C_{\text{CRM164}}$ (mg/g)	C.V. (%)
SFC	2.70	0.002
GC	3.02	0.001

cholesterol in milk fat than GC using our sample preparation method.

Ulberth and Reich [2], analyzing nine samples of the same reference material (CRM 164) by GC, have reported an overall mean value of 2.66 mg/g (C.V. 1.2%), which did not differ significantly from the indicated value; however, the sample preparation was different from our sample preparation. In the same paper, it was demonstrated that an accurate method for the analysis of cholesterol in anhydrous milk fat is also suitable for the analysis of cholesterol in foodstuffs such as sausages, mayonnaise, noodles or cheese.

Secondly, cholesterol was added to a cholesterol-free sunflower oil at a level of 3.10 mg/g. Three samples of spiked sunflower oil were prepared and analyzed by SFC and GC. The mean experimental values of the cholesterol content ( $C_{so}$ ), the coefficient of variation and the recovery are shown in Table 3.

According to our recovery studies, there is no difference between the use of SFC and GC in analyzing spiked sunflower oil at a level of 3.1 mg/g.

Finally, information about the long-term reliability of the developed SFC method is given. We have analyzed the cholesterol content in ca. 300 milk fat samples over a period of six months. We have compared the results of our experiments analyzing five samples of the reference material at the beginning and the end of a 6-

months period, and we did not find any significant changes in the cholesterol content ( $P > 0.05$ , Analysis of Variance [8]). We found it very useful to repeat the first analysis after every non-run period to get best results.

#### 4. Conclusions

A supercritical fluid chromatographic method for the determination of cholesterol in milk fat has been developed with carbon dioxide as carrier gas. The method uses sample preparation, saponification and extraction, is relatively rapid (25 min), very accurate and precise (C.V. < 1%). In our case, SFC seems to be more accurate than GC for the analysis of cholesterol in milk fat, but GC is faster and cheaper.

#### Acknowledgement

The authors would like to thank Prof. M. García Vargas (University of Cádiz) for his critical comments during the preparation of this paper.

#### References

- [1] D.M. Hegsted, in G.J. Nelson (Editor), *Health Eff. Diet. Fatty Acids*, AOCS, Ch. 5, 1991, p. 50.
- [2] F. Ulberth and H. Reich, *Food Chem.*, 43 (1992) 387.
- [3] M. Fenton and J.S. Sim, *J. Chromatogr.*, 540 (1991) 323.
- [4] F. Höfler and G. Alt, *ZFL*, 42 (1991) 18.
- [5] J.W. King, *J. Chromatogr. Sci.*, 28 (1990) 9.
- [6] C.P. Ong, H.M. Ong and S.F.Y. Li, *J. Microcol. Sep.*, 2 (1990) 69.
- [7] A. Nomura, J. Yamada and A. Takatsu, *Anal. Chem.*, 65 (1993) 1994.
- [8] J. Hartung, *Statistik*, Oldenburg Verlag, Munich, 8th ed., 1991, p. 610.

Table 3  
Mean cholesterol content of spiked sunflower oil analyzed by SFC and GC

Method	$C_{so}$ (mg/g)	V.C. (%)	Recovery (%)
SFC	3.08	0.29	99.4
GC	3.13	0.71	100



ELSEVIER

Journal of Chromatography A, 715 (1995) 337–344

JOURNAL OF  
CHROMATOGRAPHY A

# Enantiomeric resolution using the macrocyclic antibiotics rifamycin B and rifamycin SV as chiral selectors for capillary electrophoresis

Timothy J. Ward\*, Charles Dann III, Alice Blaylock

*Department of Chemistry, Millsaps College, Jackson, MS 39210, USA*

Received 28 February 1995; revised manuscript received 10 May 1995; accepted 22 May 1995

## Abstract

Rifamycin B and rifamycin SV belong to the class of macrocyclic antibiotics known as ansamycins. These macrocyclic antibiotics were used as chiral selectors in capillary electrophoresis to enantioselectively resolve a number of chiral compounds. They contain groups capable of providing the types of multiple interactions necessary to achieve chiral recognition between enantiomers. In fact, they appear to be complimentary in the types of compounds they can enantiomerically resolve. Rifamycin B is shown to be enantioselective towards positively charged compounds, while rifamycin SV was enantioselective towards negatively charged solutes. The choice of wavelength for detection significantly affects sensitivity. Monitoring one of the wavelengths which coincide with the absorption minima of the chiral selector enhances sensitivity. Resolution is enhanced by keeping the amount of analyte injected on column as low as possible and it is demonstrated that it is possible to detect as little as 0.1% of one enantiomer in the presence of the other enantiomer using indirect detection.

## 1. Introduction

The separation of chiral compounds continues to be an area of significant interest, in part due to recent government regulations regarding the marketing of optically active drugs [1]. There are several approaches one can take to achieve enantiomeric separation using capillary electrophoresis (CE) [2–4]. Adding a chiral selector to the free solution is by far the most common approach [5,6], while immobilizing the chiral selector in a gel or other suitable packing in the capillary has also proven to be effective [7,8]. Other workers have demonstrated that wall-im-

mobilized chiral stationary phases are feasible for enantiomeric separations [9,10].

The most common and successful additives for CE chiral separations have been the cyclodextrins and their derivatives [2,11]. This is due to the fact that cyclodextrins are of the optimal size to form inclusion complexes with a significant number of chiral compounds. Another contributing factor to their widespread use is the ability to derivatize the secondary hydroxyls at the rim of the cyclodextrin with various functional groups which can improve solubility and provide unique selectivity for separation. In spite of their use, the need for more diverse and potentially more powerful chiral selectors still remains an intensive area of research. Recently Armstrong and

\* Corresponding author.

co-workers suggested macrocyclic antibiotics would be useful as a broad new class of chiral selectors in CE, HPLC, and TLC [12–14]. These compounds which are structurally diverse and commercially available have opened a new area of research into chiral selectors that appear promising for enantioseparations.

Rifamycins have a characteristic ring structure or chromophore spanned by an aliphatic chain and differ from one another in the type and location of the substituents on their naphtho-hydroquinone ring. Fig. 1 shows how rifamycin B differs from rifamycin SV by the R group attached to the naphtho-hydroquinone ring. In rifamycin B this group is an oxy-acetic acid ( $-\text{OCH}_2\text{COOH}$ ) while in rifamycin SV the R group is a hydroxyl ( $-\text{OH}$ ). Changing this substituent has profound effects on the selector's selectivity toward charged compounds. Since the carboxylic and hydroxyl groups on rifamycin B are ionizable it can exist as a dibasic acid while rifamycin SV is essentially neutral at the pHs used in this study. In addition to the functional groups mentioned above, each rifamycin has nine stereogenic centers, four hydroxy groups, one carboxymethyl group, and one amide bond.

In this work the macrocyclic antibiotics rifamycin SV and rifamycin B were examined as chiral selectors for CE. These macrocyclic antibiotics appear to be complimentary in the types of compounds they can enantiomerically resolve. Rifamycin B seems to be well suited for separat-

ing positively charged analytes while rifamycin SV is capable of resolving negatively charged solutes. Previous work used rifamycin B as a chiral selector in CE for the resolution of a racemic amino alcohols [13]. They examined the effect of chiral selector concentration, pH, and organic modifier on enantiomeric resolution. In this work novel separations are presented using these chiral selectors and the effects of column loading and wavelength detection on sensitivity and separation are investigated.

## 2. Experimental

Sodium dihydrogen phosphate, sodium hydroxide, and 2-propanol were obtained from Fisher (Atlanta, GA, USA); rifamycin B and rifamycin SV were acquired from Advanced Separation Technologies (Whippany, NJ, USA); and all chiral analytes were obtained from Sigma (St. Louis, MO, USA). All reagents in this study were used as received.

Electrophoretic experiments were performed using an Isco model 3850 (Isco, Lincoln, NE, USA) equipped with an on-column variable-wavelength UV detector, and a Chrom-Jet integrator was used to record electropherograms (Spectra-Physics, San Jose, CA, USA). The regulated high-voltage power supply capable of delivering up to 30 kV, was used in the constant voltage mode. An Ultra-Ware degassing system with helium gas supplied by Union Carbide (Danbury, CT, USA) was used to degas all solutions.

The fused-silica capillary tube was 65 cm  $\times$  50  $\mu\text{m}$  I.D. (Isco), with the detector cell window 40 cm from the column inlet. All solutions were degassed and filtered prior to their use with 0.45- $\mu\text{m}$  polypropylene filters (Alltech, Deerfield, IL, USA). The capillary was purged daily with 1.0 M NaOH, followed by water and run buffer for 3 min each. All samples, unless noted otherwise, were dissolved in distilled water at approximately 0.3 mg/ml and injected into the capillary using electrokinetic injection at 5 kV for 5 s. The capillary was purged with run buffer

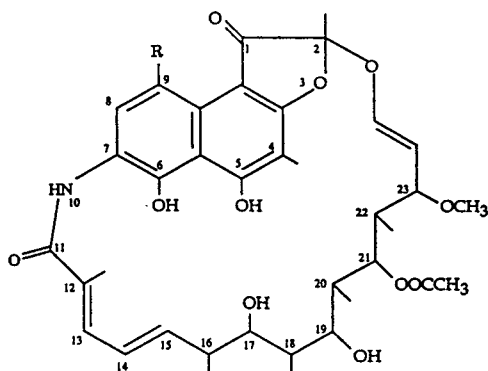


Fig. 1. Structures of rifamycin B ( $\text{R} = -\text{OCH}_2\text{COOH}$ ) and rifamycin SV ( $\text{R} = -\text{OH}$ ).

for 3 min between injections. All separations were carried out at ambient temperature (21°C).

The aqueous buffer solutions were prepared by adjusting the pH of a solution containing the appropriate amount of sodium phosphate monobasic with NaOH. The phosphate buffer–2-propanol solvent mixtures are volume percents prior to mixing. Run buffers containing rifamycin B and rifamycin SV were prepared by weighing the proper amount of the macrocyclic antibiotic into a volumetric flask, adding the phosphate buffer–2-propanol solution, and sonicating to dissolve the antibiotic.

The absorbance spectra were obtained using a Perkin-Elmer Model 553 double beam UV–Vis spectrophotometer. The solution for the spectra was prepared in 70% 0.1 M phosphate buffer pH 7–30% 2-propanol, prepared as described above.

### 3. Results and discussion

#### 3.1. Separations using rifamycin B as chiral selector

Recently, Armstrong and workers investigated the effect of pH, organic modifier and chiral selector concentration on the resolution of  $\alpha$ -amino alcohols [13]. They found that enantioresolution increased with pH, reached a maximum at pH 7, and decreased with increasing pH. This can be explained by examining the charge on the chiral selector and analyte being separated. Rifamycin B, a dibasic acid, loses some fraction of the negative charge present on the molecule as pH is lowered which precludes a strong charge–charge interaction with the positively charged amine containing analyte. As pH is increased to pH 7, rifamycin B exists primarily as a di-anion while the analyte is positively charged, providing a strong electrostatic interaction. At higher pHs, the amine group on the analyte is deprotonated again precluding a strong charge–charge interaction. While other parameters such as electroosmotic flow are also affected, clearly charge–charge interactions play a prominent role in enantioresolution.

No enantioselectivity was observed in the

absence of organic modifier in the run buffer. Of the organic modifiers investigated, 2-propanol provided the greatest enhancement to enantioresolution. Increasing the 2-propanol concentration in the run buffer increased enantioresolution, decreased electrophoretic mobilities and increased migration times. Increasing chiral selector concentration increased enantioresolution but tended to slightly increase migration times due to the small decrease in electrophoretic mobility. Increasing the chiral selector concentrations above 30 mM produced an extremely small signal-to-noise ratio due to the strong UV absorption of the chiral selector.

Considering all the factors discussed above, we chose a buffer containing 25 mM rifamycin B in 70% 0.1 M phosphate buffer pH 7–30% 2-propanol for our studies.

#### *Influence of wavelength on sensitivity*

Rifamycin SV and rifamycin B absorb strongly in both the ultraviolet and visible spectral regions as shown in Fig. 2. This makes direct detection of analytes difficult at commonly employed wavelengths such as 254 nm. Also in Fig. 2, it can be seen that rifamycin SV has absorption maxima at slightly longer wavelengths than rifamycin B, but each exhibit minima at approximately 205, 275 and 350 nm. A series of racemic

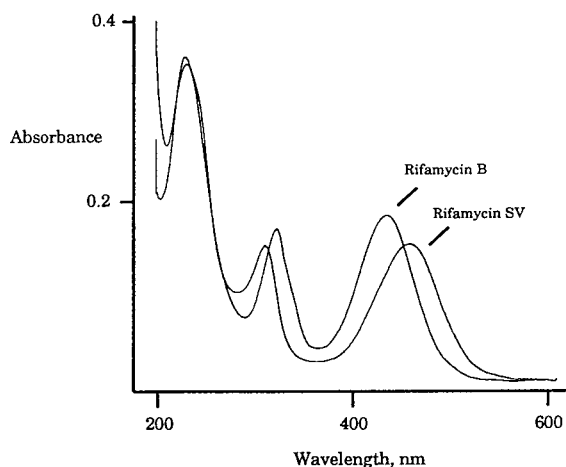


Fig. 2. UV–Vis spectra of rifamycin B and rifamycin SV at pH 7.

amino alcohols were previously resolved using a wavelength of 254 nm by indirect detection [13]. In this work we examined the effect of wavelength detection on sensitivity, specifically looking at regions where an absorption minima occurred. Fig. 3 shows the separation of epinephrine injected under identical conditions at 275 nm and 350 nm. It is apparent from Fig. 3 that the sensitivity is much greater at 350 nm than at 275 nm. This can be attributed to the fact that at absorption minima the baseline noise is substantially reduced resulting in improved sensitivity. Since the sensitivity was greater at 350 nm than at 275 nm or 254 nm, we chose this wavelength for all subsequent injections.

#### Effect of column loading on resolution

Table 1 shows the results of injecting seven compounds most of which had resolutions factors ( $R_s$ ) of 1.0 or less from the previous work [13]. In that work the authors found that a concentration of 25 mM rifamycin B in 60% 0.1 M phosphate buffer pH 7–40% 2-propanol afforded the best enantioselectivity. We used the same buffer system with the exception of adding 30% 2-propanol instead of 40% 2-propanol. Using a larger percent of 2-propanol increases resolution

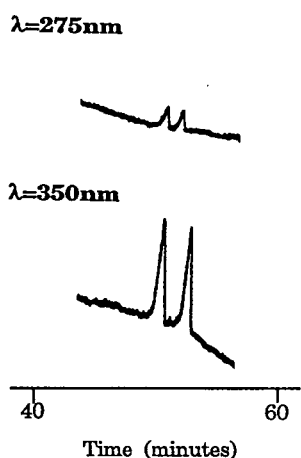


Fig. 3. CE separation of enantiomers of epinephrine at 275 nm and 350 nm. Run buffer consisted of 2-propanol–0.1 M phosphate buffer pH 7 (30:70, v/v) containing 25 mM rifamycin B. Separation voltage was 8 kV and 1.0 mg/ml of epinephrine was loaded at 5 kV for 5 s.

but also substantially increases solute migration times. As a compromise we chose 30% 2-propanol since enantioresolutions at this percent organic modifier were good and migration times were substantially shortened. By injecting approximately 0.2 to 0.3 mg/ml at 5 kV, 5 s, we were able to triple the  $R_s$  value of oxprenolol (0.4 to 1.2), double the values for alprenolol (0.7 to 1.4) and epinephrine (1.5 to 3.1), and substantially improve the values for normetanephrine (0.9 to 1.3) and octapamine (1.1 to 1.4). It should be noted from Table 1 that most of these separations could be improved further by increasing the amount of 2-propanol at the expense of longer analysis time. Interestingly, reducing the amount of metoprolol and norepinephrine loaded on column appeared to have little effect on their resolution. Resolution and peak-to-peak separation are affected by the amount of analyte loaded on the capillary column. With the increase in sensitivity at 350 nm (greatest UV minima), loading less analyte (approximately 80% less) on column substantially improved separation resolutions for five of the seven solutes studied.

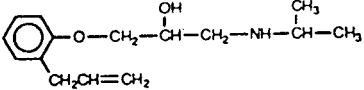
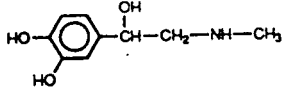
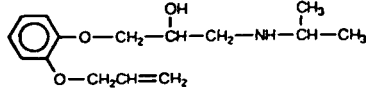
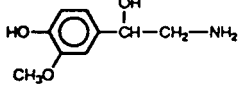
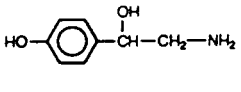
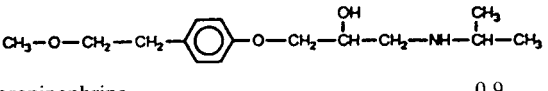
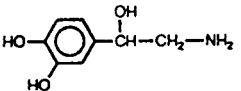
The amount of analyte loaded on column clearly affects chiral resolution as noted above. The effect on resolution as well as peak shape is shown in Fig. 4. As more epinephrine was loaded on column, separation gradually eroded. From the figure it is apparent that the separation began degrading significantly between 0.3 mg/ml and 60 mg/ml and is nearly lost at 200 mg/ml. As the concentration loaded increased above 100 mg/ml, peak tailing became very pronounced and resolution began to degrade rapidly. Thus separations of amounts larger than what could be termed analytical, are not feasible with this system due to the loss of resolution as well as poor peak symmetry at higher loadings of analyte on column.

#### Separation of compounds containing more than one ring

Table 2 shows the first separation of several new solutes using either rifamycin B or rifamycin SV as indicated in the table. The first three solutes were all positively charged under the

Table 1

Increased enantiomeric resolutions of selected compounds, migration times and apparent mobilities with 25 mM rifamycin B in 2-propanol–0.1 M phosphate buffer pH 7.0 (30:70, v/v)

Compound	$R_s$	Time <sup>a</sup>	$\mu(a)^b$	$R_s^c$	Time	$\mu(a)$
Alprenolol 	1.4	19.2	16.9	0.7	63.9	5.6
Epinephrine 	3.1	48.2	6.7	1.5	62.1	5.8
Oxprenolol 	1.2	35.8	9.1	0.4	60.3	6.0
Normetanephrine 	1.3	29.2	11.1	0.9	55.6	6.5
Octapamine 	1.4	37.6	8.6	1.1	55.6	6.5
Metaprolol 	0.7	46.1	7.0	0.8	62.1	5.8
Norepinephrine 	0.9	32.8	9.9	0.9	57.0	6.3

<sup>a</sup> Migration times are given in minutes for first eluting isomer.

<sup>b</sup>  $\mu(a)$  is the apparent mobility in  $\text{cm}^2 \text{kV}^{-1} \text{min}^{-1}$  of the first eluting isomer.

<sup>c</sup> Data from Ref. [13].

conditions employed, while the last three solutes were negatively charged. Rifamycin B had previously been shown to be adept at separating single-ring structures but appeared to exhibit no enantioselectivity towards double-ring or larger structures. Pindolol and propranolol were both resolved even though both contain multiple-ring structures. In the case of pindolol, it is composed of an indole ring which is substituted at the 4 position with an aliphatic chain containing an

amine. It exhibits an absorption profile in the UV range similar to that of the previous single-ring aromatic structures monitored by indirect detection, in that it does not absorb appreciably at 350 nm. Propranolol on the other hand contains a naphthyl moiety which absorbs UV light significantly at longer wavelengths and was monitored by direct detection at 350 nm. While pindolol was poorly resolved, propranolol exhibited good resolution. It is of interest to note

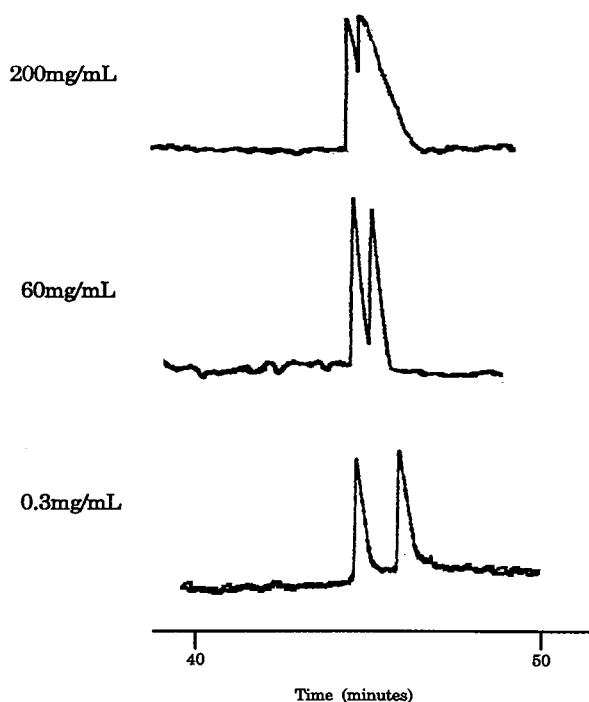


Fig. 4. The effect of solute concentration versus resolution at 350 nm using indirect detection. Conditions: same as Fig. 3. Separation voltage was 8 kV and indicated concentration of epinephrine was loaded at 5 kV for 5 s.

that the two compounds contain one identically substituted ring and differ only in that pindolol is composed of an indole instead of a naphthyl ring. This further illustrates the point that structure type and size obviously play an important role in enantioselectivity. It also demonstrates that two-ring and possibly larger solutes can be resolved using rifamycin B.

### 3.2. Separations using rifamycin SV as the chiral selector

The last three solutes in Table 2 were resolved using rifamycin SV as the chiral selector in the run buffer. All three were negatively charged at the buffer pH employed, and eluted after the larger water perturbation of the baseline. Fig. 5 shows the separation of hexobarbital using indirect UV detection. Interestingly, rifamycin SV seems particularly suited for separating systems

containing at least two rings. Hexobarbital and glutethimide each contain two rings which are not conjugated while dansyl aspartic acid has a conjugated ring system. Dansyl aspartic acid absorbs at longer wavelengths, and was monitored by direct UV detection at 350 nm while hexobarbital and glutethimide were both monitored by indirect UV detection. Rifamycin SV separates negatively charged solutes and is a complimentary chiral selector to rifamycin B, which can resolve positively charged solutes.

### 3.3. Enantiomeric purity assessment

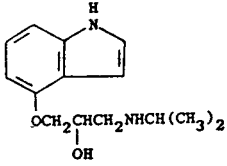
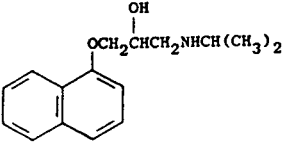
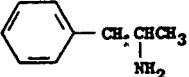
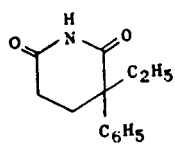
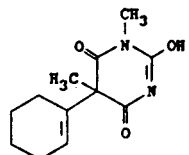
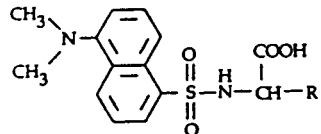
The ability to monitor one enantiomer in the presence of the other remains an important consideration for any viable chiral analysis. Fig. 6 shows the separation of isoproterenol with spiked concentrations of each enantiomer. Using indirect UV detection at 350 nm we could accurately see 0.1% of the (–)-enantiomer in the presence of the (+)-enantiomer. In this case the enantiomer as the minor constituent eluted first, which makes monitoring optical purity easier.

## 4. Conclusions

We have demonstrated the utility of rifamycin B and rifamycin SV in the chiral resolution of several compounds. We found that performing separations at 350 nm versus 275 or 254 nm results in increased sensitivity due to the decrease in baseline noise at longer wavelengths. This increase in signal-to-noise ratio allows for smaller amounts of solute to be injected on column which can increase chiral resolution for some compounds. While solutes containing single aromatic groups are especially suited for chiral resolution using rifamycin B, solutes containing more than one ring are also amenable to separation. Rifamycin SV resolved negatively charged solutes making it a complimentary chiral selector to rifamycin B which resolves positively charged solutes. It was shown that it is possible to measure as little as 0.1% of one enantiomer in the presence of the other demonstrating the feasibility of using these chiral selectors for



Table 2  
Enantiomeric resolutions, migration times and apparent mobilities with 25 mM macrocyclic antibiotic in 2-propanol–0.1 M phosphate buffer pH 7.0 (30:70, v/v)

Compound	$R_s$	Time <sup>a</sup>	$\mu(a)^b$
Pindolol <sup>c</sup>	0.3	36.7	8.8
			
Propranolol <sup>c</sup>	1.3	27.8	11.7
			
Amphetamine sulfate <sup>c</sup>	1.1	36.1	9.0
			
Glutethimide <sup>d</sup>	4.0	34.8	9.3
			
Hexobarbital <sup>d</sup>	1.9	40.8	8.0
			
Dansyl aspartic acid <sup>d</sup>	1.5	36.8	8.8
			

<sup>a</sup> Migration times are given in minutes for first eluting isomer.

<sup>b</sup>  $\mu(a)$  is the apparent mobility in  $\text{cm}^2 \text{kV}^{-1} \text{min}^{-1}$  of the first eluting isomer.

<sup>c</sup> Positively charged compounds resolved with rifamycin B.

<sup>d</sup> Negatively charged compounds resolved with rifamycin SV.

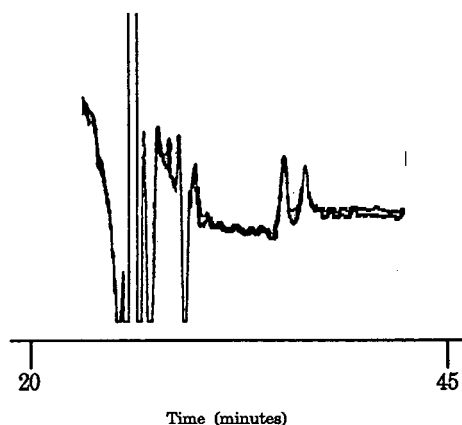


Fig. 5. Separation of enantiomers of hexobarbital. Conditions: run buffer, 2-propanol-0.1 M phosphate buffer pH 7 (30:70, v/v) containing 25 mM rifamycin SV. Voltage was 8 kV, indirect detection at 350 nm.

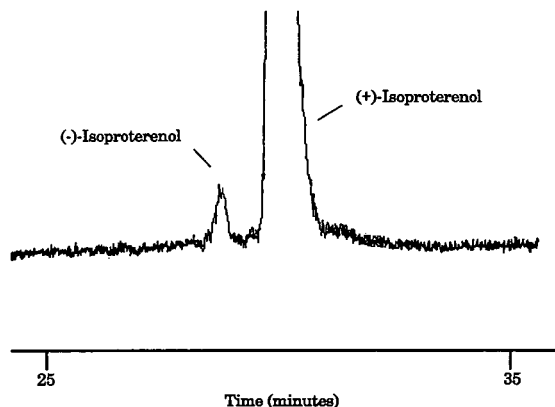


Fig. 6. Separation of enantiomers of isoproterenol at concentrations of 500  $\mu\text{g/ml}$  (+)-isoproterenol and 0.50  $\mu\text{g/ml}$  (-)-isoproterenol using indirect UV detection at 350 nm. Injection was at 5 kV for 8 s. Other conditions same as Fig. 3.

enantiomeric purity assay. Increasing the amount of solute loaded on column rapidly degrades separation, thus for best results, solute loadings should be kept as low as feasible for detection.

Work is continuing in our laboratory to further characterize the parameters which affect separation and investigation of the mechanism of separation for these macrocyclic chiral selectors.

### Acknowledgements

The authors thank the William and Flora Hewlett Foundation Award of Research Corporation and Howard Hughes Medical Institute for their generous support of this project.

### References

- [1] S.C. Stinson, *Chem. Eng. News*, 27 (1993) 38.
- [2] T.J. Ward, *Anal. Chem.*, 66 (1994) 633A.
- [3] R. Kuhn and S. Hoffstetter-Kuhn, *Chromatographia*, 34 (1992) 505.
- [4] S. Terabe, *Trends Anal. Chem.*, 8 (1989) 129.
- [5] S. Fanali, *J. Chromatogr.*, 545 (1991) 437.
- [6] T.J. Ward, M. Nichols, L. Sturdivant and C.C. King, *Amino Acids*, 8 (1995) 337.
- [7] A. Guttman, A. Paulus, A.S. Cohen, N. Grinberg, and B.L. Karger, *J. Chromatogr.*, 448 (1988) 41.
- [8] S. Li and D.K. Lloyd, *Anal. Chem.*, 65 (1993) 3684.
- [9] D.W. Armstrong, Y. Tang, T. Ward and M. Nichols, *Anal. Chem.*, 65 (1993) 1114.
- [10] S. Mayer and V. Schurig, *J. Liq. Chromatogr.*, 16 (1993) 915.
- [11] S. Fanali, *J. Chromatogr.*, 474 (1989) 441.
- [12] D.W. Armstrong, K.L. Rundlett and J. Chen, *Chirality*, 6 (1994) 496.
- [13] D.W. Armstrong, K. Rundlett and G. Reid, *Anal. Chem.*, 66 (1994) 1690.
- [14] D.W. Armstrong and A.Y. Zhou, *J. Liq. Chromatogr.*, 17 (1994) 1695.

# Optimization of the separation of $\beta$ -agonists by capillary electrophoresis on untreated and $C_{18}$ bonded silica capillaries

S. Chevolleau\*, J. Tulliez

*Laboratoire des Xénobiotiques, INRA, B.P. 3, 31931 Toulouse Cedex, France*

First received 14 March 1995; revised manuscript received 23 May 1995; accepted 23 May 1995

## Abstract

The conditions of the separation of ten  $\beta$ -agonists by capillary zone electrophoresis were studied. Several buffers were tested at different ionic strengths and different pH values. The experiments were carried out on two different supports, i.e. an untreated fused-silica capillary and a  $C_{18}$  covalently bonded silica capillary. The results showed that the optimum pH value was the same for the two capillaries. Separation efficiencies were slightly better for the fused-silica capillary whereas better selectivity and repeatability were obtained with the  $C_{18}$  bonded capillary, under optimal conditions.

## 1. Introduction

Beta-adrenergic agonists, commonly named  $\beta$ -agonists, are used as bronchodilators in human and veterinary therapeutics for the treatment of pulmonary diseases. When used as animal feed additives,  $\beta$ -agonists can also act as repartitioning agents, by increasing protein accretion and decreasing the lipogenesis. Thus, they cause a shift in carcass composition, improving the yield of the farm animals [1].

$\beta$ -Agonists are considered anabolic substances within the European Community and their use as animal feed additives is prohibited. A number of  $\beta$ -agonists are however known to be illegally used, thus imposing serious food safety problems. Consequently, accurate multi-compound analyses are required for effective control.

$\beta$ -Agonists are mainly phenylethanolamines, variously substituted on their aryl moiety and terminal amino group. In simple chemical terms, the chemical structure of this diverse group of drugs can be defined as aryhydroxyalkylamines possessing a common functionality: the presence of a  $\beta$ -hydroxyamino group on the side-chain.

Although not known accurately, the  $pK_a$  values of the  $\beta$ -agonists, are assumed to be in the range 7–9 [2].

Several analytical techniques have already been used for the analysis of these polar and ionic compounds, including GC–MS [3–5] and HPLC with UV [6], fluorescence [7], or MS detection [8,9]. Several authors have also demonstrated the use of capillary electrophoresis for their analysis in pharmaceutical formulations [10], determination of drug related impurities [11] and chiral analysis of enantiomeric forms of  $\beta$ -agonists [12,13]. Recently, four  $\beta$ -agonists have been analysed in calf urine using on-line

\* Corresponding author.

isotachopheresis-capillary zone electrophoresis (ITP-CZE) prior to mass spectrometric detection [2].

Capillary zone electrophoresis (CZE) is a very efficient separation technique with a high resolution power, suitable for the separation of ionic compounds even with very small differences in their electrophoretic mobilities. The separation mechanism is based on differences in solute size and charge at a given pH.

In a non-coated fused-silica capillary, the interface between the silanol groups of the tube wall and the electrophoretic buffer consists of a double-layer which tends to make the flow of liquid migrate towards the cathode. This bulk movement of liquid is called the electroosmotic flow (EOF). In CZE, the control of this EOF is very important for improving the separation and shortening the analysis time. It can be adjusted by changing the nature of the buffer, its viscosity (temperature), its ionic strength, or by controlling the voltage of the separation. The most commonly used optimization techniques in CZE are changing the pH of the running buffer to change the charge/mass ratio of the ions, using

additives to decrease the EOF, or the use of coated columns.

Some of the problems encountered when using a non-coated fused-silica capillary are the possible variations in the EOF and the adsorption of charged molecules on the capillary surface. Thus rinsing of unmodified capillaries is an important factor in obtaining stable results.

Coated capillary columns are employed to reduce the EOF, to control the migration time and to improve column efficiency by minimizing solute adsorption on the bare silica wall. Among the different coated columns, the highly hydrophobic  $C_{18}$  bonded phase—well-known in HPLC—attracted attention because of its stability over time at neutral pH and its ability to reduce EOF and decrease solute-wall interactions [14].

In this paper, after preliminary experiments, we have studied the separation of ten  $\beta$ -agonists by CZE on two supports (uncoated fused-silica and  $C_{18}$  bonded phase). The structures of these  $\beta$ -agonists are shown in Fig. 1. The influence of the pH of running buffer has been examined for both columns. The separation efficiency of the two systems is evaluated, and their repeatability

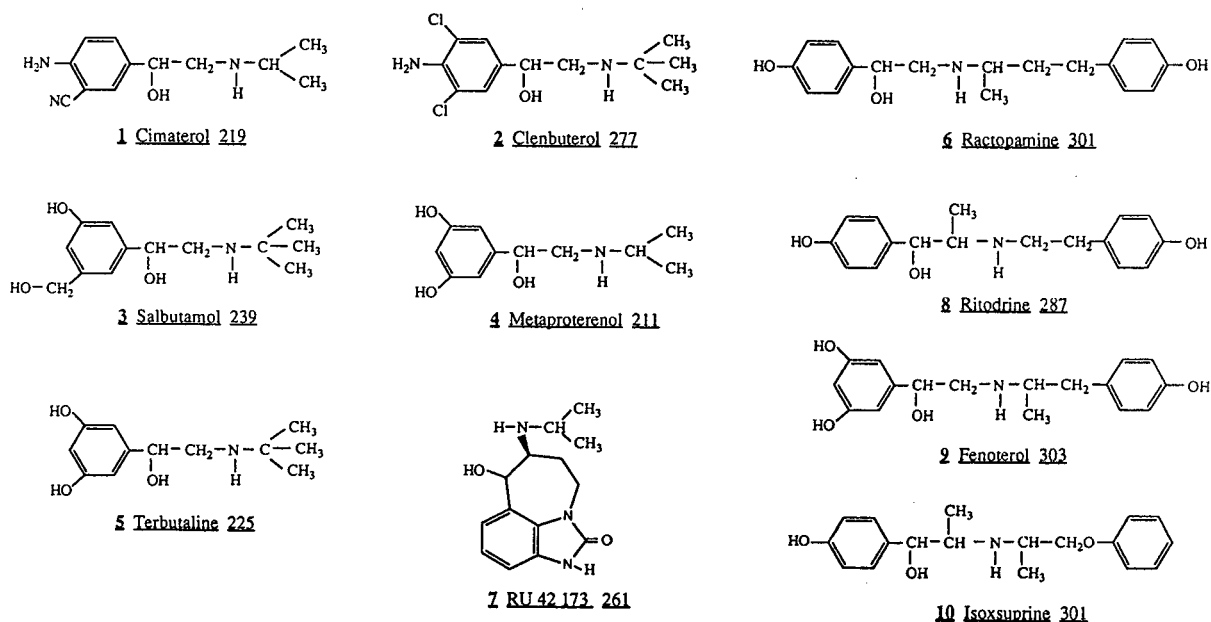


Fig. 1. Structures of the ten  $\beta$ -agonists studied.

is discussed in terms of migration times, relative migration times, separation efficiencies, and normalized peak areas.

## 2. Experimental

### 2.1. Apparatus

Electrophoresis was carried out on a Hewlett-Packard HP <sup>3D</sup>CE system (Hewlett-Packard, Wilmington, DE, USA) with a built-in UV diode-array detector and DOS Windows-type, data-analysis software.

Separations were performed using two different columns. A non-coated fused-silica capillary (68.5 cm × 50 μm I.D., 60 cm effective length) (Hewlett-Packard) and a C<sub>18</sub> bonded phase capillary column (CElect-H250) (68.5 cm × 50 μm I.D., 60 cm effective length) (Supelco, Bellefonte, PA, USA).

All experiments were carried out in the cationic mode, applying a voltage of 15–30 kV. Hydrostatic injection was applied for 2–6 s at 50 mbar, followed by a 4-s flush with buffer. Detection was performed at a wavelength of 200 nm. The temperature was kept constant at 25°C.

Before its use, a new fused-silica capillary was conditioned with 1 M NaOH for 20 min at 40°C, then with 0.1 M NaOH for 10 min at 40°C, rinsed with water for 20 min at 25°C and finally with the running buffer. In order to improve the migration-time and peak-shape reproducibilities, after each run the system was programmed for the following successive operations: 5 min rinsing with 0.1 M NaOH followed by 5 min with running buffer.

The C<sub>18</sub> bonded phase capillary was conditioned for 1 min with 0.1 M NaOH, for 5 min with water and for 5 min with running buffer, repeating the wash/rinse cycle over a 2-h period. After each run the column was rinsed for 5 min with the running buffer, and every ten runs, washed for 1 min with 0.1 M NaOH, and for 5 min with the running buffer.

The running buffers used in these experiments were prepared with tris(hydroxymethyl)amino-methane (Tris) (Sigma, La Verpillière, France) in

deionized water (Milli Q system, Millipore, Bedford, MA, USA) and adjusted at pH 5–9 with acetic acid. All buffer solutions were filtered through 0.45-μm membrane filters (Millipore, Molsheim, France) before use.

### 2.2. Samples

Salbutamol, fenoterol hydrobromide, metaprotorenol hemisulfate salt, ritodrine hydrochloride, isoxsuprine hydrochloride, and terbutaline hemisulfate salt were purchased from Sigma. Cimeterol and clenbuterol hydrochloride were obtained from Boehringer (Ingelheim, Germany) and ractopamine hydrochloride from Eli Lilly (St. Cloud, France). RU 42 173 was kindly provided by Roussel Uclaf (Romainville, France).

Standard solutions were prepared in deionized water at a concentration of 100 ng μl<sup>-1</sup>. A working solution was prepared by mixing 100 μl of the ten standard solutions, which resulted in a concentration of 10 ng μl<sup>-1</sup> for each compound.

Each β-agonist was identified in the mixture by automated spiking achieved by co-injection of each individual component and the mixture under the same conditions as described by McLaughlin et al. [15] and Altria and Luscombe [16].

## 3. Results and discussion

### 3.1. Preliminary experiments

The optimization of the β-agonists separation was performed on the fused-silica capillary. The first parameters studied were the nature and the ionic strength of the running buffer, and the applied voltage.

For preliminary experiments, the applied voltage was set at 15 kV, and the following buffer solutions (20 mM) were tested: sodium citrate (pH 5), acetate (pH 5), phosphate (pH 7), borate (pH 9) and finally Tris (pH 5).

None of the first four buffer systems gave satisfying results. Indeed, when sodium citrate

was used, a high current was produced and baseline instability was observed. With acetate, peak shape distortions were obtained, which should be explained by differences in conductivity between the sample and the buffer [17]. Phosphate gave no satisfactory separation and borate gave no separation at all of the compounds studied. Ackermans et al. [10] obtained some satisfactory results with Tris (pH 5) for the determination of some  $\beta$ -agonists, and this buffer system was selected for further optimization.

The influence of the ionic strength of the Tris buffer was then studied at pH 5. The use of Tris at 50 mM instead of 20 mM resulted in improvement of the resolution without increasing too much the current intensity. A 100 mM Tris solution increased the migration times but did not improve the separation. Thus, the Tris buffer concentration was fixed at 50 mM.

An increase of the applied voltage from 15 kV to 30 kV neither improved the separation, nor changed the elution order. It did, however, reduce the migration times of the  $\beta$ -agonists. A similar trend was observed by Lukkari et al. [18] in a study using micellar electrokinetic capillary chromatography (MEKC) for the separation of nine  $\beta$ -blockers. From these observations, 30 kV was chosen as the working voltage.

### 3.2. Influence of buffer pH

The influence of buffer pH on the migration times of the  $\beta$ -agonists was investigated with a buffer concentration of 50 mM Tris and an applied voltage of 30 kV. The pH was changed from 5 to 9 and two different capillaries were compared: an uncoated fused-silica capillary and a  $C_{18}$  bonded capillary.

The plots of the migration times of each  $\beta$ -agonist studied versus pH are given in Figs. 2a and b, for the uncoated and  $C_{18}$  bonded capillaries, respectively. It appears that, for a given pH, migration times are longer for the  $C_{18}$  bonded capillary than for the untreated one. This can be attributed to the well-known decrease of the EOF on bonded capillaries [14].

Moreover it can be seen that for a given capillary, the shapes of the plots are very similar

from one compound to another, indicating that each  $\beta$ -agonist shows the same behaviour on changing the buffer pH. Little difference is observed between the two types of capillaries. Indeed, the migration times of all compounds decrease with increasing pH. This is in agreement with an increase of the electroosmotic mobilities with pH [17,19]. Nevertheless, some differences between the two capillaries can be pointed out, especially for the pH range 8–9.

For the uncoated fused-silica capillary, the migration times did not change from pH 5 to pH 6, and then decreased uniformly from pH 6 to pH 9. For the  $C_{18}$  bonded capillary, the migration times decreased gradually with an increase of the pH from 5 to 8. A minimum was observed at pH 8, and then the migration times increased with a further increase of the pH to 8.3. At a pH above 8.6, the migration times decreased again, whereas some little discrepancy could be observed for some of the  $\beta$ -agonists in the pH range 8.3–8.6.

This particular behaviour of the  $\beta$ -agonists on the  $C_{18}$  bonded capillary between pH 8 and 9 remains unexplained. In a study on the separation of metallothioneins on an untreated fused-silica capillary, Liu et al. [20] obtained an incurved graph, which was interpreted to be a consequence of the variations in the ionic strength of the solutions due to the buffer pH titration. In our case, with Tris buffer a decrease in pH corresponds to an increase of the number of ions, and hence an increase in the ionic strength, which results in an increased migration time, as described by Vindevogel and Sandra [21]. Thus, it seems that the migration-time variations between pH 8 and pH 8.6 observed on the  $C_{18}$  capillary are not related to the titration of the Tris buffer.

The increased migration times observed on the  $C_{18}$  bonded capillary at pH 8–8.6 could be tentatively interpreted, considering that for these pH values close to the  $pK_a$  values of  $\beta$ -agonists, some solute partitioning should occur between the running buffer and the hydrophobic octadecyl groups bonded to the capillary wall. Thus, some retention should participate in the separation process, resulting in a kind of electrically

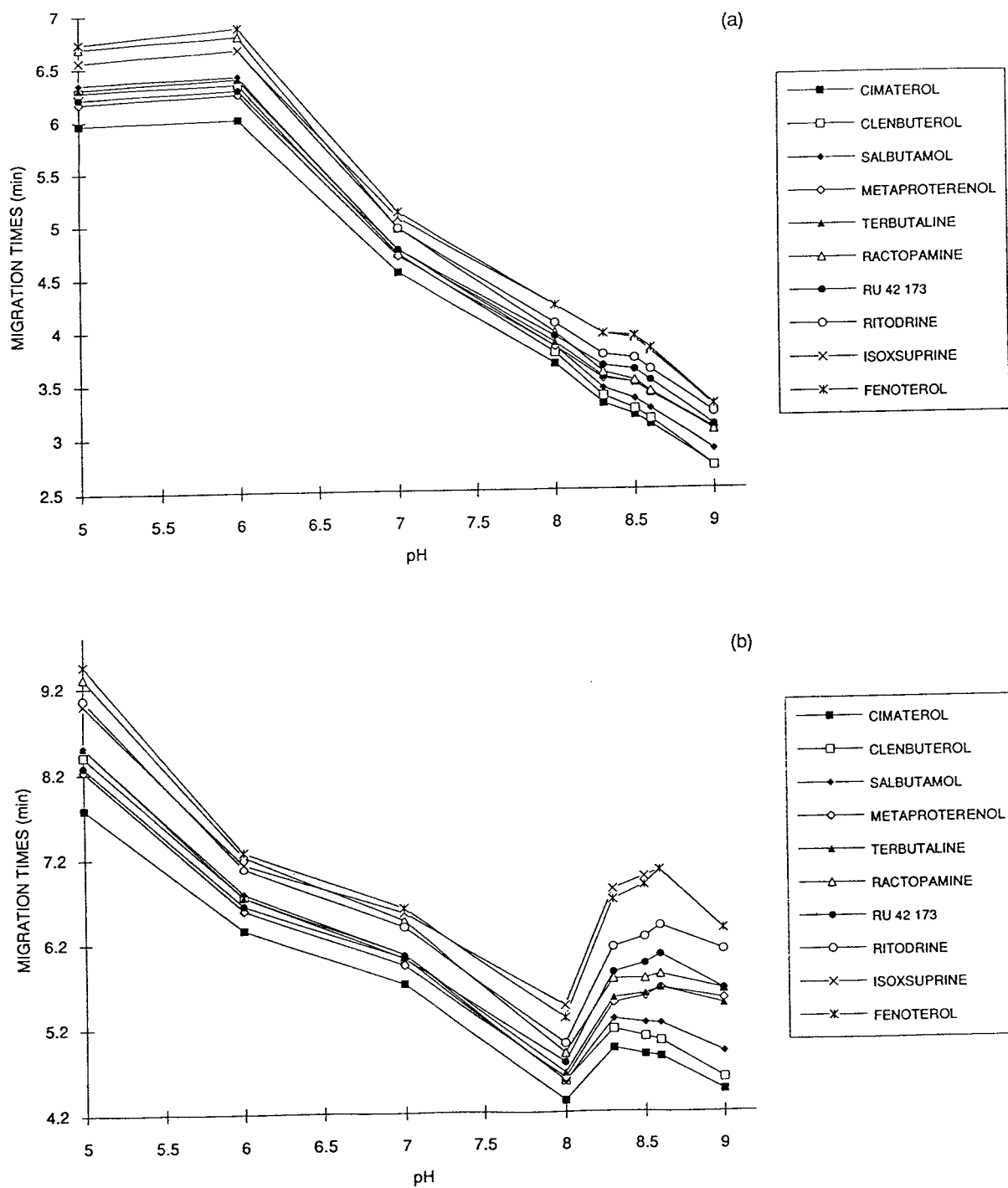


Fig. 2. Plot of migration times of the  $\beta$ -agonists versus pH obtained (a) on fused-silica capillary and (b) on  $C_{18}$  bonded capillary. Conditions: running buffer, Tris 50 mM; voltage, 30 kV; temperature, 25°C; UV detection at 200 nm.

driven open-tubular liquid chromatography as described by Bruin et al. [22].

The elution orders of the  $\beta$ -agonists at pH 5 to pH 9 are shown in Figs. 3a and b, for the uncoated and  $C_{18}$  bonded capillaries respectively, according to a scheme proposed by Lukkari et al. [23]. These orders are identical for the two capillaries for a given pH, although no complete separation could be obtained on the silica capillary. On the other hand, a small change in pH can change the elution order, except for cimaterol which is always eluted first, irrespective of the capillary employed. This effect could result in some limitation concerning the robustness of the separation.

No clear correlation between the migration times and the structure of the  $\beta$ -agonists could be deduced from our experiments, since numerous factors—such as the tendency of some  $\beta$ -agonists to interact with the capillary wall and their ability to form doubly-charged species—pre-

vent precise predictions. Nevertheless, at pH 5, at which one can consider all  $\beta$ -agonists positively charged, the elution order is very close to the order of increasing molecular masses of the compounds. Exceptions are for cimaterol, clenbuterol and RU 42 173 (Fig. 1) which bear two amino groups and thus can be eluted faster.

Finally, complete separation of the mixture of  $\beta$ -agonists can be achieved on the  $C_{18}$  bonded capillary within 6.8 min at pH 8.3. For the untreated fused-silica capillary the optimum pH is also set at 8.3, which allows the separation of nine of the ten  $\beta$ -agonists studied, within 4 min. The electropherograms obtained under these conditions are shown in Figs. 4a and b for the two types of capillaries.

### 3.3. Repeatability

The repeatability of the separations was assessed for the two capillaries and at different pH values. Repeatabilities were estimated from the means and relative standard deviations (R.S.D.), for migration times (MT) and for relative migration times (RMT) calculated relatively to cimaterol:

$$RMT = MT/MT_c$$

where MT is the migration time of the actual  $\beta$ -agonist, and  $MT_c$  is the migration time of cimaterol, for which the RMT is unity. Selected results are shown in Table 1.

The R.S.D. ( $n = 10$ ) of MT values varied from 0.30 to 1.62% for untreated silica and from 0.10 to 2.83% for  $C_{18}$  bonded capillary. For RMT, values ranging from 0.07 to 0.20% and from 0.07 to 0.50% were obtained for the untreated and bonded capillaries, respectively. These values show that highly repeatable separations were obtained on the  $C_{18}$  bonded support as well as on the silica capillary. Moreover, it should be noted that the stability of the MT is better on the bonded capillary for pH values near the optimum value (see bold values in Table 1).

The migration-time drift described in the literature [24] for  $C_{18}$  bonded capillaries, was not observed in this study, especially for pH values close to the optimum pH (8.3). A slight drift was

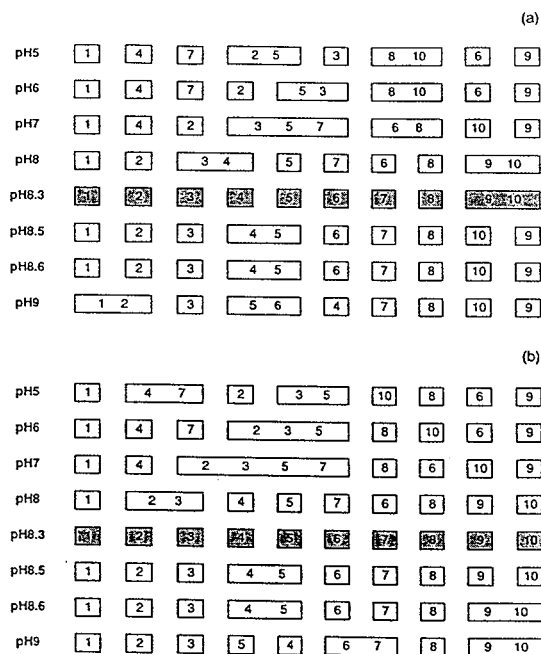


Fig. 3. Elution order of the ten  $\beta$ -agonists from pH 5 to pH 9 obtained (a) on fused-silica capillary and (b) on  $C_{18}$  bonded capillary. Conditions: running buffer, Tris 50 mM; voltage, 30 kV; temperature, 25°C; UV detection at 200 nm. (for compound numbers see Fig. 1).



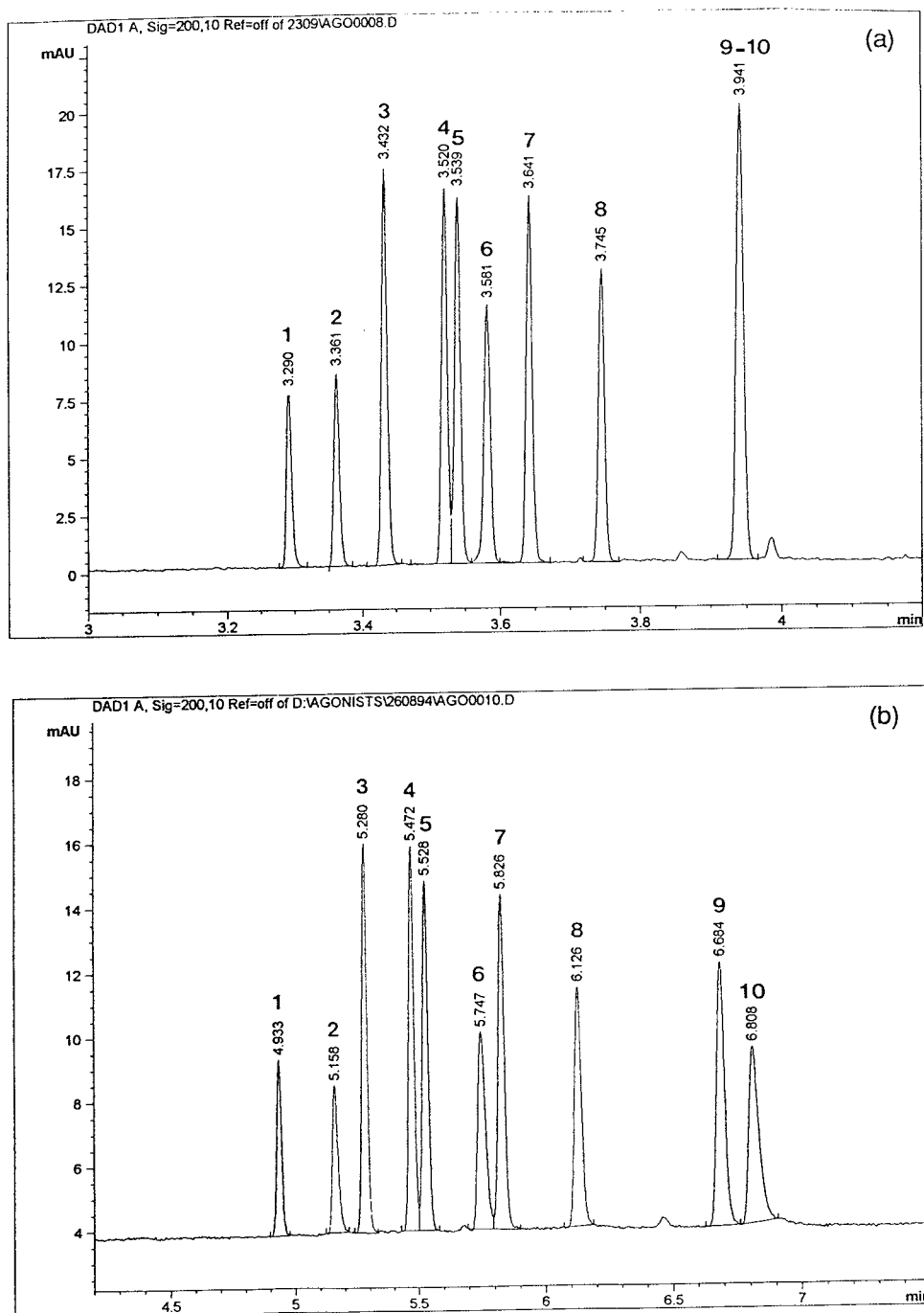


Fig. 4. Electropherograms of the  $\beta$ -agonists mixture obtained (a) on fused-silica capillary and (b) on  $C_{18}$  bonded capillary. Conditions: running buffer, Tris 50 mM (pH 8.3); voltage, 30 kV; temperature, 25°C; UV detection at 200 nm.

Table 1  
Selected results of relative standard deviations (R.S.D.) of migration times (MT) and relative migration times (RMT)

		Metaproterenol			Terbutaline			RU 42173		
		pH 5	pH 7	pH 8.3	pH 5	pH 7	pH 8.3	pH 5	pH 7	pH 8.3
R.S.D. (%)	MT silica	0.41	0.33	1.45	0.41	0.32	1.49	0.42	0.32	1.52
	MT C <sub>18</sub>	2.5	2.08	<b>0.15</b>	2.61	2.13	<b>0.14</b>	2.52	2.07	<b>0.17</b>
R.S.D. (%)	RMT silica	0.07	0.07	0.1	0.18	0.09	0.11	0.08	0.09	0.14
	RMT C <sub>18</sub>	0.18	0.13	<b>0.07</b>	0.25	0.19	<b>0.07</b>	0.26	0.13	<b>0.09</b>

nevertheless observed at pH 5, which is the cause of the higher R.S.D. values obtained for RMT at this pH (Table 1).

The performance stability of the two systems was also assessed from the separation efficiency, measured by the number of theoretical plates according to the formula:

$$N = 5.54(MT/w_{h1/2})^2$$

where  $N$  is the number of theoretical plates and  $w_{h1/2}$  is the peak width at half-height.

The results indicated that for the two capillaries, best efficiencies were obtained at pH 8.3. At this pH, efficiencies vary between 200 000 and 500 000 theoretical plates, which corresponds to approximately 350 000–800 000 theoretical plates per meter of capillary. As a general rule, slightly better efficiencies are obtained with the untreated silica capillary, irrespective of the pH selected. However, especially at the optimum pH, a constant decrease in efficiency was observed from injection to injection for the silica capillary (Fig. 5). This phenomenon was not

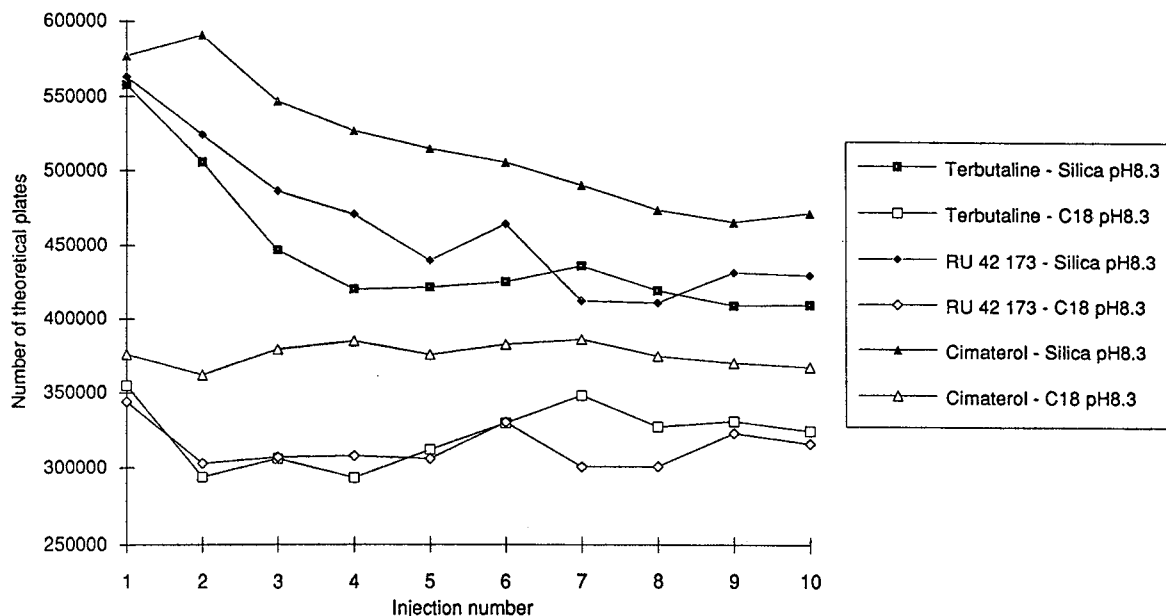


Fig. 5. Number of theoretical plate versus injection number on fused-silica capillary (filled symbols) and on C<sub>18</sub> bonded capillary (open symbols).

observed for the bonded capillary, which showed a stable performance over time (Fig. 5), resulting in better R.S.D. values of the efficiency.

Adsorption phenomena on fused-silica capillary walls have been extensively described [17,24], and they seem to occur not only for proteins, but also for small ionic molecules like  $\beta$ -agonists, in spite of frequent sodium hydroxide rinsing. In the case of the  $C_{18}$  bonded capillary, adsorption is much less important and performance stability seems better, and sodium hydroxide rinsing between runs is unnecessary.

To evaluate the suitability of the method for quantitative determinations, we measured the peak areas of each  $\beta$ -agonist. Normalized peak areas (NPAs) (i.e. peak areas divided by migration times [15,25]) were used in mean and R.S.D. calculations ( $n = 9$ ).

Table 2 shows the mean and R.S.D. values of NPAs calculated for cimaterol, RU 42 173 and ractopamine at two different pH values. Results show that NPA values obtained on the fused-silica capillary are always lower than on the  $C_{18}$  bonded capillary for all  $\beta$ -agonist studied. This observation is quite surprising since the two columns have identical internal diameters (50  $\mu\text{m}$ ) as well as external diameters (360 and 363  $\mu\text{m}$ , respectively). It may, however, be consistent with an adsorption phenomenon as revealed by the previously mentioned need to frequently rinse the silica capillary. Moreover, adsorption would be associated with lower theoretical plate numbers; work is in progress to tentatively explain this discrepancy.

The R.S.D. values vary in the same range (i.e. between 0.5 and 2.5%, depending on the compound considered) for the two pH values and the two capillaries. Although HPLC has been mentioned to give even better results [10], these values indicate a good precision of the method for quantitative purposes, taking into account the low concentration test mixture employed in this study (10  $\mu\text{g ml}^{-1}$ ). The use of higher sample concentrations would give better R.S.D. values since in CE it is well known that peak area precision improves with increased sample concentration [26,27].

#### 4. Conclusion

Good separation of the  $\beta$ -agonists studied was obtained with both capillary systems under the conditions applied. The ten  $\beta$ -agonists studied can be separated with high efficiency in less than 7 min, with good repeatability. The ten peaks are baseline resolved in a migration window of less than 120 s using a  $C_{18}$  bonded silica capillary.

For separation of  $\beta$ -agonists, capillary electrophoresis was found to give significantly higher efficiency and speed compared to HPLC which requires the use of an ion-pairing agent [6–8]. The present CZE method offers certain advantages, including simple background electrolyte preparation, and does not require the long preconditioning and stabilization periods which are needed in ion-pairing HPLC.

Table 2  
Selected results of means and R.S.D. of normalized peak areas (NPA) on fused and  $C_{18}$  bonded silica capillaries

pH		NPA-silica		NPA- $C_{18}$	
		Means	R.S.D. (%)	Means	R.S.D. (%)
5	Cimaterol	1.34	1.81	1.61	0.9
	RU 42 173	2.74	2.07	3.31	0.78
	Ractopamine	2.51	0.56	2.58	1.29
8.3	Cimaterol	1.34	1.42	1.45	1.67
	RU 42 173	2.82	1.95	3.04	1.87
	Ractopamine	2.12	1.54	2.24	1.13

The use of the C<sub>18</sub> bonded capillary seems advantageous compared to the untreated capillary taking into account its greater stability, which results in a greater reproducibility with time. However, some potential drawbacks, such as batch-to-batch variability or coating stability, should be considered for this type of capillary which is still not widely used. Rinsing between runs was found to be necessary for the untreated fused-silica capillary, in order to bring the system back to the initial conditions, to keep the current constant from run to run, and to reduce adsorption on the capillary wall. Also the fact that no between-run rinsing is needed makes the C<sub>18</sub> bonded capillary easier to use.

## References

- [1] L.O. Fiems, *Ann. Zootech.*, 36 (1987) 271.
- [2] M.H. Lamoree, N.J. Reinhoud, U.R. Tjaden, W.M.A. Niessen and J. van der Greef, *Biol. Mass Spectrom.*, 23 (1994) 339.
- [3] M.C. Dumasia and E. Houghton, *J. Chromatogr.*, 564 (1991) 503.
- [4] L.A. van Ginkel, R.W. Stephany and H.J. van Rossum, *J. Assoc. Off. Anal. Chem.*, 75 (1992) 554.
- [5] M.P. Montrade, B. Le Bizec, F. Monteau, B. Siliart and F. Andre, *Anal. Chim. Acta*, 275 (1993) 253.
- [6] W. Haasnoot, M.E. Ploum, R.J.A. Paulussen, R. Schilt and F.A. Huf, *J. Chromatogr.*, 519 (1990) 323.
- [7] R.N. Gupta, H.D. Huller and M.B. Dolovich, *J. Chromatogr. A*, 654 (1994) 205.
- [8] L. Debrauwer, G. Delous and G. Bories, *Chromatographia*, 36 (1993) 218.
- [9] L. Debrauwer and G. Bories, *Anal. Chim. Acta*, 275 (1993) 231.
- [10] M.T. Ackermans, J.T. Beckers, F.M. Everaerts and I.G.J.A. Seeten, *J. Chromatogr.*, 590 (1992) 341.
- [11] K.D. Altria, *J. Chromatogr.*, 634 (1993) 323.
- [12] M.M. Rogan, K.D. Altria and D.M. Goodall, *Electrophoresis*, 15 (1994) 808.
- [13] A. Aumatell, R.J. Wells and D.K.Y. Wong, *J. Chromatogr. A*, 686 (1994) 293.
- [14] A.M. Dougherty, C.L. Wolley, D.L. Williams, D.F. Swaile, R.O. Cole and M.J. Sepaniak, *J. Liq. Chromatogr.*, 14 (1991) 907.
- [15] G.M. MC Laughlin, J.A. Nolan, J.L. Lindahl, R.H. Palmieri, K.W. Anderson, S.C. Morris, J.A. Morrison and T.J. Bronzert, *J. Liq. Chromatogr.*, 15 (1992) 961.
- [16] K.D. Altria and D.C.M. Luscombe, *J. Pharm. Biomed. Anal.*, 11 (1993) 415.
- [17] S.F.Y. Li, *Capillary Electrophoresis: Principles, Practice and Applications*, Elsevier, Amsterdam, 1992.
- [18] P. Lukkari, A. Ennelin, H. Sirén and M.-L. Riekkola, *J. Liq. Chromatogr.*, 16 (1993) 2069.
- [19] K. Otsuka and S. Terabe, *J. Microcol. Sep.*, 1 (1989) 150.
- [20] G.-Q. Liu, W. Wang, X.-Q. Shan, *J. Chromatogr. A*, 653 (1994) 41.
- [21] J. Vindevogel and P. Sandra, *J. Chromatogr.*, 541 (1991) 483.
- [22] G.J.M. Bruin, P.P.H. Tock, J.C. Kraak and H. Poppe, *J. Chromatogr.*, 517 (1990) 557.
- [23] P. Lukkari, H. Vuorela, M.-L. Riekkola, *J. Chromatogr. A*, 652 (1993) 451.
- [24] N.A. Guzman (Editor), *Capillary Electrophoresis Technology*, Chromatographic Science Series, Marcel Dekker, New York, NY, 1993.
- [25] K.D. Altria, *Chromatographia*, 35 (1993) 177.
- [26] H. Wätzig and C. Dette, *J. Chromatogr.*, 636 (1993) 31.
- [27] K.D. Altria, R.C. Harden, M. Hart, J. Hevizi, P.A. Hailey, J.V. Makwana and M.J. Portsmouth, *J. Chromatogr.*, 641 (1993) 147.



ELSEVIER

Journal of Chromatography A, 715 (1995) 355–360

JOURNAL OF  
CHROMATOGRAPHY A

# Determination of aminopyrine and its metabolite by capillary electrophoresis–electrochemical detection

Weihong Zhou, Jun Liu, Erkang Wang\*

*Laboratory of Electroanalytical Chemistry, Changchun Institute of Applied Chemistry, Chinese Academy of Sciences, Changchun 130022, China*

First received 8 December 1994; revised manuscript received 18 May 1995; accepted 19 May 1995

## Abstract

An electrochemical pretreatment regime for a cylindrical carbon fibre microelectrode was optimized for the determination of aminopyrine (AM) and its metabolite 4-aminoantipyrine (AAN) by capillary electrophoresis (CE)–electrochemical detection (ED). Under optimized conditions, a response of high sensitivity and stability was obtained for AM and AAN at a detection voltage as low as 0.9 V following CE–ED, by which AM and AAN were separated satisfactorily. The calibration graph was linear over three orders of magnitude and the limits of detection for AM and AAN were in the femtomole range.

## 1. Introduction

Aminopyrine has been widely used as an analgesic and antipyretic drug, and one of its major metabolites in human fluids is 4-aminoantipyrine. Several methods have been developed for the determination of AM and AAN [1–7], such as spectrophotometry [1], thin-layer chromatography [2], gas chromatography–mass spectrometry [3] and high-performance liquid chromatography [4–7].

Since its introduction over a decade ago, capillary electrophoresis (CE) has been shown to be a powerful tool for the separation of a wide range of analytes, and has become a very important technique in the area of liquid-phase separations. To make full use of its advantages, sensitive detection systems are required. Although much of the research in CE has been

carried out with UV detection, these detectors lack sensitivity because of their path-length-dependent response. Laser-based fluorescence detectors can provide more sensitive detection but are limited to analytes with fluorescence. Originally described by Wallingford and Ewing [8], electrochemical detection (ED) has an advantage over these methods in that the response is not dependent on pathlength, so both sensitivity and selectivity can be provided.

The carbon fibre microelectrode has been widely used in CE–ED, but the surface of the electrode changes with time owing to adsorption of species from solution. These changes often result in variations in sensitivity or reversibility and sometimes lead to complete inhibition of charge transfer. In order to observe reproducible and well defined electrochemical behaviour, pretreatment of carbon fibre microelectrodes is required.

A variety of methods have been devised for

\* Corresponding author.

pretreating solid electrodes, including polishing, electrochemical treatment, chemical treatment, flaming, vacuum heat treatment, radiofrequency plasma treatment and laser treatment. Electrochemical pretreatment has been used successfully for the activation of carbon fibre microelectrodes [9,10]. For CE–ED it is very convenient to use electrochemical pretreatment because it can be performed while the microelectrode is inserted in the capillary column with the buffer flowing past its surface.

The purpose of the work reported here was to investigate various parameters concerning the electrochemical pretreatment of carbon fibre microelectrodes for the determination of AM and AAN. Electrochemical activation was evaluated with respect to duration of applied potential, potential range and solution conditions.

## 2. Experimental

### 2.1. Apparatus

The power supply (Beijing Strong Biological and Electronic) provided a 30 kV d.c. high voltage. An uncoated fused-silica capillary of 50  $\mu\text{m}$  I.D. was obtained from Yongnian Optical Fibre Factory (Hebei, China). The CE–ED system has been described previously [11]. The electrochemical detector is isolated from the applied electrical field by using a Nafion joint as described by O'Shea et al. [12]. This joint is positioned in the cathodic buffer reservoir and permits ion movement but not bulk electrolyte flow. Both the Nafion joint and electrochemical cell were shielded in an aluminium box to reduce external noise. An EI-400 dual microelectrode potentiostat (Ensmen Instrumentation) was used as an amperometric detector. A Model 056 recorder (Hitachi) was used.

The electrochemical cell is similar to that described by Wallingford and Ewing [13]. Electrochemical detection was performed with 30  $\mu\text{m}$  diameter carbon fibres protruding 1–2 mm from drawn glass capillaries as the working electrodes.

The microelectrode was mounted on an X–Y–Z micromanipulator (laboratory-built) and positioned in the electrochemical detection cell. With the aid of an optical microscope, the microelectrode was aligned and inserted into the capillary column. The cell was operated in a two-electrode configuration, with an Ag–AgCl reference electrode. UV–Vis detection was carried out on a CV<sup>4</sup> capillary absorbance detector (ISCO).

Sample introduction was accomplished using an electromigration system and the volume injected was calculated in the continuous fill mode by recording the time required for the sample to reach the detector.

### 2.2. Cyclic voltammetry

Cyclic voltammetric experiments were performed in a three-electrode system cell. A platinum wire was employed as the auxiliary electrode. Cyclic voltammetry was used to evaluate the effect of various electrochemical pretreatments on the chemical nature and electrochemical reversibility of electrochemically treated carbon fibre surfaces.

### 2.3. Reagents

AM and AAN were obtained from Beijing Chemical. All reagents were of analytical-reagent grade and were used as received. All solutions were prepared with doubly distilled water and passed through a membrane filter (0.45  $\mu\text{m}$ ) before use. Phosphate solution (4 mM) was used as the separation buffer and was adjusted to the appropriate pH with phosphoric acid.

### 2.4. Sample preparation

Human urine samples were diluted immediately in 4 mM buffer (1:5) and filtered with a 2- $\mu\text{m}$  pore size filter. This solution was injected directly on to the capillary column.

### 3. Results and discussion

#### 3.1. Effect of pretreatment parameters

Electrochemical pretreatment methods involve anodization, anodization followed by cathodization, alternating potential applying a triangular or square wave form to the microelectrode, etc. However, simply holding the microelectrode at positive potentials can give good results. Fig. 1 shows cyclic voltammograms of (A) AM and (B) AAN at (a) untreated and (b) anodized carbon fibre microelectrodes. It can be seen that the peak obtained with the pretreated electrode was much higher than that with the untreated electrode. AM yields irreversible oxidation waves at ca. 0.7 and 1.3 V and AAN at 0.5 and 1.1 V on the pretreated electrode, revealing a significant improvement in magnitude and sharpness of the anodic peaks. Several workers have noted that anodic pretreatment of glassy carbon electrodes introduces oxygen functionalities, including hydroxyl, carbonyl and carboxyl groups, on the surface [14,15]. The work of Rice et al. [16] on carbon paste electrodes [16] indicated that anodic pretreatment made the graphite surface more hydrophilic, thus removing some of the

adherent organic layer. The activation of the pretreated carbon fibre electrode in our work may also be as a result of the introduction of oxygen functionalities and the removal of passivating layers that hinder electron transfer.

The dependence of the peak current of both AM and AAN on the pH of the buffer solution illustrates that the peak current decreased with increase in pH. This may be the reason why anodic treatments in acidic media can produce a greater increase in carbon–oxygen bonds than that in neutral or basic pH buffers. Because a low pH of the solution leads to comparatively long migration times, pH 5 was selected in the CE separation.

Apart from pH, other treatment parameters had few effects on AM. The effect of the treatment conditions on AAN is illustrated in Fig. 2. The data points on the graphs were obtained with the same microelectrode; once inserted into the outlet of the capillary and positioned in the direction cell, the same electrode was used in CE–ED without replacement. The duration of pretreatment was evaluated for periods ranging from 15 to 60 s. As shown in Fig. 2A, after 30 s there was no improvement in sensitivity and actually a decline in the peak

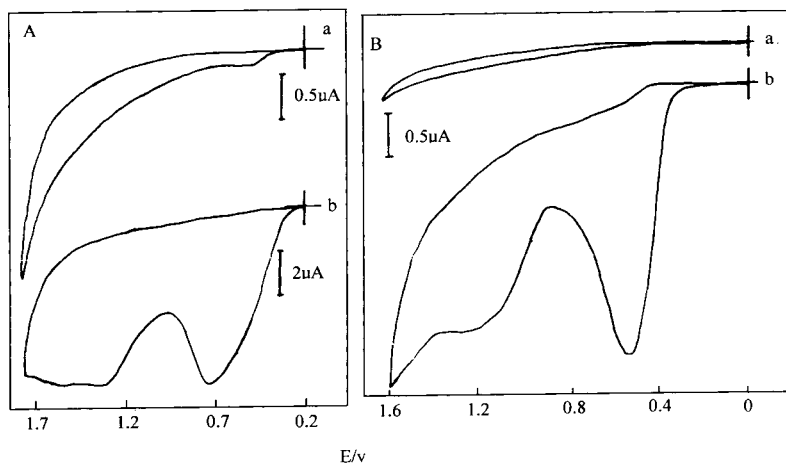


Fig. 1. Cyclic voltammograms of (A)  $10^{-3}$  M AM and (B)  $10^{-3}$  M AAN obtained at carbon fibre microelectrodes (a) untreated and (b) treated at 1.5 V for 30 s. Supporting electrolyte, 4 mM phosphate buffer (pH 4.82); scan rate,  $100 \text{ mV s}^{-1}$ ; electrode diameter,  $30 \mu\text{m}$ .  $E$  (V) vs. Ag–AgCl.

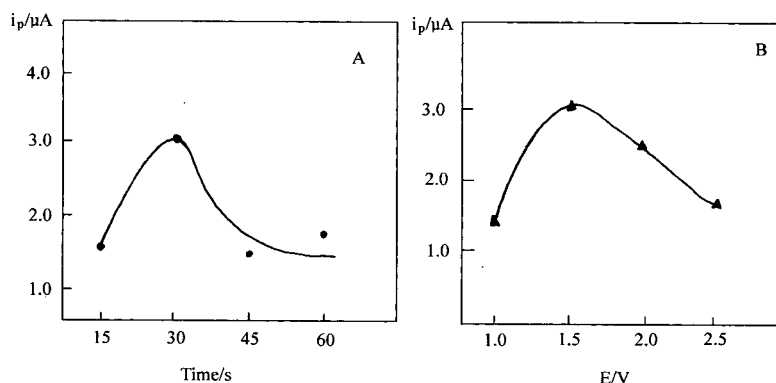


Fig. 2. Effect of AAN treatment conditions: (A) pretreatment time and (B) upper potential limit. Supporting electrolyte, 4 mM phosphate buffer (pH 4.82); analyte concentration, 1 mM; electrode diameter, 30  $\mu\text{m}$ .

current occurred. Such a process has also been observed on carbon fibre microelectrodes by other workers [9,10]. We assumed that with the increase in oxygen functionalities on the microelectrode by anodization, the electrode surface was cleaned and possessed more active sites than before, but with the increasing time, more and more oxygen functionalities were introduced and thus might have formed a passivating film coating on the surface, which would deactivate the electrode. A maximum point was also observed when we investigated the effect of potential limits (Fig. 2B). An increase in the voltammetric response was obtained on changing the potential limit from 0 to 1.5 V, followed by a gradual decrease in current.

In order to be practical for routine applications in capillary electrophoresis, the initial catalytic activity should be maintained over a long period of time. After pretreatment, the electrode was kept in the buffer for 3–20 min. An equilibration period is necessary for a more stable response. The electrode showed a steady response after being kept in buffer for over 5 min and retained its catalytic activity for 15 min.

The pretreatment conditions selected as optimum were a potential of 1.5 V for 30 s in pH 5 buffer and maintaining the treated electrode in buffer for 5 min or longer. Using the optimum pretreatment between each scan, the response

was constant with the precision, calculated as the relative standard deviation, being better than 1.8% for AAN.

### 3.2. CZE with electrochemical detection

Insufficient stability and reproducibility are often drawbacks of electrochemical detectors. Fig. 3 shows the stability of the electrochemically treated electrode after one pretreatment. The

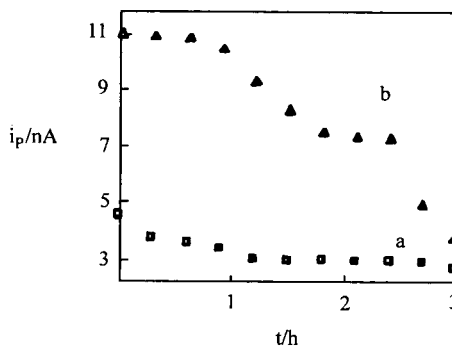


Fig. 3. CE-ED peak current change for (a) 0.5 mM AM and (b) 1 mM AAN at an electrochemically pretreated carbon fibre microelectrode. 50  $\mu\text{m}$  I.D. capillary; 33 cm long separation capillary; 1.7 cm detection capillary; injection by electromigration, 10 s at 12 kV; separation voltage, 12 kV; 4 mM phosphate buffer (pH 4.82).



activity of treated electrodes used in the CE–ED system was observed to decrease slightly with time for AM within 3 h after eleven successive injections, but for AAN it changed quickly. It is recommended that pretreatment be performed between each run. The detector response was also found to be very reproducible when the electrode was pretreated between injections.

The effect of the CZE flow conditions on the anodic current response as a function of the applied potential was examined by means of hydrodynamic voltammograms (HDVs) as shown in Fig. 4. The HDVs obtained under CZE conditions for AM and AAN were peak-shaped and reached their maximum current at 0.91 and 1.2 V, respectively. Because high potential give rise to a higher background current, 0.9 V was selected for the simultaneous determination of AM and AAN. Under the optimized conditions, a response of high sensitivity and stability was obtained for AM and AAN at a detective voltage as low as 0.9 V following CE–ED, by which AM and AAN were separated satisfactorily in short capillary length and eluted within 5 min as shown in Fig. 5. Regression analysis for AM

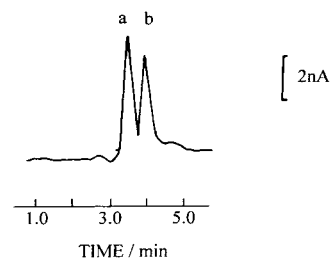


Fig. 5. Electropherogram of (a) AM ( $1 \cdot 10^{-3}$  M) and (b) AAN ( $1 \cdot 10^{-3}$  M). Other conditions as in Fig. 4.

over the concentration range  $5 \cdot 10^{-5}$ – $1 \cdot 10^{-2}$  M (based on an injection volume of 14.4 nl, corresponding to 144–144 pmol) resulted in a correlation coefficient of 0.984 ( $n = 6$ ). Regression analysis for AAN over the range of 430 fmol–172 pmol resulted in a correlation coefficient of 0.995 ( $n = 6$ ). The slope of the curves obtained was 8.24 nA/mM for AM and 7.15 nA/mM for AAN. Detection limits of 0.40 pg for AM and 1.46 pg for AAN were estimated (signal-to-noise ratio = 3).

To compare the sensitivity of ED with UV–Vis absorbance detection, an on-column UV detector (234 nm) was used under the same separation conditions as in CE–ED. The detection limit with the UV–Vis method was  $1 \cdot 10^{-4}$  M, corresponding to 142 pg for AM and 111 pg for AAN. The mass detection limits with CE–ED are also more sensitive than those obtained by LC–ED in previous studies with an unmodified electrode (10 ng or  $4.3 \cdot 10^{-6}$  M for AM [6]) and a glassy carbon electrode dispersed with  $\alpha$ -alumina particles (1.4 ng or  $3.0 \cdot 10^{-7}$  for AM and 0.8 ng or  $2.0 \cdot 10^{-7}$  M for AAN [7]).

To evaluate the performance of the system for the analysis of real samples, the detection of AM and AAN added to human urine sample was studied. Fig. 6A illustrates a typical electropherogram obtained at a carbon fibre electrode for a diluted (1:5) urine sample from a healthy female volunteer. Also shown for comparison (Fig. 6B) is the electropherogram of a urine sample with  $6 \cdot 10^{-5}$  M AM and AAN added. Good sensitivity and selectivity can be achieved

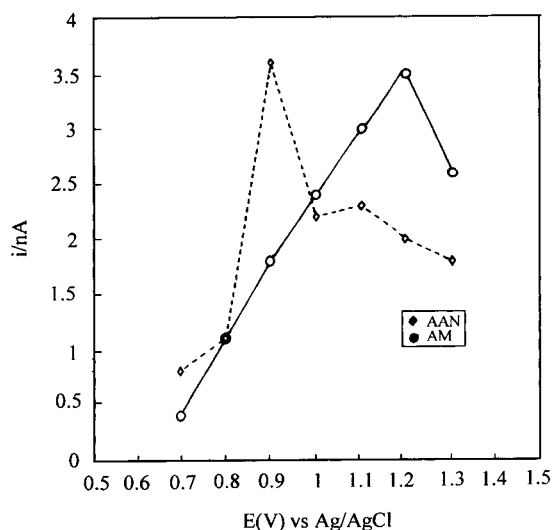


Fig. 4. Hydrodynamic voltammograms of 0.01 M each of AM and AAN at a carbon fibre microelectrode. Injection by electromigration, 5 s at 12 kV; other conditions as Fig. 3.

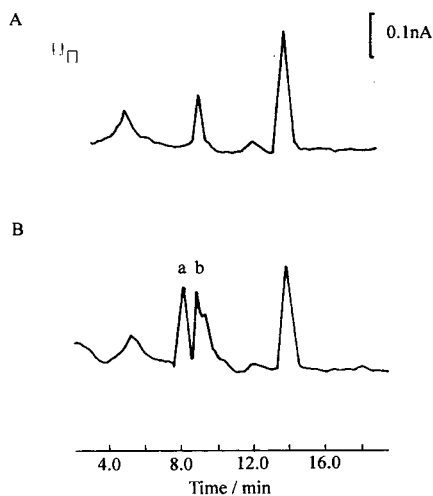


Fig. 6. Electropherogram of (A) diluted (1:5) urine sample and (B) urine sample with (a)  $6 \cdot 10^{-5}$  M AM and (b)  $6 \cdot 10^{-5}$  M AAN added. 52 cm long separation capillary; 1.5 cm detection capillary; other conditions as in Fig. 3.

with application of the proposed method to the determination of the drug in urine.

#### 4. Conclusion

This is the first report dealing with the detection of AM and AAN using CE–ED. The method has proved to have good reproducibility, a wide linear response range and low mass detection limits at a lower detection voltage compared with LC–ED [6,7].

#### Acknowledgement

This project was supported by the National Natural Science Foundation of China.

#### References

- [1] B.B. Brodie and J. Axelrod, *J. Pharmacol. Exp. Ther.*, 99 (1950) 171.
- [2] R. Gradnik and L. Fleischmann, *Pharm. Acta Helv.*, 48 (1973) 181.
- [3] T. Goromaru, T. Furuta, S. Baba, A. Noda and S. Iguchi, *Chem. Pharm. Bull.*, 29 (1981) 1724.
- [4] K. Inoue, K. Fujimori, K. Mizokami, M. Sunouchi, A. Takanaka and Y. Omori, *J. Chromatogr.*, 274 (1983) 201.
- [5] N. Miyagi, N. Hikich and H. Niwa, *J. Chromatogr.*, 375 (1986) 1.
- [6] E. Wang and J. Zhou, *Microchem. J.*, 42 (1990) 259.
- [7] H. Li and E. Wang, *Electroanalysis*, in press.
- [8] R.A. Wallingford and A.G. Ewing, *Anal. Chem.*, 59 (1987) 1762.
- [9] J. Wang, P. Tuzhi and V. Villa, *J. Electroanal. Chem.*, 234 (1987) 119.
- [10] T.J. O'Shea, A.C. Garcia, P.T. Blanco and M.R. Smyth, *J. Electroanal. Chem.*, 307 (1991) 63.
- [11] W. Zhou, L. Xu, M. Wu, L. Xu and E. Wang, *Anal. Chim. Acta*, 299 (1994) 189.
- [12] T.J. O'Shea, R.D. Greenhagen, S.M. Lunte and C.E. Lunte, *J. Chromatogr.*, 593 (1992) 305.
- [13] R.A. Wallingford and A.G. Ewing, *Anal. Chem.*, 60 (1988) 258.
- [14] R.C. Engstrom and V.A. Strasser, *Anal. Chem.*, 56 (1984) 136.
- [15] T. Nagaoka and T. Yoshino, *Anal. Chem.*, 58 (1986) 1037.
- [16] M.E. Rice, Z. Gulus and R.N. Adams, *J. Electroanal. Chem.*, 143 (1983) 89.

Short communication

# GABA-B agonists: enantiomeric resolution of 4-amino-3-(5-chlorothien-2-yl)butyric acid and analogues on chiral crown ether stationary phase

Claude Vaccher\*, Pascal Berthelot, Michel Debaert

*Laboratoire de Pharmacie Chimique, Université de Lille II, BP 83, 3 rue du Pr. Laguesse, 59006 Lille Cédex, France*

First received 21 April 1995; revised manuscript received 23 May 1995; accepted 23 May 1995

## Abstract

The enantiomeric resolution of 4-amino-3-(5-chlorothien-2-yl)butyric acid, an analogue of baclofen [4-amino-3-(4-chlorophenyl)butyric acid], was examined by HPLC using a chiral stationary phase consisting of a crown ether and perchloric acid–methanol as the mobile phase. Optimization of the separation was achieved by variation of temperature, pH and eluent composition. The absolute configuration may be assigned by comparison with authentic enantiomers of baclofen of known absolute configuration. The best results obtained were  $\alpha = 1.15$  and  $R_s = 2.72$  at 20°C with  $\text{HClO}_4$  (pH 1.3)– $\text{CH}_3\text{OH}$  (90:10). The study was extended to analogues, viz., 3-(substituted thienyl) and 3-(substituted furanyl)-4-amino acids.

## 1. Introduction

Following our interest in the preparation of 4-amino acids (4-AAs), we recently described [1] potent and specific GABA<sub>B</sub> receptors agonists 1–5 [2]; the most efficient one, 3 (Fig. 1), was commercially available as the racemate from Tocris-Cookson (Langford, Bristol, UK) until 1991 and is used as a neurochemical ligand in pharmacology. As this molecule has a chiral centre, a detailed investigation of its pharmacodynamic properties could require a knowledge of the individual biological behaviour of each of the enantiomers. This kind of research in the GABA<sub>B</sub> field has recently received much attention [3,4]. As a first step, a method has to be developed that would allow the chromatographic

separation of these optical isomers. In order to obtain a more rapid method, the direct resolution, without any prederivatization, of the enantiomeric components was studied with a newly introduced phase using a chiral crown ether moiety as chiral selector.

In this paper, we describe the direct separation and an optimization study of the potent 4-AA 3 and its comparison with the less active 4-AAs 1 and 2 and the inactive 4-AAs 4 and 5, in order to collect information about the influence on the chromatographic parameters of the heteroaromatic ring and substituents.

## 2. Experimental

Chromatographic resolution was accomplished with an LKB 2249 metering pump and detection

\* Corresponding author.

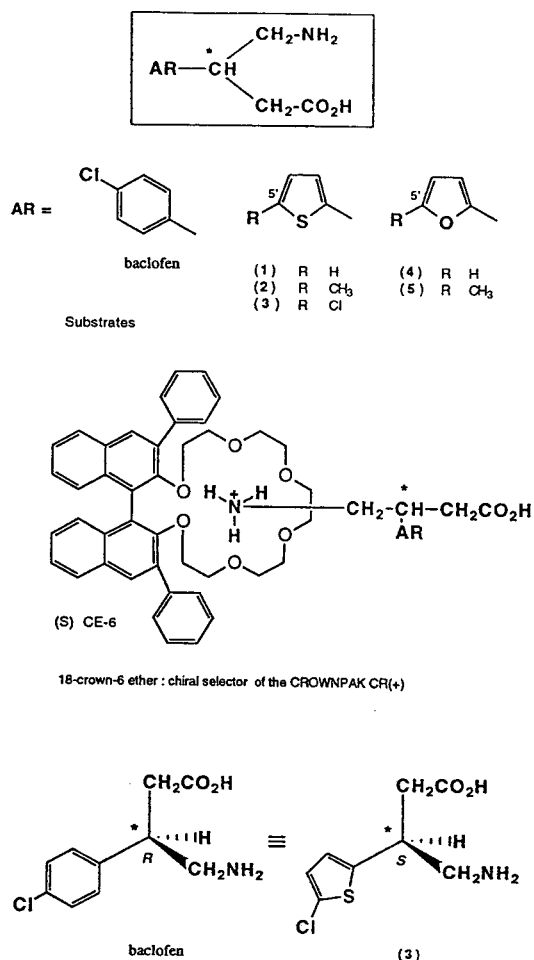


Fig. 1. Structures of substrate 4-AAs and of the selector and illustration of nomenclature.

with an HP 1040 photodiode-array spectrophotometer connected to an HP 9000 S300 computer. The column eluate was monitored at 225, 220 and 200 nm (4 nm bandwidth) with a reference at 550 nm (100 nm bandwidth). The column was Crownpak CR(+) (5  $\mu$ m) (150  $\times$  4 mm I.D.) packed with a chiral stationary phase (CSP) composed of a chiral crown ether (Fig. 1) (Daicel Chemical Industries, Baker, France). The sample loop was 10  $\mu$ l (Rheodyne Model 7125 injector). Elution was carried out isocratically using perchloric acid at the required pH and methanol at a flow-rate of 0.9 ml/min. The temperature of the column was controlled with

water circulating through a jacket surrounding the column.

Baclufen and its enantiomers were kindly supplied by Ciba-Geigy. The 4-AAs 1–5 were obtained as described previously [1]. Water was purified through a Milli-Q unit (Millipore). Methanol was of gradient grade from Merck and perchloric acid was of analytical-reagent grade from Prolabo. All the solutions were filtered (0.45  $\mu$ m), degassed and purged with helium. All amino acids were dissolved in the mobile phase at a concentration of about 1.6 mM (which corresponds to  $1.6 \cdot 10^{-8}$  mol injected) and passed through a 0.45- $\mu$ m membrane filter prior to injection. To prevent corrosion and decomposition of the stationary phase, the column and all

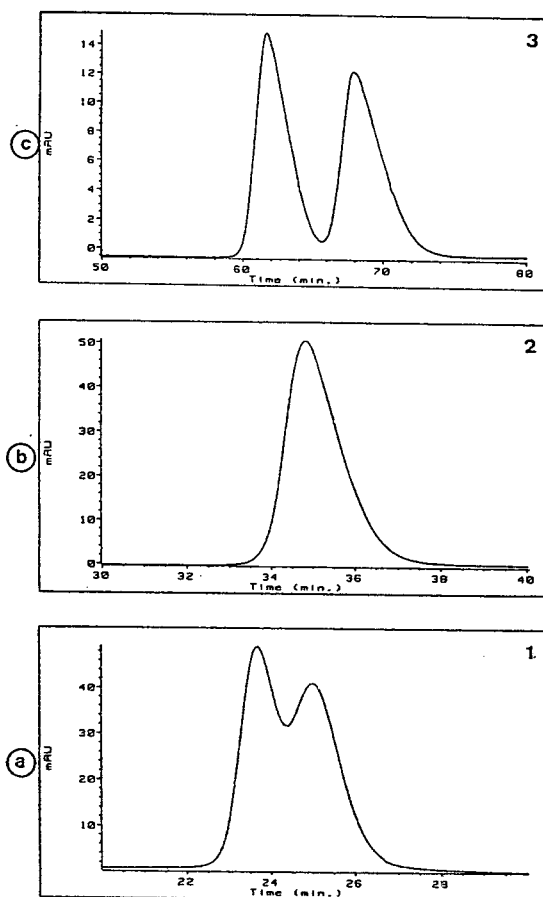


Fig. 2. Chromatograms obtained for (a) 1 (eluent D; 10°C); (b) 2 (eluent D; 20°C); (c) 3 (eluent A; 20°C).

Table 1  
Analytical HPLC: retention factors ( $k'$ ), enantioselectivity ( $\alpha$ ) and resolution ( $R_s$ ) of compounds 1–5

Compound	Eluent <sup>a</sup>	10°C			20°C			30°C			40°C		
		$k'_1$	$\alpha$	$R_s$	$k'_1$	$\alpha$	$R_s$	$k'_1$	$\alpha$	$R_s$	$k'_1$	$\alpha$	$R_s$
Baclofen	A				37.0	1.84	10.02	25.4	1.65	8.07	17.4	1.48	6.11
1	A				8.40	1	– <sup>b</sup>	5.57	1	– <sup>b</sup>			
	B				5.33	1	– <sup>b</sup>						
	C				7.66	1.05	0.81						
	D	15.44	1.06	0.91	8.55	1.06	0.91						
2	A				25.20	1	– <sup>b</sup>	15.70	1	– <sup>b</sup>			
	B				14.50	1	– <sup>b</sup>						
	C				20.50	1	– <sup>b</sup>						
	D	41.76	1	– <sup>b</sup>	23.34	1	– <sup>b</sup>						
3	A				36.50	1.11	1.76	23.56	1.10	1.34	15.25	1.09	1.21
	B				21.40	1.15	1.90						
	C				34.80	1.15	2.72						
4	A				3.93	1.09	0.86						
	B				2.66	1.09	0.66	1.70	1.07	0.48	1.12	1	– <sup>b</sup>
5	A				10.46	1.15	1.64						
	B				6.47	1.18	1.52	4.08	1.15	1.21	2.64	1.12	0.98

$k' = (t_x - t_0)/t_0$ ;  $\alpha = (t_2 - t_0)/(t_1 - t_0)$ ;  $R_s = 2(t_2 - t_1)/(w_1 + w_2)$ , where  $w$  = width at baseline,  $t_0$  = retention time of an unretained compound and  $t_x$  = retention times of compounds,  $S$  or  $R$ .

<sup>a</sup> Eluent A = HClO<sub>4</sub> (pH 2); eluent B = HClO<sub>4</sub> (pH 2)–CH<sub>3</sub>OH (90:10); eluent C = HClO<sub>4</sub> (pH 1.3)–CH<sub>3</sub>OH (90:10); eluent D = HClO<sub>4</sub> (pH 1.1)–CH<sub>3</sub>OH (90:10).

<sup>b</sup> No resolution.

the apparatus were thoroughly washed with water at the end of every day.

### 3. Results and discussion

The enantiomeric separation of 4-AAs 1–5 on the crown ether CSP is summarized in Table 1 and shown in Figs. 2 and 3. According to the structural spatial analogy, one could think that the same elution order may be observed for each pair of enantiomers of the 4-AAs 1–5 as for the enantiomers of baclofen. The designation of  $k'_S$  and  $k'_R$  as the first and second peaks for baclofen can be deduced by chromatographing samples of pure enantiomers of known absolute configuration. Following the Cahn–Ingold–Prelog rules, (i) for baclofen the substituent order is CH<sub>2</sub>N > phenyl > CH<sub>2</sub>CO > H, but (ii) for 4-AAs 1–5 this order becomes thienyl (or furyl) > CH<sub>2</sub>N >

CH<sub>2</sub>CO > H. Hence for an identical spatial structure the order is reversed. For 1–5, the first and the second peaks should be  $k'_R$  and  $k'_S$ , respectively.

For each compound we tried to optimize the separation either by addition of an organic modifier to the mobile phase or by varying the temperature or the pH. The enantioselectivity factor ( $\alpha$ ) and resolution ( $R_s$ ) slowly increase while significant retention factors ( $k'$ ) reduction are observed with increasing concentration of methanol for 3. Methanol proportions above 15% are not recommended for this column. For 4 and 5 the selectivity  $\alpha$  increases or remains unchanged whereas  $R_s$  and  $k'$  decrease [5,6]. Variation of the pH of the mobile phase [5,6] between 1.1 and 2.0 influences the retention ( $k'$ ) and enantioselectivity ( $\alpha$ ) factors of 1–3 as demonstrated in Table 1. The enantioselectivity factor decreases slightly or remains unchanged

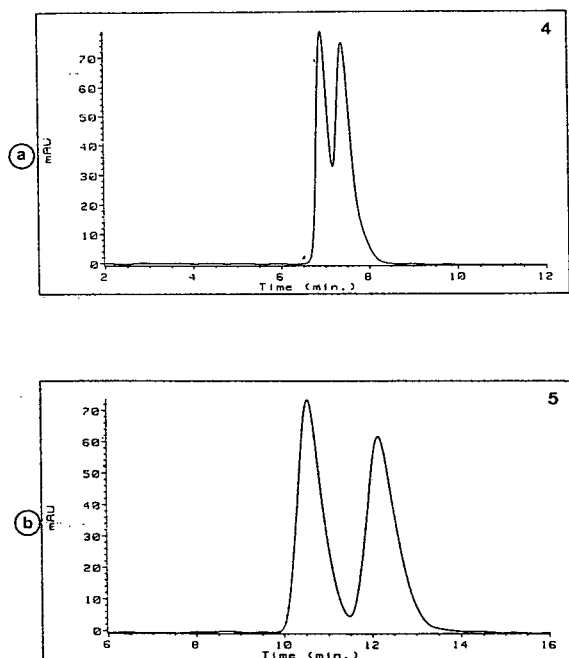


Fig. 3. Chromatograms obtained for (a) 4 (eluent A; 20°C); (b) 5 (eluent B; 20°C).

with increasing pH, whereas the retention factors are much more affected. The resolution ( $R_s$ ) also shows a progressive decrease with increasing pH. The large separations exhibited at lower pH are presumably because of the ability of the preferred enantiomers to fill the chiral cavity [5].

The factors  $k'$ ,  $\alpha$  and  $R_s$  were found to be increased with decreasing temperature from 40 to 10°C. As might be expected, the resolution increased at the expense of lengthened retention times and broadened peak shapes [5–8].

Under the same elution conditions, 1–5 are much less retained than baclofen. The order of elution in each system is (Table 1)  $4 < 1 < 5 < 2 < 3 < \text{baclofen}$ . Compounds 1–5 are certainly less hydrophobic than baclofen. The literature data for  $\log P$  values of the aromatic moieties are 1.36 (1.34), 1.59 (1.81), 1.87 (1.90), 2.10 (2.37), 2.34 (2.52) and 2.81 for 4, 1, 5, 2, 3 and baclofen, respectively ( $P$  = partition coefficients measured in *n*-octanol–water following Rekker [9] or Hansch and Leo [10] (in parentheses)).

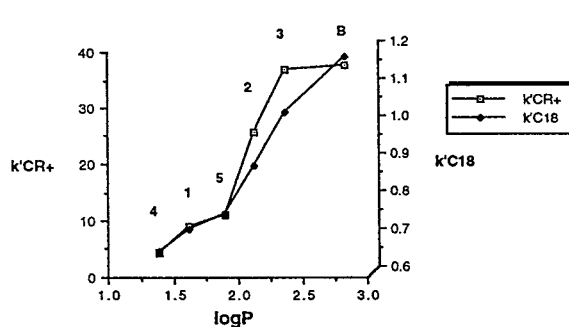


Fig. 4. Retention factors vs.  $\log P$ :  $k'_{\text{CR}(+)}$  (eluent A; 20°C);  $k'_{\text{C}_{18}}$  [eluent  $\text{CH}_3\text{OH}-\text{H}_2\text{O}$  (60:40); 20°C].

They are in perfect accordance with the order of capacity factors both on Crownpak CR(+) and reversed ( $\text{C}_{18}$ ) stationary phases (Fig. 4). For the latter, the  $k'_{\text{C}_{18}}$  values are 0.66, 0.72, 0.76, 0.89, 1.03 and 1.18 for 4, 1, 5, 2, 3 and baclofen, respectively.

The limit of detection (at a signal-to-noise ratio of 3) for each enantiomer of 3 was  $6.2 \cdot 10^{-6}$  mol/l, corresponding to  $6.2 \cdot 10^{-11}$  mol injected. Fig. 5 illustrates the enantioseparation

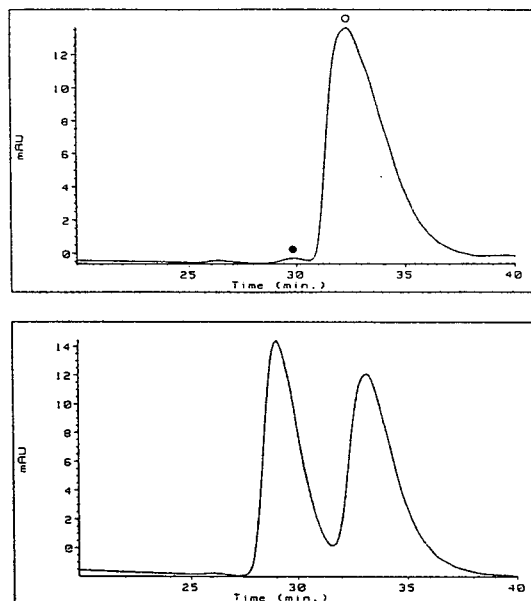


Fig. 5. Chromatograms of 3 (eluent B; 20°C): (a) racemate; (b) a major component (○) with a minor enantiomer (●).

of racemate **3** and its comparison with one of its enantiomers, the minor enantiomer (*R*) eluting first in front of the main component (*S*). These enantiomers were prepared according to a previously described method [11]. The *S* antipode is much more potent than the *R* antipode (bioassays will be published elsewhere). This is in accordance with the fact that the biological activity of baclofen, phaclofen [3] and saclofen [4] resides in the single enantiomer (*R*). Using the crown ether phase we were able to determine the minor enantiomer in a relative proportion of less than 1% [12,13] (Fig. 5: 0.4% *R* versus *S*).

The good separation of the optical isomers of the commercially available 4-AA **3** as efficiently as for the reference baclofen makes this chromatographic method suitable for studies designed to probe the enantiomeric distribution of the antipodes of **3** in biological media.

## References

- [1] P. Berthelot, C. Vaccher, N. Flouquet, M. Debaert, M. Luyckx and C. Brunet, *J. Med. Chem.*, 34 (1991) 2557.
- [2] J. Ong, D.I.B. Kerr, P. Berthelot, C. Vaccher, N. Flouquet and M. Debaert, *Eur. J. Pharmacol.*, 218 (1992) 343.
- [3] K. Frydenvang, J.J. Hansen, P. Krogsgaardlarsen, A. Mitrovic, H. Tran, C.A. Drew and G.A.R. Johnston, *Chirality*, 6 (1994) 583.
- [4] N.I. Carruthers, J.M. Spitler, S.C. Wang, D.J. Blythin, X. Chen, H.J. Shue and S. Mittelman, *Bioinorg. Med. Chem. Lett.*, 5 (1995) 237.
- [5] P.M. Udvarhelyi and J.C. Watkins, *Chirality*, 2 (1990) 200.
- [6] B.S. Kersten, *J. Liq. Chromatogr.*, 17 (1994) 33.
- [7] T. Shinbo, T. Yamaguchi, K. Nishimura and M. Sugiura, *J. Chromatogr.*, 405 (1987) 145.
- [8] M. Hilton and D.W. Armstrong, *J. Liq. Chromatogr.*, 14 (1991) 3673.
- [9] R.F. Rekker, in W.T. Nauta and R.F. Rekker (Editors), *Pharmacochemistry Library—The Hydrophobic Fragmental Constant*, Elsevier, Amsterdam, 1977.
- [10] C. Hansch and A. Leo, *Substituent Constants for Correlation Analysis in Chemistry and Biology*, Wiley, New York, 1979, p. 48.
- [11] C. Vaccher, P. Berthelot, N. Flouquet and M. Debaert, *J. Chromatogr.*, 542 (1991) 502.
- [12] P.M. Udvarhelyi, D.C. Sunter and J.C. Watkins, *J. Chromatogr.*, 519 (1990) 69.
- [13] A. Shibukawa and T. Nakagawa, in A.M. Krstulovic (Editor), *Chiral Separations by HPLC*, Ellis Horwood, Chichester, 1989, p. 477.

Short communication

## Nickel(II) chelates of some tetradentate Schiff bases as stationary phases for gas chromatography

M.Y. Khuhawar<sup>a,\*</sup>, Ashfaq A. Memon<sup>a</sup>, M.I. Bhangar<sup>b</sup>

<sup>a</sup>*Institute of Chemistry, University of Sindh, Jamshoro, Sindh, Pakistan*

<sup>b</sup>*National Centre of Excellence in Analytical Chemistry, University of Sindh, Jamshoro, Sindh, Pakistan*

First received 24 January 1995; revised manuscript received 12 May 1995; accepted 24 May 1995

### Abstract

Nickel(II) chelates of four tetradentate Schiff bases, bis(acetylaceton)ethylenediimine ( $H_2AA_2en$ ), bis(acetylaceton)propylenediimine ( $H_2AA_2pn$ ), bis(acetylaceton)-*dl*-stilbenediimine (*dl*- $H_2AA_2S$ ) and bis(acetylaceton)-*meso*-stilbenediimine (*meso*- $H_2AA_2S$ ), were examined as stationary phases for gas chromatography. The complexes were coated with 3% OV-101 in the range 3–5%. The phases were packed in stainless-steel columns (3 m × 3 mm I.D.) and were examined for the separation of saturated aromatic hydrocarbons, heteroaromatic aldehydes, ketones, amines and alcohols. Kováts retention indices of alcohols, aldehydes and ketones increased with improvement in the separation when using mixed stationary phases, particularly 3% OV-101–5% *dl*- $AA_2S$  compared with 3% OV-101.

### 1. Introduction

A number of attempts have been made to modify the stationary phases in gas chromatographic (GC) columns with inorganic electrolytes and metal chelate compounds. The copper, nickel, palladium and platinum chelates of *N*-dodecylsalicylaldehydes, nickel, palladium and platinum chelates of *n*-octylglyoximes [1], beryllium, aluminium and nickel chelates of *n*-nonyl  $\beta$ -diketones [2], transition metal chelates of phthalocyanine [3], 1,10-phenanthroline and 2,2'-bipyridine [4], nickel chelates of bis[3-(trifluoroacetyl)-1R-camphorate] [5], 2,2'-biphenyl-enephosphoric acids [6], triphenylphosphine complexes of rhodium(I) and ruthenium(II) [7] and copper and nickel chelates of tetradentate

Schiff bases [8–10] have been examined as stationary phases for GC individually or together with squalane or silicone oils. Wasiak [11] reported chemically bonded chelates as selective complexing sorbents for GC. The stationary phases have been evaluated for the separation of different organic compounds including hydrocarbons, alcohols and amines. Their relative retention and thermodynamic functions have been calculated [8,9,12]. Nickel chelates have also been used in kinetic studies of enantiomerization [5], enantiomer separations [13,14] and temperature-dependent reversal of elution sequences in complexation GC on chiral phases [15]. Some useful separations have been reported using Schiff base metal chelates as stationary phases with squalane [10], but in this work four tetradentate Schiff bases, bis(acetylaceton)ethylenediimine ( $H_2AA_2en$ ), bis(acetylaceton)propy-

\* Corresponding author.



lenediimine ( $H_2AA_2pn$ ), bis(acetylacetonate)-*dl*-stilbenediimine (*dl*- $H_2AA_2S$ ) and bis(acetylacetonate)-*meso*-stilbenediimine (*meso*- $H_2AA_2S$ ), were investigated separately and as mixed stationary phase with OV-101. Their resolution was compared with 3% OV-101 on Chromosorb G/NAW (60–80 mesh). The nickel chelates of the ligands *dl*- $H_2AA_2S$  and *meso*- $H_2AA_2S$  containing phenyl groups were considered promising because their higher thermal stability was more suited to GC [16].

## 2. Experimental

The reagents  $H_2AA_2en$ ,  $H_2AA_2Pn$ , *dl*- $H_2AA_2S$  and *meso*- $H_2AA_2S$  and their nickel(II) chelates (Fig. 1) were prepared as reported [17,18], by heating acetylacetonate with the appropriate 1,2-diamine in a 2:1 molar ratio in ethanol. An equimolar solution (0.01 M) of nickel acetate and the reagent was warmed together to obtain nickel chelates.

A Hitachi Model 163 gas chromatograph connected with a flame ionization detector and a Model 056 recorder was used.

An appropriate amount of the nickel chelates, individually or together with OV-101 (BDH), dissolved in chloroform, was added by thorough-

ly mixing with the appropriate amount of Chromosorb G/NAW (60–80 mesh) (Merck). The solvent was removed at reduced pressure on a Rotavapor (Buchi). For  $AA_2enNi$  and  $AA_2PnNi$ , ethanol was used as a solvent. The dried materials were packed in columns (3 m × 3 mm I.D.) using the usual procedure. Each of the columns was conditioned at 130°C for at least 24 h before use. Injections (10–15) of different compounds were made on each of the columns, before measuring the analytical responses.

Thermogravimetry (TG) and differential thermal analysis (DTA) were carried out on a Shimadzu TG30 thermal analyser in the temperature range from room temperature to 500°C at a heating rate of 10°C/min and with a nitrogen flow-rate 45 cm<sup>3</sup>/min. Sample amounts of 7–15 mg were used.

## 3. Results and discussion

The nickel complex *meso*- $AA_2SNi$ , having the highest thermal stability [10], was selected for coating at 3%, 5% and 10% on Chromosorb G/NAW (60–80 mesh size). However, difficulties were encountered in coating 10% uniformly on the solid support, some crystals of metal chelates being visible in the coated material. When DTA and TG were applied to each of the materials, a decrease in mass started at 220°C and losses of 3% and 5% occurred up to 300°C. However, with the material with 10% coating, a loss of 8% was observed within the same temperature range.

Each of the phases after packing and conditioning was examined for elution and GC separation of saturated and aromatic hydrocarbons, heteroaromatic aldehydes, ketones and alcohols. Their chromatographic characteristics were compared with those for an uncoated Chromosorb G/NAW (60–80 mesh) solid support packed in the same column. It was observed that the retention times of alcohols and heteroaromatics increased and tailing of the peaks decreased in the order (1) Chromosorb G/NAW (60–80 mesh size) (2) 3%, (3) 5% and (4) 10% *meso*- $AA_2SNi$  on Chromosorb G/NAW

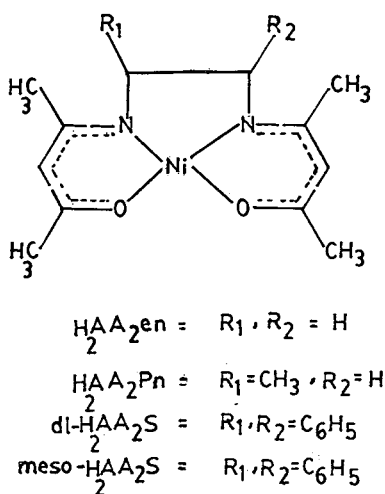


Fig. 1. Structure of metal chelates.

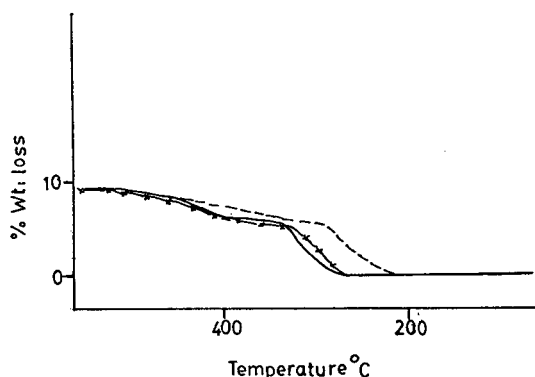


Fig. 2. TG of (---) 3% OV-101-5% AA<sub>2</sub>PnNi (×) *dl*-AA<sub>2</sub>SNi and (—) 3% OV-101-5% *meso*-AA<sub>2</sub>SNi on Chromosorb G/NAW (60–80 mesh). Heating rate, 10°C/min; nitrogen flow-rate, 45 ml/min.

(60–80 mesh). The retention times of *n*-pentanol on columns 1, 2, 3 and 4 were 2.28, 3.0, 3.36 and 3.48 min, respectively. However, the columns did not seem to serve a useful purpose for the separation of organic compounds. Mixed stationary phases were therefore considered.

The thermoanalytical studies of mixed phases of 5% nickel chelates plus 3% OV-101 on Chromosorb indicated that the decrease in mass for AA<sub>2</sub>PnNi, AA<sub>2</sub>enNi, *dl*-AA<sub>2</sub>SNi and *meso*-AA<sub>2</sub>SNi started from 215, 220, 265 and 270°C, respectively, and losses of ca. 5%, corresponding to nickel chelates occurred, up to 270, 285, 325 and 335°C, respectively. This was followed by a secondary loss of 3% in the temperature range 380–500°C, corresponding to OV-101 (Fig. 2).

After the necessary conditioning, each of the columns was injected with saturated long-chain hydrocarbons and the logarithm of adjusted retention time with *n*-hexane was plotted versus carbon number; a linear correlation was obtained (Fig. 3). This was followed by the injection of different aromatic hydrocarbons, alcohols, aldehydes, ketones and heteroaromatics. It was observed that the retention times, theoretical plate numbers and Kováts retention indices on mixed stationary phases increased in comparison with 3% OV-101 (Tables 1 and 2).

The utility of the mixed stationary phases for

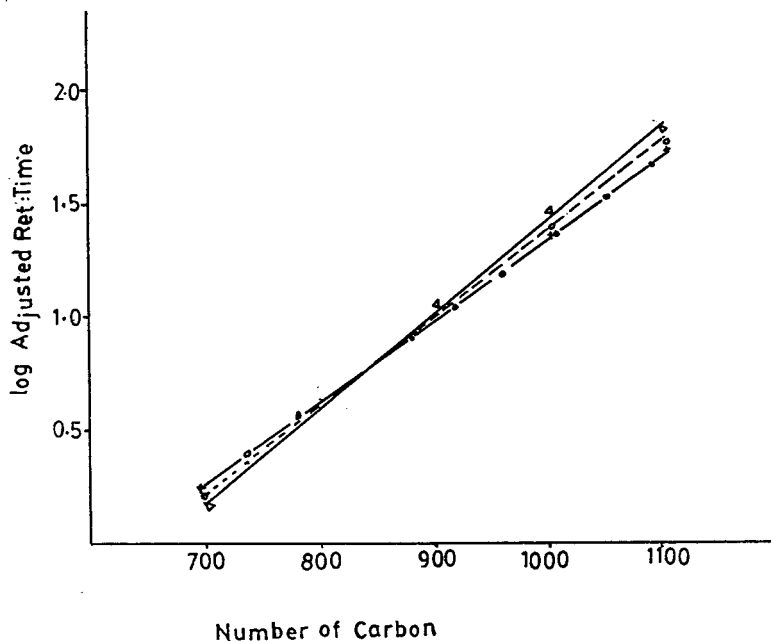


Fig. 3. Variation of log (adjusted retention time) with carbon number. ▽ = 3% OV-101, ○ = 3% OV-101-5% *meso*-AA<sub>2</sub>SNi and × = 3% OV-101-5% *dl*-AA<sub>2</sub>SNi on Chromosorb G/NAW (60–80 mesh). Column, 3 m × 3 mm I.D.; column temperature, 80°C; injection port temperature, 100°C; nitrogen flow-rate, 12 ml/min. X-axis shows number of carbon × 100.

Table 1  
Total number of theoretical plates ( $n$ ) on each phase packed in a 3 m × 3 mm I.D. column

Compound	3% OV-101	3% OV-101– 5% AA <sub>2</sub> PnNi	3% OV-101– 5% AA <sub>2</sub> enNi	3% OV-101– 5% <i>meso</i> -AA <sub>2</sub> SNi	3% OV-101– <i>dl</i> -AA <sub>2</sub> SNi
Pyridine	417	429	529	576	981
2-Picoline	655	704	860	913	1216
3-Picoline	676	882	981	1239	1354
2,6-Dimethylpyridine	690	986	1244	1745	1897
Toluene	661	711	700	900	1337
Paraldehyde	601	892	952	1024	1273
Pentanol	437	1024	1273	1422	1554
Hexanol	601	2136	2885	3076	3317

the separation of aromatic hydrocarbons, hetero-aromatics and alcohols was examined. The separation of alcohols showed pronounced tailing on 3% OV-101, but using mixed-phase columns some improvement in peak shape was observed. The optimum separation was obtained using 3% OV-101–5% *dl*-AA<sub>2</sub>SNi (Fig. 4). Similarly, when a mixture of pyridine, 2-picoline, 3-picoline and 2,6-dimethylpyridine was injected on to the column packed with 3% OV-101 and mixed stationary phases, better peak shapes were obtained on the latter and 3-picoline and 2,6-dimethylpyridine, which co-eluted on 3% OV-101, were separated on 3% OV-101–5% *dl*-AA<sub>2</sub>SNi (Fig. 5). The resolution factors ( $R_s$ ) calculated for the separation of 1,2-xylene and 1,3-xylene on columns (5) 3% OV-101; 3% OV-101–5% (6) AA<sub>2</sub>PnNi, (7) AA<sub>2</sub>enNi, (8) *meso*-

AA<sub>2</sub>SNi and (9) *dl*-AA<sub>2</sub>SNi were 1.52, 1.62, 1.63, 1.64 and 1.71, respectively, using the same operating conditions. The improvement in resolution may be due to adsorption on planar nickel chelates due to electron donor–acceptor complexation [8–10].

#### 4. Conclusion

Four nickel chelates, AA<sub>2</sub>PnNi, AA<sub>2</sub>enNi, *meso*-AA<sub>2</sub>SNi and *dl*-AA<sub>2</sub>SNi, were examined as stationary phases individually and as mixed phases with 3% OV-101 on Chromosorb G/NAW (60–80 mesh). The mixed stationary phases showed some promise for the separation of aromatic hydrocarbons, alcohols and heteroaromatics compared with 3% OV-101. The

Table 2  
Comparison of Kováts retention indices on different stationary phases packed in a 3 m × 3 mm I.D. column

Compound	3% OV-101	3% OV-101– 5% AA <sub>2</sub> PnNi	3% OV-101– 5% AA <sub>2</sub> enNi	3% OV-101– 5% <i>meso</i> -AA <sub>2</sub> SNi	3% OV-101– <i>dl</i> -AA <sub>2</sub> SNi
1-Pentanol	770	790	814	805	820
1-Hexanol	875	880	890	900	910
1-Heptanol	970	980	986	990	1015
2-Octanol	995	1005	1008	1012	1030
Aniline	940	978	975	988	1012
Toulene	745	760	770	775	790
<i>p</i> -Xylene	844	876	870	880	890
Benzaldehyde	926	950	948	955	976
Methyl isobutyl ketone	710	720	720	730	742
Cyclohexanone	870	890	885	893	912

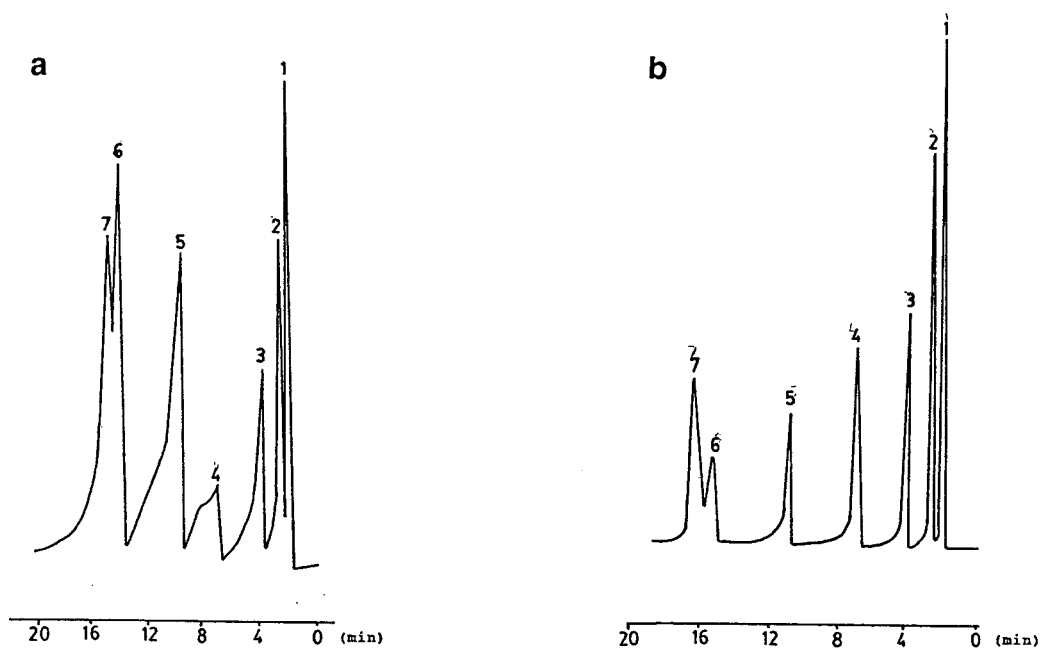


Fig. 4. Separation of (1) ethanol, (2) *n*-propanol, (3) *n*-butanol, (4) *n*-pentanol, (5) *n*-hexanol, (6) *n*-heptanol and (7) octan-2-ol. Column, 3 m  $\times$  3 mm I.D., packed with (a) 3% OV-101 and (b) 3% OV-101–5% *dl*-AA<sub>2</sub>SNi, on Chromosorb G/NAW (60–80 mesh). Column temperature, 80°C for 4.40 min, then programmed at 4°C/min to 120°C; injection port temperature, 130°C; nitrogen flow-rate, 12 ml/min; flame ionization detection.

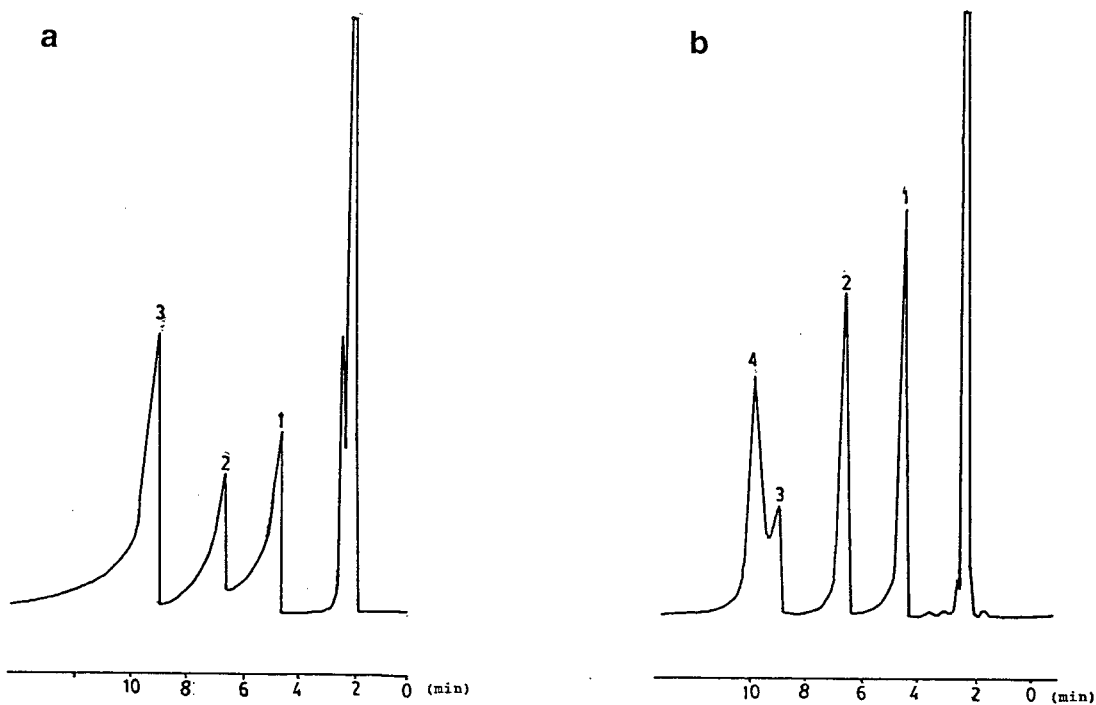


Fig. 5. Separation of (1) pyridine, (2) 2-picoline, (3) 3-picoline and (4) 2,6-dimethylpyridine. Columns as in Fig. 4. Column temperature, 80°C; injection port temperature, 100°C; nitrogen flow-rate, 12 ml/min; flame ionization detection. In (a) peaks 3 and 4 overlap.

mixed stationary phase 3% OV-101–5% dl-AA<sub>2</sub>SNi on Chromosorb G/NAW (60–80) gave the best results.

## References

- [1] G.P. Cartoni, R.S. Lowrie, C.S.G. Phillips and L.M. Venanzi, in R.P.W. Scott (Editor), *Gas Chromatography 1960*, Butterworths, London, 1960, p. 273.
- [2] G.P. Cartoni, A. Liberti and R. Palombari, *J. Chromatogr.*, 20 (1965) 278.
- [3] C.V. Madjar and G. Guiochon, *J. Chromatogr. Sci.*, 9 (1971) 664.
- [4] V. Ilie, *Rev. Chim. (Bucharest)*, 20 (1969) 43.
- [5] W. Burkle, H. Karfunkel and V. Schurig, *J. Chromatogr.*, 288 (1984) 1.
- [6] W. Kuchen and H.F. Mahler, *Z. Naturforsch.*, 336 (1978) 1049.
- [7] W. Wasiak, *Chem. Anal. (Warsaw)*, 33 (1988) 573.
- [8] J. Masłowska and G. Bazylak, *J. Chromatogr.*, 298 (1984) 211.
- [9] J. Masłowska and G. Bazylak, *Pol. J. Chem.*, 62 (1988) 331.
- [10] J. Masłowska and G. Bazylak, *Collect. Czech. Chem. Commun.*, 54 (1989) 1530.
- [11] W. Wasiak, *J. Chromatogr.*, 547 (1991) 259; 653 (1993) 63.
- [12] W. Wasiak, *Chem. Anal. (Warsaw)*, 39 (1994) 325.
- [13] V. Schurig, H. Laderer, D. Wistuba, A. Morandl, V. Schubert and U. Hagenauer-Hener, *J. Essent. Oil Res.*, 1 (1989) 209.
- [14] V. Schurig, W. Buerkle, K. Hintzer and R. Weber, *J. Chromatogr.*, 475 (1989) 23.
- [15] V. Schurig, J. Ossig and R. Link, *Angew. Chem.*, 101 (1989) 197.
- [16] M.Y. Khuhawar, *Arab. Gulf J. Sci. Res.*, 4 (1986) 463.
- [17] H. Kanatomi, I. Murase and A.E. Martell, *J. Inorg. Nucl. Chem.*, 38 (1976) 1465.
- [18] R. Belcher, K. Blesel, T. Cardwell, M. Pravica, W.I. Stephen and P.C. Uden, *J. Inorg. Nucl. Chem.*, 35 (1973) 1127.

Short communication

# Modified and convenient preparation of silica impregnated with silver nitrate and its application to the separation of steroids and triterpenes

Tong-Shuang Li\*, Ji-Tai Li, Hui-Zhang Li

*Department of Chemistry, Hebei University, Baoding 071002, Hebei Province, China*

First received 12 January 1995; revised manuscript received 23 May 1995; accepted 24 May 1995

## Abstract

Modified and convenient procedures are reported for the preparation of flash columns and thin-layer chromatographic plates using silica impregnated with silver nitrate. The application of this adsorbent to the separation of steroids and triterpenes is also reported.

## 1. Introduction

In connection with our research on the synthesis of steroidal and triterpenoidal biological markers [1–5], the separation of olefinic hydrocarbons was frequently necessary. Silica gel impregnated with silver ions has been successfully used in the separation of unsaturated compounds by thin-layer (TLC) and column chromatography [6–23]. However, no significant modification of the preparation of this kind adsorbent has been introduced. The reported procedures [8,15,18,20,21,23] for the preparation of silica impregnated with silver nitrate involve the addition of silver nitrate solution to silica and drying the mixture under reduced pressure in a rotary evaporator. When these procedures were repeated in our laboratory, however, there were always problems as about one third of the adsorbent rose up the condenser of the

evaporator. Therefore, the rotary evaporator had to be cleaned and reassembled and the yield of the adsorbent was only around 70%.

TLC plates coated with silica impregnated with silver ions, prepared by literature [6,7,10,11] methods have the defect that the adsorbent is not strong enough and might be destroyed by spraying agents or by heating, and all the plates must be used within 1 week as otherwise they become dark.

We report here modified and convenient procedures for the preparation of flash columns and TLC plates using silica impregnated with silver nitrate and their application to the separation of steroids and triterpenes.

## 2. Experimental

### 2.1. Preparation of TLC plates coated with silica impregnated with silver nitrate

A 10 × 2.5 cm TLC plate coated with silica gel

\* Corresponding author.

60 (Merck) was developed once with an aqueous solution of silver nitrate (2.0 g) in distilled water (5 ml). The plate was then dried and activated with a heat gun for 2 min. Silver nitrate consti-

tuted around 25% of the adsorbent. The plate can be used as usual and the movement of solvent was usually controlled at 2 cm from the upper edge.

Table 1  
 $R_F$  values of steroids and triterpenes

Mixture	$R_F$	Solvent
Cholesterol	0.37	Hexane–ethyl acetate
Cholestanol	0.47	(3:1)
3 $\beta$ -Acetoxycholest-5-ene	0.48	Hexane–diethyl ether
3 $\beta$ -Acetoxycholestane	0.62	(10:1)
3 $\beta$ -Acetoxycholest-8(14)-ene	0.42	Hexane–diethyl ether
3 $\beta$ -Acetoxycholest-14-ene	0.27	(5:1)
4 $\beta$ -Methylcholest-2-ene	0.43	Hexane
4-Methylcholest-3-ene	0.33	
4-Methylcholest-4-ene	0.55	
Cholest-4-ene	0.68	Hexane–toluene
Cholest-3-ene	0.57	(10:1)
Cholest-2-ene	0.54	
Cholesta-3,5-diene	0.32	
(20 <i>R</i> )-Diacholest-13(17)-ene	0.46	Hexane–toluene
(20 <i>S</i> )-Diacholest-13(17)-ene	0.61	(10:1)
4,4-Dimethylcholest-5-ene	0.35	Hexane
4,5 $\alpha$ -Dimethylcholest-3-ene	0.64	
(20 <i>R</i> )-4,4-Dimethyldiacholest-13(17)-ene	0.46	Hexane–toluene
(20 <i>S</i> )-4,4-Dimethyldiacholest-13(17)-ene	0.61	(10:1)
Lupeol	0.42	Hexane–ethyl acetate
Dihydrolupeol	0.53	(3:1)
Betulin	0.39	Hexane–ethyl acetate
Dihydrobetulin	0.50	(2:1)
Lup-2-ene	0.34	Hexane
$\gamma$ -Lup-3(4)-ene	0.50	
$\gamma$ -Lup-3(5)-ene	0.29	
Lupa-2,20(29)-diene	0.37	Hexane–toluene
$\gamma$ -Lupa-3(4),20(29)-diene	0.46	(10:1)
19 $\alpha$ (H)-28-Norlup-17-ene	0.82	Hexane
19 $\beta$ (H)-28-Norlup-17-ene	0.70	
28-Norlup-16-ene	0.51	
28-Norlup-17(22)-ene	0.38	

## 2.2. Preparation of silica impregnated with silver nitrate (10%) for flash column chromatography

An aqueous solution of 5.5 g of silver nitrate in 30 ml of distilled water was mixed with 50 g of 200–300-mesh silica and ground for 5 min in a mortar. The mixture was then dried in an oven at 150°C for 1 h. The resulting powder was almost white, stored in a beaker wrapped with dark paper and dried over phosphorus pentoxide in a vacuum desiccator. The adsorbent could be stored for several months without significant darkening or decrease in activity. Columns were packed in the same way as ordinary silica columns and wrapping with dark paper was not necessary for flash chromatography. Most mixtures were separated by using 50 g of adsorbent for each gram of mixture.

## 3. Results and discussion

To prepare TLC plates coated with silica impregnated with silver nitrate, 0.5, 1.0, 1.5, 2.0 and 3.0 g of silver nitrate in 5 ml of distilled water were tried as development solvents. The first three caused double fronts and the last led to overloading with silver nitrate. Consequently, a solution of 2.0 g of silver nitrate in 5 ml of distilled water was adopted and thus silver nitrate constituted ca. 25% of the adsorbent. For flash column chromatography, 10% silver nitrate on 200–300-mesh silica was found to be efficient enough for the separation of olefinic mixtures of steroids and triterpenes.

Thirteen olefinic mixtures, containing 32 steroids and triterpenes, were separated satisfactorily by flash column chromatography on silica impregnated with silver nitrate (10%), except for the mixture of cholest-2-ene and cholest-3-ene. The  $R_F$  values of the 32 compounds obtained by TLC are given in Table 1. The mixtures in Table 1 could not be separated by the usual TLC and column chromatography on silica. TLC plates prepared in this manner were mainly used for analysis purposes. For example, the hydrogenation of cholesterol, 3 $\beta$ -acetoxycholest-5-ene,

lupeol and betulin was usually checked by  $^1\text{H}$  NMR spectroscopy, but now the evolution of these hydrogenation reactions can be monitored by silica–silver nitrate TLC. The fractions from flash column chromatography on silica impregnated with silver nitrate could also be checked by this kind of TLC instead of GC.

In conclusion, very convenient and practical procedures for the preparation of flash columns and TLC plates using silica impregnated with silver nitrate have been developed.

## Acknowledgement

This work was supported by the State Education Commission of China via a Research Grant for Returned Chinese Scholars.

## References

- [1] T.-S. Li, Y.-L. Li and X.-T. Liang, *Acta Chim. Sin.*, Engl. Ed., (1989) 544.
- [2] T.-S. Li, Y.-L. Li and X.-T. Liang, *Youji Huaxue*, 10 (1990) 240.
- [3] T.-S. Li, Y.-L. Li and X.-T. Liang, *Steroids*, 55 (1990) 263.
- [4] T.-S. Li, Y.-L. Li and X.-T. Liang, *Steroids*, 57 (1992) 67.
- [5] T.-S. Li, Y.-T. Yang and Y.-L. Li, *J. Chem. Res. (S)*, (1993) 28.
- [6] C.B. Barrett, M.S. Dallas and F.B. Padley, *Chem. Ind. (London)*, (1962) 1050.
- [7] A.S. Gupta and S. Dev, *J. Chromatogr.*, 12 (1963) 189.
- [8] T. Norin and L. Westfelt, *Acta Chem. Scand.*, 17 (1963) 1828.
- [9] B.M. Lawrence, *J. Chromatogr.*, 38 (1968) 535.
- [10] R.S. Prasad, A.S. Gupta and S. Dev, *J. Chromatogr.*, 92 (1974) 450.
- [11] J.C. Kohli and K.K. Badaisha, *J. Chromatogr.*, 320 (1985) 455.
- [12] B. De Vries, *J. Am. Oil Chem. Soc.*, 40 (1963) 184.
- [13] R. Vivilecchia, M. Thiebaut and R.W. Frei, *J. Chromatogr. Sci.*, 10 (1972) 411.
- [14] F. Mikes, V. Schurig and E. Gil-Av, *J. Chromatogr.*, 83 (1973) 91.
- [15] R.R. Heath, J.H. Tumlinson, R.E. Doolittle and A.T. Proveaux, *J. Chromatogr. Sci.*, 13 (1975) 380.
- [16] R. Aigner, H. Spitzzy and R.W. Frei, *Anal. Chem.*, 48 (1976) 2.
- [17] R. Aigner, H. Spitzzy and R.W. Frei, *J. Chromatogr. Sci.*, 14 (1976) 381.



- [18] R.R. Heath, J.H. Tumlinson and R.E. Doolittle, *J. Chromatogr. Sci.*, 15 (1977) 10.
- [19] S. Lam and E. Grushka, *J. Chromatogr. Sci.*, 15 (1977) 234.
- [20] M. Özcimder and W.E. Hammers, *J. Chromatogr.*, 187 (1980) 307.
- [21] E.C. Smith, A.D. Jones and E.W. Hammond, *J. Chromatogr.*, 188 (1980) 205.
- [22] Y. Yamauchi, R. Oshima and J. Kumanotani, *J. Chromatogr.*, 198 (1980) 49.
- [23] R.P. Evershed, E.D. Morgan and L.D. Thompson, *J. Chromatogr.*, 237 (1982) 350.



ELSEVIER

Journal of Chromatography A, 715 (1995) 376–384

JOURNAL OF  
CHROMATOGRAPHY A

Short communication

## Determination of the petroleum tracers nitrate and thiocyanate in subterranean waters by capillary ion electrophoresis

Liguo Song<sup>a,\*</sup>, Qingyu Ou<sup>a</sup>, Weile Yu<sup>a</sup>, Lingcheng Fang<sup>b</sup>, Yanbo Jin<sup>b</sup>

<sup>a</sup>Lanzhou Institute of Chemical Physics, Chinese Academy of Sciences, Lanzhou 730000, China

<sup>b</sup>Tuha Research Institute of Petroleum Exploration and Development, Shanshan 838201, China

First received 2 January 1995; revised manuscript received 9 May 1995; accepted 22 May 1995

### Abstract

The petroleum tracers nitrate and thiocyanate in subterranean waters were determined by capillary ion electrophoresis using direct UV detection. The high concentrations of salts in subterranean waters made the determination difficult. Taking sodium chloride to represent salts in subterranean waters, the effect of high concentrations of salts in samples on the determination was examined. Because of electrostacking and its inverse process, different concentrations of salts in samples could cause different peak heights and peak widths of constant concentration of an anion, but the peak area remained constant. The experimental results showed that the determination of the tracers was feasible using peak areas. By using 100 mM sodium chloride with 2.0 mM cetyltrimethylammonium chloride as carrier electrolyte solution, determination of nitrate and thiocyanate was accomplished at concentrations of sodium chloride in the sample from 0 to 200 mM. Standard addition recoveries of the tracers in four subterranean water samples were between 91 and 113%.

### 1. Introduction

Capillary ion electrophoresis (CIE), introduced at the beginning of this decade [1–4] is a capillary electrophoretic technique optimized for the rapid determination of low-molecular-mass inorganic and organic ions. Although CIE is a recent separation and analysis technique, it has gained many applications after several years of development. It has been used to determine anions in environmental waters [5], high-purity

water in the power industry [6], urine [7], milk [8], food samples [9], in the pulp and paper industry [10], alumina production [11], prenatal vitamin formulations [12], bulk drugs and intermediates [13] and explosives residues [14], etc. A number of difficult and challenging problems in ion chromatography (IC) can be solved by using CIE.

Jones and Jandik [15] determined anions with disparate concentrations, e.g., impurities in 99.9% pure solid terephthalic acid. Whereas in IC consideration must be given to the total ion-exchange capacity of the column, moderate ion-exchange capacity columns reduce the risk of sample overloading at the cost of short analysis times. The re-equilibration time alone can ex-

\* Corresponding author. Present address: Research Laboratory of Analytical Chemistry, Department of Chemistry, Wuhan University, Wuhan 130072, China.

ceed 1 h after a column is overloaded. In the determination of the petroleum tracers nitrate and thiocyanate, a similar situation will be encountered.

Nitrate and thiocyanate are used as petroleum tracers in the Tuha oil field to investigate the stratigraphic structure, the distribution of oil deposits and the effectiveness of water blocking. Since subterranean water contains very high concentrations of chloride, sulfate and carbonate salts, etc., e.g., the concentration of chloride can reach tens of grams per litre, the determination of tracers by IC is difficult. In a previous study [16] we investigated a CIE method using direct UV detection for their separation, and the effect of high concentrations of salts in samples on the separation was examined. The experimental results showed that because of electrostacking, the high concentrations of salts in subterranean water caused quantification problems. The CIE separation studied was unsatisfactory, so the determination of the tracers was not carried out.

In this work, 100 mM sodium chloride solution containing 2.0 mM cetyltrimethylammonium chloride (CTAC) was used as a carrier electrolyte solution, and the CIE determination of the petroleum tracers nitrate and thiocyanate was accomplished at concentrations of sodium chloride in the sample from 0 to 200 mM.

## 2. Experimental

### 2.1. Apparatus

The CE system employed was a Quanta 4000 (Waters Chromatography Division of Millipore, Milford, MA, USA) with a negative power supply. Direct UV detection was accomplished with a zinc lamp and a 214-nm optical filter. Data acquisition was carried out with a Waters Millennium 2010 Chromatography Manager with a bus satellite interface and a LAC/E module connecting the data station with the CE system. Data collection was initiated by a signal cable connection between the Quanta 4000 and the bus satellite interface.

### 2.2. Carrier electrolyte solution

CTAC was used as an electroosmotic flow modifier and a carrier electrolyte solution of 100 mM sodium chloride containing 2.0 mM CTAC was prepared as described previously [16].

### 2.3. Standard solutions

Analytical-reagent grade sodium or potassium salts were used to prepare 1000 ppm anion stock standard solutions containing a single anion. All mixed anion solutions consisted of ten anions: fluoride, chloride, bromide, iodide, nitrite, nitrate, sulfate, phosphate, carbonate and thiocyanate; of these, only five, bromide, iodide, nitrite, nitrate and thiocyanate, have UV absorbance at 214 nm and gave response signals in our experiments. Five mixed anion solutions containing 1, 4, 10, 20 and 40 ppm of each anion were prepared to obtain calibration graphs. Another five mixed anion solutions containing 10 ppm of each of the above-mentioned ten anions with an additional 20 ppm of thiocyanate, 10 ppm of nitrate, 10 ppm of nitrite, 20 ppm of bromide or 20 ppm of iodide separately were prepared for the purpose of peak identification on the electropherograms. Mixed anion solutions were prepared not only with deionized water, but also with 12.5, 50 or 100 mM sodium chloride solutions. Polyethylene containers were utilized for the mixed anion solutions.

### 2.4. Electrophoresis

A Waters Accu-Sep polyimide-coated fused-silica capillary was used throughout. The capillary dimensions were 75  $\mu\text{m}$  I.D., 60 cm total length and 52 cm from the point of injection to the detector cell. The capillary was flushed with 1 M potassium hydroxide for 1 h and then equilibrated with carrier electrolyte solution before use. All injections were performed in the hydrostatic mode at a height of 10 cm for 30 s. The applied voltage for each run was 10 kV. A 2-min capillary purge with carrier electrolyte solution by a vacuum applied to the receiving

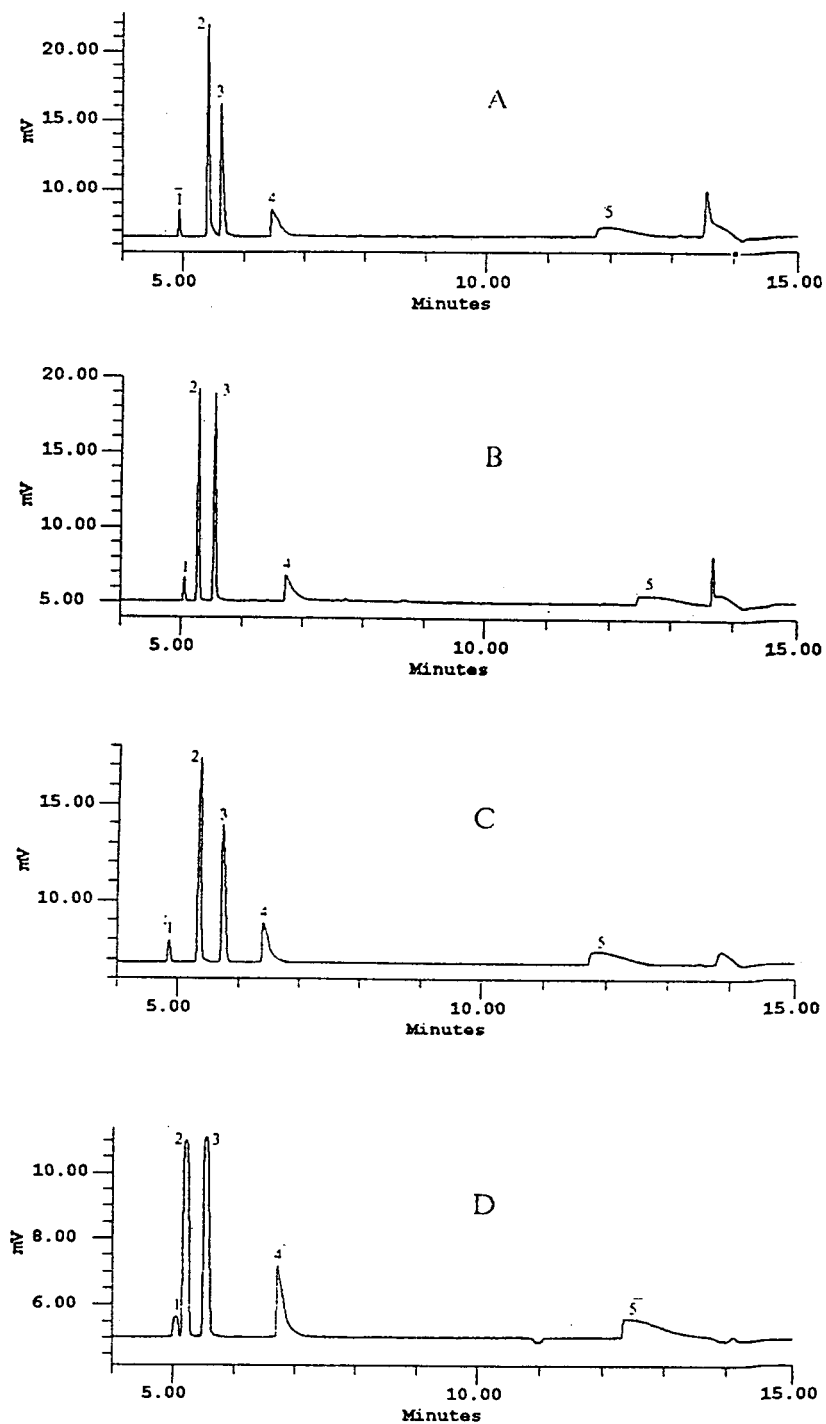


Fig. 1. Effect of the concentration of sodium chloride in the sample on the CIE separation of anions. Current:  $85 \mu\text{A}$ . Concentration of sodium chloride in sample: (A) 0; (B) 12.5; (C) 50; (D) 100 mM. Peaks: 1 = bromide; 2 = nitrite; 3 = nitrate; 4 = iodide; 5 = thiocyanate. The concentration of each anion in sample was 20 ppm.

electrolyte vial was performed prior to each injection.

### 3. Results and discussion

Taking sodium chloride to represent salts in subterranean water, the effect of high concentrations of salts in the samples on the CIE separation of anions was examined and the results are illustrated in Fig. 1.

It can be seen from Fig. 1 that high concentrations of chloride in the samples did not cause any baseline disturbances, such as negative peaks covering the bromide peak as occurred in our previous study [16]. The different anionic form of the electroosmotic flow modifier, previously bromide and now chloride, was the reason. Bromide made the carrier electrolyte solutions generate UV absorption at 214 nm, and the presence of chloride in the samples displaced bromide and caused a decrease in absorbance. Chloride is a UV-transparent anionic form, so negative peaks disappeared. Similar phenomena were also observed by Jones and Jandik [15] and Jackson and Haddad [17].

In Fig. 1, there are five peaks belonging to bromide, nitrite, nitrate, iodide and thiocyanate. Because iodide and thiocyanate are hydrophobic anions, their peaks were asymmetric and showed strong tailing due to hydrophobic interactions between them and CTAC. In comparison with iodide and thiocyanate, bromide, nitrite and nitrate gave more symmetrical peaks. It can be seen from Fig. 1 that an increase in the concentration of sodium chloride in the sample caused changes in peak height and width of the

symmetrical peaks of bromide, nitrite and nitrate, but caused less change in the asymmetric peaks of iodide and thiocyanate. When the concentration of sodium chloride in the sample was 12.5 mM, the highest and narrowest peaks of nitrite and nitrate were observed. On increasing the concentration of sodium chloride in the sample from 12.5 to 50 and 100 mM, the peaks widened.

The detection limit was defined as a detectable concentration of an anion giving a peak twice as high as the background noise ( $N$ ). For a defined change in anion concentration, its corresponding change in peak height was calculated from the slope ( $SL$ ) of the calibration graph of the anion of peak height versus anion concentration from 1 to 40 ppm. All correlation coefficients of the calibration graphs were calculated and were higher than 0.99. Detection limits calculated as  $2N/SL$  (experimental data for  $N = 55 \mu\text{V}$ ) are given in Table 1 for different concentrations of sodium chloride in the samples. It can be seen that when the concentration of sodium chloride in the sample was 12.5 mM, nitrite and nitrate had the lowest detection limits. The detection limits of nitrite and nitrate increased with increasing concentration of sodium chloride in the sample from 12.5 to 100 mM. However, the detection limit of bromide increased steadily with increasing concentration of sodium chloride in sample, whereas the detection limits of iodide and thiocyanate was relatively unchanged.

The separation efficiency was represented by the theoretical plate number,  $N$ , which was calculated from  $N = 5.54 (t_R/w)^2$ , where  $t_R$  is the migration time and  $w$  is the peak width at half-height. Theoretical plate numbers for bromide,

Table 1  
Effect of concentration of sodium chloride in sample on detection limit

Concentration of NaCl in sample (mM)	Detection limit (ppb)				
	Bromide	Nitrite	Nitrate	Iodide	Thiocyanate
0	996	162	278	1468	5036
12.5	1396	154	182	1853	6820
50	1762	204	332	1617	4785
100	3088	368	350	1709	6286

Table 2  
Effect of concentration of sodium chloride in sample on separation efficiency of bromide, nitrite and nitrate

Concentration of NaCl in sample (mM)	Theoretical plate number		
	Bromide	Nitrite	Nitrate
0	147 300	120 100	82 900
12.5	167 000 <sup>a</sup>	142 800	127 200
50	63 000 <sup>b</sup>	57 700	46 100
100	21 300 <sup>b</sup>	15 700	17 900

<sup>a</sup> Average of only four values because of detection sensitivity limitation.

<sup>b</sup> Average of only three values because of detection sensitivity limitation.

nitrite and nitrate at different concentrations of sodium chloride in the sample were calculated and are given in Table 2. Each theoretical plate number in Table 2 is the average of five results which were obtained by the separation of five mixed anion solutions containing 1, 4, 20 and 40 ppm of each anion. It can be seen from Table 2 that when the concentration of sodium chloride in the sample was 12.5 mM, bromide, nitrite and nitrate had the highest theoretical plate numbers, and then increasing the sodium chloride concentration in sample from 12.5 to 50 and 100 mM resulted in a decrease in the theoretical plate numbers. The theoretical plate numbers of iodide and thiocyanate are not shown in Table 2 because they varied with the concentration of iodide and thiocyanate in sample, as illustrated in Table 3. Because the peaks of iodide and thiocyanate were not significantly affected by high concentrations of sodium chloride in the

Table 3  
Effect of concentration of iodide and thiocyanate in sample on their separation efficiency (theoretical plate number)

Anion	Concentration (ppm)				
	1	4	10	20	40
Iodide	— <sup>a</sup>	35 500	21 300	11 000	6 200
Thiocyanate	— <sup>a</sup>	7 900	4 100	2 100	1 200

<sup>a</sup> Not measured because of detection sensitivity limitation.

samples, each value in Table 3 is the average of four values obtained by the separation of four mixed anion solutions with 0, 12.5, 50 and 100 mM of sodium chloride in the sample. It can be seen from Table 3 that increasing concentrations of iodide and thiocyanate in the sample resulted in a decreased separation efficiency, which could be attributed to the tailing peaks.

The reason for the above effects of high concentrations of sodium chloride in samples on the CIE separation of anions can be explained as follows. In capillary electrophoresis, when the ionic strength of the sample is lower than that of the carrier electrolyte solution, electrostacking occurs and the sample ion will be stacked in a narrow zone [17–23]. However, when the ionic strength of the carrier electrolyte solution is lower than that in the sample, a peak broadening mechanism will result from anti-stacking and the sample ion will be diffused in a broad zone. When stacking or anti-stacking occurs, there is also an accompanying phenomenon, laminar flow, which originates from the different local electroosmotic flow caused by the non-uniform distribution of the electric field strength and will broaden a separated sample zone [19]. When the concentration of sodium chloride in the sample is higher than that in the carrier electrolyte solution, it can be concluded that the length of the separated zone will always increase with increasing concentration of sodium chloride in the sample because of the effects of anti-stacking and laminar flow broadening. However, when the concentration of sodium chloride in the sample is lower than that in the carrier electrolyte solution, it can be concluded that stacking and laminar flow broadening will function against each other so that the optimum concentration of sodium chloride in the sample for a minimum length of a separated zone is somewhere between zero and the concentration of sodium chloride in carrier electrolyte solution. In this experiment, the concentration of sodium chloride in the carrier electrolyte solution was 100 mM, and the optimum concentration of sodium chloride in the sample was 12.5 mM.

In the determination of anions in subterranean water, 100 mM sodium chloride solution con-

Table 4

Statistics of migration time of each anion at different concentrations of sodium chloride (0, 12.5, 50 and 100 mM) and different concentrations of each anion (1, 4, 10, 20 and 40 ppm) in sample

Anion	Br <sup>-</sup>	NO <sub>2</sub> <sup>-</sup>	NO <sub>3</sub> <sup>-</sup>	I <sup>-</sup>	SCN <sup>-</sup>
Average (min)	5.0 <sup>a</sup>	5.3	5.6	6.6 <sup>b</sup>	12.2 <sup>b</sup>
Lowest (min)	4.8	5.2	5.5	6.3	11.4
Highest (min)	5.1	5.5	5.8	6.9	12.9
R.S.D. (%)	1.9 <sup>a</sup>	1.6	2.1	3.0 <sup>b</sup>	3.5 <sup>b</sup>

<sup>a</sup> Calculated from only fourteen values because of detection sensitivity limitation.

<sup>b</sup> Calculated from only sixteen values because of detection sensitivity limitation.

taining 2.0 mM CTAC was chosen as the carrier electrolyte solution because it gave lower detection limits in comparison with a lower concentration of sodium chloride, and it was also suitable for samples with higher concentrations of salts. With a concentration of sodium chloride in the sample of 0, 12.5, 50 or 100 mM, separations of five mixed anion standard solutions that contained 1, 4, 10, 20 and 40 ppm of each anion were accomplished, and the statistics of the migration times of each anion at different concentrations of sodium chloride and each anion in the sample are presented in Table 4. It can be seen from Table 4 that considering the differences between the migration times of each anion and the reproducibility of the migration

Table 6

Regression equations between peak area ( $A$ ,  $\mu\text{V s}$ ) and anion concentration ( $C$ , ppm)

Anion	Regression equation	Correlation coefficient
Bromide	$A = 178C + 15$	0.9998
Nitrite	$A = 1682C + 858$	0.9998
Nitrate	$A = 1589C + 808$	0.9997
Iodide	$A = 967C - 205$	0.9816
Thiocyanate	$A = 1324C + 965$	0.9999

time of each anion, it was feasible to identify a peak from the migration time when a real sample with unknown concentrations of salts and anions was separated. This is very useful for routine analysis.

As different concentrations of salts in samples could cause different peak heights at a constant concentration of an anion, the simplest approach to achieve accurate quantification by peak height was to use the standard additions calibration technique [16]. However, it was discovered that the peak area for a constant concentration of an anion remained constant regardless of the concentration of salts in the sample, which is demonstrated in Table 5. Although the R.S.D.s of the peak areas in Table 5 was not very low, the data were still acceptable for quantification purposes. Using the average peak area calculated from four values at different concentrations of sodium chloride in the sample (0, 12.5, 50 and 100 mM), regression equations between peak

Table 5

Reproducibility of peak area at different concentrations of sodium chloride in sample (0, 12.5, 50 and 100 mM)

Concentration of anion in sample (mM)	R.S.D. (%)				
	Bromide	Nitrite	Nitrate	Iodide	Thiocyanate
1	— <sup>a</sup>	18.0	20.3	— <sup>a</sup>	— <sup>a</sup>
4	19.9 <sup>b</sup>	11.8	7.2	14.9 <sup>c</sup>	10.3
10	18.8 <sup>b</sup>	5.1	10.8	15.8	11.3
20	9.7	8.2	15.8	7.2	15.4
40	13.5	9.3	11.3	6.6	8.4

<sup>a</sup> Not measured because of detection sensitivity limitation.

<sup>b</sup> Three values were measured because of detection sensitivity limitation.

<sup>c</sup> Two values were measured because of detection sensitivity limitation.

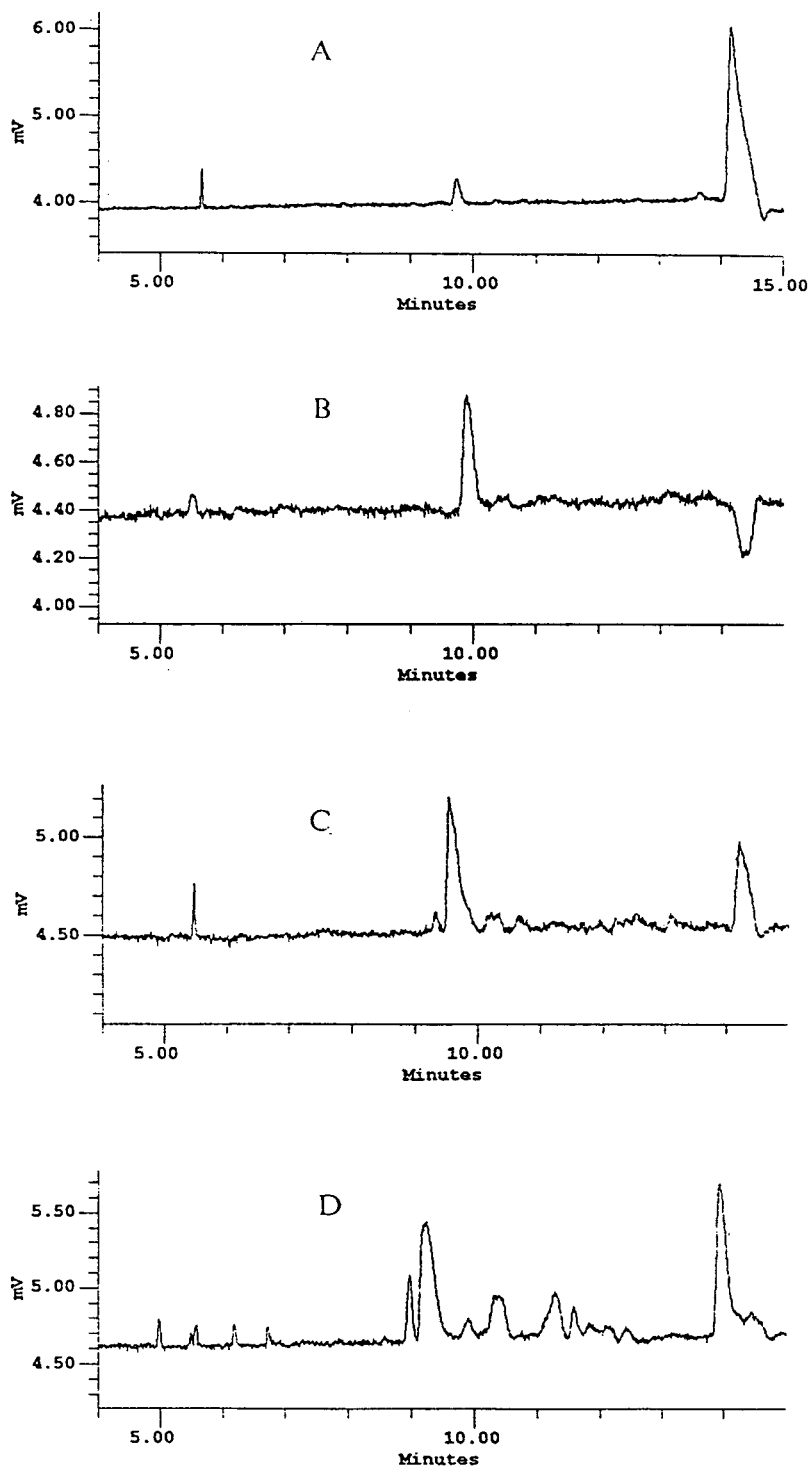


Fig. 2. CIE separations of four subterranean water samples. (A) L8-19; (B) WX3-82; (C) HT1; (D) S13-12.



Table 7  
Compositions of four subterranean water samples

Ion	Concentration <sup>a</sup> (mM)			
	L8-19	WX3-82	HT1	S13-12
Na <sup>+</sup> K <sup>+</sup>	11.2	557.3	269.3	57.7
Ca <sup>2+</sup>	0.7	37.9	2.6	2.1
Mg <sup>2+</sup>	0.4	2.7	2.1	0.3
Cl <sup>-</sup>	3.4	619.1	228.7	37.9
SO <sub>4</sub> <sup>2-</sup>	3.1	1.6	5.9	0.8
HCO <sub>3</sub> <sup>-</sup>	3.7	16.1	36.8	22.8
CO <sub>3</sub> <sup>2-</sup>	0.1	0.0	0.7	0.8

<sup>a</sup> Determined by titrimetric method.

area and anion concentration were obtained and are given in Table 6. It can be seen from Table 6 that the correlation coefficients of each regression equation were very good. It should be notified that when the concentration of sodium chloride in the sample was 200 mM, a successful separation of anions by using 100 mM sodium chloride solution containing 2.0 mM CTAC as carrier electrolyte solution was also achieved, and the peak area at a constant concentration of an anion remained the same as that when the concentration of sodium chloride in the sample was 0, 12.5, 50 and 100 mM. However, when the concentration of sodium chloride in the sample was 400 mM, the separation deteriorated because too broad peaks of bromide, nitrite and

nitrate caused the resolution to decrease significantly.

A standard additions recovery test was applied to four subterranean water samples, L8-19, WX3-82, HT1 and S13-12. The compositions of the four samples are given in Table 7. CIE separations of these samples are illustrated in Fig. 2, where it can be seen that S13-12 had a more complex composition, leading to many small peaks on its electropherogram. The last peak in the four electropherograms near 15 min was probably caused by water and other neutral compounds. The four subterranean water samples contained nitrate, iodide and thiocyanate, which were determined from the migration times shown in Table 4, and their concentrations were described as the blank concentrations of the three samples and calculated with the equation  $C = A/SL$ , where  $C$  is the concentration,  $A$  the area of the peak and  $SL$  the slope of the regression equation given in Table 6. Because the linearity range of the regression equation was from 1 to 40 ppm, concentrations lower than 1 ppm were calculated by the above method. After 10 ppm of nitrate, thiocyanate and/or iodide had been added to the four samples, after CIE separation the recoveries of the three anions in the four samples were calculated and are given in Table 8. It can be seen that the recoveries were between 90.8 and 113.4%.

Table 8  
Recoveries of nitrate, thiocyanate and/or iodide in four subterranean water samples

Sample	Dilution	Ion	Concentration (ppm)		Recovery (%)
			Blank	Determined	
L8-19	1:2	Nitrate	0.5	11.8	113
		Thiocyanate	0.0	9.1	91
WX3-82	1:5	Nitrate	0.4	10.5	101
		Thiocyanate	0.0	9.4	94
HT1	1:10	Nitrate	0.0	11.1	111
		Thiocyanate	0.0	10.1	101
		Iodide	0.0	10.0	100
S13-12	1:2	Nitrate	0.0	10.6	106
		Thiocyanate	0.6	10.0	93
		Iodide	0.5	10.1	96

## Acknowledgement

This work was financially supported by the Chinese Academy of Sciences.

- [1] W.R. Jones and P. Jandik, *Am. Lab.*, 22 (1990) 51.
- [2] W.R. Jones, P. Jandik and R. Pfeiter, *Am. Lab.*, 23 (1991) 40.
- [3] P. Jandik, W.R. Jones, A. Weston and P.R. Brown, *LC·GC*, 9 (1991) 634.
- [4] P. Jandik and W.R. Jones, *J. Chromatogr.*, 546 (1991) 431.
- [5] J.P. Romano and J. Krol, *J. Chromatogr.*, 640 (1993) 403.
- [6] G. Bondoux, P. Jandik and W.R. Jones, *J. Chromatogr.*, 602 (1992) 79.
- [7] B.J. Wildman, P.E. Jackson, W.R. Jones and P.G. Alden, *J. Chromatogr.*, 546 (1991) 459.
- [8] M. Schmitt, F. Saulnier, L. Malhautier and G. Linden, *J. Chromatogr.*, 640 (1993) 419.
- [9] B.F. Kenney, *J. Chromatogr.*, 546 (1991) 423.
- [10] D.R. Salomon, *J. Chromatogr.*, 602 (1992) 219.
- [11] S.C. Grocott, L.P. Jefferies, T. Bowser, J. Carnevale and P.E. Jackson, *J. Chromatogr.*, 602 (1992) 252.
- [12] M.E. Swartz, *J.A. Chromatogr.*, 640 (1993) 411.
- [13] J.B. Nair and C.G. Izzo, *J. Chromatogr.*, 640 (1993) 445.
- [14] K.A. Hargadon and B.R. McCord, *J. Chromatogr.*, 602 (1992) 241.
- [15] W.R. Jones and P. Jandik, *J. Chromatogr.*, 608 (1992) 385.
- [16] L.G. Song, Q.Y. Ou, W.L. Yu and G.F. Xu, *J. Chromatogr. A*, 699 (1995) 371.
- [17] P.E. Jackson and P.R. Haddad, *J. Chromatogr.*, 640 (1993) 481.
- [18] D.S. Burgi and R.L. Chien, *J. Microcol. Sep.*, 3 (1991) 199.
- [19] D.S. Burgi and R.L. Chien, *Anal. Chem.*, 63 (1991) 2042.
- [20] D.S. Burgi and R.L. Chien, *Anal. Biochem.*, 202 (1992) 306.
- [21] A. Vinther, H. Soeberg, L. Nielsen, J. Petersen and K. Biedermann, *Anal. Chem.*, 64 (1992) 187.
- [22] R.L. Chien and D.S. Burgi, *Anal. Chem.*, 64 (1992) 1046.
- [23] D.S. Burgi, *Anal. Chem.*, 65 (1993) 3726.



ELSEVIER

Journal of Chromatography A, 715 (1995) 385–386

---

---

JOURNAL OF  
CHROMATOGRAPHY A

---

---

---

## Book Review

---

*Techniques and Practice of Chromatography (Chromatographic Science Series, Vol. 70)*, by R.P.W. Scott, Marcel Dekker, New York, 1995, XII + 395 pp., price US\$ 85.00, ISBN 0-8247-9460-5.

The structure of this book by Raymond Scott, one of the pioneers in gas and efficient liquid chromatography, reflects his theoretical and practical experience. The text is divided into four parts: The chromatographic process, covering separation mechanisms, retention phenomena, peak dispersion, qualitative and quantitative analysis in a manner valid both for GC and LC; Gas chromatography, and Liquid chromatography both with the same structure (apparatus, detectors, columns and examples of application), and Thin-layer chromatography with two subchapters: Apparatus and Techniques. All parts contain thoroughly selected basic material necessary to understand the essential minimum from which it is possible for anybody to enlarge knowledge—if necessary—by further study.

In the preface, Scott formulates his philosophy: for the 21st century, it seems to be more beneficial to have books like this one rather than books written as reference texts on special subjects. This is really valid as experienced lecturers, giving basic education courses for those unfamiliar with the subject, can confirm.

Nevertheless, in such a case it is necessary not to overlook books like those by Smith [1] or Poole and Poole [2] which have appeared between the time of issue of the cited Mikes [3] and the author's book on the same (or a little bit broader) topic. The author emphasizes the precision in the use of nomenclature and definitions

but does not refer on a recent and excellent booklet by Etre and Hinshaw [4].

There are some weaknesses following from the title of the book which is broader than the content. E.g., supercritical fluid chromatography is overlooked also in otherwise very instructive subchapters about phases; gel chromatography is not mentioned although it is more significant than size exclusion on silica summarized in entropically driven separations; ion chromatography is marginally mentioned in connection with ionic forces and with few examples illustrating them; GC and LC separations based on complexation, and affinity chromatography are not mentioned at all. A few more minor comments follow: among hyphenated techniques (Chapter 4), the combinations with spectrometric methods such as atomic absorption and atomic emission spectrometry are missing. Calibration technique (Chapter 5) is not discussed although it is often erroneously used due to its apparent simplicity. Frontal analysis (Figure 4) is oversimplified because the second, third or further analytes are not simply superimposed on a *constant concentration* of solutes A, B, etc. In Fig. 19, the omitted description of axes as well as of peaks decreases the value of the example of application.

With the exception of the above weaknesses, I can recommend the book for the first approach to gas, liquid and thin-layer chromatography because of a didactically instructive presentation

of basic intermolecular forces and processes playing a substantial role in understanding the selectivity and resolution of separations, and a nice broad set of practical examples of applications.

*Brno, Czech Republic*

**Jaroslav Janák**

[1] R.M. Smith, *Gas and Liquid Chromatography in Analytical Chemistry*, Wiley, New York, 1988.

[2] C.F. Poole and S.K. Poole, *Chromatography Today*, Elsevier, Amsterdam, 1991.

[3] O. Mikeš, *Laboratory Handbook of Chromatographic Methods*, Van Nostrand, London, 1966.

[4] L.S. Ettre and J.V. Hinshaw, *Basic Relationships of Gas Chromatography*, Avanstar Communications, Cleveland, OH, 1993.



ELSEVIER

Journal of Chromatography A, 715 (1995) 387–388

---

---

JOURNAL OF  
CHROMATOGRAPHY A

---

---

---

## Book Review

---

*Ion Chromatography*, by J. Weiss, VCH, Weinheim, New York, 2nd ed., 1995, XII + 465 pp., price DM 164.00, ISBN 3-527-28698-5.

This edition of *Ion Chromatography* follows from the first edition published almost ten years ago. The original text has proved to be an excellent reference work for suppressed ion chromatography (SIC) and this new edition promises to be just as successful.

The layout and content of the book have been revised extensively from the first edition and there is substantially more material included. The first two chapters are devoted to an introduction to SIC and basic chromatographic theory. The main separation modes in SIC, namely ion-exchange, ion-exclusion and ion-pair chromatography, are covered in the next three chapters which together account for more than half of the book. Detection methods are treated in Chapter 6, with quantitative analysis (e.g. methods for determination of sample composition and statistical data assessment) and applications being covered in the final two chapters. The applications chapter is quite extensive (more than 100 pages) and is structured around the main application areas and industries which use SIC, including environmental analysis, power generation, electroplating, the semiconductor industry, detergents, foods and beverages, the pharmaceutical industry and clinical chemistry. A well-compiled and extensive index is included. The first question one must ask when looking at a second edition is whether it offers significant

new information. In this case, the answer undoubtedly is yes.

The text is written in an easily readable style, the topics are covered in a systematic and logical manner and the book is well illustrated with numerous chromatograms and figures. In addition, the layout of the printing is clear and pleasing to the eye. I found the content to be accurate and thorough and the book is certainly the best source of information on SIC that I have seen to date.

My criticisms are both very few and minor and could be considered more to be matters of opinion and personal preference rather than shortcomings of a scientific nature. Whilst there is some treatment of non-suppressed IC methods (more so than in the first edition), the book is dominated by SIC methods, particularly the applications chapter. The many users of non-suppressed IC will therefore find limited information only. Detection methods are treated much less comprehensively than separation methods, when in practice the correct choice of detector is usually just as important as the choice of the separation mode. Finally, sample preparation methods are treated in only three pages and this aspect often governs the success or otherwise of an analysis. None of these criticisms detracts significantly from the text.

In summary, the second edition of *Ion Chro-*

*matography* raises the already high standard of the first edition and will find widespread appeal among the practitioners of SIC who will derive sound theoretical knowledge and good practical

information from the book. I am sure that it will be a success and I recommend it strongly.

*Hobart, Australia*

**Paul R. Haddad**

## Author Index Vol. 715

- Abdul-Wajid, A., see Gadowski, L. 715(1995)241
- Adachi, T., Nemoto, M. and Ito, Y.  
Method of increasing the sensitivity of liquid chromatography-atmospheric pressure chemical ionization mass spectrometry using a semi-micro column 715(1995)13
- Albanesi, C., see Castelnovo, P. 715(1995)143
- Andersson, P.E., see Engström, A. 715(1995)151
- Anspach, F.B., see Beeskow, T.C. 715(1995)49
- Araki, T., see Harino, H. 715(1995)135
- Asztemborska, M., see Sybilska, D. 715(1995)309
- Baiocchi, C., Marengo, E., Roggero, M.A., Giacosa, D., Giorcelli, A. and Toccari, S.  
Chromatographic and chemometric investigation of the chemical defence mechanism of poplar tree genotypes against a bark fungine parasite 715(1995)95
- Beeskow, T.C., Kusharyoto, W., Anspach, F.B., Kroner, K.H. and Deckwer, W.-D.  
Surface modification of microporous polyamide membranes with hydroxyethyl cellulose and their application as affinity membranes 715(1995)49
- Berthelot, P., see Vaccher, C. 715(1995)361
- Bhanger, M.I., see Khuhawar, M.Y. 715(1995)366
- Billiet, H.A.H., see Corstjens, H. 715(1995)1
- Bisello, A., see Casazza, A. 715(1995)227
- Blaylock, A., see Ward, T.J. 715(1995)337
- Bockhardt, A., see Krause, I. 715(1995)67
- Bogillo, V.I. and Voelkel, A.  
Solution properties of amorphous co- and terpolymers of styrene as examined by inverse gas chromatography 715(1995)127
- Bu, Q., see Panda, S. 715(1995)279
- Buchmann, T., see Fricke, B. 715(1995)247
- Carlsson, H. and Östman, C.  
Retention mechanisms of polycyclic aromatic nitrogen heterocyclics on bonded amino phases in normal-phase liquid chromatography 715(1995)31
- Carrier, D.-J., Cunningham, J.E., Hogge, L.R., Taylor, D.C. and Dunstan, D.I.  
Gas chromatographic-mass spectrometric characterization of some fatty acids from white and interior spruce 715(1995)317
- Casazza, A., Curcuruto, O., Hamdan, M., Bisello, A. and Peggion, E.  
Investigation of crudes of synthesis of neuropeptide Y by high-performance liquid chromatography-electrospray mass spectrometry 715(1995)227
- Castells, R.C., Romero, L.M. and Nardillo, A.M.  
Thermodynamic consideration of the retention mechanism in a poly(perfluoroalkyl ether) gas chromatographic stationary phase used in packed columns 715(1995)299
- Castelnovo, P. and Albanesi, C.  
Determination of the enantiomeric purity of 5,6-dihydroxy-2-aminotetralin by high-performance capillary electrophoresis with crown ether as chiral selector 715(1995)143
- Cherkaoui, S., Faupel, M. and Francotte, E.  
Separation of formoterol enantiomers and detection of zeptomolar amounts by capillary electrophoresis using laser-induced fluorescence 715(1995)159
- Chevolleau, S. and Tulliez, J.  
Optimization of the separation of  $\beta$ -agonists by capillary electrophoresis on untreated and  $C_{18}$  bonded silica capillaries 715(1995)345
- Chmelík, J., see Pazourek, J. 715(1995)259
- Corstjens, H., Billiet, H.A.H., Frank, J. and Luyben, K.Ch.A.M.  
Optimisation of selectivity in capillary electrophoresis with emphasis on micellar electrokinetic capillary chromatography 715(1995)1
- Cunningham, J.E., see Carrier, D.-J. 715(1995)317
- Curcuruto, O., see Casazza, A. 715(1995)227
- Dann III, C., see Ward, T.J. 715(1995)337
- Debaert, M., see Vaccher, C. 715(1995)361
- Deckwer, W.-D., see Beeskow, T.C. 715(1995)49
- DeMontigny, P., see Faulkner, A. 715(1995)189
- Dunstan, D.I., see Carrier, D.-J. 715(1995)317
- Engström, A., Wan, H., Andersson, P.E. and Josefsson, B.  
Determination of chiral reagent purity by capillary electrophoresis 715(1995)151
- Fang, L., see Song, L. 715(1995)376
- Faulkner, A. and DeMontigny, P.  
High-performance liquid chromatographic determination of denatonium benzoate in ethanol with 5% polyvinylpyrrolidone 715(1995)189
- Faupel, M., see Cherkaoui, S. 715(1995)159
- Francotte, E., see Cherkaoui, S. 715(1995)159
- Frank, J., see Corstjens, H. 715(1995)1
- Fricke, B., Buchmann, T. and Friebe, S.  
Unusual chromatographic behaviour and one-step purification of a novel membrane proteinase from *Bacillus cereus* 715(1995)247
- Friebe, S., see Fricke, B. 715(1995)247
- Fülöp, F., see Péter, A. 715(1995)219
- Funazo, K., see Harino, H. 715(1995)135
- Gadowski, L. and Abdul-Wajid, A.  
Quantitation of monoclonal antibodies by perfusion chromatography-immunodetection 715(1995)241
- Galceran, M.T. and Moyano, E.  
Determination of hydroxy-substituted polycyclic aromatic hydrocarbons by high-performance liquid chromatography with electrochemical detection 715(1995)41
- Giacosa, D., see Baiocchi, C. 715(1995)95
- Giang, Y.-S., see Wang, S.-M. 715(1995)325
- Giddings, J.C., see Shiundu, P.M. 715(1995)117
- Giese, R.W.  
Editorial 715(1995)v
- Gifford, L.A., Owusu-Daaku, F.T.K. and Stevens, A.J.  
Acenaphthene fluorescence derivatisation reagents for use in high-performance liquid chromatography 715(1995)201

- Gill, D.S., Roush, D.J., Shick, K.A. and Willson, R.C.  
Microcalorimetric characterization of the anion-exchange adsorption of recombinant cytochrome b<sub>5</sub> and its surface-charge mutants 715(1995)81
- Giorcelli, A., see Baiocchi, C. 715(1995)95
- Gmahl, E., see Tegeler, A. 715(1995)195
- Goronowicz, J., see Sybilska, D. 715(1995)309
- Govers, H.A.J., Van der Wielen, F.W.M. and Olie, K.  
Derivation of solubility parameters of chlorinated dibenzofurans and dibenzo[*p*]dioxins from gas chromatographic retention parameters via SOFA 715(1995)267
- Gump, E.L. and Monnig, C.A.  
Pre-column derivatization of proteins to enhance detection sensitivity for sodium dodecyl sulfate non-gel sieving capillary electrophoresis 715(1995)167
- Haddad, P.R.  
Ion Chromatography (edited by J. Weiss) (Book Review) 715(1995)387
- Hamdan, M., see Casazza, A. 715(1995)227
- Harino, H., Tanaka, M., Araki, T., Yasaka, Y., Masuyama, A., Nakatsuji, Y., Ikeda, I., Funazo, K. and Terabe, S.  
Double-chain surfactants with two sulfonate groups as micelle-forming reagents in micellar electrokinetic chromatography of naphthalene derivatives 715(1995)135
- Henle, T., see Krause, I. 715(1995)67
- Hogge, L.R., see Carrier, D.-J. 715(1995)317
- Huber, W., Molero, A., Pereyra, C. and Martínez de la Ossa, E.  
Determination of cholesterol in milk fat by supercritical fluid chromatography 715(1995)333
- Ikeda, I., see Harino, H. 715(1995)135
- Ito, Y., see Adachi, T. 715(1995)13
- Janvion, P., Motellier, S. and Pitsch, H.  
Ion-exchange mechanisms of some transition metals on a mixed-bed resin with a complexing eluent 715(1995)105
- Jin, Y., see Song, L. 715(1995)376
- Josefsson, B., see Engström, A. 715(1995)151
- Khuhawar, M.Y., Memon, A.A. and Bhangar, M.I.  
Nickel(II) chelates of some tetradentate Schiff bases as stationary phases for gas chromatography 715(1995)366
- Klampfl, C.W. and Spanos, E.  
Separation of priority pollutant phenols on chemically modified poly(styrene-divinylbenzene) resins by high-performance liquid chromatography 715(1995)213
- Klostermeyer, H., see Krause, I. 715(1995)67
- Krause, I., Bockhardt, A., Neckermann, H., Henle, T. and Klostermeyer, H.  
Simultaneous determination of amino acids and biogenic amines by reversed-phase high-performance liquid chromatography of the dabsyl derivatives 715(1995)67
- Kroner, K.H., see Beeskow, T.C. 715(1995)49
- Kusharyoto, W., see Beeskow, T.C. 715(1995)49
- Janák, J.  
Technique and Practice of Chromatography (edited by R.P.W. Scott) (Book Review) 715(1995)385
- Li, H.-Z., see Li, T.-S. 715(1995)372
- Li, J.-T., see Li, T.-S. 715(1995)372
- Li, T.-S., Li, J.-T. and Li, H.-Z.  
Modified and convenient preparation of silica impregnated with silver nitrate and its application to the separation of steroids and triterpenes 715(1995)372
- Ling, Y.-C., see Wang, S.-M. 715(1995)325
- Liu, J., see Zhou, W. 715(1995)355
- Luyben, K.Ch.A.M., see Corstjens, H. 715(1995)1
- Marengo, E., see Baiocchi, C. 715(1995)95
- Martínez de la Ossa, E., see Huber, W. 715(1995)333
- Masujima, T., see Razee, S. 715(1995)179
- Masuyama, A., see Harino, H. 715(1995)135
- Memon, A.A., see Khuhawar, M.Y. 715(1995)366
- Meyerhoff, M.E., see Xiao, J. 715(1995)19
- Mitov, I.P. and Petrov, L.A.  
Assessment of some possibilities for improving the performance of gas chromatographic thermal conductivity detectors with hot-wire sensitive element 715(1995)287
- Molero, A., see Huber, W. 715(1995)333
- Monnig, C.A., see Gump, E.L. 715(1995)167
- Motellier, S., see Janvion, P. 715(1995)105
- Moyano, E., see Galceran, M.T. 715(1995)41
- Nakatsuji, Y., see Harino, H. 715(1995)135
- Nardillo, A.M., see Castells, R.C. 715(1995)299
- Neckermann, H., see Krause, I. 715(1995)67
- Nemoto, M., see Adachi, T. 715(1995)13
- Olie, K., see Govers, H.A.J. 715(1995)267
- Östman, C., see Carlsson, H. 715(1995)31
- Ou, Q., see Song, L. 715(1995)376
- Owusu-Daaku, F.T.K., see Gifford, L.A. 715(1995)201
- Panda, S., Bu, Q., Yun, K.S. and Parcher, J.F.  
Repetitive liquid injection system for inverse gas chromatography 715(1995)279
- Parcher, J.F., see Panda, S. 715(1995)279
- Pazourek, J. and Chmelík, J.  
Experimental study on the separation of silica gel supports by gravitational field-flow fractionation. II. Sample preparation, stop-flow procedure and overloading effect 715(1995)259
- Peggion, E., see Casazza, A. 715(1995)227
- Pereyra, C., see Huber, W. 715(1995)333
- Péter, A. and Fülöp, F.  
High-performance liquid chromatographic method for the separation of isomers of *cis*- and *trans*-2-amino-cyclopentane-1-carboxylic acid 715(1995)219
- Petrov, L.A., see Mitov, I.P. 715(1995)287
- Pitsch, H., see Janvion, P. 715(1995)105
- Razee, S., Tamura, A. and Masujima, T.  
Improvement in the determination of food additive dyestuffs by capillary electrophoresis using  $\beta$ -cyclodextrin 715(1995)179
- Roggero, M.A., see Baiocchi, C. 715(1995)95
- Romero, L.M., see Castells, R.C. 715(1995)299
- Roush, D.J., see Gill, D.S. 715(1995)81
- Ruess, W., see Tegeler, A. 715(1995)195
- Shick, K.A., see Gill, D.S. 715(1995)81



- Shiundu, P.M. and Giddings, J.C.  
Influence of bulk and surface composition on the retention of colloidal particles in thermal field-flow fractionation 715(1995)117
- Song, L., Ou, Q., Yu, W., Fang, L. and Jin, Y.  
Determination of the petroleum tracers nitrate and thiocyanate in subterranean waters by capillary ion electrophoresis 715(1995)376
- Spanos, E., see Klampfl, C.W. 715(1995)213
- Stevens, A.J., see Gifford, L.A. 715(1995)201
- Sybiliska, D., Asztemborska, M., Zook, D.R. and Goronowicz, J.  
Glycerol as a new dissolution medium for  $\alpha$ -,  $\beta$ - and  $\gamma$ -cyclodextrins for preparing stereoselective stationary phases for gas-liquid chromatography 715(1995)309
- Tamura, A., see Razez, S. 715(1995)179
- Tanaka, M., see Harino, H. 715(1995)135
- Taylor, D.C., see Carrier, D.-J. 715(1995)317
- Tegeler, A., Ruess, W. and Gmahl, E.  
Determination of amphoteric surfactants in cosmetic cleansing products by high-performance liquid chromatography on a cation-exchange column 715(1995)195
- Terabe, S., see Harino, H. 715(1995)135
- Toccori, S., see Baiocchi, C. 715(1995)95
- Tsai, L.-C., see Wang, S.-M. 715(1995)325
- Tulliez, J., see Chevolleau, S. 715(1995)345
- Vaccher, C., Berthelot, P. and Debaert, M.  
GABA-B agonists: enantiomeric resolution of 4-amino-3-(5-chlorothien-2-yl)butyric acid and analogues on chiral crown ether stationary phase 715(1995)361
- Van der Wielen, F.W.M., see Govers, H.A.J. 715(1995)267
- Voelkel, A., see Bogillo, V.I. 715(1995)127
- Wan, H., see Engström, A. 715(1995)151
- Wang, E., see Zhou, W. 715(1995)355
- Wang, S.-M., Ling, Y.-C., Tsai, L.-C. and Giang, Y.-S.  
Headspace sampling and gas chromatographic-mass spectrometric determination of amphetamine and methamphetamine in betel 715(1995)325
- Ward, T.J., Dann III, C. and Blaylock, A.  
Enantiomeric resolution using the macrocyclic antibiotics rifamycin B and rifamycin SV as chiral selectors for capillary electrophoresis 715(1995)337
- Willson, R.C., see Gill, D.S. 715(1995)81
- Xiao, J. and Meyerhoff, M.E.  
High-performance liquid chromatography of  $C_{60}$ ,  $C_{70}$ , and higher fullerenes on tetraphenylporphyrin-silica stationary phases using strong mobile phase solvents 715(1995)19
- Yasaka, Y., see Harino, H. 715(1995)135
- Yu, W., see Song, L. 715(1995)376
- Yun, K.S., see Panda, S. 715(1995)279
- Zhou, W., Liu, J. and Wang, E.  
Determination of aminopyrine and its metabolite by capillary electrophoresis-electrochemical detection 715(1995)355
- Zook, D.R., see Sybiliska, D. 715(1995)309





# Journal of Chromatography A



## NEWS SECTION

### SYMPOSIUM PROGRAMME

#### 4th International Symposium on HYPHENATED TECHNIQUES IN CHROMATOGRAPHY AND HYPHENATED CHROMATOGRAPHIC ANALYZERS (HTC 4)

The Saint John's Conference Center,  
Bruges (Belgium), February 6 - 9, 1996

The symposium will be preceded by a series of workshops (hands-on training as well as tutorial).

#### Introduction

The Fourth International Symposium on Hyphenated Techniques in Chromatography and Hyphenated Chromatographic Analyzers (HTC 4) will again cover all fundamental aspects, instrumental developments and applications of the various hyphenated chromatographic techniques (e.g. coupling of GC or LC to LC, GC and SFC-SFE; MS, FTIR, AED and other techniques coupled with GC, (HP)LC, SFC and CZE; PTV-GC-MS; on-line air traps-, purge-and-trap-, extractors-, and GPC-GC (or LC); LC to NMR, FIA-DAD, light scattering; ITP-MS, etc.). Emphasis will also be placed on the design of hyphenated, on-line and at-line, chromatographic analyzers.

The scientific programme will include oral presentations in plenary and parallel sessions, poster presentations and tutorials given by prominent scientists. A technical exhibition will give an overview of instruments, books and accessories. The latest developments in instrumentation will be presented during workshop type product seminars. Finally, a social and an accompanying persons programme including optional tours in Bruges and Northern Belgium will be offered.

#### HTC-4 Award

During the Fourth International Symposium on Hyphenated Techniques in Chromatography, an HTC-Award will be presented to the most innovative paper- or poster contribution of the Conference. An international jury under the chairmanship of Prof. F. Adams, will ensure that the most outstanding and innovative work in the field of hyphenated chromatographic techniques will be awarded. The award will be presented during the closing session on the last symposium-day.

#### Call for papers

Abstracts for last minute poster presentations will be accepted up to December 30, 1995. Abstracts will be considered by a panel of referees for inclusion in the programme. Please note that an accepted paper will only be included in the final programme if the author has formally registered and paid the fee. Abstracts of all papers will be available to registered participants.

The abstract book will have an ISBN number and can thus be cited as an official publication.

### Publication

A special volume of the *Journal of Chromatography A* will be dedicated to the accepted and reviewed papers, which will be channelled through the usual refereeing system. Deadline for manuscripts is the last day of the symposium (i.e. February 9, 1996).

### Further information

Submission forms for papers, enquiries about the technical exhibition and all other information may be obtained from the HTC 4-Congress Secretariate, Ordibo bvba, Lucas Henninckstraat 18, B-2610 Wilrijk (Belgium), tel./fax : + 32 (3) 828.89.61.

## Workshops preceeding the HTC 4 Symposium

A number of workshops (hands-on training as well as tutorials) will be organized on Monday February 5 and Tuesday February 6, 1996.

### WORKSHOP no. 1 (2 days)

Large volume injection : The Next Step in Capillary Gas Chromatography for Trace Analysis

**K. Grob** (Kantonales Labor Zürich, Switzerland), **R.C.M. Leenderts** (Interscience, Breda, The Netherlands), **F. Munari** (CE Instruments, Italy), **M. Termonia** (DCMS, Bierges, Belgium)

### WORKSHOP no. 2 (2 days)

Pre- and postcolumn techniques in HPLC for improved analyte isolation, derivatization, cleanup, separation, and detection

**I. S. Krull** (Northeastern University, Boston, Massachusetts, USA) and **H. Lingeman** (Free University of Amsterdam, The Netherlands)

### WORKSHOP no. 3 (1 1/2 day)

Isotopically labelled compounds in hyphenated GC-techniques

**M. Matucha** and **M. Kubátová** (Czech Academy of Science, Prague, Czech Republic)

### WORKSHOP no. 4 (2 days)

Analytical tools for GC-MS (Advanced modes of

ion-trap mass spectrometry)

**J. D. Mills** (Varian Ltd, Walton-on-Thames, United Kingdom)

### WORKSHOP no. 5 (2 days)

Biomedical applications of GC-MS

**H. G. Wahl** (University of Tübingen, Germany)

## HTC 4 - PRELIMINARY PROGRAMME

### WEDNESDAY, FEBRUARY 7, 1996

#### Opening adress

**R. Smits** (Chairman of the Organizing Committee)  
**F. Adams** (Chairman of the Scientific Committee)

#### Session 1 - Hyphenated Chromatography - Environmental Analysis and Instrumental Techniques (Part I)

**Hawthorne S.B.** (University of North Dakota, Grand Forks, USA)

On-line and off-line supercritical fluid extraction (SFE) for environmental analysis

**Brinkman U.A.Th.** (Free University of Amsterdam, The Netherlands)

The potential of hyphenation and coupled-column techniques in applied analysis

#### Break - Coffee - Visit to the exhibition - Poster session

#### Product Seminar : CE Instruments

#### Session 2 - Environmental Analysis with Hyphenated Chromatography (Part II)

**Bartle K.D.** (University of Leeds, U.K.)

LC-GC-MS in the analysis of atmospheric polycyclic aromatic compounds

**Louter A.J.H.**, **Slobodník J.**, **Hogenboom A.C.** and **Brinkman U.A.Th.** (Free University of Amsterdam, The Netherlands)

Comparison of negative chemical and electron impact ionization in on-line solid-phase extraction gas chromatography-mass spectrometry for the ultra-trace-level analysis of contaminants in water and sediment

**Möder M.**, **Schrader St.** and **Popp P.** (Center for Environmental Research Leipzig-Halle Ltd, Germany)

The comparison of solid-phase micro extraction (SPME) coupled with GC-MS and LC-MS for phenol determination in strong matrix loaded waste water

*Session 3 - Biomedical Analysis with Hyphenated Chromatography (Part I)*

Dovich N.J. (University of Alberta, Edmonton, Canada)

Laser induced fluorescence detection for DNA sequencing by capillary electrophoresis

Ogorka J. (Sandoz Pharma, Basle, Switzerland)

On-line coupled RP-LC-GC-MS including on-line derivatization a lucrative approach to the structure elucidation of unknown organic impurities in pharmaceutical products

Appfel A., Chakel J.A., Hancock W.S., Souders C.\*, M'Timkulu T.\* and Pungor E. Jr.\* (Hewlett Packard Laboratories, Palo Alto and \*Berlex Biosciences, Brisbane, CA, USA)

Application of affinity techniques in combination with HPLC, ESI-LC-MS and MALDI-TOFMS to the characterization of post-translational glycosylation of single chain plasminogen activator

**Tutorial 1 - Adams F.C.** (University of Antwerp, Belgium)

Organometal speciation analysis with metal-specific detectors

*Session 4 - Food and Organics Analysis with Hyphenated Chromatography (Part I)*

Grob K. (Kantonales Labor, Zürich, Switzerland)

Large volume injection or on-line LC-GC through a vaporizing chamber

*Break - Coffee - Visit to the exhibition - Poster session*

*Product Seminar : Bruker*

*Session 5 - Instrumental techniques in Hyphenated Chromatography (Part II)*

Regnier F.E. (Purdue University, Indiana, USA)

Integration of chromatography into multidimensional analytical systems

Webster C., Clarkson P. and Cooke M. (Sheffield Hallam University, Sheffield, UK)

Atomic emission detection — sometimes a very useful technique

Henion J.D. (Cornell University, Ithaca, New York, USA)

New strategies in trace level sample analyses using HPLC coupled with tandem mass spectrometry

Matz G., Märkl H. and Lennemann F. (Technical University of Hamburg-Harburg, Germany)

On-line monitoring of biotechnological processes by GC-MS analysis of fermentation suspensions

Prokisch J., Kovács B. and Gyóri Z. (Debrecen Agricultural University, Hungary)

Theoretical and practical problems in hyphenation of a liquid chromatograph and an atomic emission (ICP) or atomic absorption (AAS) instrument

*Session 6 - Food and Organics Analysis with Hyphenated Chromatography (Part II)*

Mondello L. (University of Messina, Italy)

On-line coupled HPLC-HRGC-MS in food analyses

Stan H.-J. (Technical University Berlin, Germany)

Capillary gas chromatography-atomic emission detection. A useful instrumental method in pesticide residue analysis of plant foodstuffs and water

De Brabander H.F., Batjoens P. and De Wasch K. (University of Ghent, Belgium)

Comparison of the possibilities of magnum GC-MS and GCQ MS-MS for the analysis of anabolics in biological material

Planck C. and Lorbeer E. (University of Vienna, Austria)

On-line normal-phase LC-GC for the analysis of liquid biofuels

Jickells S. (Ministry of Agriculture, Norwich, UK)

Analysis of plastics monomers, oligomers and additives in food contact materials and measurement of migration to foods and food simulants using LC-MS, ICP-MS and SEC-FTIR

**THURSDAY, FEBRUARY 8, 1996**

*Session 7 - Speciation Analysis with and Statistics Techniques in Hyphenated Chromatography (Part I)*

Donard O.F.X. (University of Bordeaux, France)

Hyphenated methods applications for trace metal speciation in marine environments

Cuesta-Sanchez F. and Massart D.L. (Free University of Brussels, Belgium)

Chemometrics for hyphenated data

*Break - Coffee - Visit to the exhibition - Poster session*

*Product Seminar : Finnigan MAT*

*Session 8 - Speciation Analysis with Hyphenated Chromatography (Part II)*

Quevauviller Ph. (Commission of the European Communities, Brussels, Belgium)

Improvement of quality control of speciation analysis using hyphenated techniques – a decade of progress within the European Community

Caruso J.A. (University of Cincinnati, Ohio, USA)

Chromatography-plasma mass spectrometry: new departures for elemental speciation

Michalke B. and Schramel P. (GSF Environmental and Health Research Center, Oberschleissheim, Germany)

Hyphenation of CE to ICP-MS as element specific detector for metal speciation

*Session 9 - Statistical Techniques in Hyphenated Chromatography (Part II)*

Davis J.M. (Southern Illinois University, Carbon-dale, USA)

Statistical interpretation of two-dimensional separations developed by microbore-LC-TLC

Rosenberg E., Peck M. and Grasserbauer M. (Vienna University of Technology, Austria)

Multifactorial optimisation of an atomic emission detector with microwave-induced He-plasma for the analysis of trace organic compounds

Škrbi B., Cvejanov J. and Pavi-Suzuki L. (University of Novi Sad, Yugoslavia)

Unified retention concept – Statistical interpretation of Kovats retention index

**Tutorial 2 - Cramers C.A., Mol J.G.J., Bosboom J.C. and Janssen J.G.M.** (Eindhoven University of Technology, The Netherlands)

PTV-based methods for large volume sampling in capillary gas chromatography

*Session 10 - Instrumental techniques in Hyphenated Chromatography (Part III)*

Sandra P. (University of Ghent, Belgium)

Hyphenation in capillary GC – Toward the 21st century

*Break - Coffee - Visit to the exhibition - Poster session*

*Product Seminar : Waters*

*Session 11 - Instrumental techniques in Hyphenated Chromatography (Part IV)*

Pawliszyn J., Yang M., Luo Y., Zhang Z., Gorecki T. and Chen J. (University of Waterloo, Ontario, Canada)

Hyphenated techniques based on SPME and MESI  
Van Ysacker P.G., Janssen H.-G., Leclercq P. and Cramers C.A. (Eindhoven University of Technology, The Netherlands)

High-speed narrow-bore capillary gas chromatography with high-resolution mass spectrometric detection

Lingeman H. (Free University of Amsterdam, The Netherlands)

On-line, membrane based, chromatographic techniques

Albert K. (University of Tübingen, Germany)

On-line use of NMR detection in separation chemistry

Koel M. and Kaljurand M. (Academy of Sciences, Tallinn, Estonia)

Thermochromatography – hyphenated evolved gas analysis technique

*Session 12 - Environmental Analysis with Hyphenated Chromatography (Part III)*

Grasserbauer M. (Vienna University of Technology, Austria)

Potential of GC-MIP for environmental trace analysis

De Smaele T., Vanhaecke F., Moens L. and Dams R. (University of Ghent, Belgium)

ICP mass spectrometry: a highly sensitive and selective detection method for the determination of organometals after separation with CGC

Blomberg J., Kerkvliet S. and Schoenmakers P. (Shell Research, Amsterdam, The Netherlands)

Development and application of a family of hyphenated separation systems

Hankemeier Th., van der Laan H.T.C., Vreuls J.J., Brinkman U.A.Th., Vredenburg M.J.\* and Visser T.\* (Free University of Amsterdam and \* National Institute of Public Health and Environmental Protection, Bilthoven, The Netherlands)

Large volume injections in cryotrapping GC-FTIR for trace level environmental analysis

Van Lieshout M., Janssen H.-G. and Cramers C.A.

(Eindhoven University of Technology, The Netherlands)

A PTV-based on-line solid-phase extraction disk large volume GC-MS system (SPE-LV-GC-MS) for water analysis

#### FRIDAY, FEBRUARY 9, 1996

##### *Session 13 - Instrumental techniques in Hyphe-nated Chromatography (Part V)*

Janssen H.-G. (Eindhoven University of Technology, The Netherlands)

On-line thermal sample pretreatment and large volume sampling in capillary GC using programmed temperature injection systems

*Break - Coffee - Visit to the exhibition - Poster session*

*Product Seminar : Varian*

##### *Session 14 - Biomedical Analysis with Hyphe-nated Chromatography (Part II)*

Esmans E.L. (University of Antwerp, Belgium)

Applications of electrospray mass spectrometry in biochemical and biomedical research

Krull I.S., Cho B.-Y., Zou H., Strong R. Li G., Fisher D.\* and Nappier J.L.\*\* (Northeastern University, Boston, Massachusetts, \* Oculon Corporation, Cambridge, Massachusetts and \*\* The Upjohn Company, Kalamazoo, Michigan, USA)

Immuno-chromatographic analysis (ICA), HPICA, and immunodetection for recombinant proteins in biofluids

Wahl H.-G. (University of Tübingen, Germany)

GC-MS and related hyphenated techniques in clinical chemistry

Kabzinski A. and Takagi T.\* (Technical University of Łódź, Poland and \* Osaka University, Japan)

The application of classical GPC and HPGPC-LALLS method for the determination of the physicochemical changes in thiolproteins and metallothiolproteins structure during separation by covalent affinity chromatography

Opiteck G.J., Jorgenson J.W.\* and Rose D.J.\* (University of North Carolina, Chapel Hill and \* Glaxo-Wellcome Inc, Research Triangle Park, North Carolina, USA)

Comprehensive two-dimensional LC-LC-MS separations of complex mixtures relevant to biomedical

and pharmaceutical research

##### *Session 15 - Food and Organics Analysis with Hyphe-nated Chromatography (Part III)*

Vreuls R., Louter A.J.H., Hankemeier Th. and Brinkman U.A.Th. (Free University of Amsterdam, the Netherlands)

On-line LC-GC based studies for the determination of micropollutants in various samples

Moyano E., Games D.E. and Galceran M.T.\* (University of Wales, Swansea, UK and \* University of Barcelona, Spain)

Determination of Quats by capillary electrophoresis-mass spectrometry

Dean J.R., Fowles I.A. and Ludkin E. (University of Northumbria, Newcastle upon Tyne, UK)

In-line concentration, extraction and analysis of herbicides using SPE-SFE-pSFC

van der Hoff G.R., Baumann R.A., Hogendoorn E.A. and van Zoonen P. (National Institute of Public Health and Environmental Protection, Bilthoven, The Netherlands)

Determination of organochlorine compounds by LC-GC-ECD

González-Vila F. J., Del Rio J.C., Martin F. and Verdejo T. (Institute of Natural Resources and Agrobiology, Sevilla, Spain)

Thermally assisted hydrolysis and methylation (THM) in combination with GC-MS as a modern analytical approach for the structural characterization of macromolecules

**Tutorial 3 - Grob K.** (Kantonales Labor, Zürich, Switzerland)

Control of edible oils: five key methods relying on on-line LC-GC — or how LC-GC became indispensable for routine analysis

##### *Session 16 - Instrumental techniques in Hyphe-nated Chromatography (Part VI)*

Wilkins C.L. (University of California, Riverside, USA)

Multidimensional GC with infrared and mass spectrometric detection

Matucha M. (Czech Academy of Science, Prague, Czech republic)

Isotopically labelled compounds in hyphenated GC techniques — Isotope effects

Lou X. (Eindhoven University of Technology, The

Netherlands)

Investigation of parameters affecting the extraction kinetics in supercritical fluid extraction combined on-line or off-line with capillary gas chromatography Zhang M., Liu Z.\* and Phillips J.B.\*\* (Xinjiang Institute of Technology, Urumgi, P.R. China, \* US Center for Disease Control and Prevention, Atlanta, Georgia, USA and \*\* Southern Illinois University, Carbondale, USA)

Narrow bore column GC analysis of organics in aqueous samples by direct large volume sample injection into Nafion tubing for concentration and thermal desorption for signal averaging

*Session 17 - Environmental Analysis with Hyphe-nated Chromatography (Part IV)*

Noij Th.H.M. (The Netherlands Waterworks, Nieuwegein, The Netherlands)

Monitoring polar organic compounds in water by on-line coupling of sample pre-concentration and chromatographic analysis

Pörschmann J., Remmler M. and Kopinke F.-D. (Centre for Environmental Research Leipzig-Halle Ltd, Germany)

Hyphe-nated techniques in characterizing coal waste-waters and associated sediments

Wedel A., Müller K.-P., Ratte M. and Rudolph J. (Institute for Atmospheric Chemistry, Jülich, Ger-many)

Measurements of aldehydes and terpenes in ambient air applying an on-line GC-MS technique

Nielen M.W.F. (Akzo Nobel Central Research, Arn-hem, The Netherlands)

Characterization of synthetic resins by hyphe-nated chromatographic and mass spectrometric techniques

*Break - Coffee*

*Session 18 - Instrumental techniques in Hyphe-nated Chromatography (Part VII)*

Cortes H.J. (Dow Chemical Company, Midland, Mi-chigan, USA)

The role of miniaturization in hyphe-nated chromato-graphy

*Closing Ceremony - Remittance of the HTC 4 - Award*

**PRELIMINARY POSTER PRO-GRAMME**

**ENVIRONMENTAL ANALYSIS WITH HYPHE-NATED CHROMATOGRAPHY**

Ahmad U.K. and Salleh N.M. (Malaysian University of Technology, Johor, Malaysia) On-line SFE-HPLC for the analysis of polycyclic aromatic hydro-carbons

Beltran J., David F.\* and Sandra P.\*\* (University of Jaume, Castello, Spain, \* Research Insitute for Chromatography, Kortrijk, Belgium and \*\* University of Ghent, Belgium)

Determination of atrazine and metabolites in water and soil by CGC-MS-MS

Hogenboom A.C., Slobodník J., Louter A.J.H. and Brinkman U.A.Th. (Free University of Amsterdam, The Netherlands)

Integrated system for on-line gas and liquid chroma-tography using a single mass spectrometric detector for automated analysis of environmental samples

Hogenboom A.C., Slobodník J., Minnaard W.A. and Brinkman U.A.Th. (Free University of Amsterdam, The Netherlands)

Rapid trace-level identification of environmental micropollutants using a single short-column for en-richment and separation combined with diode array UV and MS detection

Jia C., Wang X.\* and Ou Q.\* (Nankai University, Tianjin and \* Chinese Academy of Sciences, Lanz-hou, P.R. China)

Microwave-induced plasma atomic emission spec-trometer used as the detector of on-line coupled high-perfomance LC-GC. (LC-GC-MIP)

Mahler H. (Siemens AG, Karlsruhe, Germany)

Monitoring of chloromethyl methyl ether emissions at sub-ppb level around working areas - an on-line air trap GC-GC system

Matz G. and Kibelka G. (Technical University of Hamburg-Harburg, Germany)

Rapid trace analysis by large volume injection and thermal desorption

Matz G., Harder A., Schillings A. and Rechenbach P.\* (Technical University of Hamburg-Harburg and \* Fire Department of Hamburg, Germany)

Fast GC-MS analysis of hazardous organics in fires and chemical accidents

Matz G., Schillings A. and Harder A. (Technical University of Hamburg-Harburg, Germany)



Simple calibration procedure for field GC-MS analysis of Tenax air samples

Ollesch T., Schröder W., Matz G. and Francke W.\* (Technical University of Hamburg-Harburg and \* University of Hamburg, Germany)

A new fast method for field screening of PCBs in air  
Rosenberg E., Silgoner I. and Grasserbauer M. (Vienna University of Technology, Austria)

Determination of volatile organic compounds in water by GC-AED - A comparison between purge & trap and solid-phase micro extraction

Scilingo A., Buttini P., Gigantiello N., Latella A. (Eniricerche S.p.A., S. Donato Milanese, Italy)

Supercritical fluid extraction (SFE) of polycyclic aromatic hydrocarbons (PAHs) in emissions from gasoline engines

Steketee P.C., Hankemeier Th., Vreuls J.J. and Brinkman U.A.Th.

(Free University of Amsterdam, The Netherlands)

Automated analysis of micropollutants in water with at-line SPE-GC using the prepsation

#### **INSTRUMENTAL TECHNIQUES IN HYPHENATED CHROMATOGRAPHY**

Cabaleiro O., Lores M. and Cela R. (University of Santiago de Compostella, Spain)

Post-column photochemical derivatization for microcolumn HPLC

Hehn W. and Maurer T. (Siemens AG, Karlsruhe, Germany)

On-line PINA analysis - advanced process GC-GC of light gasoline

Jiang X., Zhang X. and He D. (Sichuan Union University, P.R. China)

Analysis of copper content in alloy copper by combination of electrography and flow injection analysis

Jönsson J. Å. and Mathiasson L. (University of Lund, Sweden).

Sample preparation using supported liquid membranes

Kishi H. and Fujii T.\* (Oyama National College of Technology and \* National Institute for Environmental Studies, Ibaraki, Japan)

A new design of a surface ionization detector for gas chromatography: a use of supersonic free jet

Lores M. and Cela R. (University of Santiago de Compostella, Spain)

Variable power post-column photochemical derivatization for conventional HPLC

Matz G., Walte A., Mnmeyer W. and Harder A. (Technical university Hamburg-Harburg, Germany)

Peak-hopping - A new technique to increase analyse speed in short column GC-MS

Ooms J.B., Haak G.S.J. and Kerkdijk H. (Spark Holland, Emmen, The Netherlands)

Automated on-line solid phase extraction coupled to mass spectrometry

Oriák A.<sup>a</sup>, Matisová E.<sup>b</sup>, Timerbaev A.R.<sup>c</sup>, Vojtek J.<sup>d</sup>, Ubik K.<sup>e</sup> and Gyoryova K.<sup>a</sup>

(<sup>a</sup>University of P.J. Šafárik, Košice, Slovakia, <sup>b</sup>Slovak Technical University, Bratislava, Slovakia, <sup>c</sup>Johannes Kepler University, Linz, Austria, <sup>d</sup>State Veterinary Institute, Košice, Slovakia and <sup>e</sup>Academy of Science of the Czech Republic, Prague, Czech Republic)

Hyphenation of TLC and AAS, MS, IR methods in the study of zinc carboxylate complexes stability

Andrews R. and Richardson H. (Waters Corporation, Milford, Massachusetts, USA)

Contribution of detector linearity and resolution to the identification of co-elution in HPLC peaks with photodiode array detection

Spraul M. and Hofman M. (Bruker, Rheinstetten, Germany)

Improvements in LC-NMR

Zhang X., Jiang X. and Liu M. (Sichuan Union University, P.R. China)

Analysis of chrome content in steel by combination of electrography and ion chromatography

#### **FOOD AND ORGANICS ANALYSIS WITH HYPHENATED CHROMATOGRAPHY**

Andrews R. and Richardson H. (Waters Corporation, Milford, Massachusetts, USA)

Characterization of vanilla extracts with HPLC with particle beam MS and photodiode array detection

Auger J. and Ferary S. (University F. Rabelais, Tours, France)

Direct cryotrapping-HPLC-MS analysis of Allium volatiles

Badjah-Hadj-Ahmed A. Y., Ghrib A. and Meklati B.Y. (C.P.A.P.C., Insitute of Chemistry, Alger, Algeria)

Analysis of mint essential oils by GC-FTIR

Batjoens P., De Brabander H.F. and De Wasch K. (University of Ghent, Belgium)

Rapid and high performing analysis of tapazole using tandem MS

Batjoens P., De Brabander H.F., De Wasch K.,

Courtheyn D.\* and Vercammen J.\* (University of Ghent and \* State Laboratory ROL, Gentbrugge, Belgium)

Tandem GC-MS analysis of Clenbuterol residues in faeces

Bondoux G. (Waters European Marketing, St. Yvelines, France)

Positive identification of polar pesticides in drinking water using HPLC with on-line UV diode array and PB-EI-MS detectors

Chanegriha N., Foudil-Cherif Y., Baaliouamer A. and Meklati B.Y. (Institute of Chemistry U.S.T.H.B., Alger, Algeria)

Use of series-coupled capillary gas chromatography columns for identification of Algerian Cypress and Eucalyptus essential oils

Chen Z., Li Z., Specht K. and Hu X. (Sino-German Research Institute, Nanchang, P.R. China)

Determination of purity of a delicious octapeptide by RP-HPLC

Chen Z., Li Z. and She S. (Sino-German Research Institute, Nanchang, P.R. China)

A comparative study on peptide maps from fresh milk protein by RP-HPLC and SPE-HPLC

Chilla C., Guillén D.A., Barroso C.G. and Pérez-Bustamante J.A. (University of Cádiz, Spain)

Automated on-line SPE-HPLC-DAD method for the analysis of the phenolic compounds in Sherry wine

Dallüge J., Hankemeier T.\*, Vreuls R.\*, Brinkman U.A.Th.\* and Werner G. (University of Leipzig, Germany and \* Free University of Amsterdam, the Netherlands)

On-line coupling of immunoaffinity-based solid phase extraction and gas chromatography for the determination of s-triazines in aqueous samples

De Swaef S.I., Kleiböhmer W.\* and Vlietinck A.J. (University of Antwerp, Belgium and \* Institute for Chemo- and Biosensors, Münster, Germany)

Comparison of capillary GC and capillary SFC for the quantitative determination of free fatty acids and fatty acid ethyl esters in Sabal Serrulata

Decolin D., Leroy P., Ambroggi G.\*, Archimbault P.\* and Nicolas A. (Faculty of Pharmaceutical and Biological Sciences, Nancy and \* Laboratory Virbac S.A., Carros, France)

Determination of colistin residues in bovine edible tissues and milk using HPLC with pre-column derivatization and column switching clean-up step

Gaspar G., Roselier E.\* and Stremple P.\*\* (J&W Scientific, Courtaboeuf, France, \*Fisons Instruments, Arcueil, France and \*\* J&W Scientific, Folsom, California, USA)

Trace analysis of pesticides by means of large volume injector – Special fused capillary column bred for GC-MS

Hogendoorn E.A. and van Zoonen P. (National Institute of Public health and Environmental Protection, Bilthoven, the Netherlands)

The scope of coupled-column LC in trace analysis

Matz G., Walte A. and Münchmeyer W. (Technical University Hamburg-Harburg, Germany)

A probe for the on-line analysis of gaseous organic compounds with a membrane inlet mass spectrometer

Sandra P., Ferraz V. and Modvedovici A. (University of Ghent, Belgium)

LC and SFC analysis of lipids with on-line UV light scattering detection

Senoráns F.J., Villén J.\*, Tabera J. and Herraiz M. (Institute of Industrial Fermentation, Madrid and \* University of Castilla-la Mancha, Ciudad Real, Spain)

On-line reversed phase liquid chromatography-gas chromatography in food analysis

Snyder J.M., King J.W. and Vorhauer J.J. (National Center for Agricultural Utilization Research, Peoria, Illinois, USA)

Development of an automated SFE-SFR-GC procedure for the analysis of total fat content of foods

Veness R.G. and Evans C.S. (University of Westminster, London, UK)

Identification of oligosaccharides by gas chromatography Fourier transform Infrared spectroscopy (GC-FTIR)

Bacaud R. and Rouleau L. (Catalysis Research Institute C.N.R.S, Villeurbanne, France)

Coupled simulated distillation-MS for the evaluation of hydroconverted petroleum residues

Naeemi E.D., Ahmad N. and Al-Kandari S. (Kuwait Institute for Scientific Research, Safat, Kuwait)

Determination of stabilizer/antioxidant in petroleum middle distillates by GC-MS

Pascual-Termens V., Zoete N. and Smits R. (BASF Antwerpen N.V., Belgium)

Simultaneous determination of the molecular weight distribution and the reactivity of polymers by gel permeation chromatography and gas chromatography

graphy

Planck C. and Prankl H.\* (University of Vienna and \* Federal Institute of Agricultural Engineering, Wieselburg, Austria)

On-line NP-LC-GC based studies on lubricating oils from vegetable oil methyl ester-fuelled diesel engines  
Robert E., Frances F., Pasquereau M., Codet G. and Beboulene J.J. (French Institute for Petroleum, Rueil Malmaison, France)

On-line coupling of HPLC with capillary GC – Application to the determination of fuel and lubricant parts in diesel particulate extracts

Van Broeck P.I. (Betz Europe, Heverlee, Belgium)

The application of head-space and pyrolysis gas chromatography mass spectrometry to solve paper and hydrocarbon processing customer problems

Verdurmen E.M., Verstappen R., Swagten J., Nelligen H. and Bart J.C.J. (DSM Research, Geleen, The Netherlands)

Hyphenated chromatographic techniques for the identification and quantification of additives extracted from polymeric materials

Vilaplana J. and Marin M.L.\* (Institute of Technology, Alicante and \* University of Alicante, Spain)

Analysis of DBP and DOP in poly(vinylchloride) (PVC) formulations by supercritical fluid extraction and capillary gas chromatography

#### **BIOMEDICAL ANALYSIS WITH HYPHENATED CHROMATOGRAPHY**

Bergkvist H., Eyem J.\* and Lundberg L. (National Laboratory of Forensic Science, Linköping and \*Hewlett-Packard Sverige, Kista, Sweden)

Fast automatic identification of drugs of abuse by means of an extraction robot and combined GC-FTIR

Cordonnier J., Van Moortel T., Goetyn W. and Vandrimck A. (Chemiphar, Brugge, Belgium)

Systematic toxicological blood screening by means of a standardized HPLC-DAD system

David F., Billiet H.\* and Sandra P.\*\* (Research institute for Chromatography, Kortrijk, Belgium, \* University of Delft, the Netherlands and \*\* University of Ghent, Belgium)

Analysis of Seaminoacids by CGC-AED

De Boeck G., Van Cauwenberghe K., Eggermont A.A.M., Van Oosterom A.T. and De Bruijn E.A. (University of Antwerp, Belgium)

Determination of melphalan and hydrolysis products in body fluids by GC-MS

Deforce D., Lemièrre F.\*, Esmans E.\* and Van den Eeckhout E. (University of Ghent and \* University of Antwerp, Belgium)

Capillary zone electrophoresis on-line coupled to electrospray MS in the elucidation of DNA adduct formation with phenylglycidyl ethers as carcinogenic compounds

Dirksen T.A. and Wells D.A.\* (3M Chemicals, Zwijndrecht, Belgium and \* 3M I&C, St Paul, Minnesota, USA)

A new approach to solid phase extraction of drugs and metabolites with capability for in-line LC-MS analysis

Haupt K. and Vijayalakshmi M.A. (University of Technology, Compiègne, France)

Immobilized metal ion affinity capillary electrophoresis (IMACE)

Herraez-Hernandez R., Louter A.J.H., Van de Merbel N.C. and Brinkman U.A.Th. (Free University of Amsterdam, the Netherlands)

Automated on-line dialysis as sample preparation for gas chromatography : determination of benzodiazepines in human plasma

Schütz S., Weibbecker B., Bitsch N., Klein A. and Hummel H.E. (Justus Liebig University, Giessen, Germany)

Analysis of leaf volatiles by GC-GC-FID-EAD and GC-MS

Shintani H. (National Institute of Health Sciences, Tokyo, Japan)

Automated solid phase extraction, automated dialysis and HPLC for uremic toxins in blood

Vanhoutte K., Joos P., Lemièrre F. and Esmans E. (University of Antwerp, Belgium)

The use of combined liquid chromatography electrospray tandem mass spectrometry in detecting and identifying carcinogen DNA-adducts



## PUBLICATION SCHEDULE FOR THE 1996 SUBSCRIPTION

### Journal of Chromatography A

MONTH	Oct. 1995	Nov. 1995	Dec. 1995 <sup>a</sup>	
Journal of Chromatography A	715/1	715/2 716/1 + 2 717/1 + 2	718/1 718/2	The publication schedule for further issues will be published later.
Bibliography Section				

<sup>a</sup> Vol. 701 (Cumulative Indexes Vols. 652–700) expected in December.

### INFORMATION FOR AUTHORS

(Detailed *Instructions to Authors* were published in *J. Chromatogr. A*, Vol. 657, pp. 463–469. A free reprint can be obtained by application to the publisher, Elsevier Science B.V., P.O. Box 330, 1000 AH Amsterdam, Netherlands.)

**Types of Contributions.** The following types of papers are published: Regular research papers (full-length papers), Review articles, Short Communications, Discussions and Letters to the Editor. Short Communications are usually descriptions of short investigations, or they can report minor technical improvements of previously published procedures; they reflect the same quality of research as full-length papers, but should preferably not exceed five printed pages. Discussions (one or two pages) should explain, amplify, correct or otherwise comment substantively upon an article recently published in the journal. Letters to the Editor (max. two printed pages) bring up ideas, comments, opinions, experiences, advice, disagreements, insights, etc. For Review articles, see inside front cover under Submission of Papers.

**Submission.** Every paper must be accompanied by a letter from the senior author, stating that he/she is submitting the paper for publication in the *Journal of Chromatography A*.

**Manuscripts.** Manuscripts should be typed in **double spacing** on consecutively numbered pages of uniform size. The manuscript should be preceded by a sheet of manuscript paper carrying the title of the paper and the name and full postal address of the person to whom the proofs are to be sent. As a rule, papers should be divided into sections, headed by a caption (e.g., Abstract, Introduction, Experimental, Results, Discussion, etc.). All illustrations, photographs, tables, etc., should be on separate sheets. Manuscripts should be accompanied by a 5.25- or 3.5-in. disk. Your disk and (**exactly matching**) printed version (printout, hardcopy) should be submitted together to the accepting editor or Editorial Office **according to their request**. Please specify the type of computer and word-processing package used (do not convert your textfile to plain ASCII). Ensure that the letter "l" and digit "1" (also letter "O" and digit "0") have been used properly, and format your article (tabs, indents, etc.) consistently. Characters not available on your word processor (Greek letters, mathematical symbols, etc.) should not be left open but indicated by a unique code (e.g.  $\alpha$ , @, #, etc., for the Greek letter  $\alpha$ ). Such codes should be used consistently throughout the entire text. Please make a list of such codes and provide a key. Do not allow your word processor to introduce word splits and do not use a "justified" layout. Please adhere strictly to the general instructions on style/arrangement and, in particular, the reference style of the journal. Further information may be obtained from the Publisher.

**Abstract.** All articles should have an abstract of 50–100 words which clearly and briefly indicates what is new, different and significant. No references should be given.

**Introduction.** Every paper must have a concise introduction mentioning what has been done before on the topic described, and stating clearly what is new in the paper now submitted.

**Experimental conditions** should preferably be given on a *separate* sheet, headed "Conditions". These conditions will, if appropriate, be printed in a block, directly following the heading "Experimental".

**Illustrations.** The figures should be submitted in a form suitable for reproduction, drawn in Indian ink on drawing or tracing paper. Each illustration should have a caption, all the *captions* being typed (with double spacing) together on a *separate sheet*. If structures are given in the text, the original drawings should be provided. Coloured illustrations are reproduced at the author's expense. The written permission of the author and publisher must be obtained for the use of any figure already published. Its source must be indicated in the legend.

**References.** References should be numbered in the order in which they are cited in the text, and listed in numerical sequence on a separate sheet at the end of the article. Please check a recent issue for the layout of the reference list. Abbreviations for the titles of journals should follow the system used by *Chemical Abstracts*. Articles not yet published should be given as "in press" (journal should be specified), "submitted for publication" (journal should be specified), "in preparation" or "personal communication".

Vols. 1–651 of the *Journal of Chromatography*; *Journal of Chromatography, Biomedical Applications* and *Journal of Chromatography, Symposium Volumes* should be cited as *J. Chromatogr.* From Vol. 652 on, *Journal of Chromatography A* should be cited as *J. Chromatogr. A* and *Journal of Chromatography B: Biomedical Applications* as *J. Chromatogr. B*.

**Dispatch.** Before sending the manuscript to the Editor please check that the envelope contains four copies of the paper complete with references, captions and figures. One of the sets of figures must be the originals suitable for direct reproduction. Please also ensure that permission to publish has been obtained from your institute.

**Proofs.** One set of proofs will be sent to the author to be carefully checked for printer's errors. Corrections must be restricted to instances in which the proof is at variance with the manuscript.

**Reprints.** Fifty reprints will be supplied free of charge. Additional reprints can be ordered by the authors. An order form containing price quotations will be sent to the authors together with the proofs of their article.

**Advertisements.** The Editors of the journal accept no responsibility for the contents of the advertisements. Advertisement rates are available on request. Advertising orders and enquiries may be sent to: Elsevier Science, Advertising Department, The Boulevard, Langford Lane, Kidlington, Oxford, OX5 1GB, UK; Tel: (+44) (0) 1865 843565; Fax (+44) (0) 1865 843952. *USA and Canada:* Weston Media Associates, Dan Lipner, P.O. Box 1110, Greens Farms, CT 06436-1110, USA; Tel (203) 261 2500; Fax (203) 261 0101. *Japan:* Elsevier Science Japan, Ms Noriko Kodama, 20-12 Yushima, 3 chome, Bunkyo-Ku, Tokyo 113, Japan; Tel (+81) 3 3836 0810; Fax (+81) 3 3839 4344.

# Retention and Selectivity in Liquid Chromatography

## Prediction, Standardisation and Phase Comparisons

Edited by R.M. Smith

Journal of Chromatography Library Volume 57

This book brings together a number of studies which examine the ways in which the retention and selectivity of separations in high-performance liquid chromatography are dependent on the chemical structure of the analytes and the properties of the stationary and mobile phases. Although previous authors have described the optimisation of separations by alteration of the mobile phase, little emphasis has previously been reported of the influence of the structure and properties of the analyte.

The initial chapters describe methods based on retention index group increments and log P increments for the prediction of the retention of analytes and the ways in which these factors are influenced by mobile phases and intramolecular interactions. The values of a wide range of group increments in different eluents are tabulated.

Different scales of retention indices in liquid chromatography are described for the comparison of separations, the identification of analytes and the comparison of stationary phases. Applications of these methods in the pharmaceutical, toxicology, forensic, metabolism, environmental, food and other fields are reviewed. The effects of different mobile phases on the selectivity of the retention indices are reported. A compilation of sources of reported retention index values are given.

Methods for the comparison of stationary phases based on the interactions of different analytes are covered; including lipophilic and polar indices, shape selectivity comparisons, their application to novel stationary phases, and chemometric methods for column comparisons.

### Contents:

1. Retention prediction based on molecular structure (R.M. Smith).
2. Retention prediction of pharmaceutical compounds (K. Valkó).
3. Retention index scales used in high-performance liquid chromatography (R.M. Smith).
4. Application of retention indices for identification in high-performance liquid chromatography (R.M. Smith).
5. Application of nitroalkanes and secondary retention index standards for the identification of drugs (M. Bogusz).

6. Identification using retention indices in gradient HPLC (P. Kuronen).
  7. Characterization of retention and selectivity in reversed phase LC using interaction indices (P. Jandera).
  8. Lipophilic and polar indices (P. Jandera).
  9. Solvent selectivity (S.D. West).
  10. Retention and selectivity for polycyclic aromatic hydrocarbons in reversed-phase liquid chromatography\* (L.C. Sander, S.A. Wise).
  11. Comparison of novel stationary phases (J.J. Pesek, E.J. Williamsen).
  12. Multivariate characterization of RP-HPLC stationary phases (A. Bolck, A.K. Smilde).
- Subject index.

©1995 480 pages Hardbound  
Price: Dfl. 425.00 (US\$ 250.00)  
ISBN 0-444-81539-2

### ORDER INFORMATION

**ELSEVIER SCIENCE**  
Customer Service Department  
P.O. Box 211

1000 AE Amsterdam  
The Netherlands  
Fax: +31 (20) 485 3432

For USA and Canada:

**ELSEVIER SCIENCE**  
Customer Service Department  
P.O. Box 945, New York  
NY 10159-0945  
Fax: +1 (212) 633 3764

US\$ prices are valid only for the USA & Canada and are subject to exchange rate fluctuations; in all other countries the Dutch guilder price (Dfl.) is definitive. Customers in the European Union should add the appropriate VAT rate applicable in their country to the price(s). Books are sent postfree if prepaid.



**ELSEVIER**

An imprint of Elsevier Science



0021-9673(19951103)715:2;1-8